



Bacteriophages of *Brevibacterium aurantiacum*: diversity, host interactions, and impact in washed rind cheeses

Thèse

Alessandra Gonçalves de Melo

Doctorat en microbiologie
Philosophiæ doctor (Ph. D.)

Québec, Canada

Résumé

Brevibacterium aurantiacum est l'un des principaux micro-organismes utilisés dans la production de fromages à croûte lavée dans le monde. L'utilisation de cette bactérie est dû à sa richesse métabolique, car elle produit des composés soufrés volatils, des pigments caroténoïdes et des enzymes lipolytiques et protéolytiques, qui sont nécessaires à la maturation d'une variété de fromages. Des souches de cette espèce bactérienne sont inoculées à la surface de fromages au cours de l'affinage et sont sensibles à des infections virales. Les bactériophages (phages), virus qui infectent les bactéries, sont omniprésents dans divers écosystèmes. Dans l'industrie laitière, ils sont reconnus pour perturber les procédés de production lors de l'infection de ferments lactiques, mais leur implication sur des fromages présentant des défauts de couleur et de saveur reste à démontrer. Ces anomalies de maturation de fromages à croûte lavée ont conduit à cette thèse.

Le premier objectif de cette thèse de doctorat consistait à analyser le génome de la souche industrielle *B. aurantiacum* SMQ-1335 et qui est aussi sensible à des phages. Le deuxième objectif de la thèse visait à étudier les phages virulents infectant cette souche. D'ailleurs, cette étude rapporte la première description et caractérisation de phages infectant cette espèce bactérienne. Malgré la similitude entre ces phages, des répétitions en tandem d'ADN ont été identifiées dans des génomes viraux et une analyse approfondie a montré que ces segments d'ADN sont répandus parmi les phages. Le troisième objectif visait à étudier l'interaction phage-hôte via l'analyse du génome de souches mutantes insensibles aux phages. En étudiant ces souches mutantes, des gènes potentiellement nécessaires pour l'infection phagique ont été identifiés. Enfin, le quatrième et dernier objectif visait à évaluer l'impact des phages de *B. aurantiacum* dans la production de fromages à croûte lavée et ce, à l'aide des caillé modèles. À noter que le reclassement de la souche SMQ-1335, avant identifiée auparavant comme *Brevibacterium linens*, est décrit en annexe de cette thèse.

Malgré des décennies d'études sur les phages laitiers, les phages de *B. aurantiacum* étaient encore inconnus. Mes travaux auront permis le développement d'un protocole reproductible pour isoler ces phages. Ces travaux ont également apporté de nouvelles connaissances sur les interactions phage-hôte et de leur impact dans les fromages affinés en surface.

Abstract

Brevibacterium aurantiacum is one of the key players in the production of washed rind cheeses produced worldwide. The importance of this bacterium to the dairy industry is due to its metabolic richness, as it produces volatile sulfur compounds, carotenoid pigments, and lipolytic and proteolytic enzymes, which play roles in the maturation of washed rind cheeses. As strains of this species are regularly inoculated on the cheese surface during ripening, there is a significant risk of viral attacks. Bacteriophage (phages), viruses that infect bacteria, are ubiquitous in the cheese environment. In the dairy industry, virulent phages have long been known to disrupt cheese processes by infecting lactic acid bacteria. The recent observations of color and flavor defects in washed rind cheeses suggested that phages may also infect strains of *B. aurantiacum*. These observations led to this thesis.

The first objective of this PhD dissertation was to study the genomics of *B. aurantiacum* SMQ-1335, an industrial strain used in the production of washed rind cheeses. The second objective of the thesis was to study the diversity and biology of virulent phages infecting this industrial strain. This study was the first report of phages infecting *B. aurantiacum*. Despite the low diversity of the isolated *B. aurantiacum* phages, DNA tandem repeats were found in an intragenic region of the viral genomes and extended analysis showed that these DNA segments are widespread among phages. The third objective was to investigate phage-host interactions through the genome analyses of bacteriophage insensitive mutants, which were selected by challenging SMQ-1335 with phage AGM1. Host genes likely necessary for phage infection were identified and may explain why some of these mutants are phage-resistant. Finally, the fourth objective of this thesis evaluated the impact of virulent phages on the production of washed rind cheeses using model curds. Of note, the reclassification of the strain SMQ-1335, long believed to be *Brevibacterium linens*, is described in the annex of the thesis.

Despite decades of studies on dairy phages, *B. aurantiacum* phages were still unknown. Here, a reproducible protocol to isolate these phages was developed, which may allow the isolation of new phages. This work also led to increased knowledge on phage-host interactions as well as on and their roles in surface-ripened cheeses.

Table of contents

Résumé	ii
Abstract.....	iii
Table of contents	iv
List of figures.....	viii
List of tables	ix
List of abbreviations	x
Acknowledgments	xiii
Foreword.....	xv
Introduction	19
Cheese and washed rind cheeses	19
<i>Brevibacterium</i> spp.....	21
<i>Brevibacterium aurantiacum</i>	22
Bacteriophages (phages).....	26
<i>B. aurantiacum</i> phages	31
Phage-host interactions.....	32
Phage as friends and enemies in food processing.....	35
Résumé	36
Abstract.....	36
Abbreviations.....	37
Introduction	38
Phages as a threat in food processing	38
Phage diversity	39
The arms race of phage and bacteria	40
Beneficial applications of bacteriophages in the food industry.....	41
Pathogenic infection of crops, fishes and farm animals	43
Food processing and packaging.....	43
Problems and risks associated with phage biocontrol	44
Conclusion	46
Conflicts of interest	46
Acknowledgements	46
References	47
Problematic, hypothesis and objectives of the study	50
Chapter 1 – Article 1	52
Résumé	53
Abstract.....	53

Abbreviations.....	54
Nucleotide sequence accession number	56
Funding Information.....	56
References	57
Chapter 2 – Article 2	59
Résumé	60
Abstract.....	61
Abbreviations.....	62
Introduction	63
Results	64
<i>B. aurantiacum</i> phage detection	64
Isolation of <i>B. aurantiacum</i> phages.....	65
Morphological analysis.....	65
Phage lytic cycle and host range.....	66
Molecular characterization	66
Genome termini	66
Genome sequencing.....	66
Genome and comparative analysis	67
DNA tandem repeats and phage groups	72
TR analysis in other phage genomes	74
Comparative genome and proteomic analysis with other <i>Brevibacterium</i> spp. phages.....	75
Discussion.....	77
Experimental Procedures.....	81
Bacterial culture and growth conditions.....	81
Phage detection.....	81
Isolation, propagation and titration of <i>B. aurantiacum</i> phages	82
Phage morphology	82
DNA isolation and restriction.....	83
Genome sequencing and primer walking	84
Determination of phage genomic termini.....	84
Genome analysis and annotation	84
Phage structural proteins analysis.....	85
Comparative genome analysis	85
DNA tandem repeat analyses in <i>B. aurantiacum</i> phage isolates.....	86
<i>In silico</i> analyses of tandem repeats in phage genomes	86
Data availability.....	86
Supporting information.....	86
Acknowledgements	87
Competing interests	87
References	88

Chapter 3 – Article 3	94
Résumé	95
Abstract.....	96
Abbreviations.....	97
Introduction	98
Results and Discussion	99
Generation of bacteriophage-insensitive mutants (BIMs).....	99
Characterization experiments show BIMs with three different phenotypes.....	102
BIMs are derivatives of SMQ-1335	104
The new genome sequence of SMQ-1335 wild-type has divergences in comparison to the previously sequenced reference genome	104
Mutations in the genome of BIMs from different phenotypic groups.....	105
Adsorption-blocking BIMs do not share exclusive mutations in similar genes or operons.....	107
An ATP-Binding Cassette (ABC) transport system is likely involved in phage insensitivity.....	110
Analysis of the ABC-transport system of <i>B. aurantiacum</i> SMQ-1335	113
<i>Lactococcus lactis</i> MG1363 as a model to study the role of permeases in phage resistance	115
Conclusion.....	116
Materials and Methods	117
Bacterial growth and phage assays.....	117
Generation of bacteriophage insensitive mutants (BIMs)	117
Confirmation of BIMs as derivatives of SMQ-1335	119
Adsorption assays	119
DNA isolation, genome sequencing and mutations mapping.....	120
Verification of mutations using PCR and Sanger sequencing.....	120
<i>In silico</i> analysis of ABC transport system and other mutated regions in the BIMs..	121
Genome editing of <i>L. lactis</i> MG1363.....	121
References	125
Chapter 4 – Article 4	128
Résumé	129
Abstract.....	130
Abbreviations.....	131
Introduction	132
Results and Discussion	133
Microbiological development on the cheese rind.....	133
<i>B. aurantiacum</i> phages on the cheese rind	138
Phage tolerance to thermal treatments.....	141
Materials and Methods	143

Culture methods and phage assays	143
Model curd preparation	143
Rind care.....	144
pH measurements of the model curds.....	144
Microbial composition of the rind	144
Development of the rind color.....	146
Thermal stability of <i>Brevibacterium aurantiacum</i> phages	146
Acknowledgements	146
References	147
Conclusion and perspectives	149
References	153
Annex A: Mobilome of <i>Brevibacterium aurantiacum</i> sheds light on its genetic diversity and its adaptation to smear-ripened cheeses.....	158

List of figures

Figure 1. Examples of washed rind cheeses from where <i>B. aurantiacum</i> has been isolated.....	4
Figure 2. <i>B. aurantiacum</i> growth.....	5
Figure 3. Current phage families according to ICTV latest report.....	10
Figure 4. Schematization of phage life cycles.....	12
Figure 5. Examples of phage defense mechanisms and counter defenses.....	16
Figure 6. Graphical abstract for “Phages as friends and enemies in food processing”	17
Figure 7. Development of phage cocktails for the biocontrol of pathogens in food.....	27
Figure 8. Electron micrograph of siphophage AGM1.....	47
Figure 9. Schematic representation and comparisons of 16 <i>B. aurantiacum</i> phage genomes.....	52
Figure 10. Mutation mapping using complete genome alignment of <i>B. aurantiacum</i> phages compared to phage AGM1.....	53
Figure 11. Schematic representations of repeat groups in the <i>orf50</i>	55
Figure 12. Schematic representation of the genome alignment and organization of phage AGM1 compared to other phages.....	58
Figure 13. Schematic representation of mutants’ selection from liquid media.....	82
Figure 14. Schematic representation of mutants’ generation and selection in solid media.....	83
Figure 15. Characterization of phage insensitive mutants.....	85
Figure 16. Schematic representation of the ABC-transport system of SMQ-1335 and mutations in the BIMs.....	94
Figure 17. Deacidification of the model curd rinds during the first 8 days of ripening.....	115
Figure 18. The growth of the yeast <i>Cryptococcus albicans</i> and <i>Geotrichum candidum</i> during model cheese ripening.....	116
Figure 19. Development of secondary bacteria on the model cheese surface.....	117
Figure 20. Development of <i>B. aurantiacum</i> and its phages during cheese ripening.....	118
Figure 21. Development of the color of the rind of model curds.....	120
Figure 22. PCR of the tandem repeats region of isolated plaques from the model curds.....	121
Figure 23. Stability of <i>B. aurantiacum</i> phages (AGM1 – AGM16) after heat treatment at 60 to 90°C for 5 min in Elliker medium.....	123
Figure 24. Basic steps for the preparation of model cheeses from cheese curd.....	126

List of tables

Table 1. Examples of commercially available bacteriophage products.....	24
Table 2. General genomic characterizations of <i>B. aurantiacum</i> phages.....	51
Table 3. Divergences between the reference genome of SMQ-1335 (GenBank accession CP017150.1) and the new sequence from Illumina.....	87
Table 4. Mutations shared among all BIMs.....	87
Table 5. Non-shared mutations in the genome of the BIMs.....	89
Table 6. Codon usage for WT and mutated codons of BIMs synonymous mutations.....	91
Table 7. List of <i>B. aurantiacum</i> strains and phages used in this study.....	100
Table 8. List of primers used for <i>B. aurantiacum</i> SMQ-1335 and its derivatives.....	101
Table 9. Primers designed for the genome editing of MG1363.....	104
Table 10. List of bacterial strains, phages and plasmids used in the genome editing of MG1363.....	105
Table 11. Analyses of the model cheeses during ripening.....	126

List of abbreviations

Abi	abortive infection
anti-CRISPR	proteins that inhibit CRISPR-Cas systems
attB	Attachment site in the bacterial genome
attP	Attachment site in the phage genome
BIM	Bacteriophage insensitive mutant
bp	Base pair
BreLI	<i>Brevibacterium</i> lanthipeptide island
BREX	Bacteriophage exclusion system
Cas	CRISPR associated
CRISPR	Clustered regularly interspaced short palindromic repeats
DISARM	Defense islands system associated with R-M
DNA	Deoxyribonucleic acid
ds	Double stranded
HGT	Horizontal gene transfer
HNH	A motif containing conserved histidine and arginine present in the catalytic site of nucleases
ICTV	International Committee on Taxonomy of Viruses
kb	Kilo bases (1000 base pairs)
kDa	Kilo Dalton
LAB	Lactic acid bacteria
mRNA	Messenger RNA
NaCl	Sodium chloride
ORF	Open reading frame
RBP	Receptor binding protein
RM	Restriction modification
RNA	Ribonucleic acid
rRNA	Ribosomal RNA
16S rRNA	Small subunit of ribosomes
RUSTI	iRon Uptake/Siderophore Transport Island
ss	Single strand
TA	toxin-antitoxin
TM	Transmembrane domain

To my mom, who taught me to persist.

*“Education does not change the world.
Education changes people.
People change the world.”*

—
Paulo Freire

Acknowledgments

This journey into my PhD was part of dream that took a long road until it happened. As long as it took to start and finish this journey, it truly led to a process that changed me as a student, researcher and human being. I would do it again. Certainly, it would not have been the same without wonderful and supporting people around me.

First of all, I would like to thank CNPq for funding my PhD studies, granting me a fellowship to perform my PhD studies. I also thank the Canadian consortium CALDO, which had a partnership with CNPq, for helping with my PhD application at Université Laval as I felt supported during the entire process. I also thank my advisory committee, Michel Frenette and Steve Labrie, for the assistance, time and helpful suggestions during the doctorate.

I have not enough words to thank my advisor Sylvain Moineau for having accepted me as a graduate student in his lab. This journey was very precious, and you helped to develop my potential with your guidance, leadership, kindness and scientific brilliance. I feel very privileged for having learned from you, as a scientist, leader and human being.

Sylvain's lab is a very dynamic, cooperative and friendly environment. In this almost five years, I could learn with great scientists and this was priceless. Among them, I would like to give a special thank you to Denise Tremblay and Geneviève Rousseau. I wish all labs could have people like you that teach and inspire. I really appreciated all the time that you put to teach me something new, suggest troubleshooting or give me support when I needed. It was really a pleasure to work with you. I thank also Stephanie Loignon and Bruno Martel that came later to the lab but were also available to answer questions and help as needed.

During the course of five years, I had many lab mates, from whom I learned so much by listening to during lab meetings, sharing protocols, discussing results or collaborating with. Be around you guys, helped me to grow as a scientist and I appreciate the time you spent with me for troubleshooting or for ways to improve my work or for simply encouraging me.

Some of my lab mates also became good friends and made my life in Quebec city much happier. First, I would like to thank Cas Mosterd, Hany Geagea and Sana Hamdi, who

welcomed me in a totally new environment and made me feel comfortable. Also, André Xavier, my Brazilian lab mate that became a great collaborator and close friend, with whom I enjoy spending hours talking about science. My Portuguese-speaking lab mates, Jessica Carvalhais (Brazil) and Priscila Pires (Portugal), which were there in different times of my life, but with whom I was able to speak Portuguese and feel a bit home; thank you for your support. Also, the sweet Honghui Liu, with whom I learned by example and it was always good to be around. And, of course, Cécile Philippe, who became a dear friend in and outside the lab. Many thanks to you all.

To my friends and people that were close to me at some moment outside the lab, I thank you for all the love and support. Thanks also for those that encouraged me when everything was only a plan, so this dream could become a reality. In special, I would like to thank my former house mate and friend, Elisa, who became like family for me. I cannot thank you enough for your friendship.

To my family, I thank you for always being there for me, encouraging and supporting this adventure. I thank especially my mom, Rute, that even with all the physical distance was present in every step of my journey and, since I was very young, stamped on me the value of pursuing higher education as a transforming experience. To my father, Elder; my brother, Alexandre; and my “little” sister, Victoria, thank you for being there for me.

Foreword

This PhD dissertation is organized in an introduction, which contains a review article; four chapters, each organized as a research article, and a conclusion. In addition, a collaborative article within the subject and relevant for the discussion has been included as an annex.

Introduction

Cheeses and washed rind cheeses are presented in the introduction of the thesis. I also present the genus *Brevibacterium* and its importance in cheese production. In particular, the species *Brevibacterium aurantiacum* is detailed and highlighted for its role in the ripening of washed rind cheeses. Phages are described in detail, including an overview on *B. aurantiacum* phages. I also discussed the interaction between phages and their hosts as well as their two sides in the review "Phage as friends and enemies in food processing". In this review, we discussed that these bacterial viruses may represent a risk to industrial fermentations, but they may also be valuable tools to control foodborne pathogens.

This review article was published in the journal *Current Opinion in Biotechnology*, in February 2018, volume 49, from page 185 to 190. I am the first author of this review. In collaboration with Sébastien Levesque and Sylvain Moineau. I performed the literature review, wrote the article and revised the manuscript. At the time of the publication, all authors were affiliated to the Département de biochimie, de microbiologie et de bio-informatique of Université Laval and to the Groupe de recherche en écologie buccale. Sylvain Moineau was also affiliated to the Félix d'Hérelle Reference Center for Bacterial Viruses. Figure, tables and references were modified to be in accordance to the dissertation format.

The problematic, hypothesis and objectives of this study were also presented at the end of the introduction section.

First research article (Chapter 1)

Complete Genome Sequence of Brevibacterium linens SMQ-1335. This short article was published in the journal *Genome Announcements*, on November 10th, 2016.

I am the first author of this article. I planned and performed the experiments, data analysis and also wrote the manuscript. Simon J. Labrie performed bioinformatics analysis. Jeannot Dumaresq carried out experiments to test antibiotic resistance of SMQ-1335. Richard J. Roberts performed analysis for the presence of restriction-modification systems. Denise Tremblay and Sylvain Moineau participated in the design and supervision of the study as well as manuscript revision. At the time of publication, Richard J. Roberts was affiliated to the New England Biolabs and Jeannot Dumaresq to the Département de microbiologie et d'infectiologie of the Centre hospitalier affilié universitaire Hôtel-Dieu de Lévis. All the other authors were affiliated to the Département de biochimie, de microbiologie et de bio-informatique of Université Laval, to the Groupe de recherche en écologie buccale. Denise Tremblay and Sylvain Moineau were also affiliated to the Félix d'Hérelle Reference Center for Bacterial Viruses.

Second research article (Chapter 2)

DNA tandem repeats contribute to the genetic diversity of Brevibacterium aurantiacum phages. This article was accepted for publication in the journal Environmental Microbiology, on June 8th, 2020.

I am the first author of this article. I conceived and performed the experiments, bioinformatics and data analysis. I also wrote and revised the manuscript. Geneviève Rousseau participated in the supervision and elaboration of experiments as well as revision of the manuscript. Denise Tremblay sequenced the genome of the phages. Simon Labrie performed bioinformatics analysis and phage genome assembly. Sylvain Moineau participated in the design and supervision of the study, as well as in the writing and revision of the manuscript. At the time of the publication, Simon Labrie was affiliated to SyntBioLab. All the other authors were affiliated to the Département de biochimie, de microbiologie et de bio-informatique of Université Laval, to the Groupe de recherche en écologie buccale. Denise Tremblay and Sylvain Moineau were also affiliated to the Félix d'Hérelle Reference Center for Bacterial Viruses of Université Laval. Figure, tables and references were modified to be in accordance to the dissertation format. The supplementary information is available online at doi: 10.1111/1462-2920.15113.

Third research article (Chapter 3)

*Mutations in an ATP-binding cassette transporter confer phage resistance in *Brevibacterium aurantiacum*.* This article is in preparation for submission.

I am the first author of this article. I conceived and performed the experiments, bioinformatics and data analysis. I also wrote and revised the manuscript. Geneviève Rousseau participated in the design of experiments as well as the revision of the manuscript. Denise Tremblay sequenced the genome of the *Brevibacterium aurantiacum* SMQ-1335 and its phage-insensitive derivatives. She also participated in the design of the experiments. Simon Labrie and Pier-Luc Plante performed bioinformatics analysis, BIMs genome assembly and mutations mapping. Sylvain Moineau participated in the supervision and design of the study as well as in the writing and revision of the manuscript. At the moment of the publication, Simon Labrie was affiliated to SyntBioLab. Pier-Luc Plante was affiliated to the Centre de recherche en infectiologie de l'Université Laval, Centre de recherche du CHU de Québec, Centre de recherche en données massives and also to Département de médecine moléculaire. All the other authors were affiliated to the Département de biochimie, de microbiologie et de bio-informatique of Université Laval, to the Groupe de recherche en écologie buccale. Denise Tremblay and Sylvain Moineau were also affiliated to the Félix d'Hérelle Reference Center for Bacterial Viruses.

Fourth research article (Chapter 4)

*The impact of virulent phages of *Brevibacterium aurantiacum* in the production of smear surface-ripened cheeses.* This article is in preparation for submission.

I am the first author of this article. I conceived and performed experiments and data analysis. Hany Geagea performed experiments of thermo-stability and revised the manuscript. Sylvain Moineau participated in the design and supervision of the study as well as in the writing and revision of the manuscript. All the authors were affiliated to the Département de biochimie, de microbiologie et de bio-informatique of Université Laval and to the Groupe de recherche en écologie buccale in the time of the experiments. Sylvain Moineau is also affiliated to the Félix d'Hérelle Reference Center for Bacterial Viruses.

Fifth research article (Annex A)

Mobilome of Brevibacterium aurantiacum sheds light on its genetic diversity and its adaptation to smear-ripened cheeses. This research article was published in the journal *Frontiers in Microbiology*, in June 2019.

I am the second author of this article. Sébastien Levesque planned and performed the experiments, data analysis and also wrote the manuscript. I performed experiments, data analysis and participated in the manuscript writing and revision. Simon Labrie performed bioinformatics analysis. Sylvain Moineau designed and supervised the study and participated in the revision of the manuscript. At the time of the publication, all the other authors were affiliated to the Département de biochimie, de microbiologie et de bio-informatique of Université Laval, to the Groupe de recherche en écologie buccale. Sylvain Moineau was also affiliated to the Félix d'Hérelle Reference Center for Bacterial Viruses.

Introduction

Cheese and washed rind cheeses

Cheese is one of the oldest fermented foods created by man (Irlinger et al., 2015). It is believed that cheese evolved in a region known as the “Fertile Crescent,” around 8000 years ago, where the so-called “Agricultural Revolution” occurred with the domestication of plants and animals (Fox and McSweeney, 2017). Bacterial growth and acid production would have likely occurred during storage or from attempts to dry milk produced by domesticated animals in a warm and dry climate, with the goal of preserving milk into a stable product (Fox and McSweeney, 2017). When sufficient acid is produced, the major milk proteins (i.e. caseins) coagulate to form a gel in which the milk fat is entrapped (Fox and McSweeney, 2017). Consequently, cheese microbial communities have been “in culture” for thousands of years, with the knowledge of how to grow these organisms passed down by generations of cheesemakers (Dutton and Wolfe, 2013).

Although cheesemaking is an ancient art, modern cheese production now relies on state-of-the-art science and technology, including the use of industrial enzymes, complex microbial fermentations, and a dynamic biochemistry during cheese ripening (McSweeney et al., 2017b). Even if derived from the same raw material, a variety of cheese types can be made around the world as the result of milk fermentation and transformation. The composition of the cheese ecosystem is defined by three elements that are the ripening agents (microorganisms and enzymes), the composition of the fresh milk, and the environmental conditions during aging (Almena-Aliste and Mietton, 2014). These factors will define the composition of the cheese ecosystem that affects not only the sensory quality but also the diversity of cheeses worldwide (Almena-Aliste and Mietton, 2014).

Cheese is often the habitat of at least two different microbial communities. The first is found in the cheese core, containing starter cultures, primarily lactic acid bacteria, while the second is found on the surface of the cheese, where a diverse collection of microbes make up the rind (Dutton and Wolfe, 2013). The primary function of starter bacteria is to produce sufficient lactic acid from lactose fermentation during cheese manufacture to reduce the pH of milk at the desired level (Cotter and Beresford, 2017). The secondary microbiota may be divided into a number of groups, including nonstarter lactic acid bacteria (e.g. nonstarter lactobacilli, *Pediococcus*, *Enterococcus*,

and *Leuconostoc*); propionic acid bacteria; molds; bacteria and yeast, which grow on the surface of smear-ripened cheeses (Cotter and Beresford, 2017). In addition to the microbial ecosystem, the variability among processing and ripening influence both the chemical composition of the fresh cheese and its enzymatic potential during ripening, which altogether contribute to the diversity and differentiation of cheese types (Almena-Aliste and Mietton, 2014).

The ripening cheese process is complex and involves microbiological and biochemical changes to the curd resulting in the flavor and texture characteristics of a particular variety (McSweeney, 2004). Microbiological changes during cheese ripening include the death and lysis of starter cells, the growth of nonstarter lactic acid bacteria and, in many varieties, the development of molds in mold-ripened varieties and a complex Gram-positive bacterial flora in smear cheeses (McSweeney, 2004). Moreover, the characteristics of the ripening conditions (temperature, relative humidity, and rates of O₂, CO₂, and NH₃) ultimately influence the character and diversity of the cheese microbiota (Almena-Aliste and Mietton, 2014).

Bacterial surface-ripened (“smear-ripened,” “washed-rind”) cheeses are a diverse group of varieties characterized by the growth of a complex and adapted Gram-positive bacterial flora on the cheese surface during ripening (McSweeney et al., 2017b). During manufacture, the surface of the cheeses is washed periodically with a brine solution, a process referred to as “smearing” (McSweeney et al., 2017b). The heterogeneous physicochemical composition of the surface of washed rind cheeses offers the possibility of simultaneous occupation by multiple microbial groups through the utilization of different carbon sources (Irlinger and Mounier, 2009). During the first days of ripening, yeasts and mold, such as *Geotrichum candidum* and *Debaryomyces hansenii*, dominate the surface microflora, where they metabolize the lactate present in the curd and release growth factors (Irlinger and Mounier, 2009). They also produce alkaline metabolites, such as ammonia from deamination of amino acids, which leads to an pH increase enabling the growth of acid-sensitive bacteria such as *Arthrobacter* spp., *Brevibacterium* spp., *Corynebacterium casei*, micrococci and staphylococci (Arfi et al., 2006; Corsetti et al., 2001; Irlinger and Mounier, 2009; Rattray and Fox, 1999). This dynamic and complex secondary microflora (molds, yeasts and surface bacteria) contribute with proteolytic and lipolytic enzymes for cheese texture, flavor, and quality (Bonomo and Salzano, 2012; Caridi et al., 2003). As such, these cheeses are characterized by a strong aroma and high levels of proteolysis and lipolysis (McSweeney et al., 2017b).

***Brevibacterium* spp.**

The metabolism and physiology of the microorganisms will determine their growth on smear surface-ripened cheeses (Motta and Brandelli, 2008). The ability to grow on the cheese surface depends on various properties such as salt tolerance and iron acquisition systems as well as the ability to use the energy compounds present in the cheese (Motta and Brandelli, 2008). Due to its enzymatic richness, *Brevibacterium* spp. strains are widely used for the manufacturing of orange-pigmented surface-ripened cheeses, contributing to the breakdown of lipids and proteins as well as producing volatile sulfur compounds (Pham et al., 2017).

Brevibacterium linens is the type species of the genus *Brevibacterium* that belongs to the *Brevibacteriaceae* family, order *Actinomycetales*, and class *Actinobacteria* (Breed et al., 1957). Species of the *Brevibacterium* genus present similarities with members of others coryneform genera, such as *Arthrobacter*, *Corynebacterium* and *Rhodococcus*, for having meso-diaminopimelic acid in the cell wall or showing a rod-coccus growth cycle (Onraedt et al., 2005). However, the presence of teichoic acids in the polysaccharide cell wall of *Brevibacteria* distinguishes them from all others coryneform bacteria (Motta and Brandelli, 2008).

For a long time, *B. linens* was considered the major component of the bacterial flora present in the smear of a variety of surface-ripened cheeses, such as Appenzeller, Brick, Gruyère Limburger, Münster, Romadour, Tilsit, and other cheeses produced worldwide (Bonnarme et al., 2000; Onraedt et al., 2005). However, as *Brevibacterium* taxonomic classification previously indicated that *B. linens* was the only member of the genus to produce orange-pigmented colonies, such *Brevibacterium* strains were usually assigned to this species (Gavrish et al., 2004). Since the taxonomy of *Brevibacterium* has been updated (Gavrish et al., 2004), the role of *B. linens* as the major *Brevibacterium* species in cheeses has been reconsidered. Strains of *B. linens*, *B. aurantiacum*, *B. antiquum*, and *B. casei* have been isolated from cheeses (Pham et al., 2017). Furthermore, recent studies using complete genome sequencing have been showing that several strains previously classified as *B. linens* are instead *B. aurantiacum* (Levesque et al., 2019; Pham et al., 2017) and also that this species is prevalent on the surface of several cheeses (Bonham et al., 2017; Cogan et al., 2014).

Brevibacterium aurantiacum

The *B. aurantiacum* species was first described by Gavrish et al. (2004) in a taxonomic study of orange-pigmented strains that were phenotypically close to *B. linens*. The study also included the new species *B. antiquum* and *B. permense* (Gavrish et al., 2004). The *B. linens* group was divided into these new species on the basis of their physiological and biochemical characteristics, the sugar and polyol composition of their teichoic acids, their 16S rRNA sequence and the DNA-DNA hybridization levels (Forquin et al., 2009). While the strain ATCC 9172 remains *B. linens*, the strain ATCC 9175 isolated from cheese represents the type strain of the *B. aurantiacum* species (Forquin et al., 2009; Gavrish et al., 2004). The isolation of *B. aurantiacum* strains have been reported in cheeses such as Camembert, Beaufort, Langres, Reblochon, Romadur, Limburger, Havarti, Livarot, Danbo and Gubbeen (Mounier et al., 2017; Pham et al., 2017). Figure 1 shows some examples of cheeses in which strains of *B. aurantiacum* have been isolated.

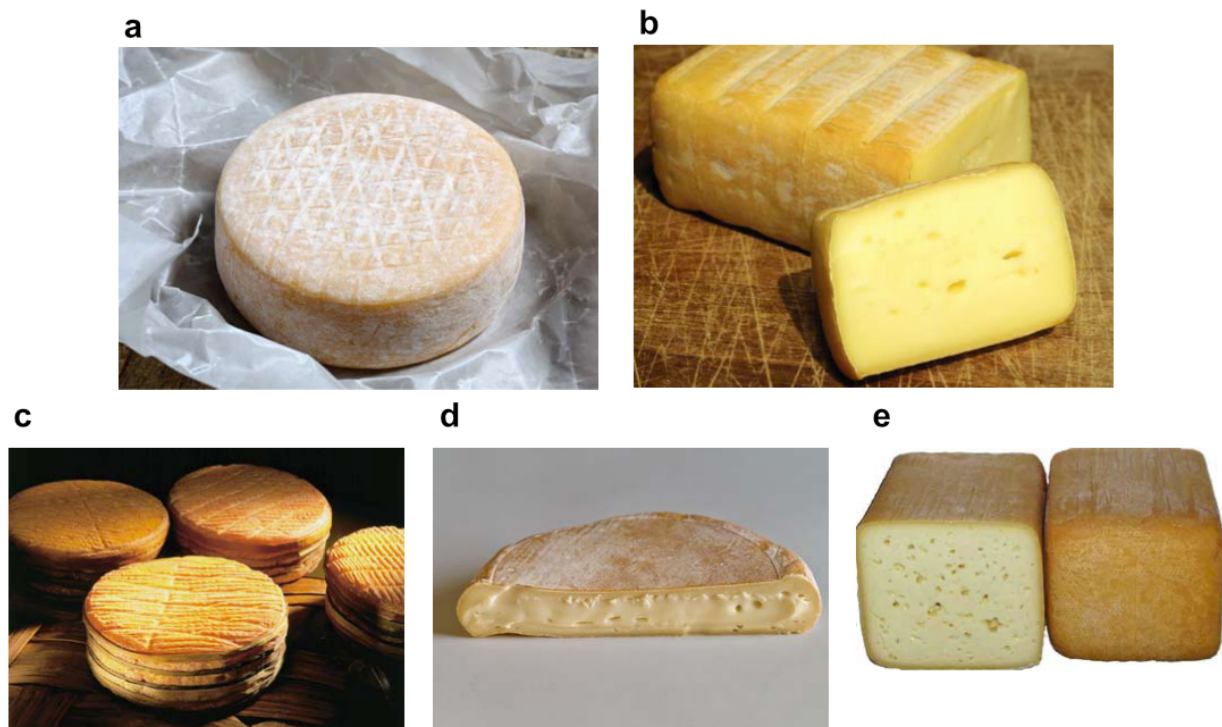


Figure 1. Strains of *B. aurantiacum* have been isolated from several washed rind cheeses.

Adapted from Cogan et al. 2014. (a) Gubbeen; (b) Limburger; (c) Livarot; (d) Reblochon; and (e) Tilsit.

B. aurantiacum is a Gram-positive, non-motile, and non-spore-forming bacterium (Gavrish et al., 2004). It produces orange colonies and undergoes a rod-coccus growth cycle, with older cultures dominated by coccoid cells (Figure 2). Furthermore, *B. aurantiacum* is aerobic and its optimal growth temperature is around 24-26°C, while being able to grow at 7°C but not at 37°C (Gavrish et al., 2004). Moreover, this species grows in 15% NaCl, hydrolyzes casein, and uses several carbon sources, such as cellobiose, fructose, galactose, glucose, glycerol, mannitol, mannose, and xylose. The peptidoglycan contains meso-diaminopimelic acid and its teichoic acids are composed of galactose, glucose and glycerol (Gavrish et al., 2004).

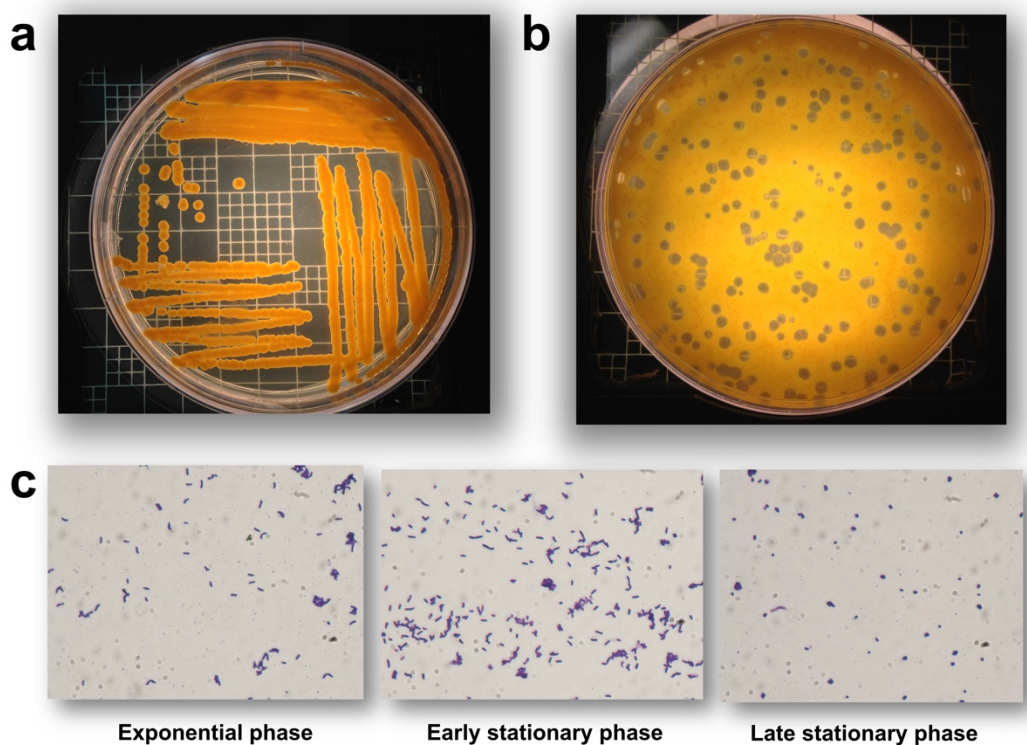


Figure 2. *B. aurantiacum* growth. (a) *B. aurantiacum* produces orange pigments during growth, a desirable feature in cheese production. (b) Phage plaques on a lawn of *B. aurantiacum* SMQ-1335. (c) *B. aurantiacum* cells transform from bacilli to coccoid shape during growth.

The recent complete genome sequencing of *B. aurantiacum* strains involved in cheese production have shown the metabolic arsenal of this bacterial species (Anast et al., 2019; Bonham et al., 2017; Levesque et al., 2019; Pham et al., 2017). For example, Pham et al. (2017) performed the comparative genome analysis of 23 *Brevibacterium* strains, including twelve strains isolated from cheeses, among which five were *B. aurantiacum* (8(6), CNRZ 920, 6(3), ATCC 9174 and ATCC

9175^T). These strains were investigated for key genetic determinants known to be important for growth in cheeses, such as the ability to use energy compounds, iron acquisition, salt tolerance, and bacteriocin production (Pham et al., 2017). Regarding the catabolism of energy compounds present in cheeses, no beta-galactosidase gene was found in the *Brevibacterium* genomes, which is consistent with the fact that most *Brevibacterium* spp., including *B. aurantiacum*, are not able to consume lactose (Gavrish et al., 2004; Pham et al., 2017). On the other hand, several strains of *B. aurantiacum*, including the type strain (ATCC 9175), encode enzymes involved in the Leloir pathway for galactose utilization and two of them (8(6) and CNRZ 920) have the complete pathway for D-galactonate catabolism (Pham et al., 2017).

Biochemical reactions, which occur in cheese during ripening, are conventionally grouped into three major categories: (1) glycolysis of residual lactose and catabolism of lactate and citrate; (2) lipolysis and the catabolism of free fatty acids; and (3) proteolysis and the catabolism of amino acids (McSweeney, 2017). During the manufacture of cheese curd, lactose is converted to lactic acid (or lactate) by starter bacteria and the resulting lactate is a substrate for a series of reactions during cheese ripening (McSweeney et al., 2017a). Enzymes involved in the lactate catabolism (NAD-independent lactate dehydrogenases) and transport (lactate permeases) have been identified in the genome of *B. aurantiacum* (Pham et al., 2017). Additionally, *B. aurantiacum* genomes encode enzymes involved in the catabolism of ethanol (alcohol dehydrogenase and acetaldehyde dehydrogenases), acetate (monocarboxylic acid transporter MctC and acetyl-CoA synthase), and also in the import of citrate (Pham et al., 2017).

Lipid catabolism involves the release of free fatty acids and glycerol as well as the subsequent breakdown of these compounds (Pham et al., 2017). As they are hydrophobic, lipids are excellent carriers and also precursors of numerous flavor compounds, such as esters, methyl ketones, lactones, and secondary alcohols (Thierry et al., 2017). The *B. aurantiacum* genomes analyzed encode several proteins with putative lipase or esterase activity in addition to enzymes involved in the catabolism of glycerol and short chain fatty acids transporters (Pham et al., 2017). *Brevibacterium* lipases release volatile fatty acid components from milk triacylglycerol, influencing the taste of ripened cheese (Motta and Brandelli, 2008; Onraedt et al., 2005).

Cheese contains a large amount of proteins, mainly caseins, which can be degraded by various

proteolytic microorganisms (Pham et al., 2017). *Brevibacterium* strains synthesize highly active proteases and peptidases during its growth (Onraedt et al., 2005; Rattray and Fox, 1999). Indeed, the genome analysis of *B. aurantiacum* strains revealed several genes coding for proteolytic enzymes (9-12), with some strains encoding extracellular proteases, one of which was previously characterized for its activity on caseins (Pham et al., 2017). The free amino acids resulted from proteolysis of caseins (Gavriš et al., 2004) can be used as an energy source by the cheese ripening microorganisms while they also have a crucial role in cheese aroma formation as precursors of volatile flavor compounds produced by a range of catabolic reactions (Ardö et al., 2017; Pham et al., 2017). The production of volatile sulfur compounds arises mostly from the degradation of the sulfur-carbon bond of L-methionine to form methanethiol (Arfi et al., 2006; Bonnarme et al., 2000). *B. aurantiacum* strains encode in their genomes enzymes for methionine degradation and also de degradation pathways for several amino acids, such as proline, alanine, arginine, glutamate, histidine, phenylalanine, serine, threonine, and tyrosine (Pham et al., 2017).

In order to survive under hyperosmotic stress in this environment, *Brevibacterium* strains accumulate compatible solutes to maintain a positive cellular turgor (Onraedt et al., 2005). *B. aurantiacum* strains have been shown to encode enzymes involved in the synthesis of the osmoprotectants ectoine, glycine-betaine and trehalose, which may help to protect these strains of the osmotic stress resulting from high salt concentrations in cheeses (Pham et al., 2017). Bacteriocins are antibacterial peptides that are inhibitory to microorganisms that are usually, but not always, closely related to the producer strain (Motta and Brandelli, 2008). Predicted bacteriocin biosynthesis genes are present in most of the strains, and one of the corresponding gene clusters is located in a probable conjugative transposon found only in cheese-associated strains and named *Brevibacterium* Lanthipeptide Island (BreLI) (Pham et al., 2017). This region was later identified also in the genome of *B. aurantiacum* SMQ-1417 and shown to circularize, although the bacteriocin activity could not be confirmed in the strains tested (Levesque et al., 2019).

As a result of growing in novel human-made environments, the microbial communities of fermented foods experience strong selection (Bonham et al., 2017). As a consequence of the selective pressure exerted by the growth on cheeses, *B. aurantiacum* strains seem to have recently acquired genes, especially those involved in iron uptake, from other actinobacteria such as *Glutamicibacter arilaitensis*, *Corynebacterium variabile*, and *Corynebacterium casei*, which are

also part of the cheese rind community (Levesque et al., 2019). Growing evidence suggests that the availability of iron is a driving force in adaptation of microorganisms that grow on cheeses (Bonham et al., 2017). As iron availability is limited in cheeses (Monnet et al., 2012), iron acquisition genes obtained through horizontal gene transfer (HGT) are very abundant in *B. aurantiacum* and other cheese bacteria (Bonham et al., 2017; Levesque et al., 2019; Pham et al., 2017). For instance, a large region of ~47 kb and 34 genes, named RUSTI (i.e. iRon Uptake/Siderophore Transport Island), was found in a study investigating the extensive HGT in cheese-associated bacteria, including *Brevibacterium* (Bonham et al., 2017). In addition to iron acquisition genes, mobile genetic elements contributed to the expansion of *B. aurantiacum* pan-genome and to its genetic diversity, with significant differences found between the mobilome of *B. aurantiacum* dairy strains and environmental strains of *B. linens* and *B. epidermidis* (Levesque et al., 2019).

Regarding defense strategies against foreign nucleic acids, no CRISPR-Cas system has been identified in the genome of *B. aurantiacum* strains (Levesque et al., 2019; Pham et al., 2017). However, a new type I restriction-modification (R-M) system was identified in the genome of *B. aurantiacum* SMQ-1335 and this strain may contain additional R-M systems (types II, III, and IV) (de Melo et al., 2016). Of note, the phage-sensitive strain SMQ-1335 was previously identified as *Brevibacterium linens* (Chapter 1), but phylogenetic analysis described in Annex A showed that this strain belongs to the *B. aurantiacum* species (Levesque et al., 2019). Additionally, an anti-plasmid system Wadjet was recently described (Doron et al., 2018) and orthologs of its proteins were identified in the genome of several *B. aurantiacum* strains, which could be partly responsible for the absence of plasmids in the referred strains (Levesque et al., 2019).

Bacteriophages (phages)

Because high numbers of bacterial cells are cultivated each day in large vats, cheese manufacturing can be disrupted by strictly lytic phages. In fact, most bacterial fermentation industries have experienced phage contaminations at varying frequencies (Labrie et al., 2010; Marcó et al., 2012). As with all viruses, phages are made of at least two components: nucleic acids and proteins (Campbell, 2003; Mc Grath et al., 2007). They are the most abundant biological entities on our planet, often outnumbering coexisting bacterial cells in ecosystems (Brüssow and Hendrix, 2002).

In the non-sterile environment of heat-treated milk, the added cultures will come into contact with virulent phages naturally contaminating milk (Garneau and Moineau, 2011). Although the phage concentration is usually low in milk, a specific phage population can increase rapidly if phage-sensitive cells are part of the added bacterial culture used to ferment milk (Garneau and Moineau, 2011). Fluctuating phage titers can be observed if a starter strain rotation system is adopted (Chibani-Chennoufi et al., 2004). The occurrence of phage outbreaks leads to economical loss as the lysis of a larger number of sensitive bacterial cells will delay the milk fermentation process and lead to low-quality products (Garneau and Moineau, 2011; Mc Grath et al., 2007). Over the past decades, the dairy industry has adopted different strategies to control phage propagation in the industrial settings, including the adaptation of factory design and processes, improved sanitation, strain rotation, and the use of phage-resistant strains (Garneau and Moineau, 2011). Despite these efforts, new viral variants keep emerging as a result of phage evolution (Garneau and Moineau, 2011).

Historically, phages were classified into ten families based on characteristics such as genome type (ssDNA, ssRNA, dsDNA or dsRNA), morphological properties of the virion and host range (Dion et al., 2020). However, in the past few years, phage taxonomy has been revisited by the Bacterial and Archaeal Viruses Subcommittee of the International Committee on Taxonomy of Viruses (ICTV) (Adriaenssens et al., 2018, 2020) and it is currently undergoing a major overhaul, moving from a mostly morphology-based approach to a genome-based taxonomy (Dion et al., 2020). Since then, nine new families of bacterial viruses were added and many more are expected to be described in the coming years.

The most predominant bacterial viruses belong to the *Caudovirales* order, which are tailed phages containing double strand DNA (dsDNA) (Brüssow and Hendrix, 2002; Dion et al., 2020; Hatfull, 2008). Previously, the *Caudovirales* order comprised three families based on the tail morphology, which were *Myo*-, *Sipho*- and *Podoviridae*. Phages from the *Myoviridae* family have a long, contractile tail whereas *Siphoviridae* and *Podoviridae* phages have long and short non-contractile tail, respectively (Brüssow and Hendrix, 2002). However, six new families were included into the *Caudovirales* order in recent years based on genome content and host, and many more are coming. Three of these new phage families, *Ackermannviridae*, *Chaseviridae* and *Herelleviridae*, share the myovirus morphology. Members of the *Demerecviridae* and *Drexelviriidae* have the siphovirus

morphology, whereas phages from the *Autographiviridae* family have a podoviral morphology (Adriaenssens et al., 2018, 2020). The minimal genome of tailed phages encodes DNA packaging, capsid, tail, DNA replication, transcription regulation, and lysis genes (Brüssow and Hendrix, 2002). The virion structure and assembly genes typically encompass at least 15 kb of genome space. Therefore, the majority of siphophages have genomes larger than 20 kb (Hatfull, 2008). Other apparently less common phages can pack their single-stranded DNA (ssDNA), dsDNA, single-stranded RNA (ssRNA) or double-stranded RNA (dsRNA) genome into non-tailed virions (Dion et al., 2020) that can be polyhedral (*Microviridae*, ssDNA; *Corticoviridae*, dsDNA; *Tectiviridae*, dsDNA; *Leviviridae*, ssRNA; *Cystoviridae*, dsRNA; and *Finnlakeviridae*, ssDNA), filamentous (*Tubuvirales* order, ssDNA; *Inoviridae*, *Plectroviridae*), or pleomorphic (*Plasmaviridae*, dsDNA) (Adriaenssens et al., 2020; Dion et al., 2020).

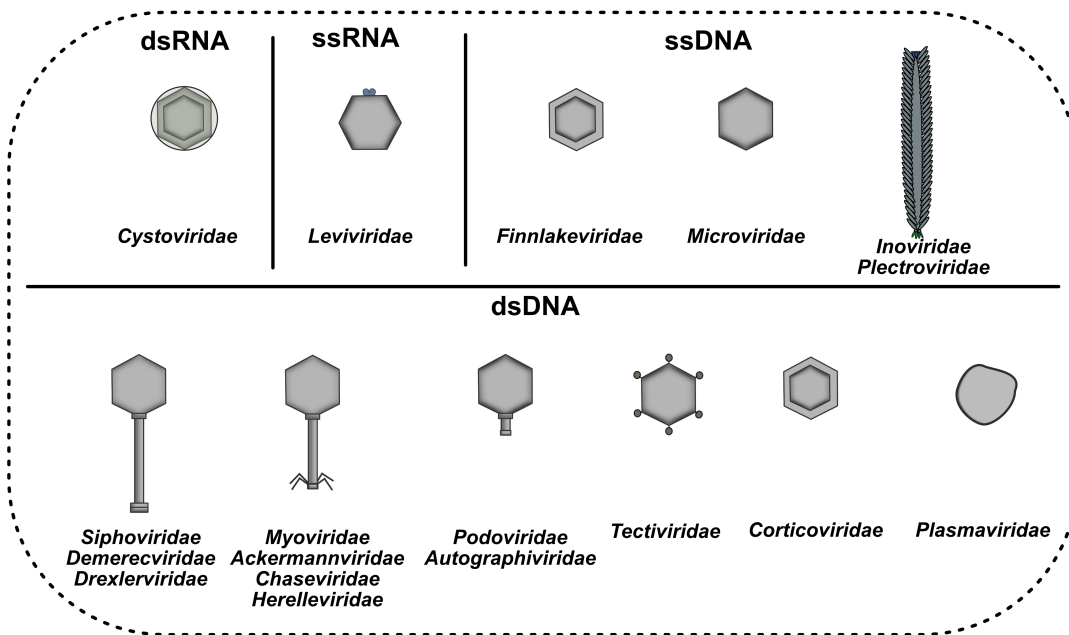


Figure 3. Current phage families according to ICTV latest reports.

Phages have evolved diverse strategies to exploit prokaryotic host cells for their own reproduction (Koskella and Brockhurst, 2014). Based on their genetics and interactions with the host bacteria, phages can undergo distinct cycles, such as lysogenic, lytic (Feiner et al., 2015; Mc Grath et al., 2007) or chronic infection (Koskella and Brockhurst, 2014) (Figure 4). In general, lytic phages immediately enter in a productive cycle upon infection, in which the phage genome is replicated and packaged into new phage particles that are then released through bacterial lysis (Bondy-Denomy and Davidson, 2014; Feiner et al., 2015). On the other hand, phages can enter in a symbiotic cycle with the host bacteria, during which the phage genome is integrated into the bacterial chromosome in a lysogenic state, or forms an extrachromosomal plasmid in pseudolysogeny (Bondy-Denomy and Davidson, 2014; Feiner et al., 2015). Additionally, filamentous phages have the ability to establish a chronic infection in which the viral genome resides within the cell in either an exclusively episomal state or integrated into the host chromosome, while virions are continuously released from the productive cycle without killing the host (Roux et al., 2019).

The adsorption, the first step of phage infection (Duplessis and Moineau, 2001), involves recognition of receptors located on the bacterial cell surface by the phage receptor-binding proteins (RBPs) (Duplessis et al., 2006; Mahony and van Sinderen, 2012). Secondly, the phage genome is then injected through the cell wall into the bacterial cytoplasm, in a process facilitated by peptidoglycan hydrolases, enzymes that are able to locally degrade the peptidoglycan without lysing the cell (Kenny et al., 2009; Oliveira et al., 2013). Phage genome entry generates a cycle of phage production initiated by phage-specified proteins, which are translated from phage mRNA after infection (Campbell, 2003). Subsequently, the components of the biosynthetic apparatus (such as ribosomes and ATP generators) are diverted from their normal tasks in bacterial growth to the production of phages, in which the replication of nucleic acids occurs first, followed by the synthesis of phage structural proteins (Campbell, 2003). Afterwards, the new phage capsids are then assembled, and the genetic material is packaged into them. In most phages, a tail will be connected to nucleic acid-filled capsid. At the end of the infection cycle, the progeny is released from the infected cell by the action of phage-encoded endolysins that hydrolyze the bacterial cell wall (Chapot-Chartier, 2014; Oliveira et al., 2013).

Alternatively, phages genome can integrate into the bacterial chromosome. The phage is then

described as a prophage and the bacterial cell harboring a prophage is known as a lysogen (Campbell, 2003). The excision and integration of a phage genome are mediated by phage-encoded DNA recombinases, such as integrases and excisionases, and take place at specific attachment sites, which are identical in both bacterial (*attB*) and phage genomes (*attP*) (Feiner et al., 2015). Prophages are replicated together with the bacterial chromosome, and this lysogenic state is maintained by the repression of phage lytic genes (Feiner et al., 2015). Moreover, the action of the repressor proteins expressed by prophages leads to resistance to superinfection by the same phage (Bondy-Denomy and Davidson, 2014; Marcó et al., 2012). Hence, the lysogenic cell can survive and replicate without the production of phage particles or deleterious phage proteins, and even be “immune” to another infection (Bondy-Denomy and Davidson, 2014; Feiner et al., 2015; Marcó et al., 2012). Ultimately, certain conditions can induce the phage genome excision, and lead lysogenic cells to re-enter the lytic cycle (Campbell, 2003).

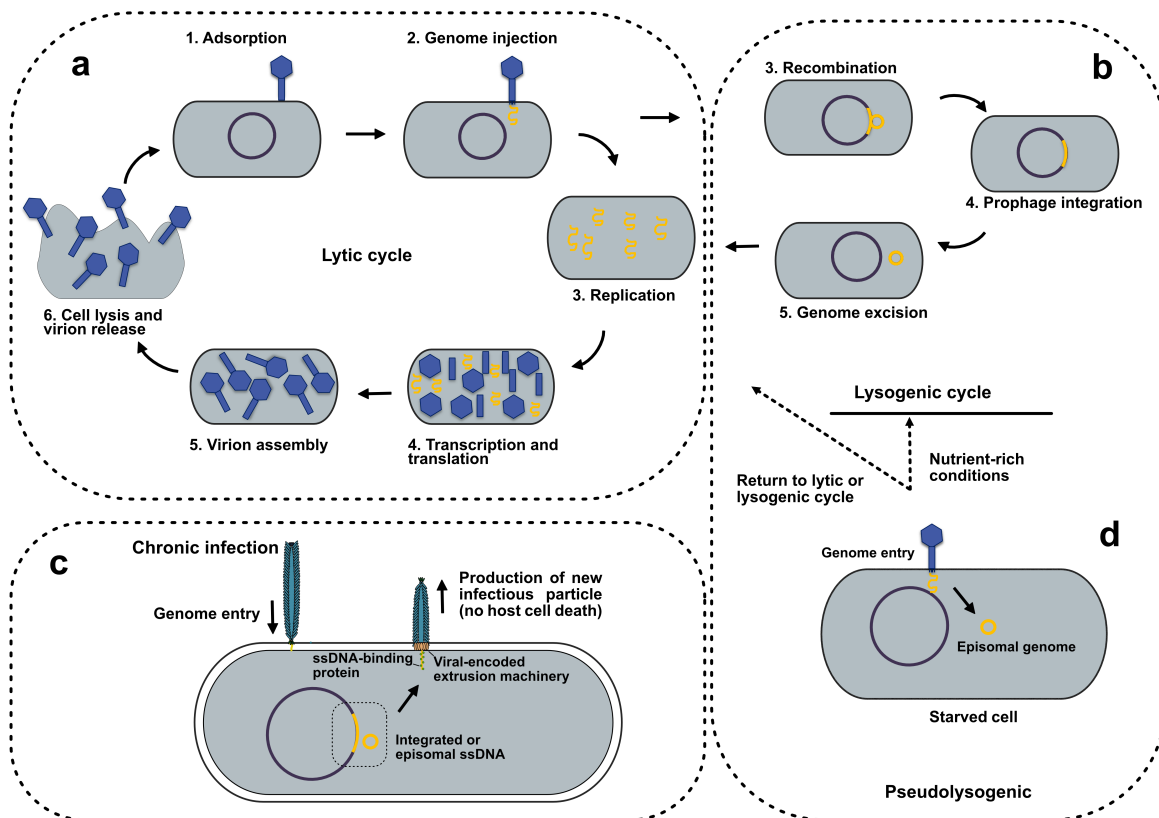


Figure 4. Schematization of phage cycles.

Most phages will perform a lytic (a) or lysogenic (b) life cycles. Filamentous phages can perform chronic infections (c) and some phages can have episomal genomes in a pseudolysogenic state (d).

***B. aurantiacum* phages**

It was recently pointed out that the phage sensitivity of ripening cultures containing *Brevibacterium* strains was unknown, and the impact of phages on these cultures was probably overlooked (Pham et al., 2017). In fact, studies on *Brevibacterium* phages are rare. To date, two different virulent phages of *Brevibacterium iodinum* and *Brevibacterium fuscum* has been described, which are phage LuckyBarnes (*Siphoviridae*) (Underwood et al., 2019) and phage Cantare (*Myoviridae*). Besides these two phages, two seemingly complete prophages have been identified in the genome of the strains *B. linens* VCM10 (Melo et al., 2020) and *B. aurantiacum* SMQ-1419 (Levesque et al., 2019). Except for *B. aurantiacum* SMQ-1419, none of the prophages or phages have been associated to the dairy environment, being instead isolated from environmental samples, such as soil.

Recently, virulent phages infecting a sensitive dairy strain of *B. aurantiacum* have been isolated in cheese manufacturing facilities after defective color and flavor development in smear surface-ripened cheeses (Melo et al., 2020). These observations suggested that these cheese defects might be related to the presence of virulent phages in this environment. Our group led the investigation of this phenomenon and the discovery of the first *B. aurantiacum* virulent phages (Chapter 2). We isolated 16 highly related virulent *Siphoviridae* phages, named AGM1 to AGM16, which all seem to have evolved from a prophage that lost the ability to integrate in the bacterial genome. *B. aurantiacum* virulent phages are unrelated to the prophage found in the cheese-associated strain *B. aurantiacum* SMQ-1419, which is closer to LuckyBarnes, but their genes coding for the phage structural proteins are related to the structural genes found in the prophage VCM10 (Melo et al., 2020). Although there is a narrow diversity among the sixteen phages, the major contributor to their genetic diversity is the presence of tandem repeats in their genomes.

An increasing interest on *B. aurantiacum* has been observed in recent years with the isolation and characterization of new strains from several parts of the world (Anast et al., 2019; Bonham et al., 2017; de Melo et al., 2016; Levesque et al., 2019; Pham et al., 2017). Although *B. aurantiacum* phage research is still in its infancy, new virulent phages will likely be isolated in forthcoming years as there is a growing industrial interest of the bacterial host strains.

Phage-host interactions

The reciprocal evolution of bacteria and phages is an important driver of ecological processes in microbial communities (Koskella and Brockhurst, 2014). This continuous cycles of co-evolution leads to the emergence of phage-insensitive hosts that help to preserve bacterial lineages, whereas counter-resistant phages threaten these new bacterial strains (Labrie et al., 2010). Bacteria have evolved numerous immune mechanisms, both innate and adaptive, to cope with this evolutionary pressure (Hampton et al., 2020). Different bacterial defense mechanisms can interfere with each step of phage infection while phages have evolved ways to impede the interference and proceed with the infection (Figure 5). An understanding of phage and host genetics and biology is essential to define phage requirements for infection and to determine how they co-evolve to counteract and adapt to the threat posed by the other (Mahony et al., 2012).

The nature and location of the phage receptors at the cell surface vary greatly depending on the phage and host. The receptors may be polysaccharides, surface proteins and other structures such as flagella, pili and capsules (Bertozzi Silva et al., 2016). The adsorption of phage particles to a bacterium leads to the activation of molecular mechanisms of infection in the virion (tail contraction, DNA ejection, etc.). The interaction between viral proteins and receptor structures on the bacterial cell surface is necessary for the conformational triggering of phage infection (Letarov and Kulikov, 2017). To prevent adsorption, bacteria can alter or disguise receptors through surface modification (Hampton et al., 2020). As such, phages lose the ability to effectively infect its host as the receptors become inaccessible or non-complementary to the phage receptor-binding protein (Bertozzi Silva et al., 2016).

Phage DNA entry can also be prevented by either mutating the bacterial components used during genome injection or through superinfection exclusion (Sie) systems. The latter are membrane proteins that block the entry of phage DNA into host cells, thereby conferring immunity against specific phages (Labrie et al., 2010). The genes encoding these membrane anchored proteins are often found in prophages (Labrie et al., 2010). They also inhibit subsequent infection of related phages with mechanisms that include interacting with the cytoplasmic membrane and blocking phage genome injection as well as interacting with the phage receptor on the bacterial outer membrane and blocking phage adsorption (Bondy-Denomy et al., 2016).

The ability to cleave phage DNA in a sequence-specific manner is shared by both restriction-modification (R-M) and clustered regularly interspaced short palindromic repeats (CRISPR)–CRISPR-associated protein (Cas) systems (Hampton et al., 2020). However, other defense systems also act during the DNA replication, including systems recently discovered, such as BacteRiophage Exclusion (BREX) (Goldfarb et al., 2015), and the Defense Islands System Associated with R-M (DISARM) (Ofir et al., 2018). Although the modes of action have yet to be elucidated, nine families of new anti-phage defense systems (i.e. Thoeris, Hachiman, Shedu, Gabija, Septu, Lamassu, Zorya, Kiwa and Druantia) were recently discovered by searching for enriched gene families within the so-called defense islands (Doron et al., 2018), which are clusters of defense genes associated to transposable mobile elements (Makarova et al., 2011). Additionally, bacteria carry “altruistic” defense systems, such as abortive infection (Abi) and toxin-antitoxin (TA) systems, that provide population resistance by sacrificing infected cells. Abi systems provide resistance through the abortion of phage infection targeting a crucial step of phage multiplication such as replication, transcription or translation, leading to the death of the infected cell (Labrie et al., 2010). In the TA systems, a toxic molecule is produced by the cell and neutralized by the antitoxin product, but when the balance between the two regulatory halves is altered, an available toxin can kill the bacterium (Labrie et al., 2010). Taken altogether, there is a clear diversity of phage resistance mechanisms (Hampton et al., 2020).

As phages face a wide range of antiviral mechanisms when infecting bacterial cells, they have evolved multiple tactics to avoid, circumvent or subvert these mechanisms (Labrie et al., 2010). For example, phage can produce their own antitoxin that acts by inactivating the host toxin (Samson et al., 2013). Additionally, phages have the ability to overcome CRISPR–Cas defenses through point mutations in the protospacer-adjacent motif (PAM) or protospacer, deletions or modifications of the DNA to prevent cleavage by Cas complexes and also by encoding anti-CRISPR proteins that can interfere with CRISPR immunity (Hampton et al., 2020). More recently, it was shown that some (jumbo) phages form a protein shell that protects viral DNA from DNA targeting defense mechanisms, such as R-M and CRISPR-Cas systems, while still susceptible to RNA targeting systems (Malone et al., 2019; Mendoza et al., 2019). Phages can also subvert other bacterial defense strategies, such as R-M systems by encoding, for example, their own methyltransferase or enzymes that are co-inject with the genome and mask the restriction sites

(Samson et al., 2013).

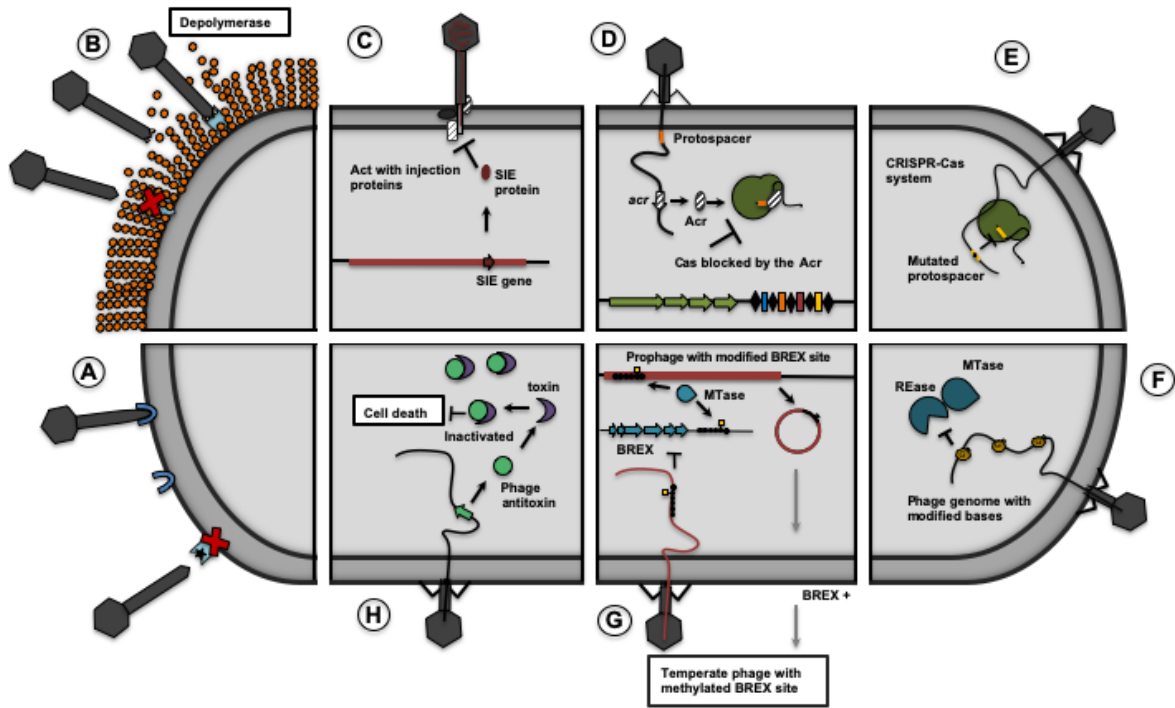


Figure 5. Examples of phage defense mechanisms and counter defenses.

Several other strategies used by phages to circumvent the anti-phage defense systems have been described (Hampton et al., 2020; Samson et al., 2013) and surely new ones will be discovered in the years to come as phage research gains more interest. A better understanding of phage–host interactions has already benefited applications that rely on phage-resistant bacteria to produce foods and biotechnological products (Samson et al., 2013). Additionally, as phage-resistant strains are required in different industries, the fundamental research into phage defense systems has supported the development of applications, such as gene editing and diagnostics (Hampton et al., 2020).

Phage as friends and enemies in food processing

Alessandra Gonçalves de Melo ¹, Sébastien Levesque ¹, and Sylvain Moineau ^{1,2*}

¹ Département de biochimie, de microbiologie, et de bio-informatique, Faculté des sciences et de génie, Groupe de recherche en écologie buccale, Faculté de médecine dentaire, Université Laval, Québec City, QC, G1V 0A6, Canada

² Félix d'Hérelle Reference Center for Bacterial Viruses, Université Laval, Québec City, QC, G1V 0A6, Canada

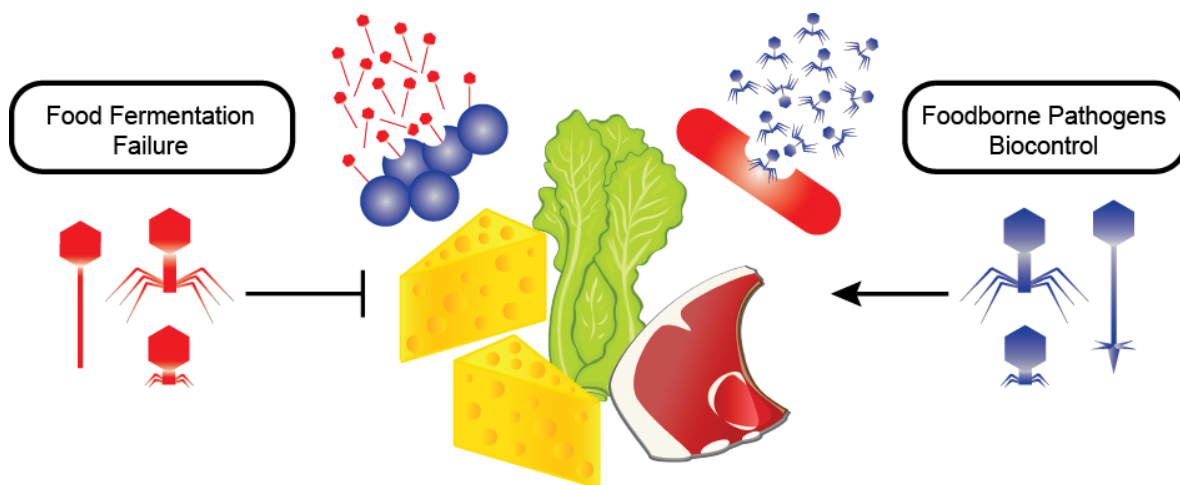


Figure 6. Graphical abstract for “Phages as friends and enemies in food processing”.

Résumé

Les phages peuvent infecter tous les genres bactériens expliquant ainsi leur grande abondance dans les écosystèmes. Bien que ces virus bactériens puissent représenter un risque pour les fermentations industrielles, ils peuvent également être des outils précieux pour contrôler les bactéries pathogènes d'origine alimentaire. Dans cette opinion, nous avons révisé ces deux aspects des phages. Comme les fermentations bactériennes sont constamment menacées par des attaques phagiques, nous discutons de la diversité des phages et des stratégies employées par l'industrie pour réduire leur impact négatif sur la transformation des aliments. De plus, nous explorons l'utilisation de phages afin de réduire les risques associés aux maladies bactériennes d'origine alimentaire.

Abstract

Phages can infect all bacterial genera on the planet leading to their abundance in ecosystems. While these bacterial viruses may represent a risk to industrial fermentations, they may also be valuable tools to control foodborne pathogens. Here we review these two sides of phage replication. As bacterial fermentations are constantly under threat of phage attacks, we will discuss phage diversity and the strategies employed by the industry to reduce their impact on food processing. Furthermore, we will explore the use of pathogen-infecting phages to reduce the risks associated with foodborne diseases over the steps of the food chain.

Abbreviations

Anti-CRISPR	Proteins that acts to inhibit CRISPR-Cas systems
ARGs	Antibiotic resistance genes
BIMs	Bacteriophage insensitive mutants
CaCO₃	Calcium carbonate
CRISPR-Cas	Clustered regularly interspaced short palindromic repeats and CRISPR-associated proteins
CRISPR-Cas9	Gene-editing tool using the nuclease Cas9
LAB	Lactic acid bacteria
MTP	Major capsid protein
<i>mtp</i>	Gene encoding for the major capsid protein
NPS	Neck passage structure
<i>tpeX</i>	Gene encoding a tail extension protein
TpeX	Tail protein extension
US FDA	United States Food and Drug Administration

Introduction

Bacteriophages or phages are recognized as the most abundant biological entities on our planet, outnumbering bacteria by an estimated ten-fold (Brüssow and Hendrix, 2002). They are ubiquitous and, as such, can be found in natural and man-made environments, especially those in which their bacterial host thrives (Chibani-chennoufi et al., 2004). Because many food fermentation processes rely on the metabolic richness of bacterial cells to transform products, they are constantly threatened by the prospect of phage contamination (Mc Grath et al., 2007). Sensitive host encounters with lytic phages can result in fermentation arrest or delay, leading to low-quality products and at worst, production loss (Emond and Moineau, 2007). Although phages are usually acknowledged as a menace, they can also be considered allies against pathogenic bacteria that represent a persistent food safety hazard. This review will highlight the character of phages as the enemies of food manufacturing, using dairy phages as examples. Furthermore, we will also focus on the role of phages as biocontrol agents in several steps of the food chain and the advances made for the application of phage cocktails to control bacterial pathogens.

Phages as a threat in food processing

Due to the nature of food fermentation processes, performed at large scale, under non-sterile conditions (Samson and Moineau, 2013) and often relying on the same bacterial cultures in successive batches (Emond and Moineau, 2007), it is not surprising that virulent phages can cause fermentation failures (Samson and Moineau, 2013). The food industry has adopted several antiphage strategies as countermeasures to prevent and diminish contamination. Example strategies include developing bacteriophage insensitive mutants (BIMs), establishing bacterial rotations as well as using chemical and physical treatments to decontaminate the factory and the substrates (Moineau and Lévesque, 2004; Samson and Moineau, 2013). The state of knowledge on phage-host interaction to prevent viral contamination in food processing (Mahony and van Sinderen, 2015) as well as standard phage control strategies have been extensively reviewed lately (Emond and Moineau, 2007; Moineau and Lévesque, 2004). Only very recent developments will be highlighted here.

Heat is a primary measure used to inactivate undesirable microorganisms found in raw milk

(Campagna et al., 2014). However, several dairy phages are thermal-stable, surviving for example pasteurization (Murphy et al., 2014). Moreover, whey proteins can provide an additional protective effect to phages (Geagea et al., 2017). Because thermal inactivation of phages would require higher temperatures and lead to protein denaturation, other alternatives, such as membrane filtration, are being investigated as a mean to reduce phage levels without changing protein structure (Samtlebe et al., 2017).

Several biocides have proven to be effective antivirals to clean industrial environs (Campagna et al., 2014; Hayes et al., 2017; Murphy et al., 2014). However, increasing resistance to chemical compounds has been observed, leading to phage persistence in manufacturing sites (Hayes et al., 2017). For example, some members of the highly prevalent *Lactococcus lactis* phage genus Sk1virus (formerly 936) are broadly tolerant to multiple classes of compounds found in commonly used sanitizers (Hayes et al., 2017). A similar conclusion was made in another study, in which the virulent lactococcal phages CB13 (isolated in Canada) and P1532 (isolated in Germany) were less sensitive to biocides than other phages (Campagna et al., 2014). These observations, and the phylogenetic separation between resistant and non-resistant phages, suggest that biocide resistance is due to the intrinsic robustness of the phage, rather than to the biocide's mechanism of action (Hayes et al., 2017). Therefore, rotation of sanitizers should be a recommended precautionary measure to avoid selection of increasingly resistant viruses (Campagna et al., 2014; Murphy et al., 2014).

Phage diversity

Dairy phages are by far the best-characterized food-related phages due to their global impact on milk fermentation processes. Carefully selected strains of lactic acid bacteria (LAB), e.g., *L. lactis*, *Lactobacillus* sp., *Leuconostoc* sp., and *Streptococcus thermophilus*, are repetitively added to milk to manufacture yogurt, fermented milks, and various cheeses on artisanal and industrial scales and, therefore, are ideal targets for virulent phages (Moineau and Lévesque, 2004). In recent years, several studies have focused on phage biodiversity, including genomic characterization of the most predominant phage groups as well as rarely isolated phage types (Mahony et al., 2017), new emerging groups (Casey et al., 2015; McDonnell et al., 2016), prophages in dairy strains (Eraclio et al., 2017) and also other LAB phages (Wagner et al., 2017).

The understanding of phage evolution and diversity at food processing sites can shed light on phage population dynamics to ensure more efficient strategies to control them (McDonnell et al., 2016). For instance, a novel emerging group of *S. thermophilus* phages, the 987 phages, was recently discovered (McDonnell et al., 2016) and compared to the three other known *S. thermophilus* phage groups (Mahony and van Sinderen, 2014). Interestingly, genomic relatedness of 987-type phages to the morphogenesis and replication modules from some lactococcal phages (P335 group) and *S. thermophilus* phages, respectively, suggests genetic exchanges that resulted in a new mosaic architecture and emerging phage group. Additionally, adsorption of the 987 phages to both *S. thermophilus* and *L. lactis* indicated that cell surface molecules might be shared between both bacterial species (McDonnell et al., 2016). The recent industrial practice of mixing *L. lactis* and *S. thermophilus* strains in a single starter culture may have led to the rise of this new phage group. Another example involves recent lactococcal phage isolates of the Sk1virus genus that are able to cross-infect various groups of *L. lactis* strains, thereby displaying a more dynamic host range than previously described for this group of phages (Murphy et al., 2013). Clearly, phage populations are dynamic in industrial environments and they need to be constantly monitored in order to adapt the antiviral strategies, particularly for bacterial strain rotation.

A comparative genomic analysis of ninety siphophages has established the core genome and variable elements of the Sk1virus genus (Murphy et al., 2016). Interestingly, a probable hotspot for gene rearrangements was identified surrounding the major tail protein-encoding gene (*mtp*), including the presence or absence of a gene encoding the neck passage structure (NPS) and/or a gene encoding a tail protein extension (*tpeX*). For the latter phenotype, MTP-TpeX was arranged as a spiral structure on the phage tail (Murphy et al., 2016). Both structures were also observed on phage persisting over several years in whey powders, suggesting that they might be beneficial for phage structural stability in harsh conditions (Wagner et al., 2017).

The arms race of phage and bacteria

Whenever they encounter each other, bacteria and phages are continuously outcompeting in an antagonistic co-evolution process. In this arms race, bacterial derivatives acquire resistance to phages using several strategies (frequently through receptor mutations), whereas phages counter-attack to overcome antiviral barriers in order to infect and propagate (Labrie et al., 2010). Bacteria

can also harbor phage-resistance mechanisms, such as restriction modification systems, abortive infections, CRISPR-Cas systems and others. These mechanisms have been extensively reviewed elsewhere as well as the strategies used by phages to respond to these challenges (see (Labrie et al., 2010; Samson et al., 2013)). Of particular interest in the past decade, the CRISPR-Cas system allows the “immunization” of bacterial strains against several phages. While this can be observed by challenging bacteria with virulent phages, the system can also be “programmed” via a plasmid to protect bacteria against multiple phages in a single assay (Hynes et al., 2016). This programming was described for *S. thermophilus*, using a high copy plasmid with highly conserved protospacers and specific protospacer adjacent motifs targeting the greatest number of virulent phages (Hynes et al., 2016). This strategy was very efficient at conferring resistance to multiple phages at once and offers the possibility of rapidly developing specific BIMs in strains carrying active CRISPR-Cas systems.

This natural coevolution can sometimes be directly observed when analyzing mixed starter cultures (Spus et al., 2015). Food fermentations can be performed using a limited number of defined bacterial strains as indicated above but also with mixed starter cultures. The latter are composed of undefined numbers and ratios of bacterial strains that will drive the fermentation process. These mixed cultures will also coexist with diverse phages leading to a complex dynamic of phage-host interactions. It is usually not recommended to use both defined and mixed cultures in the same industrial environment.

Beneficial applications of bacteriophages in the food industry

Phages are also prospective antimicrobial alternatives to prevent contamination by bacterial pathogens at different stages of the commercial food chain. Diseases caused by foodborne bacteria affect millions of people annually on a global scale (Amarillas et al., 2016; Schmelcher and Loessner, 2016). While the intensive use of antibiotics led to the emergence of resistant bacteria and increased the likelihood of untreatable infections (Amarillas et al., 2016; Colom et al., 2017), phages are highly specific in their bacterial targets and will only replicate if available hosts are in their surroundings (auto-dosing) (Yen et al., 2017). Consequently, phages are also being investigated for treatment of several bacterial infections (Abedon et al., 2017).

Table 1. Examples of commercially available bacteriophage products.

Manufacturer	Products	Target bacterial species	References
Intralix Ltd	ListShield® EcoShield® SalmFresh® ShigaShield®	<i>Listeria monocytogenes</i> <i>E. coli</i> O157:H7 <i>Salmonella</i> spp. <i>Shigella</i> spp.	www.intralix.com
Elanco	Finalyse®	<i>E. coli</i> O157:H7	www.elanco.us
Micreos Food Safety	PhageGuard Lystex (Lystex P100™) PhageGuard S (Salmonex™)	<i>Listeria monocytogenes</i> <i>Salmonella</i> spp.	www.micreos.com and www.phageguard.com
Omnilytics Ltd	Agriphage	<i>Xanthomonas campestris</i> <i>Pseudomonas syringae</i>	www.omnilytics.com
Brimrose Technology Corporation	Enko-phage SES-bacteriophage Pyo-bacteriophage Intesti-bacteriophage	<i>Salmonella</i> spp. <i>Shigella</i> spp. Enteropathogenic <i>E. coli</i> <i>Staphylococcus</i> spp. <i>Staphylococcus</i> spp. <i>Streptococcus</i> spp. Enteropathogenic <i>E. coli</i> <i>Staphylococcus</i> spp. <i>Streptococcus</i> spp. <i>Pseudomonas aeruginosa</i> <i>Proteus</i> spp. <i>E. coli</i> <i>Shigella</i> spp. <i>Salmonella</i> spp. <i>E. coli</i> <i>Staphylococcus</i> spp. <i>Enterococcus</i> spp. <i>Proteus</i> spp. <i>P. aeruginosa</i>	www.brimrosetechnology.com/ biotech/bacteriophages
APS biocontrol Ltd	Biolyse®	Soft rot <i>Enterobacteriaceae</i>	www.apsbiocontrol.com

Since the approval of a phage cocktail (several virulent phages) as food preservative in 2006 (ListShield™) by the US FDA, an increasing number of phage products are commercially available for pathogen control, as shown in Table 1 (Lee et al., 2016). From agricultural production to packaging, the application of phage cocktails is possible at various time points within food processes. The use of a cocktail of phages is often highly recommended, as opposed to the use of single phage, to limit the rapid emergence of phage resistant strains.

Pathogenic infection of crops, fishes and farm animals

The prospective use of phages as biocontrol agents for crops, fishes, and farm animals could reduce the economic burden caused by bacterial diseases (Abedon et al., 2017; Vincent et al., 2017). Some phage cocktails have been used successfully to prevent bacterial infections in plant and animal models (Buttimer et al., 2017; Cooper, 2016; Yen et al., 2017). However, they must have a broad host range and overcome a wide variety of adverse environmental conditions to be used as biocontrol agents. For example, phage encapsulation with milk proteins was tested as an interesting strategy to overcome acidic conditions, protecting phages at pH 2.0 for 2 hours (Samtlebe et al., 2016). Moreover, alginate/CaCO₃ capsules containing a cocktail of three phages were also shown to have greater and longer lasting efficacy than the corresponding non-encapsulated phage cocktail against *Salmonella* in broiler chickens (Amarillas et al., 2016).

Food processing and packaging

Numerous recent studies have investigated the performance of phage cocktails on *Listeria monocytogenes* (Cooper, 2016), *E. coli* (Gundogdu et al., 2016), *Salmonella* spp. (Yeh et al., 2017), *Shigella sonnei* (Soffer et al., 2017), *Staphylococcus aureus* (El Haddad et al., 2016), etc. Significant bacterial reductions were observed on artificially contaminated food products treated with commercial phage cocktails (Buttimer et al., 2017; Cooper, 2016; Samtlebe et al., 2016). Interestingly, *Listeria* phages remained stable on dry-cured ham for 14 days and were even able to eliminate *L. monocytogenes* biofilms on machinery surfaces (Cooper, 2016). Since biofilms are frequently associated with bacterial contamination in the food industry as they provide a reservoir for foodborne pathogens, these results are very encouraging (Gutiérrez et al., 2016; Pires et al., 2016). The use of phage endolysins and depolymerases to reduce the population of pathogens and biofilms has also been investigated and reviewed (Pires et al., 2016; Schmelcher and Loessner, 2016). Although they provide a wide range of applications, the addition of these enzymes to food products would likely be too expensive when compared to phages. The use of phages expressing these enzymes is perhaps more affordable. Bioactive packaging materials, using phage immobilized on solid supports or sprayed, is another appealing technology to extend food safety and shelf life (Lone et al., 2016). The use of acetate cellulose film and absorbent food pads containing phages has recently shown activity against *Salmonella* (Gouvêa et al., 2016, 2015).

Problems and risks associated with phage biocontrol

As a result of the arms race between phages and their hosts, pathogenic bacteria could also develop natural resistance when exposed to virulent phages (Labrie et al., 2010). However, antiphage barriers generate a selective pressure that forces the phage population to evolve and select for phages that will evade bacterial defense mechanisms. A relevant example is the recent discovery of four unique type II-A CRISPR-Cas9 inhibitor proteins in *L. monocytogenes* prophages (Rauch et al., 2017). The occurrence of anti-CRISPR proteins seems widespread in *Listeria*, with at least one prophage-encoded inhibitor in more than half of CRISPR-Cas9-containing *L. monocytogenes* strains (Gutiérrez et al., 2016). Although observed in prophages, anti-CRISPR proteins could potentially be widespread in virulent phages. Hence, the isolation of new phages that can overcome the CRISPR-Cas system would benefit pathogen biocontrol.

It is also important to mention that the use of biological agents raises certain safety issues. As vectors for horizontal gene transfer, some specialized phages may transfer virulence and antibiotic resistance genes (ARGs) among bacteria (Cui et al., 2017). A recent metagenomics analysis of hospital wastewater revealed that particular phages are reservoirs of ARGs (Subirats et al., 2016). Moreover, phages were shown to enable *Staphylococcus aureus* to acquire antibiotic resistance by a process described as “auto-transduction” (Haaber et al., 2016). In this process, phage-sensitive *S. aureus* strains are killed by the release of phages particles from a neighboring lysogenic subpopulation. The prophage-containing subpopulation, which is immune to the phage, can acquire ARGs that are occasionally captured in viral transducing particles, enabling the bacteria to proliferate under strong antibiotic pressure (Haaber et al., 2016). For this reason, it is crucial to use strictly lytic phages as biocontrol agents. Additionally, the genome of prospective biocontrol phages must be completely devoid of genes coding for virulence factors and antibiotic resistance, as well as for proteins that could cause allergenicity. A general process of phage cocktail development observing these safety issues is illustrated in Figure 7.

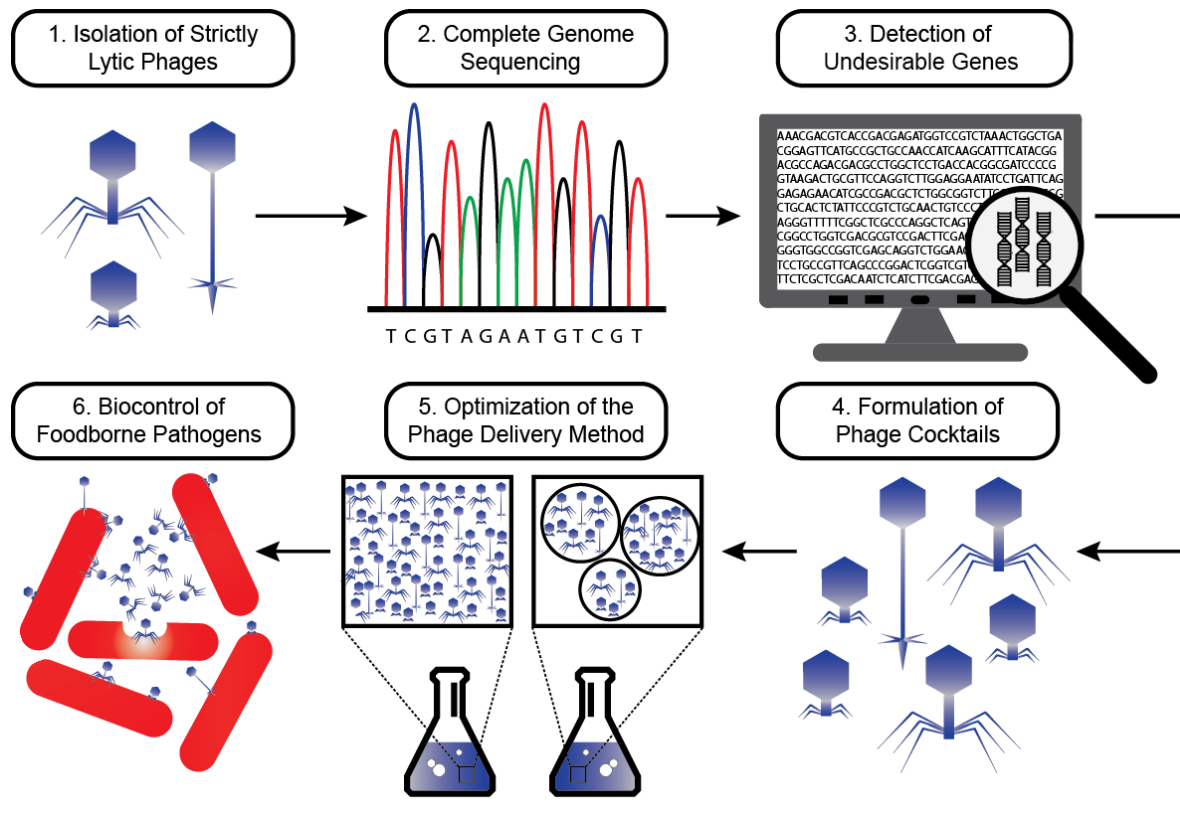


Figure 7. Development of phage cocktails for the biocontrol of pathogens in food processing. Polyvalent virulent phages can be isolated and used to target a specific bacterial species. The genome of the isolated phage must be sequenced and analyzed to ensure undesirable traits, such as a lysogeny module, antibiotic resistance genes and virulence factors are not present. Phage cocktails are then formulated and the phage delivery method is optimized according to the desired application. For example, phages can be immobilized on a solid support for food packaging or microencapsulated for direct administration to farm animals. After optimization, phage cocktails can be used at different stages of the food chain to prevent contamination by pathogens.

Conclusion

Phages are versatile entities. Because their populations are continuously evolving, the food industry faces intermittent challenges to control phage contamination. The favorable conditions for proliferation found in the food industry makes phage research, control and monitoring, a central approach to staying ahead. Phage research, for example, led to the discovery of CRISPR-Cas as a prokaryote immune system. This information directed the use of this strategy to “vaccinate” CRISPR-containing industrial bacteria against common phage groups. On the other hand, distinct phages can be employed as alternatives to antimicrobials in the control of pathogenic bacteria. Challenges such as the antiphage hurdles, potential vectors for genetic exchange and the constant need to include new phages in the cocktails, must be overcome to help phages become an efficient antimicrobial strategy in food processing. Phages are dynamic and can naturally evolve readily to overcome barriers posed by bacterial defense mechanisms. As phage biology advances, new groups of pathogen-infecting phages will likely be discovered and applied in phage cocktails to improve the fight against foodborne pathogens. The recent advent of phage genome editing tools also offers a plethora of possibilities to improve phage efficacy (Lemay et al., 2017). Finally, if one day pathogen-targeting phages find widespread use in foods and farms, it will be of utmost importance to not overuse them as it was exemplified with antibiotics.

Conflicts of interest

The authors declare that they have no conflicts of interest associated with this manuscript.

Acknowledgements

We thank Barb Conway for editorial assistance. AGM has a scholarship from the National Council for Scientific and Technological Development (CNPq-Brazil) in partnership with CALDO (Canada). S.M. acknowledges funding from NSERC (CRD program) and Agropur. SM holds a Tier 1 Canada Research Chair in Bacteriophages.

References

- Abedon, S.T., García, P., Mullany, P., Aminov, R., 2017. Editorial: Phage therapy: past, present and future. *Front. Microbiol.* 8, 981.
- Amarillas, L., Chaidez, C., González-Robles, A., León-Félix, J., 2016. Complete genome sequence of new bacteriophage phiE142, which causes simultaneously lysis of multidrug-resistant *Escherichia coli* O157:H7 and *Salmonella enterica*. *Stand. Genomic Sci.* 11, 89.
- Brüssow, H., Hendrix, R.W., 2002. Phage Genomics: Small is beautiful. *Cell* 108, 13–16.
- Buttimer, C., Mcauliffe, O., Ross, R.P., Hill, C., Mahony, J.O., Coffey, A., Abedon, S.T., Chan, B.K., 2017. Bacteriophages and bacterial plant diseases. *Front. Microbiol.* 8, 34.
- Campagna, C., Villion, M., Labrie, S.J., Duchaine, C., Moineau, S., 2014. Inactivation of dairy bacteriophages by commercial sanitizers and disinfectants. *Int. J. Food Microbiol.* 171, 41–47.
- Casey, E., Mahony, J., Neve, H., Noben, J.P., Bello, F.D., van Sinderen, D., 2015. Novel phage group infecting *Lactobacillus delbrueckii* subsp. *lactis*, as revealed by genomic and proteomic analysis of bacteriophage Ldl1. *Appl. Environ. Microbiol.* 81, 1319–1326.
- Chibani-chennoufi, S., Bruttin, A., Brüssow, H., Dillmann, M., Bru, H., 2004. Phage-host interaction: an ecological perspective. *J. Bacteriol.* 186, 3677–3686.
- Colom, J., Cano-Sarabia, M., Otero, J., Ariñez-Soriano, J., Cortés, P., MasPOCH, D., Llagostera, M., 2017. Microencapsulation with alginate/CaCO₃: a strategy for improved phage therapy. *Sci. Rep.* 7, 41441.
- Cooper, I.R., 2016. A review of current methods using bacteriophages in live animals, food and animal products intended for human consumption. *J. Microbiol. Methods* 130, 38–47.
- Cui, Z., Guo, X., Dong, K., Zhang, Y., Li, Q., Zhu, Y., Zeng, L., Tang, R., Li, L., 2017. Safety assessment of *Staphylococcus* phages of the family *Myoviridae* based on complete genome sequences. *Sci. Rep.* 7, 41259.
- El Haddad, L., Roy, J.P., Khalil, G.E., St-Gelais, D., Champagne, C.P., Labrie, S., Moineau, S., 2016. Efficacy of two *Staphylococcus aureus* phage cocktails in cheese production. *Int. J. Food Microbiol.* 217, 7–13.
- Emond, E., Moineau, S., 2007. Bacteriophage and Food Fermentations. In: Mcgrath, S., Van Sinderen, D. (Eds.), *Bacteriophage: Genetics and Molecular Biology*. Horizon Scientific Press/Caister Academic Press, Norfolk, UK, pp. 93–124.
- Eraclio, G., Fortina, M.G., Labrie, S.J., Tremblay, D.M., Moineau, S., 2017. Characterization of prophages of *Lactococcus garvieae*. *Sci. Rep.* 7, 1856.
- Geagea, H., Gomaa, A., Remondetto, G., Moineau, S., Subirade, M., 2017. Molecular structure of lactoferrin influences the thermal resistance of lactococcal phages. *J. Agric. Food Chem.* 65, 2214–2221.
- Gouvêa, D.M., Mendonça, R.C.S., Lopez, M.E.S., Batalha, L.S., 2016. Absorbent food pads containing bacteriophages for potential antimicrobial use in refrigerated food products. *LWT - Food Sci. Technol.* 67, 159–166.
- Gouvêa, D.M., Mendonça, R.C.S., Soto, M.L., Cruz, R.S., 2015. Acetate cellulose film with bacteriophages for potential antimicrobial use in food packaging. *LWT - Food Sci. Technol.* 63, 85–91.
- Gundogdu, A., Bolkvadze, D., Kilic, H., 2016. *In vitro* effectiveness of commercial bacteriophage cocktails on diverse extended-spectrum beta-lactamase producing *Escherichia coli* strains. *Front. Microbiol.* 7, 1761.

- Gutiérrez, D., Rodríguez-Rubio, L., Martínez, B., Rodríguez, A., García, P., 2016. Bacteriophages as weapons against bacterial biofilms in the food industry. *Front. Microbiol.* 7, 825.
- Haaber, J., Leisner, J.J., Cohn, M.T., Catalan-Moreno, A., Nielsen, J.B., Westh, H., Penadés, J.R., Ingmer, H., 2016. Bacterial viruses enable their host to acquire antibiotic resistance genes from neighbouring cells. *Nat. Commun.* 7, 13333.
- Hayes, S., Murphy, J., Mahony, J., Lugli, G.A., Ventura, M., Noben, J.-P., Franz, C.M.A.P., Neve, H., Nauta, A., Van Sinderen, D., 2017. Biocidal inactivation of *Lactococcus lactis* bacteriophages: efficacy and targets of commonly used sanitizers. *Front. Microbiol.* 8, 107.
- Hynes, A., Labrie, S.J., Moineau, S., 2016. Programming native CRISPR arrays for the Generation of targeted immunity. *MBio* 7, e00202-16.
- Hynes, A.P., Lemay, M.-L., Moineau, S., 2016. Applications of CRISPR-Cas in its natural habitat. *Curr. Opin. Chem. Biol.* 34, 30–36.
- Labrie, S.J., Samson, J.E., Moineau, S., 2010. Bacteriophage resistance mechanisms. *Nat. Rev. Microbiol.* 8, 317–327.
- Lee, H., Ku, H.-J., Lee, D.-H., Kim, Y.-T., Shin, H., Ryu, S., Lee, J.-H., 2016. Characterization and genomic study of the novel bacteriophage HY01 infecting both *Escherichia coli* O157:H7 and *Shigella flexneri*: potential as a biocontrol agent in food. *PLoS One* 11, e0168985.
- Lemay, M.L., Horvath, P., Moineau, S., 2017. The CRISPR-Cas app goes viral. *Curr. Opin. Microbiol.* 37, 103-109.
- Lone, A., Anany, H., Hakeem, M., Aguis, L., Avdjian, A.C., Bouget, M., Atashi, A., Brovko, L., Rochefort, D., Griffiths, M.W., 2016. Development of prototypes of bioactive packaging materials based on immobilized bacteriophages for control of growth of bacterial pathogens in foods. *Int. J. Food Microbiol.* 217, 49–58.
- Mahony, J., Moscarelli, A., Kelleher, P., Lugli, G., Ventura, M., Settanni, L., van Sinderen, D., 2017. Phage biodiversity in artisanal cheese wheys reflects the complexity of the fermentation process. *Viruses* 9, 45.
- Mahony, J., van Sinderen, D., 2014. Current taxonomy of phages infecting lactic acid bacteria. *Front. Microbiol.* 5, 7.
- Mahony, J., van Sinderen, D., 2015. Novel strategies to prevent or exploit phages in fermentations, insights from phage-host interactions. *Curr. Opin. Biotechnol.* 32, 8–13.
- Mc Grath, S., Fitzgerald, G.F., van Sinderen, D., 2007. Bacteriophages in dairy products: pros and cons. *Biotechnol. J.* 2, 450–455.
- McDonnell, B., Mahony, J., Neve, H., Hanemaaijer, L., Noben, J.P., Kouwen, T., van Sinderen, D., 2016. Identification and analysis of a novel group of bacteriophages infecting the lactic acid bacterium *Streptococcus thermophilus*. *Appl. Environ. Microbiol.* 82, 5153–5165.
- Moineau, S., Lévesque, C., 2004. Control of bacteriophages in industrial fermentations. In: Kutter, E., Sulakvelidze, A. (Eds.), *Bacteriophages*. CRC Press, Boca Raton, FL, United States of America, pp. 285–296.
- Murphy, J., Bottacini, F., Mahony, J., Kelleher, P., Neve, H., Zomer, A., Nauta, A., van Sinderen, D., 2016. Comparative genomics and functional analysis of the 936 group of lactococcal *Siphoviridae* phages. *Sci. Rep.* 6, 21345.
- Murphy, J., Mahony, J., Bonestroo, M., Nauta, A., Van Sinderen, D., 2014. Impact of thermal and biocidal treatments on lactococcal 936-type phages. *Int. Dairy J.* 34, 56–61.
- Murphy, J., Royer, B., Mahony, J., Hoyles, L., Heller, K., Neve, H., Bonestroo, M., Nauta, A., van Sinderen, D., 2013. Biodiversity of lactococcal bacteriophages isolated from 3 Gouda-type cheese-producing plants. *J. Dairy Sci.* 96, 4945–4957.

- Pires, D.P., Oliveira, H., Melo, L.D.R., Sillankorva, S., Azeredo, J., 2016. Bacteriophage-encoded depolymerases: their diversity and biotechnological applications. *Appl. Microbiol. Biotechnol.* 100, 2141–2151.
- Rauch, B.J., Silvis, M.R., Hultquist, J.F., Waters, C.S., McGregor, M.J., Krogan, N.J., Bondy-Denomy, J., 2017. Inhibition of CRISPR-Cas9 with bacteriophage proteins. *Cell* 168, 150–158.e10.
- Samson, J.E., Magadán, A.H., Sabri, M., Moineau, S., 2013. Revenge of the phages: defeating bacterial defences. *Nat. Rev. Microbiol.* 11, 675–687.
- Samson, J.E., Moineau, S., 2013. Bacteriophages in food fermentations: new frontiers in a continuous arms race. *Annu Rev Food Sci Technol* 4, 347–368.
- Samtlebe, M., Ergin, F., Wagner, N., Neve, H., Küçükçetin, A., Franz, C.M. a P., Heller, K.J., Hinrichs, J., Atamer, Z., 2016. Carrier systems for bacteriophages to supplement food systems: encapsulation and controlled release to modulate the human gut microbiota. *LWT - Food Sci. Technol.* 68, 334–340.
- Samtlebe, M., Wagner, N., Brinks, E., Neve, H., Heller, K.J., Hinrichs, J., Atamer, Z., 2017. Production of phage free cheese whey: design of a tubular laboratory membrane filtration system and assessment of a feasibility study. *Int. Dairy J.* 71, 17–23.
- Schmelcher, M., Loessner, M.J., 2016. Bacteriophage endolysins: applications for food safety. *Curr. Opin. Biotechnol.* 37, 76–87.
- Soffer, N., Woolston, J., Li, M., Das, C., Sulakvelidze, A., 2017. Bacteriophage preparation lytic for *Shigella* significantly reduces *Shigella sonnei* contamination in various foods. *PLoS One* 12, e0175256.
- Spus, M., Li, M., Alexeeva, S., Wolkers-Rooijackers, J.C.M., Zwietering, M.H., Abee, T., Smid, E.J.J., Smid, E.J.J., Valenberg, H.J.F. van, Smid, E.J.J., 2015. Strain diversity and phage resistance in complex dairy starter cultures. *J. Dairy Sci.* 98, 5173–5182.
- Subirats, J., Sánchez-Melsió, A., Borrego, C.M., Balcázar, J.L., Simonet, P., 2016. Metagenomic analysis reveals that bacteriophages are reservoirs of antibiotic resistance genes. *Int. J. Antimicrob. Agents* 48, 163–167.
- Vincent, A., Paquet, V.E., Bernatchez, A., Tremblay, D.M., Moineau, S., Charette, S.J., 2017. Characterization and diversity of phages infecting *Aeromonas salmonicida* subsp. *salmonicida*. *Sci. Rep.* 7, 7054.
- Wagner, N., Brinks, E., Samtlebe, M., Hinrichs, J., Atamer, Z., Kot, W., Franz, C.M.A.P., Neve, H., Heller, K.J., 2017. Whey powders are a rich source and excellent storage matrix for dairy bacteriophages. *Int. J. Food Microbiol.* 241, 308–317.
- Yeh, Y., Purushothaman, P., Gupta, N., Ragnone, M., Verma, S.C., De Mello, a S., 2017. Bacteriophage application on red meats and poultry: effects on *Salmonella* population in final ground products. *Meat Sci.* 127, 30–34.
- Yen, M., Cairns, L.S., Camilli, A., 2017. A cocktail of three virulent bacteriophages prevents *Vibrio cholerae* infection in animal models. *Nat. Commun.* 8, 14187.

Problematic, hypothesis and objectives of the study

Phages are especially prevalent in environments where bacteria are abundant. As bacterial strains are used daily for milk fermentation, the dairy industry is an environment particularly susceptible to phage proliferation. Beside the abundance of hosts, dairy facilities also have multiple phage entry points, such as raw milk, workers, equipment, and also the presence of prophages in the genome of industrial strains. Despite adopting phage control measures, the presence of sensitive host can potentially lead to phage outbreaks, which can delay or interrupt fermentation processes, leading to low-quality products. Phage outbreaks usually require the implementation of costly measures to stop phage spread and guarantee the quality of the fermented products.

Although a large part of our knowledge on phage-infecting dairy strains comes from studies on lactic acid bacteria, phages can also infect other key players during cheese production, such as the ripening strains. However, the complex nature of cheese rind ecosystem makes the replacement or rotation of ripening strains rather difficult. Once a ripening strain has been established in the manufacturing process of fine cheeses, changing the strain is considered a last resort, as it can alter the organoleptic attributes of the cheese, and the consumer acceptability of the final product. Yet, keeping a phage-sensitive strain in production can lead to the persistence of specific phages in the manufacturing facilities.

The main hypothesis of this thesis was that virulent phages infecting *Brevibacterium aurantiacum* strains can be isolated in specialty cheese manufacturing facilities and they can have a negative impact on cheese quality. Therefore, the study of *B. aurantiacum* phage genomics, diversity and biology is necessary to understand the dynamic of phage-host interactions and to control the proliferation of these phages in cheese industries. Additionally, the selection of phage-resistant strains of *B. aurantiacum* is essential to keep the quality of washed rind cheeses. To the best of my knowledge, this is the first thesis on phages infecting *B. aurantiacum*.

The first objective of the thesis was to study the genomics of the phage-sensitive strain, *B. aurantiacum* SMQ-1335, which was used as the host for the phages throughout my studies. The following objective led to the analysis of the first virulent phages infecting a *B. aurantiacum* strain

as well as the study of their diversity and evolution. The third objective was to study the phage-host interactions, specifically in the characterization of bacteriophage-insensitive mutants of *B. aurantiacum* SMQ-1335 and the mechanisms involved in the phage insensitivity. The fourth objective aimed to evaluate the impact of phages in the development of the rind of surface-ripened cheese. Model cheese curds were used to follow the color development of the rind as well as the phage titers and cell counts on this cheese. Finally, a collaborative work on the comparative genomics of *Brevibacterium* spp. strains that led to the reclassification of the strain SMQ-1335 (formerly classified as *Brevibacterium linens*) as *B. aurantiacum* has been included as an annex.

Chapter 1 – Article 1

Complete genome sequence of *Brevibacterium linens* SMQ-1335

Alessandra G. de Melo ^{1,2}, Simon J. Labrie ^{1,2}, Jeannot Dumaresq ³, Richard J. Roberts ⁴, Denise M. Tremblay ^{1,2,5}, and Sylvain Moineau ^{1,2,5*}

¹ Département de biochimie, de microbiologie et de bio-informatique, Faculté des sciences et de génie, 1045, avenue de la Médecine, Québec, QC, Canada.

² Groupe de Recherche en Écologie Buccale, Faculté de médecine dentaire, 2420 rue de la Terrasse, Université Laval, Québec, QC, Canada.

³ Département de Microbiologie et d'Infectiologie, Centre Hospitalier Affilié Universitaire Hôtel-Dieu de Lévis, Lévis, QC, Canada.

⁴ New England Biolabs, 240 County Road, Ipswich, MA, USA.

⁵ Félix d'Hérelle Reference Center for Bacterial Viruses, Faculté de médecine dentaire, 2420 rue de la Terrasse, Université Laval, Québec, QC, Canada.

Genome Announc. 2016. 4:e01242-16. doi: 10.1128/genomeA.01242-16.

Résumé

Brevibacterium linens est l'une des principales bactéries présente sur la croûte des fromages affinés en surface. Le génome de la souche industrielle SMQ-1335 a été séquencé en utilisant la technologie PacBio. Il comporte 4 209 935 pb, présente une teneur en G + C de 62,6%, 3 848 cadres de lecture ouverts et 61 ARN structuraux. Un nouveau système de restriction-modification de type I a été identifié.

Abstract

Brevibacterium linens is one of the main bacteria found in the smear of surface-ripened cheeses. The genome of the industrial strain SMQ-1335 was sequenced using PacBio. It has 4,209,935 bp, a 62.6% G+C content, 3,848 open reading frames, and 61 structural RNAs. A new Type I restriction-modification system was identified.

Abbreviations

BLASR	Basic local alignment with successive refinement
BLASTp	Basic local alignment search tool for proteins
bp	Base pair
DBETH	Database of bacterial exotoxins for human
DNA	Deoxyribonucleic acid
G+C	Bases guanine and cytosine
HGAP	Hierarchical genome assembly process – a tool for de novo genome assembly using PacBio reads
PHASTER	Phage search tool enhanced release – to search for prophages
RAST	Rapid annotation using subsystem technology
RM system	Restriction-modification system
RNA	Ribonucleic acid
rRNA	Ribosomal RNA
TMP-SMX	Trimethoprim-sulfamethoxazole
tRNA	Transfer RNA

Brevibacterium linens is a Gram-positive bacterium found on the surface of a variety of washed rind cheeses produced globally (Breed et al., 1957; Motta and Brandelli, 2008; Rattray and Fox, 1999). This non-spore forming, halotolerant, strictly aerobic chemoorganotroph undergoes a rod-cocci cycle during growth and possesses mesodiaminopimelic acid in its cell wall (Motta and Brandelli, 2008; Onraedt et al., 2005; Rattray and Fox, 1999). *B. linens* plays key roles during cheese ripening in the breakdown of lipids and proteins (Rattray and Fox, 1999), the production of volatile sulfur compounds (Arfi et al., 2006; Bonnarme et al., 2000), and the development of color due to carotenoid pigment production (Kim et al., 2010; Motta and Brandelli, 2008; Onraedt et al., 2005; Rattray and Fox, 1999). Furthermore, the production and accumulation of compatible solutes allows *B. linens* to grow in hyperosmotic environments (Onraedt et al., 2005). The genomes of three *B. linens* strains are currently available, of which one is complete (GCA_001606005.1) and two are scaffold and draft sequences, respectively (GCA_000167575.1 and GCA_000807915.1).

The genome of *B. linens* SMQ-1335 was sequenced using one SMRT cell in a PacBio RSII Sequencer (Génome Québec Innovation Centre, Montréal), which generated 76,075 raw subreads of an average length of 9,010 bp that provided an average coverage of 162-fold. The genome was assembled into one contig using HGAP (Chin et al., 2013). BLASR (Chaisson and Tesler, 2012) was used to align and preassemble the sequences using the longest reads as seeds to which all the other subreads were recruited and mapped to correct random errors. The Celera assembler (Myers et al., 2000) was then used to *de novo* assemble these long and corrected reads into contigs. The sequences were refined using Quiver, wherein the raw reads were aligned on the contigs to generate a consensus sequence containing the complete genome. The single contig had redundant ends of 16,018 bp that were removed from one end for the final assembly. The origin of the genome was set upstream of the gene coding for the replication initiator protein DnaA. Gene prediction and annotation was performed using RAST (Overbeek et al., 2014) and BLASTp (Altschul et al., 1997). The *B. linens* SMQ-1335 genome has a high G+C content (62.6%) and is composed of 4,209,935 bp, 3,848 genes, and 61 structural RNAs (49 tRNAs and 12 rRNAs).

In vitro tests revealed that *B. linens* SMQ-1335 is sensitive to vancomycin, daptomycin, gentamicin, tetracycline, and rifampin. However, this strain was insensitive to β -lactam antibiotics (penicillin and ceftriaxone), trimethoprim-sulfamethoxazole (TMP-SMX), and a second-

generation fluoroquinolone (ciprofloxacin). A gene likely coding for the lantibiotic, linocin, was identified using BAGEL3 (van Heel et al., 2013).

No genes coding for known toxins were found in the genome of SMQ-1335 using Virulence Finder (Joensen et al., 2014), Virulence Factor Database (Chen et al., 2012), and DBETH (Chakraborty et al., 2012). RAST and PHASTER (Arndt et al., 2016) identified a putative prophage (31,300 bp). Analysis of this prophage sequence revealed many transposases and integrases, suggesting that this may be a non-functional prophage.

The methylome (Roberts et al., 2013) of *B. linens* SMQ-1335 was analyzed to identify DNA methyltransferases and restriction endonucleases (Roberts et al., 2015) as well as specificity subunits (Murray et al., 2012). A new methyltransferase M.Bli1335I, a restriction endonuclease Bli1335IP, and a new Type I RM system were assigned, with the recognition site sequence: CGGANNNNNNTTC. The SMQ-1335 genome may contain additional RM systems (Type II, III, and IV). For the Type II, a new restriction endonuclease (Bli1335II) was also assigned with DTGAAT as the recognition sequence.

Nucleotide sequence accession number

The complete genome sequence of *B. linens* SMQ-1335 is available in GenBank under the accession number CP017150.

Funding Information

We thank Génome Québec Innovation Centre for performing PacBio sequencing and preliminary genome assembly. We acknowledge funding from the Natural Sciences and Engineering Research Council of Canada. AGM is the recipient of a graduate fellowship from National Council for Scientific and Technological Development (CNPq-Brazil)/CALDO-Canada). RJR is a full-time employee of New England Biolabs, a company that sells research reagents such as DNA MTases. SM holds a Tier 1 Canada Research Chair in Bacteriophages.

References

- Altschul, S.F., Madden, T.L., Schäffer, A.A., Zhang, J., Zhang, Z., Miller, W., Lipman, D.J., 1997. Gapped BLAST and PSI-BLAST: a new generation of protein database search programs. *Nucleic Acids Res.* 25, 3389–3402.
- Arfi, K., Landaud, S., Bonnarme, P., 2006. Evidence for distinct L-methionine catabolic pathways in the yeast *Geotrichum candidum* and the bacterium *Brevibacterium linens*. *Appl. Environ. Microbiol.* 72, 2155–2162.
- Arndt, D., Grant, J.R., Marcu, A., Sajed, T., Pon, A., Liang, Y., Wishart, D.S., 2016. PHASTER: a better, faster version of the PHAST phage search tool. *Nucleic Acids Res.* 44, W16–W21.
- Bonnarme, P., Psoni, L., Spinnler, H.E., 2000. Diversity of L-methionine catabolism pathways in cheese-ripening bacteria. *Appl. Environ. Microbiol.* 66, 5514–5517.
- Breed, R.S., Murray, E.G.D., Smith, N.R., 1957. *Bergey's manual of systematic bacteriology*, Igarss 2014.
- Chaisson, M.J., Tesler, G., 2012. Mapping single molecule sequencing reads using basic local alignment with successive refinement (BLASR): application and theory. *BMC Bioinformatics* 13, 238.
- Chakraborty, A., Ghosh, S., Chowdhary, G., Maulik, U., Chakrabarti, S., 2012. DBETH: a database of bacterial exotoxins for human. *Nucleic Acids Res.* 40, D615-620.
- Chen, L., Xiong, Z., Sun, L., Yang, J., Jin, Q., 2012. VFDB 2012 update: toward the genetic diversity and molecular evolution of bacterial virulence factors. *Nucleic Acids Res.* 40, D641-645.
- Chin, C.-S., Alexander, D.H., Marks, P., Klammer, A.A., Drake, J., Heiner, C., Clum, A., Copeland, A., Huddleston, J., Eichler, E.E., Turner, S.W., Korlach, J., 2013. Nonhybrid, finished microbial genome assemblies from long-read SMRT sequencing data. *Nat. Methods* 10, 563–569.
- Joensen, K.G., Scheutz, F., Lund, O., Hasman, H., Kaas, R.S., Nielsen, E.M., Aarestrup, F.M., 2014. Real-time whole-genome sequencing for routine typing, surveillance, and outbreak detection of verotoxigenic *Escherichia coli*. *J. Clin. Microbiol.* 52, 1501-1510.
- Kim, S.H., Park, Y.H., Schmidt-Dannert, C., Lee, P.C., 2010. Redesign, reconstruction, and directed extension of the *Brevibacterium linens* C40 carotenoid pathway in *Escherichia coli*. *Appl. Environ. Microbiol.* 76, 5199–5206.
- Motta, A.S., Brandelli, A., 2008. Properties and antimicrobial activity of the smear surface cheese coryneform bacterium *Brevibacterium linens*. *Eur. Food Res. Technol.* 227, 1299–1306.
- Murray, I.A., Clark, T.A., Morgan, R.D., Boitano, M., Anton, B.P., Luong, K., Fomenkov, A., Turner, S.W., Korlach, J., Roberts, R.J., 2012. The methylomes of six bacteria. *Nucleic Acids Res.* 40, 11450–11462.
- Myers, E., Sutton, G., Delcher, A., IM, D., DP, F., MJ, F., SA, K., CM, M., KHJ, R., KA, R., EL, A., RA, B., HH, C., CM, J., AL, H., S, L., EM, B., RC, B., L, C., PJ, D., Z, L., Y, L., DR, N., M, Z., Q, Z., X, Z., GM, R., MD, A., JC, V., 2000. A whole-genome assembly of *Drosophila*. *Science.* 287, 2196–2204.
- Onraedt, A., Soetaert, W., Vandamme, E., 2005. Industrial importance of the genus *Brevibacterium*. *Biotechnol. Lett.* 27, 527–533.
- Overbeek, R., Olson, R., Pusch, G.D., Olsen, G.J., Davis, J.J., Disz, T., Edwards, R.A., Gerdes, S., Parrello, B., Shukla, M., Vonstein, V., Wattam, A.R., Xia, F., Stevens, R., 2014. The SEED and the rapid annotation of microbial genomes using subsystems technology (RAST).

- Nucleic Acids Res. 42, 206–214.
- Ratray, F.P., Fox, P.F., 1999. Aspects of enzymology and biochemical properties of *Brevibacterium linens* relevant to cheese ripening: a review. J. Dairy Sci. 82, 891–909.
- Roberts, R.J., Carneiro, M.O., Schatz, M.C., 2013. The advantages of SMRT sequencing. Genome Biol. 14, 405.
- Roberts, R.J., Vincze, T., Posfai, J., Macelis, D., 2015. REBASE-a database for DNA restriction and modification: enzymes, genes and genomes. Nucleic Acids Res. 43, D298–D299.
- van Heel, A.J., de Jong, A., Montalbán-López, M., Kok, J., Kuipers, O.P., 2013. BAGEL3: automated identification of genes encoding bacteriocins and (non-)bactericidal posttranslationally modified peptides. Nucleic Acids Res. 41, W448-453.

Chapter 2 – Article 2

DNA tandem repeats contribute to the genetic diversity of *Brevibacterium aurantiacum* phages

Alessandra G. de Melo^{1, 2}, Geneviève M. Rousseau^{2,3}, Denise M. Tremblay^{2,3}, Simon J. Labrie⁴
and Sylvain Moineau^{1,2,3*}

¹ Département de biochimie, de microbiologie et de bio-informatique, Faculté des sciences et de génie, Université Laval, Québec, QC, Canada.

² Groupe de recherche en écologie buccale, Faculté de médecine dentaire, Université Laval, Québec, QC, Canada.

³ Félix d'Hérelle Reference Center for Bacterial Viruses, Faculté de médecine dentaire, Université Laval, Québec, QC, Canada.

⁴ SyntBioLab, Lévis, QC, Canada.

Environ. Microbiol. 2020. doi: 10.1111/1462-2920.15113.

Résumé

Ce chapitre présente la caractérisation des premiers phages virulents infectant *Brevibacterium aurantiacum*, une espèce bactérienne utilisée lors de la fabrication des fromages affinés en surface. Ces phages semblent également responsables de défauts de saveur et de couleur observés dans ce type de fromages. Seize phages (sur soixante-deux isolats) ont été sélectionnés pour le séquençage de leur génome et pour des analyses de génomique comparative. Ces phages de type *cos* à longue queue non contractile appartiennent à la famille des *Siphoviridae* (ordre des *Caudovirales*). La taille de leur génome varie de 35 637 pb à 36 825 pb et, comme leur hôte, possède une teneur élevée en GC (~ 61%). Des gènes codant pour un répresseur d'immunité, une excisionase et une intégrase tronquée ont été identifiés, suggérant que ces phages virulents seraient peut-être dérivé d'un prophage. Leur organisation génomique est hautement conservée mais la section la plus diversifiée est due à la présence de longues répétitions en tandem (TR) d'ADN (198 pb) dans un *orf* codant pour une protéine de fonction inconnue. Nous avons classé ces phages en sept groupes génomiques en fonction de leur nombre de TR, qui va de deux à huit. De plus, nous avons montré que les TR sont répandus dans les génomes phagiques, retrouvés dans plus de 85% des génomes disponibles dans les bases de données publiques.

Abstract

This report presents the characterization of the first virulent phages infecting *Brevibacterium aurantiacum*, a bacterial species used during the manufacture of surface-ripened cheeses. These phages were also responsible for flavor and color defects in surface-ripened cheeses. Sixteen phages (out of sixty-two isolates) were selected for genome sequencing and comparative analyses. These *cos*-type phages with a long non-contractile tail currently belong to the *Siphoviridae* family (*Caudovirales* order). Their genome sizes vary from 35,637 bp to 36,825 bp and, similar to their host, have a high GC-content (~61%). Genes encoding for an immunity repressor, an excisionase and a truncated integrase were found, suggesting that these virulent phages may be derived from a prophage. Their genomic organization is highly conserved, with most of the diversity coming from the presence of long (198-bp) DNA tandem repeats (TR) within an *orf* coding for a protein of unknown function. We categorized these phages into seven genomic groups according to their number of TR, which ranged from two to eight. Moreover, we showed that TRs are widespread in phage genomes, found in more than 85% of the genomes available in public databases

Abbreviations

BACON	Bacteroides-associated carbohydrate-binding often N-terminal
BLASTp	Basic local alignment search tool for proteins
BWA	Burrows-Wheeler aligner
CaCl₂	Calcium chloride
CsCl	Cesium chloride
DNA	Deoxyribonucleic acid
dsDNA	Double strand DNA
EDTA	Ethylenediaminetetraacetic acid
HCl	Hydrochloric acid
HNH	Domain with conserved histidine (H) and asparagine (N)
INDEL	Insertion-deletions
LAB	Lactic acid bacteria
MgSO₄	Magnesium sulphate
MW	Molecular weight
NaCl	Sodium chloride
ORF	Open reading frame
PCR	Polymerase chain reaction
PEG	Polyethylene glycol
pI	Isoelectric point
PFU	Plaque forming units
RNA	Ribonucleic acid
16S rRNA	Small subunit of the ribosomal RNA
RtcB	RNA-splicing ligase
SD	Shine-Dalgarno sequence
SDS	Sodium dodecyl sulfate
SNV	Single nucleotide variation
TMP	Tape measure protein
TR	Tandem repeats
Tris	Tris(hydroxymethyl)aminomethane
tRNA	Transfer RNA
UV	Ultraviolet

Introduction

As the most abundant biological entities on the planet (Brüssow and Hendrix, 2002), bacteriophages (or phages) are found in every ecosystem containing bacterial cells (de Melo et al., 2018), shaping their population and evolution (Koskella and Meaden, 2013). Virulent phages are particularly successful in environments where their bacterial hosts also thrive (Chibani-Chennoufi et al., 2004). For example, the dairy industry is an ecological niche in which large quantities of Gram-positive lactic acid bacteria (LAB) are added to non-sterile milk to control the fermentation process and to develop the sought-after organoleptic properties found in fermented dairy products such as cheeses (de Melo et al., 2018; Moineau and Lévesque, 2004). Ripening microbial cultures are also added for the manufacture of some fine cheeses as they play a role in flavor development.

Although phage titers are usually low in heat-treated milk, a specific viral population can increase very rapidly if they replicate on phage-sensitive bacterial strains used in the dairy cultures (de Melo et al., 2018). The dairy industry relies on a range of strategies to control phages but because of their diversity, they still remain today the main cause of incomplete milk fermentation.

The microbial system of washed rind cheeses is also very complex, and its balance is key to develop the specific cheese flavor and color. *Brevibacterium aurantiacum* is among the most important bacterial species used as a surface ripening culture for such cheeses (Anast et al., 2019; Bonham et al., 2017; Cogan et al., 2014; Levesque et al., 2019; Pham et al., 2017). This bacterial species is part of the taxonomic group of orange pigment-producing *Brevibacterium* genus (Gavrish et al., 2004), in which *Brevibacterium linens* is the type species (Forquin et al., 2009; Gavrish et al., 2004). As part of the diverse community found on the rinds of surface-ripened cheeses (Cogan et al., 2014; Irlinger and Mounier, 2009; Mounier, 2015; Onraedt et al., 2005; Pham et al., 2017; Wolfe et al., 2014), *B. aurantiacum* and other *Brevibacterium* species play a variety of roles during the cheesemaking process, especially in the breakdown of lipids and proteins as well as in the production of carotenoid pigments and volatile sulfur compounds (Irlinger and Mounier, 2009; Motta and Brandelli, 2008; Onraedt et al., 2005; Pham et al., 2017; Rattray and Fox, 1999). During cheese maturation, the ripening cultures are added to the curds in successive surface washes, contributing to the final organoleptic characteristics (Motta and Brandelli, 2008; Onraedt et al., 2005; Rattray and Fox, 1999). Even though these bacteria have been receiving growing interest

lately (Anast et al., 2019; Bonham et al., 2017; Pham et al., 2017), *Brevibacterium aurantiacum* phages have yet to be isolated and characterized. Although complex, cheese rind microbial communities have been shown to be a tractable system that can be used to understand the dynamics influencing microbial assembly, succession and function (Wolfe et al., 2014). This system is composed of phylogenetically diverse bacteria and fungi that interact during cheese ripening (Wolfe et al., 2014). However, the viral impact on the development and stability of cheese rind microbial communities is still poorly understood.

Here, we studied the diversity of virulent *B. aurantiacum* phages that were isolated from failed productions of smear and washed rind cheeses. These uncharacteristic cheeses did not develop the expected flavor and color during ripening. The comparative analyses of the genomes of these bacterial viruses led to the identification of not only a new viral group, but also of DNA tandem repeats (TRs) in a coding region. TRs or satellite DNA are nucleotide sequences (Zhou et al., 2014) that are directly repeated, with each repeated unit located immediately adjacent to the other, seemingly reflecting local duplications of the DNA sequence (Gemayel *et al.*, 2010; Jansen *et al.*, 2012). TRs regions are potentially hypermutable and their variability is thought to be one of the factors that influence genomic plasticity in organisms (Zhou et al., 2014). This observation of TRs in *B. aurantiacum* phages also led us to evaluate TR distribution among other phage genomes.

Results

***B. aurantiacum* phage detection**

We recently reported the genomic characterization of *B. aurantiacum* strain SMQ-1335, formerly identified as *B. linens* (de Melo *et al.*, 2016; Levesque *et al.*, 2019). This strain has been extensively used as a ripening culture for the production of washed-rind cheeses at three manufacturing sites and was used here as a phage-sensitive host. To the best of our knowledge, this is the first study on *B. aurantiacum* phages and as such, an efficient and reproducible plaque assay to detect these phages had to be adapted. After testing several parameters and growth conditions (e.g. media, temperature, bacterial inoculum, micronutrients and supplements), phage plaques were readily detected from environmental samples using a double-layer plaque assay (see Experimental

Procedures). Like many other dairy phages (Mahony et al., 2015; Pujato et al., 2015), these bacterial viruses require the presence of CaCl_2 to propagate.

Isolation of *B. aurantiacum* phages

Various cheese and environmental samples were collected between 2013 and 2016 from three manufacturing sites (S1, S2 and S3) in Canada, where flavor and color defects were observed in washed rind cheeses (Supporting Information Figure S1). Factories S1 and S3 mainly manufacture semi-hard washed-rind cheeses, whereas factory S2 produces only soft cheeses. In total, sixty-two phage isolates were recovered from these samples (Supporting Information Table S1).

Morphological analysis

Electron micrographs of these *B. aurantiacum* phage isolates showed that they all look alike, and they would currently belong to the *Siphoviridae* family of the *Caudovirales* order, as they possess a very long non-contractile tail (Figure 8). One phage isolate, named AGM1, was randomly selected for measurements ($n = 15$) and is made of an isometric capsid of 57 ± 3 nm in diameter and a long non-contractile flexible tail of 315 ± 12 nm long and 8 ± 1 nm wide.

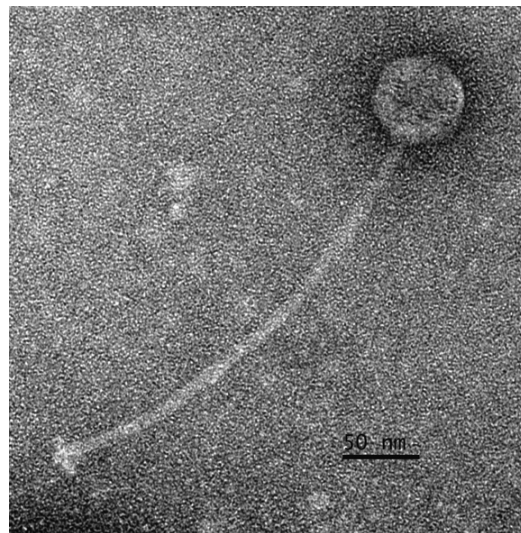


Figure 8. Electron micrograph of the siphophage AGM1.

Phage lytic cycle and host range

One-step growth curve was performed to determine the lytic cycle of phage AGM1 in laboratory conditions. This phage has a long latent period of 255 ± 77 minutes, with a burst size of only 6 ± 2 virions per infected cell at 23°C . This latent period was very long compared to other dairy phages, which complete their lytic cycle well within an hour. On the other hand, this was expected considering that its host SMQ-1335 takes approximately three hours to duplicate in laboratory conditions (data not shown). Five other distinct *B. aurantiacum* strains (SMQ-1417 to SMQ-1421) (Levesque *et al.*, 2019) were tested for phage sensitivity and were fully resistant to these phages.

Molecular characterization

We selected eighteen phage isolates for whole genome sequencing based on seemingly distinct restriction enzyme patterns using the endonuclease NarI. However, the isolates were highly related as their NarI-profiles were very similar with only slight differences (data not shown). Nevertheless, sequencing results showed that isolates 17 and 51 as well as 7 and 23 (Supporting Information Table S1) were 100% identical, therefore these pairs were assigned the same phage name (AGM11 and AGM13, respectively). We also named the remaining sixteen genetically diverse phages, from AGM1 to AGM16, while keeping the above characterized phage as AGM1.

Genome termini

PCR was performed, targeting both extremities of the genome to determine the genome packaging strategy as well as to ensure that the complete phage genomes had been sequenced. The abrupt stop and drop-off of the signals from the DNA sequencing results were indicative of the presence of *cos*-sites. The analysis showed that all sixteen of the *B. aurantiacum* phages analyzed are *cos*-type phages that possess 3' overhang *cos*-sites that are nine nucleotides long (5'-CGCCGGAGA-3').

Genome sequencing

Using the reads from both Illumina and Sanger sequencing, an in-depth analysis of *B. aurantiacum* phage genomes was performed and two particular regions were divergent. These two regions were defined as the *orf27* and the *orf50*. These divergent genomic regions with low coverage and/or

disagreements were solved using primer walking (Supporting Information Table S2). The final assembly generated the complete genomes of *B. aurantiacum* phages and they are described below.

Genome and comparative analysis

The general genomic features of the sixteen *B. aurantiacum* phages and their origin are presented in Table 2. Genome analysis and annotation were carried out using phage AGM1 as a reference, and the results were compared to the 15 other phages. *B. aurantiacum* phage genomes vary in length from 35,637 bp (AGM16) to 36,825 bp (AGM15) and do not possess tRNAs. Similar to their host, these genomes have a high GC-content (60.7-60.9%) and share a very similar codon usage (data not shown). The percentage of nucleotide identity between phage AGM1 and the 15 other phages varies from 97.80% to 99.997%, indicating that they belong to the same species.

Gene prediction and annotation revealed that *B. aurantiacum* phages have 53 open reading frames (ORFs). The detailed information on the functional annotation of these ORFs is found in Supplementary Information Table S3. In comparison to AGM1, none of the other 15 phages had frameshift or point mutations in their genes that generated stop codons or yielded nonsense mutations. Additionally, no genome rearrangement, acquisition or loss of any *orf* was observed. Therefore, these phages have a very conserved genomic organization. Figure 9 presents genome maps with the pairwise alignment of their proteins. Deduced proteins that have 100% identity have the same color. As these 16 *B. aurantiacum* phages are highly related, we mapped the differences in comparison to phage AGM1, excluding the tandem repeats in *orf50* (see below). The differences, including insertions/deletions (INDELS) and single nucleotide variations (SNVs) are summarized in Figure 10. Detailed information on these mutations are found in Supporting Information S4. Eighteen of the proteins encoded in these phage genomes have no predicted functions or associated domains (hypothetical proteins), whereas eight additional proteins (i.e. ORF30, ORF32, ORF35, ORF37, ORF42, ORF45, ORF46, ORF47) have no significant hits or homologues in the public databases (Supplementary Information Table S3).

The genome of *B. aurantiacum* phages can be divided into at least three functional modules, which include DNA packaging, morphogenesis and host lysis (Figure 9). The morphogenesis module is defined at the minimum from *orf3* (probably coding for the portal protein) to *orf21* (tailspike protein). The *orf16* likely codes for the tail tape measure protein (TMP), which would be made of

2,012 amino acid residues. As the size of the TMP determines the length of the phage tail (Abuladze et al., 1994; Belcaid et al., 2011; Katsura and Hendrix, 1984; Mahony et al., 2016), these siphophages possess a very long tail (Figure 8).

Two proteins that are involved in host lysis were also identified. The gene that encodes for the holin (*orf26*) is located downstream from the endolysin (*orf24*), which is a common organization for the host-lysis module found in other actinobacteriophages (Catalão et al., 2013). However, this gene organization is different from dairy phages, in which the holin-encoding gene is usually located upstream of the endolysin gene (Labrie et al., 2004). The presence of genes that possibly encode for a truncated integrase (ORF31) as well as putative immunity repressor (ORF33), and excisionase (ORF34), suggests that these virulent phages are likely derived from a prophage that lost the ability to integrate into the host genome. The host strain (SMQ-1335) does not contain a functional prophage as previously described (de Melo et al., 2016; Levesque et al., 2019).

Most of the genes downstream of the host-lysis module probably form the early and middle-expressed genes, although just a few proteins were assigned functions. These viral genes likely encode for proteins responsible for redirecting host metabolism and machinery for the production of the viral progeny. ORF49 shares 61% amino acid identity with the RNA-splicing ligase (RtcB) of the actinobacteria *Brachybacterium muris*. RtcB is part of a family of RNA ligases that has been shown to participate in RNA splicing and repair in prokaryotes (Chakravarty et al., 2012) but is not common in phages. Both *orf50* and *orf53* code for distinct proteins with HNH endonuclease domains. HNH proteins are common components of phage packaging machinery (Kala et al., 2014). In *E. coli* phage HK97, the HNH endonuclease forms a complex with the phage terminase, which stimulates the cleavage of phage DNA at the *cos*-site during genome packaging into the capsid (Kala et al., 2014). Additionally, in HK97, the HNH endonuclease gene is upstream of the 3' end of the linearized genome, where the *cos*-site is found. In the replicative circular form of the phage genome (Kala et al., 2014), this gene is also upstream of the terminase encoding gene.

Table 2. General genomic characterizations of *B. aurantiacum* phages.

Phage	Origin		Genome length (bp)	%GC	% Identity with AGM1	orf50 length (bp)	Groups	GenBank accession #
	Site - Period	Sample						
AGM16	S3 - 02/2016	Brine	35,637	60.7	98.80	1,515	TR2m2	MN023191
AGM1	S1 - 2013	Wash solution	36,032	60.8	–	1,911	TR4m4	MN023176
AGM2	S3 - 10/2015	Drain	36,032	60.8	99.997	1,911		MN023177
AGM3	S2 - 11/2015	Wash solution	36,034	60.8	99.96	1,911		MN023178
AGM4	S3 - 11/2015	Floor	36,083	60.8	99.81	1,911		MN023179
AGM5	S1 - 09/2015	Wall	36,231	60.8	99.44	2,109	TR5m5	MN023180
AGM6	S1 - 11/2015	Drain	36,231	60.8	99.44	2,109		MN023181
AGM7	S2 - 10/2015	Cheese	36,232	60.8	99.41	2,109		MN023182
AGM8	S2 - 11/2015	Rack	36,232	60.8	99.41	2,109		MN023183
AGM9	S1 - 11/2015	Drain	36,282	60.8	99.28	2,109		MN023184
AGM10	S3 - 10/2015	Floor	36,341	60.8	99.12	2,169	TR5m6	MN023185
AGM11	S3 - 11/2015	Cheese	36,341	60.8	99.12	2,169		MN023186
AGM12	S3 - 11/2015	Cheese	36,429	60.8	98.89	2,307	TR6m6	MN023187
AGM13	S1 - 09/2015	Drain	36,480	60.8	98.73	2,307		MN023188
AGM14	S3 - 11/2015	Rack	36,678	60.8	98.22	2,505	TR7m7	MN023189
AGM15	S3 - 02/2016	Drain	36,825	60.9	97.80	2,703	TR8m8	MN023190

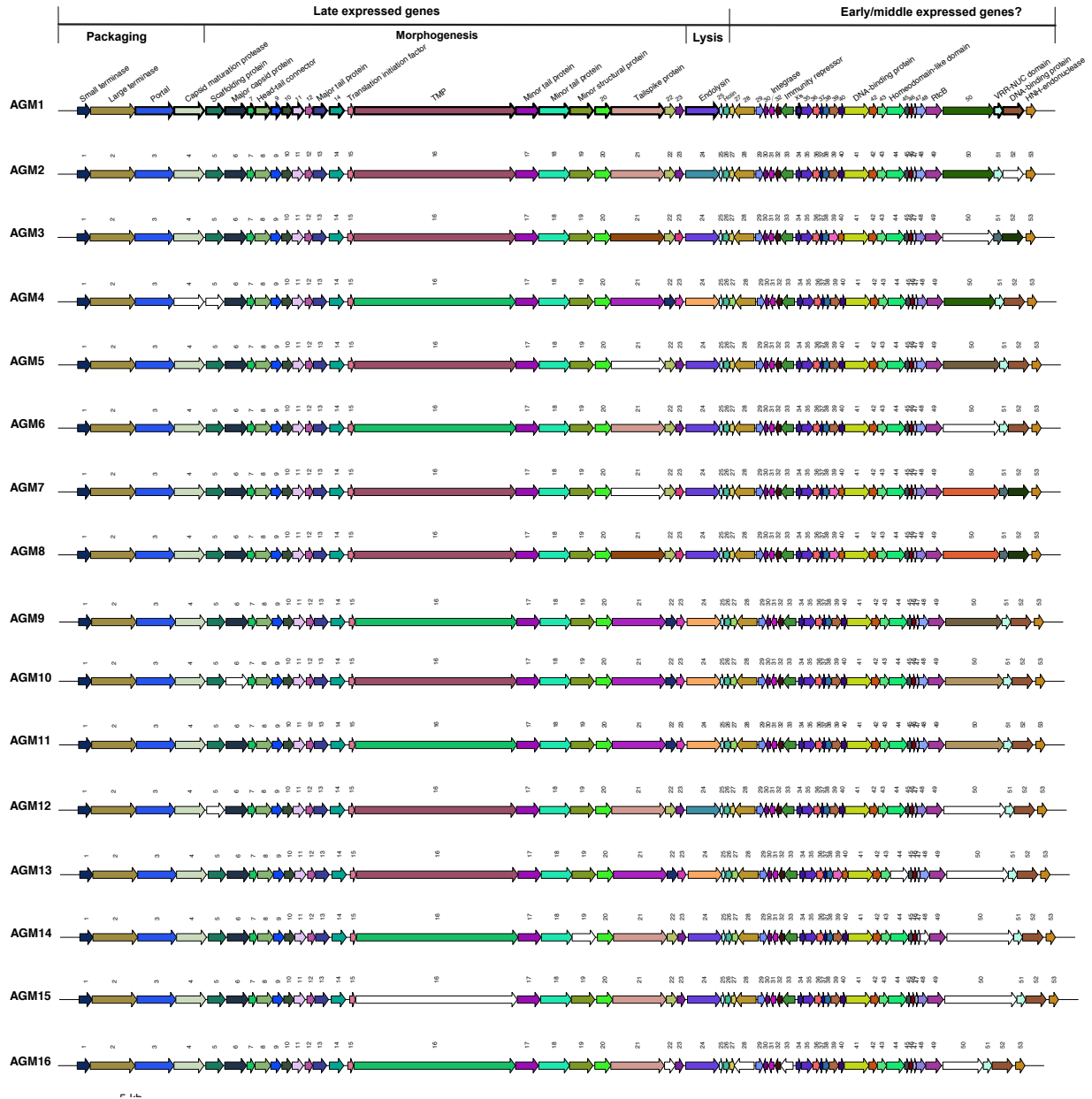


Figure 9. Schematic representation and comparisons of 16 *B. aurantiacum* phage genomes. Each line represents a phage and each arrow represents an ORF. ORFs with 100% amino acid identity share the same color. White arrows represent ORFs without a 100% identical pair.

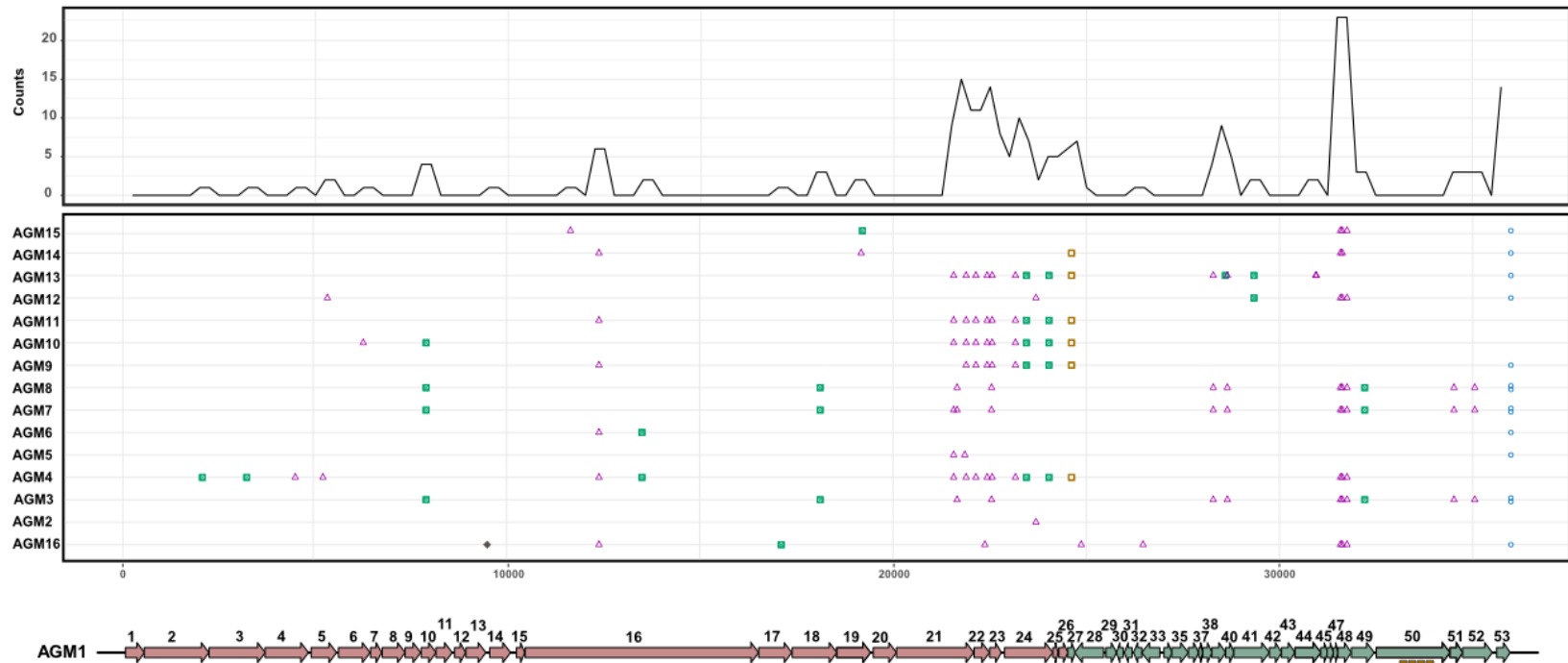


Figure 10. Mutation mapping using complete genome alignment of *B. aurantiacum* phages compared to phage AGM1.

The mutations are positioned according to the genome map of AGM1 where each arrow represents an *orf*. Counts refer to the number of mutations in an overlapping sliding window in a certain region of all sixteen phage genomes. The following symbols represent mutation types that differentiate *B. aurantiacum* phages: point mutation (\square), insertion (\square), duplication (\square), missense (\square), and silent mutation (\square). The TRs in the *orf50* were removed from this analysis but are represented as four brown rectangles below the *orf50* in AGM1 genome map. The *orfs* in pink are likely late expressed genes, whereas the ones in green are likely early- and middle-expressed genes.

DNA tandem repeats and phage groups

Differences in *B. aurantiacum* phage genomes were found in *orf50*, which codes for a protein of 636 amino acids in phage AGM1. As mentioned, this gene codes for protein containing an HNH-endonuclease domain, but it also contains tandem nucleotide repeats (TRs) within the *orf*. TRs are repeated DNA sequences positioned directly next each other (Gemayel *et al.*, 2010; Jansen *et al.*, 2012). In *B. aurantiacum* phages, the repeats are 198-bp long in the central to the final part of the *orf50* and are in frame. The HNH endonuclease domain is located approximately from the amino acid positions 125 to 179 while the repeat array starts at amino acid position 265. The HNH domain is not disrupted by the presence of TRs and each full repeat seems to add 66 amino acids to ORF50.

B. aurantiacum phages markedly vary in the number of TRs in their *orf50*. In fact, we could group these phages according to their number of TRs and a classification scheme is presented in Figure 11 and Table 2. As reported previously (Zhou *et al.*, 2014), the unit size of microbial TRs can vary from 1 to 9 bp, from 10 to 100 bp, or greater than 100 bp and are classified as micro-, mini-, and macrosatellites, respectively. The 198 bp-long TRs found in the genome of *B. aurantiacum* phages would be macrosatellites. Upon further analysis, we noticed that this 198 bp-long TR is in fact composed of two internal arrays of direct repeats: a 138-bp macrosatellite and a 60-bp minisatellite. Here, we will refer to the 198-bp macrosatellites as TRs and phages were grouped according to their number of 198-bp TRs (from 2 to 8, TR2-TR8). However, one set of phages (AGM10 and AGM11) also had a duplication of one minisatellite, displaying an extra 60 bp-long repeat that disrupted the tandem arrangement of the 198-bp macrosatellites (Figure 11). Thus, we added in the grouping scheme the number of internal 60 bp minisatellites (from 2 to 8, m2-m8) in *orf50*. Taken altogether, our *B. aurantiacum* phages were classified based on the number of TRs and minisatellites. For instance, phages from the group TR5m6 have five tandem repeats and six minisatellites, whereas the phage from TR2m2 has two tandem repeats and two minisatellites. No differences in phenotype (plaque size, host range) were observed with the various phages.

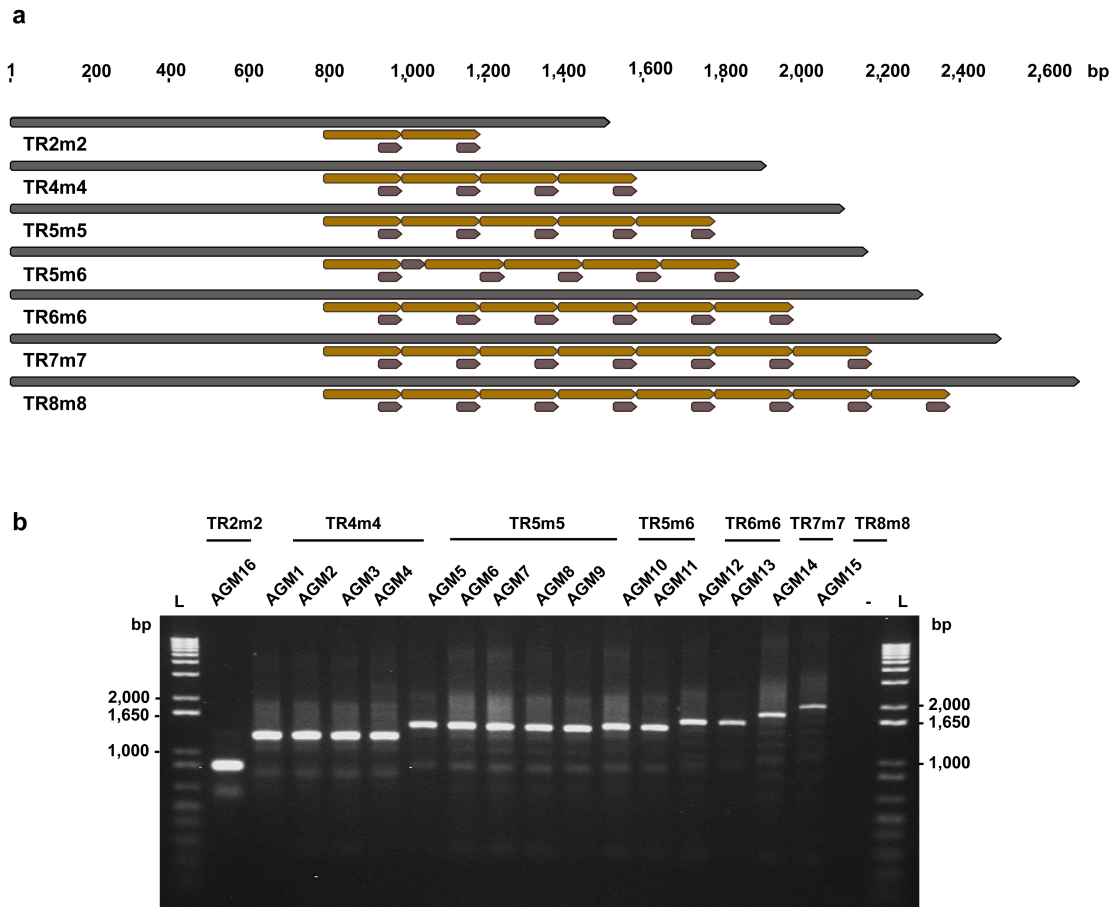


Figure 11. Schematic representations of repeat groups in the *orf50*. (a) The *orf50* (grey arrow) of *B. aurantiacum* phages contain different repeat numbers and their respective classifications are represented. TRs, represented by the 198 bp macrosatellites, are colored in light brown, and the 60-bp minisatellites are represented in dark brown. Due to the various TRs, the *orf50* has variable lengths among *B. aurantiacum* phages. (b) PCR that targets the TRs reveals amplicon sizes varying depending on the content of the repeat array.

TR analyses among *B. aurantiacum* phage isolates

Using PCR and Sanger sequencing, we further characterized the remaining *B. aurantiacum* phage isolates based on the classifications of TRs in their *orf50*. The overall results are presented in Supporting Information Table S1. TR5m5 was the most prevalent among the phages, with 51.6% of the isolates possessing such array in their *orf50*. The other most common array was TR4m4 (14.5%), TR5m6 (12.9%), TR6m6 (12.9%), and TR7m7 (4.8%). The TR2m2 and TR8m8 groups had just one member (1.6%) among all of the isolates (AGM16 and AGM15, respectively).

TR analysis in other phage genomes

The presence of TRs was also verified in phages retrieved from GenBank using the search strategy described in the Experimental procedures section. A repeat array was defined as a set of two or more repeats in a certain region of the genome. The results are available in Supporting Information Table S5 and S6. Among the 5,633 phage genomes retrieved at the time of the analyses, 85.5% (4,815 genomes) were found to contain tandem repeats (identical or degenerated). There was no noticeable correlation between GC-content and the occurrence of TRs, with similar numbers of repeats present in both low and high GC-content genomes. When considering arrays with more than 90% identity between repeat units, the most prevalent repeat type were the minisatellites (85.5% or 7,222 arrays), followed by the microsatellites (11.2% or 944 arrays). Macrosatellites, found in the *B. aurantiacum* phage genomes, are not as widespread, accounting for only 3.3% of the total analyzed arrays (280 arrays). Moreover, our analyses showed that TRs are more abundant in coding regions (75%), and most (75%) of them do not disrupt the reading frame.

The number of repeats was not directly correlated with the size of the phage genome. For example, the genome of the *Liberibacter* phage SC1 (*Podoviridae*) is composed of 40,048 bp and contains 58 repeats distributed among 21 unique arrays located in different genomic regions. In contrast, the genome of *Bacillus* phage G (*Myoviridae*) is composed of 497,513 bp and has only 10 repeats distributed among five arrays within the genome. An outstanding number of TRs were detected in *Campylobacter* phages CP220 (177,534 bp), CP21 (182,833 bp), and CPt10 (175,720 bp), with 120, 100 and 82 repeats distributed among 28, 26 and 26 genomic regions, respectively.

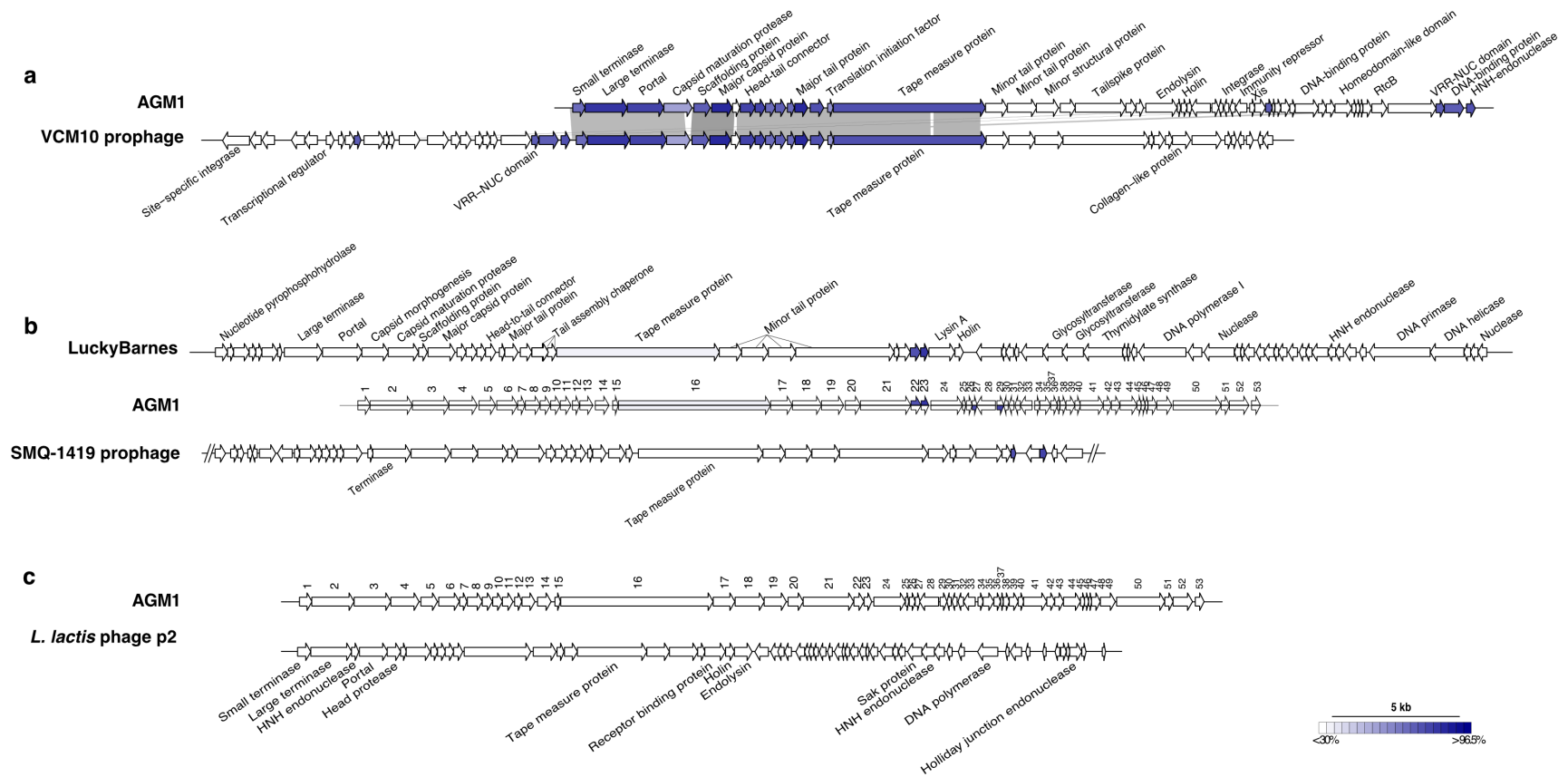
Many of the proteins that are encoded by genes with TRs have an unknown function (~36%). We observed more TRs in genes encoding for structural proteins, especially in tail proteins and fibers, but this could be a bias due to the lack of functional annotation for the non-structural phage proteins. Nonetheless, genes coding for tail proteins are overrepresented, accounting for 11% of the repeats. It is well established in the literature that tail tape measure proteins (TMP) are composed of repeated sequences (Belcaid et al., 2011). Our analysis confirms this observation as 3.7% of the TRs were in the TMP coding gene.

Comparative genome and proteomic analysis with other *Brevibacterium* spp. phages

The structural proteome of phage AGM1 was experimentally determined and the results are described in Supporting Information S7. The complete proteome of the *B. aurantiacum* phages was also determined *in silico* and compared to databases (Supporting Information Table S3). The best matches were with structural proteins found in a prophage of *Brevibacterium* sp. VCM10 (JAJB00000000.1), isolated from an environmental sample collected in Malaysia (Figure 12). Recent comparative and phylogenetic analyses of *Brevibacterium* strains identified VCM10 as a strain of *B. linens* (Levesque et al., 2019; Pham et al., 2017).

Among the structural proteins, the major capsid protein (ORF6, 90%) and the major tail protein (ORF13, 88%) of *B. aurantiacum* phages share the highest percentages of amino acid identities with VCM10 proteins (Supporting Information Table S3). There is also 92% identity between the endolysin of phage AGM1 and a phage-related protein found in *B. aurantiacum* strain 6 (3). Several other *B. aurantiacum* phage proteins have sequence identities with actinobacteriophages or host proteins from *Gordonia*, *Streptomyces Propionibacterium*, and other *Brevibacterium*.

Besides *B. linens* VCM10 prophage, two other *Brevibacterium* phage genomes are available in GenBank. Both phages, LuckyBarnes (Underwood et al., 2019) (MF668275.1) and Cantare (MK016493), were isolated from soil samples. The most evolutionarily distant *Brevibacterium* phage was *B. fuscum* phage Cantare (*Myoviridae*) and it contains a much larger genome (90,743 bp) as well as a lower GC-content (52.9%) than the other *Brevibacterium* spp. phages. *B. iodinum* phage LuckyBarnes (*Siphoviridae*) contains a 50,774 bp genome with a 61.9% GC-content (Underwood et al., 2019). A putative prophage was also recently found in the genome of *B. aurantiacum* SMQ-1419 (Levesque et al., 2019) (CP025333). LuckyBarnes, together with VCM10 and the SMQ-1419 prophages share limited protein similarities with *B. aurantiacum* phages (Figure 12). Yet, the phages characterized in this study are novel *Brevibacterium* viruses.



1

2 **Figure 12. Schematic representation of the genome alignment and organization of phage AGM1 compared to other phages.**
 3 Each arrow represents an ORF. ORFs with more than 30% amino acid identity are represented in the same color according to the gradient.
 4 ORFs with functions or domains assigned are identified. (a) The virulent *Brevibacterium* phage AGM1 is compared to *B. linens* VCM10
 5 prophage, which is the closest phage in databases. The grey shading links DNA similarities. (b) AGM1 is compared to two distant
 6 *Brevibacterium* phages. Horizontal lines split the AGM1 genome map to compare it simultaneously with *B. iodinum* phage LuckyBarnes
 7 (upper part) and *B. aurantiacum* SMQ-1419 prophage (lower part). (c) The genome map of the lactococcal dairy phage p2 was used as
 8 comparator to AGM1. Protein functions of AGM1 can be seen in (a).

9

Discussion

In this study, we isolated several virulent *B. aurantiacum* phages from dairy environmental samples collected between 2013 and 2016 as well as analyzed the genome of sixteen of them to shed light on their diversity and evolution. The 16 phages were found to be highly related at the genomic level. Greater diversity is usually found among dairy phages infecting *Lactococcus lactis* (Deveau et al., 2006; Murphy et al., 2016, 2013), *Streptococcus thermophilus* (Mahony and van Sinderen, 2014; McDonnell et al., 2016), *Leuconostoc* spp. (Kot et al., 2014; Pujato et al., 2015), *Lactobacillus* spp. (Capra et al., 2010; Casey et al., 2014; Mercanti et al., 2016), and *Propionibacterium freudenreichii* (Cheng et al., 2018).

Our data suggest that these virulent *B. aurantiacum* phages have evolved from a common ancestor, even though they were isolated from three distant manufacturing sites. A previous study suggested that dairy lactococcal phages that share a common origin may evolve differentially once they have been carried to different dairy factories (Chmielewska-Jeznach et al., 2018). On the other hand, it is not uncommon to find highly conserved genomic organization and content in phages infecting the same bacterial host. For example, the virulent lactococcal phages GR7 and CB14, which infected the same starter strain, were isolated fourteen months apart and were 100% identical at the genomic level. Such finding indicated that despite all the measures adopted by the dairy industry to control phages, they can persist and remain stable in a cheese plant over a long period of time (Rousseau and Moineau, 2009). Similarly, *B. aurantiacum* phages AGM1 and AGM2, which were isolated two years apart, exhibited only one SNV between their genomes. Additionally, phage isolates 17 (AGM11, S1/2015) and 51 (AGM11, S3/2015) were 100% identical even if they were found in different manufacturing sites (Supporting Information Table S1).

Although we isolated phages from three sites, all of them infect the same ripening strain, *B. aurantiacum* SMQ-1335. While it is possible to find remarkable genetic diversity among phages infecting a single host, as observed for mycobacteriophages (Pope et al., 2015) and *Arthrobacter* phages (Klyczek et al., 2017), the factors shaping phage diversity may also be related to ecological parameters. Some mycobacteriophages have the ability to infect other *Mycobacterium* species (Jacobs-Sera et al., 2012). This extended host range provide opportunities to acquire new genes

from other bacterial strains or viruses, leading to a dynamic and evolving phage population (Pope et al., 2015). Another example is phages infecting *Propionibacterium freudenreichii*, which is used as a ripening culture during the production of a Swiss-type cheese. *P. freudenreichii* phages have a narrow host range but a greater genetic diversity than other members of the genus (Cheng et al., 2018), suggesting that the cheese environment provided more opportunities for genetic exchange (Bonham et al., 2017). Still, two *P. freudenreichii* phages (E1 and Anatole) belonging to the same genomic cluster but isolated from different periods and geographic locations (1992 in France and 2015 in USA, respectively), shared 99% genomic identity (Cheng et al., 2018). Interestingly, we noticed that phage Anatole had a 75 bp insertion in its *orf52*, which formed a degenerated tandem repeat array when compared to phage E1. Only two SNVs were found throughout their genomes.

As *B. aurantiacum* phages were not able to infect other *B. aurantiacum* or *B. linens* strains, it may indicate that these phages are strain-specific, which could partially explain their overall low genetic diversity. Horizontal gene transfer relies on the ability of diverse phages to infect the same or related hosts (Filée et al., 2006) and host range can constrain viral evolution (Shapiro and Putonti, 2018). The evolution of phages with narrow host ranges may depend on stochastic mutations or recombination events with virulent or temperate phages that infect the same hosts.

While the comparative genomic analyses indicated high relatedness among these *B. aurantiacum* phages, most of the diversity was attributed to the presence of TRs in an intragenic genomic region. The prevalence of these structures, especially macrosatellites, in the compact genomes of phages, was surprising especially considering the genome size constraint for packaging into the capsid. Moreover, we could not attribute a function or determine whether the variable numbers of TRs provided a competitive advantage to the phages. The variability in the number of TRs in the phage genomes was striking, including in those available in GenBank. Many of these TRs are in coding regions and do not alter the reading frame, thus conserving the original amino acid sequence of the protein (Mrazek et al., 2007; Zhou et al., 2014). Conversely, the most prevalent non-coding TRs (i.e. in intergenic region) are not multiples of three nucleotides. The same trend was observed in prokaryotes (Zhou et al., 2014) and eukaryotes (Gemayel et al., 2010). Repeats that cause frameshift mutation are probably selected against in coding regions (Gemayel et al., 2010; Mrázek et al., 2007), whereas they do not have the same impact in intergenic regions.

Although little is known about these structures in the genome of bacterial viruses, they have been studied for years in eukaryote and prokaryote genomes. While considered to be nonfunctional and ignored in eukaryotes and prokaryotes for many years, the availability of whole genome sequences revealed their presence in coding regions, promoters and other regulatory regions (Gemayel et al., 2010). These repeat sequences could fulfill specific biological roles (Jansen et al., 2012). Accumulating evidences point to a potential role of TRs as engines of genetic variability and bacterial adaptation (Zhou et al., 2014). For example, they may lead a subpopulation of pathogenic cells to evade the host immune system in the processes of antigenic or phase variation (Gemayel et al., 2010; Guo and Mrázek, 2008; Zhou et al., 2014).

While no previous analyses specifically targeted the distribution of TRs in the genomes of bacterial viruses, a recently published study analyzed two million viral metagenomic contigs for the presence of a domain repeated in tandem in crAss-like phages, named the Bacteroides-associated carbohydrate-binding often N-terminal (BACON) domain (Jonge et al., 2019). This study found that crAss-BACON tandem-repeat-containing ORFs were associated to phage tail proteins, whereas single domain or domains not in tandem were not associated to this protein category. They also showed that a TR of eight crAss-BACONs was derived from multiple duplication events of the single domains.

Minisatellites (10-100 bp) were also the most prevalent repeat arrays in phage genomes, and macrosatellites (>100 bp) were the least prevalent, although abundant in *B. aurantiacum* phage genomes. It is unclear which selective barriers, if any, favor or not the formation of these arrays. While a large number of TRs was observed in *Caudovirales* genomes, their number is not correlated with the size of the viral genome. We identified a high proportion of TRs in genes coding for structural proteins, particularly for tail proteins. While it referred to another category of repeats, it was recently demonstrated that the flexibility of an interspersed repeat region in the tape measure protein (TMP) enabled the virulent *Lactococcus* phage CB14 to evolve thermal resistance (Geagea et al., 2017). In addition to the TMP, a large proportion of the TRs was identified in tail fiber proteins (3.7%). It is tempting to speculate that by rearranging the repeated regions in the tail fiber without compromising the integrity of the protein, these repeats may represent a way for phages to adapt to the diverse repertoire of bacterial receptors or to persist in certain environments.

The *B. aurantiacum* host strain is used during the production of washed rind cheeses. As a strategy to control phages, the cheese industry will typically rotate bacterial starter cultures to limit the repetitive phage infection of a strain (Garneau and Moineau, 2011). To our knowledge, no such strain rotation is regularly used in ripening microbial cultures. The complex nature of cheese rinds makes the replacement or rotation of ripening strains rather difficult. The establishment of these species on the surface of a cheese depends on their metabolism but also on their ability to interact with other members of the microbial community (Mounier et al., 2008; Pham et al., 2017). Once a ripening strain has been established in the manufacturing process, changing the strain is considered a last resort, as it can alter the organoleptic attributes of the cheese and its consumer acceptability.

One can speculate that over time, the recurrent use of the same *B. aurantiacum* culture not only favors the persistence of specific phages in the manufacturing facilities, but that viral mutations are inevitable, including change in the number of TRs. Clearly, TRs act as promoters of diversity among these phages. This phenomenon was also recently observed in *Staphylococcus* phage Sb-1 and its derivatives (Sergueev et al., 2019). After applying a so-called adaptation procedure, the host range of this Twort-like phage was expanded in part of the phage population. Genomic analyses showed that a hypervariable region composed of TRs was the genetic determinant for the expansion. While this locus was variable in the parental preparation, it displayed a stable distinct allele in the mutant with host range expansion (Sergueev et al., 2019).

In terms of phage biology, phage AGM1 has a long latency period and releases very few virions per infected cells under laboratory conditions. Cheese ripening takes place in conditions that might slow down the metabolism of the host, making the latency period even longer in manufacturing settings and possibly slowing the evolution of these phages as compared to other dairy phages. This could also be a reason as to why these phages have not been reported before. However, these phages still cause technological problems during ripening, which brings a new layer of complexity to the cheese rind microbiota. Cheese rind was recently shown as a tractable system to study microbial community formation and succession (Wolfe et al., 2014). Although phages were not addressed as part of the cheese rind microbiome, it is likely that the viral population has also an impact in the stability of the community and even represents an evolutionary pressure.

Overall, *B. aurantiacum* phages studied here evolved from the same ancestor, despite being isolated from three cheese-manufacturing sites. The presence of several long TRs arrays in their genomes may indicate a relatively recent evolutionary event that led to the expansion of DNA segments in their genomes. However, several questions remain regarding the presence of tandem repeats, and whether they impact protein structure, function and folding. Finally, as phage protocols have now been adapted, we expect that additional *Brevibacterium* spp. phages will be isolated from various geographical locations and cheese environments. Additional comparative genome analyses will also lead to more information about their diversity and evolution.

Experimental Procedures

Bacterial culture and growth conditions

B. aurantiacum cultures were grown in Elliker broth (HiMedia) supplemented with 0.5% NaCl. Co-factors such as 0.4 mM of MgSO₄ and 20 mM of CaCl₂ were added after sterilization. Cultures were incubated at 23°C under agitation (200 rpm) for 24 hours or until the optical density at 600 nm (OD₆₀₀) reached 0.8. Stocks were prepared by growing bacterial culture in 10 mL of Elliker broth (as described above). The cells were then harvested by spinning the culture in 15 mL conical tubes at 5,000 *x g* for 10 minutes. Pellets were resuspended in 1 mL of fresh Elliker broth with 15% glycerol and placed in 1.5 mL cryogenic screw cap vials. The stock tubes were flash-frozen and stored at -80°C for further use. *B. aurantiacum* SMQ-1335 (GenBank CP017150.1) was used as a host to isolate, propagate, and titer the phages. The host strain as well as the phages are available at the Félix d'Hérelle Reference Center for Bacterial Viruses (www.phage.ulaval.ca).

Phage detection

Several growth conditions were tested to establish a plaque assay for the detection of *B. aurantiacum* phages. The parameters tested include media (MRS, Elliker), temperature (20°C, 23°C, 25°C, and 30°C), bacterial inoculum, and supplements (i.e. non-fat dry milk, casein, lactose, sodium chloride, MgSO₄, CaCl₂, triammonium citrate, sodium acetate, potassium phosphate dibasic, ascorbic acid and Polysorbate 80). The final plaque assay was performed on Elliker agar made from Elliker broth, 0.5% NaCl, 0.15% Polysorbate 80, 20 mM CaCl₂ (added after sterilization) and 1% agar (bottom layer) or 0.75% agar (soft layer). Phages were propagated in

half-strength Elliker broth (50% Elliker) supplemented with 0.5% NaCl, as well as with 0.4 mM MgSO₄ and 20 mM CaCl₂ added after sterilization. Plates were incubated at 23°C for 48 h.

Isolation, propagation and titration of *B. aurantiacum* phages

Phages were isolated from 30 cheese and environmental samples obtained from three Canadian production sites after observing washed-rind cheeses with flavor and color defects (see Supporting Information Table S1). Two to three clear isolated plaques were selected per sample and purified three times to ensure purity. After the final round of purification, one isolated plaque was selected with a sterile truncated pipette tip. Each plaque was added to 10 mL of 50% Elliker broth inoculated with 100 µL of bacterial cells (OD₆₀₀ of 0.8), under the conditions stated above. A 10-mL culture containing only *B. aurantiacum* cells (100 µL) was incubated as a positive control for bacterial growth. The cultures were kept at 23°C while being agitated at 200 rpm until lysis was observed, or for up to 24 hours. Then, the cultures containing phages were spun down at 5,000 *x g*, for 10 min to separate the free phages in the supernatant from the bacterial cell debris in the pellet. The supernatants were filtered (0.45 µm) and the phage lysate were stored at 4°C until use.

Phage titration was performed using a spot test or a double layer plaque assay with bacterial cells grown for 18-24 hours at 23°C, until the OD₆₀₀ reached 0.8. Serial dilutions of the phage lysates (10⁻¹ - 10⁻⁷) were performed using phage buffer (50 mM Tris-HCl (pH 7.5), 100 mM NaCl, 8 mM MgSO₄). For double layer plaque assays, 100 µL of bacterial culture was added to a tube containing 3 mL melted soft agar (at ~50°C) together with 50 µL of each phage dilution (10⁻¹ - 10⁻⁷) or undiluted phage lysate and poured over a plate containing a bottom layer Elliker agar. For spot test, 100 µL of *B. aurantiacum* culture was added to 3 mL of melted Elliker soft agar, poured over a bottom layer Elliker agar, and let dry. Then, 10 µL of each dilution was spotted on this plate containing the sensitive host. Plates were incubated at 23°C for 48 hr. Phage glycerol stocks were prepared as described previously (Fortier and Moineau, 2009) and stored at -80°C.

Phage morphology

Phages were concentrated, from one liter of phage lysate prepared as above, using polyethylene glycol (PEG) 8000 and NaCl (Hamdi et al., 2017; Jarvis, 1978). This was followed by a

discontinuous and continuous cesium chloride (CsCl) gradients, as was previously described (Azaïez et al., 1998; Fortier et al., 2006; Sambrook and Russel, 2001), with the following modifications. After concentrating phages with PEG 8000, the pellet was resuspended in 5 mL of phage buffer. Resuspended phages were then transferred into a conical tube and centrifuged for 10 min at 5,000 x g . Both the pellet and the supernatant were kept. The supernatant was transferred to an ultracentrifuge tube, whereas the pellet was resuspended in 5 mL of phage buffer and transferred to a second tube. After CsCl discontinuous gradient, phage bands from both tubes were selected and combined for a CsCl continuous gradient (Azaïez et al., 1998; Fortier et al., 2006; Sambrook and Russel, 2001). Purified phages were then used to visualize using an transmission electron microscopy as described previously (Fortier and Moineau, 2007).

DNA isolation and restriction

Prior to DNA isolation, phage lysates (titer $> 10^9$ PFU/mL) were mixed with chloroform (1:1; v/v) and centrifuged at 14,243 x g for 10 min, in a microcentrifuge. The upper phase was carefully removed and used for DNA extraction using a modified phenol-chloroform protocol (Moineau et al., 1994). Five microliters of RNase (10 mg/mL), 5 μ L of DNase (1 mg/mL) and 10 mM MgSO₄ were added to 1 mL of filtered lysate, and the sample was incubated at 37°C, for 30 min. Afterward, 100 μ L of a pre-warmed SDS mix (2.5% SDS, 0.5 M Tris-HCl (pH 9.0), 0.25 M EDTA) was added to the solution, mixed and placed at 65°C for 30 min. Following incubation, 125 μ L of cold 8 M potassium acetate was added and the tube was kept on ice for 30 min.

The preparation was centrifuged at 21,000 x g at 4°C for 10 min, and the supernatant was transferred in equal volumes into two new microcentrifuge tubes. An equal volume of phenol-chloroform was added to each tube, vortexed, and centrifuged at 14,243 x g , at room temperature, for 10 min. This step was repeated twice. The upper phases of both tubes were carefully removed and combined in a single tube. DNA was precipitated by adding 0.7 volumes of isopropanol and centrifuged at 21,000 x g at 4°C for 10 min. The supernatant was discarded, and the pellet was carefully washed three times with 70% ethanol, while quick spins were performed to keep the pellet undisturbed. After allowing the pellet to dry, DNA was resuspended in 20 μ L of 50 mM Tris-HCl (pH 8.0) and stored at -20°C. Phage DNA was digested using the restriction endonuclease

NarI according to manufacturer instructions (Roche Diagnostics) and then migrated through a 0.8% agarose gel, stained with EZ-Vision Three (Amresco) and visualized under UV light.

Genome sequencing and primer walking

Sixteen phages containing slight differences in their restriction profiles were selected, and their genomes were sequenced using Illumina MiSeq at Université Laval. Phage DNA was first extracted as described above and quantified using a Quant-iT PicoGreen dsDNA Assay kit. Libraries were prepared using a Nextera XT DNA Sample kit, Nextera XT Index kit, and a MiSeq Reagent kit v2. The reads were assembled using RAY (v2.3.1) (Boisvert et al., 2010) or SPAdes (v3.9.0) (Nurk et al., 2013) software and the coverages obtained ranged from 556-fold to 2,333-fold. Phage genomic regions presenting low coverage or high divergence were confirmed and/or completed through primer walking using PCR and Sanger sequencing (Plateforme de Séquençage et de Génotypage des Génomes du Centre Hospitalier de l'Université Laval). The primer sets used for amplification and sequencing are listed in Supporting Information Table S2. Using Taq DNA polymerase (Bio Basic), PCR was performed by adding GC enhancer to improve the specificity of the primer-annealing step. When possible, new reads obtained using Sanger sequencing were *de novo* assembled, and then the assemblies were mapped to their respective phage contigs using Geneious® 7.0.6 (Biomatters) in order to close the genome sequences. Once the sequences were nearly completed, Illumina reads were also mapped to the phage genome for verification and to correct any possible errors.

Determination of phage genomic termini

A set of primers encompassing both extremities of the genomes was designed (Cos forward and reverse, Supporting Information Table S2) as described elsewhere (Mahony et al., 2006). PCR targeting genomic termini was performed, and amplicons as well as phage DNA were Sanger sequenced with the primers cited above.

Genome analysis and annotation

Genome analysis and annotation were performed using AGM1 as the reference phage. Open reading frames (*orfs*) were predicted using ORF finder (<https://www.ncbi.nlm.nih.gov/orffinder/>),

Glimmer (Delcher et al., 2007), Prodigal (Hyatt et al., 2010) and GeneMarkS (Besemer et al., 2001). The Shine-Dalgarno (SD) sequence was determined using the 3' end of the *B. aurantiacum* 16S RNA gene (Shine and Dalgarno, 1975, 1974). The SD sequences located upstream of all start codons were manually checked. An *orf* was considered if equal to or greater than 90 nucleotides and if it contained a SD sequence that is close to its start codon. Protein function was predicted using Blast2GO (Conesa and Götzt, 2008), BLASTp (Altschul et al., 1997) and local BLASTp with the Actinobacteriophage database (<http://phagesdb.org>). The presence of conserved domains was also checked in all predicted ORFs. Protein identity was calculated by dividing the number of identical amino acids by the total number of amino acids of the smaller protein, when comparing phage AGM1 proteins with the best BLASTp hit. Protein isoelectric point (pI) and molecular weight (MW) were predicted with the ExPASy – Compute pI/MW tool (Gasteiger et al., 2005, 2003). The presence of tRNA was verified using tRNAscan-SE 2.0 (Lowe and Eddy, 1996).

Phage structural proteins analysis

CsCl-purified phage samples were directly used for structural proteins analysis with liquid chromatography/tandem mass spectroscopy at the Plateforme de Protéomique du Centre de Génomique de Québec. The results were analyzed as described previously (Hamdi et al., 2017) and are shown in the Supplementary Information S7.

Comparative genome analysis

Genome sequences of phages AGM2 to AGM16 were compared to phage AGM1 (Figure 9) and the differences are presented in Figure 10. Illumina reads were aligned with AGM1 genome using BWA (Burrows-Wheeler aligner) (Li and Durbin, 2009). The variants were called using SAMtools and BCFtools (Li et al., 2009), and then mapped in the genome of the phages using in-house Python scripts and Biopython (Cock et al., 2009). Phage genome maps were generated in R using the package genoPlotR (Guy et al., 2010). Figure 10 containing the distribution of the mutations was generated using ggplot2 (Wickham, 2016). The closest relatives to *Brevibacterium* phages, prophage VCM10 (NZ_JAJB01000050), LuckyBarnes (MF668275.1) and prophage SMQ-1419 (CP025333), were compared to phage AGM1 at the nucleotide and protein levels (Figure 12). *Lactococcal* phage p2 (GQ979703) was also compared to AGM1 and its genome map included as

a structure comparator.

DNA tandem repeat analyses in *B. aurantiacum* phage isolates

In situ analyses of tandem repeats were performed for the sixty-two phage isolates. Primers targeting the repeats region in the *B. aurantiacum* phage genomes were used for PCR (LCR3-Forward and LCR2-Reverse) with an annealing temperature of 67°C. The resulting amplicons were separated using 0.8% agarose gel with EZ-Vision® loading buffer and TAE buffer (40 mM Tris, 20 mM acetic acid, 1 mM EDTA, pH 8.3) at 100 V. Amplicons were Sanger sequenced and reads were analyzed with Geneious® 7.0.6.

***In silico* analyses of tandem repeats in phage genomes**

The presence of TRs in the genomes of *B. aurantiacum* phages was analyzed using Tandem Repeat Finder (Benson, 1999). A search of the GenBank database (September 2018) using specific terms was also used to retrieve the available phage genomes belonging to the *Caudovirales* order (search strategy: txid28883[Organism:exp] and "complete genome"[Title]). The results contained duplicates that were removed based on the name of the phage. When duplicates were found, the most recent version of the entry was kept. All genomes were scrutinized for repeats using Tandem Repeat Finder (Benson, 1999), with a cut-off of 90% identity among the sequences. The sequences were parsed in order to remove redundant results.

Data availability

The data generated in this study are disclosed here and in the Supporting Information. Phage genome sequences were deposited in GenBank under the accession numbers found in Table 2.

Supporting information

Supporting information Tables S1 to S7 and supplementary Figure S1 can be found in the supplementary data files.

Acknowledgements

We are grateful to Pier-Luc Plante for performing genome assemblies and Crayon-Bleu for editorial assistance. We thank the Moineau's lab members for helpful discussions. AGM earned a scholarship from the National Council for Scientific and Technological Development (CNPq-Brazil) in partnership with CALDO (Canada). This work was funded by Natural Sciences and Engineering Research Council of Canada. SM holds the Tier 1 Canada Research Chair in Bacteriophages.

Competing interests

The authors declare no competing interests.

References

- Abuladze, N.K., Gingery, M., Tsai, J., Eiserling, F.A., 1994. Tail length determination in bacteriophage T4. *Virology* 199, 301–310.
- Altschul, S.F., Madden, T.L., Schäffer, A.A., Zhang, J., Zhang, Z., Miller, W., Lipman, D.J., 1997. Gapped BLAST and PSI-BLAST: a new generation of protein database search programs. *Nucleic Acids Res.* 25, 3389–3402.
- Anast, J.M., Dzieciol, M., Schultz, D.L., Wagner, M., Mann, E., Schmitz-Esser, S., 2019. *Brevibacterium* from Austrian hard cheese harbor a putative histamine catabolism pathway and a plasmid for adaptation to the cheese environment. *Sci. Rep.* 9, 6164.
- Azaïez, S.R.C., Fliss, I., Simard, R.E., Sylvan, M., 1998. Monoclonal antibodies raised against native major capsid proteins of lactococcal c2-like bacteriophages. *Appl. Environ. Microbiol.* 64, 4255–4259.
- Belcaid, M., Bergeron, A., Poisson, G., 2011. The evolution of the tape measure protein: units, duplications and losses. *BMC Bioinformatics* 12, S10.
- Benson, G., 1999. Tandem repeats finder: a program to analyse DNA sequences. *Nucleic Acids Res.* 27, 573–578.
- Besemer, J., Lomsadze, A., Borodovsky, M., 2001. GeneMarkS: a self-training method for prediction of gene starts in microbial genomes. Implications for finding sequence motifs in regulatory regions. *Nucleic Acids Res.* 29, 2607–2618.
- Boisvert, S., Laviolette, F., Corbeil, J., 2010. Ray: simultaneous assembly of reads from a mix of high-throughput sequencing technologies. *J. Comput. Biol.* 17, 1519–33.
- Bonham, K.S., Wolfe, B.E., Dutton, R.J., 2017. Extensive horizontal gene transfer in cheese-associated bacteria. *eLife* 6, e22144.
- Brüssow, H., Hendrix, R.W., 2002. Phage genomics: small is beautiful. *Cell* 108, 13–16.
- Capra, M.L., Mercanti, D.J., Reinheimer, J.A., Quiberoni, A.L., 2010. Characterisation of three temperate phages released from the same *Lactobacillus paracasei* commercial strain. *Int. J. Dairy Technol.* 63, 396–405.
- Casey, E., Mahony, J., O’Connell-Motherway, M., Bottacini, F., Cornelissen, A., Neve, H., Heller, K.J., Noben, J.P., Dal Bello, F., van Sinderen, D., 2014. Molecular characterization of three *Lactobacillus delbrueckii* subsp. *bulgaricus* phages. *Appl. Environ. Microbiol.* 80, 5623–5635.
- Catalão, M.J., Gil, F., Moniz-Pereira, J., São-José, C., Pimentel, M., 2013. Diversity in bacterial lysis systems: bacteriophages show the way. *FEMS Microbiol. Rev.* 37, 554–571.
- Chakravarty, A.K., Subbotin, R., Chait, B.T., Shuman, S., 2012. RNA ligase RtcB splices 3'-phosphate and 5'-OH ends via covalent RtcB-(histidiny)-GMP and polynucleotide-(3')pp(5')G intermediates. *Proc. Natl. Acad. Sci.* 109, 6072–6077.
- Cheng, L., Marinelli, L.J., Grosset, N., Fitz-Gibbon, S.T., Bowman, C.A., Dang, B.Q., Russell, D.A., Jacobs-Sera, D., Shi, B., Pellegrini, M., Miller, J.F., Gautier, M., Hatfull, G.F., Modlin, R.L., 2018. Complete genomic sequences of *Propionibacterium freudenreichii* phages from Swiss cheese reveal greater diversity than *Cutibacterium* (formerly *Propionibacterium*) acnes phages. *BMC Microbiol.* 18, 19.
- Chibani-chenoufi, S., Bruttin, A., Brüssow, H., Dillmann, M., Bru, H., 2004. Phage-Host interaction: an ecological perspective. *J. Bacteriol.* 186, 3677–3686.
- Chmielewska-Jeznach, M., Bardowski, J.K., Szczepankowska, A.K., 2018. Molecular, physiological and phylogenetic traits of *Lactococcus* 936-type phages from distinct dairy

- environments. *Sci. Rep.* 8, 12540.
- Cock, P.J.A., Antao, T., Chang, J.T., Chapman, B.A., Cox, C.J., Dalke, A., Friedberg, I., Hamelryck, T., Kauff, F., Wilczynski, B., De Hoon, M.J.L., 2009. Biopython: freely available Python tools for computational molecular biology and bioinformatics. *Bioinformatics* 25, 1422–1423.
- Cogan, T., Goerges, S., Gelsomino, R., Larpin, S., Hohenegger, M., Bora, N., Jamet, E., Rea, M., Mounier, J., Vancanneyt, M., Guéguen, M., Desmasures, N., Swings, J., Goodfellow, M., Ward, A., Sebastiani, H., Irlinger, F., Chamba, J.-F., Beduhn, R., Scherer, S., 2014. Biodiversity of the surface microbial consortia from Limburger, Reblochon, Livarot, Tilsit, and Gubbeen cheeses. In: *Cheese and Microbes*. American Society of Microbiology, pp. 219–250.
- Conesa, A., Götz, S., 2008. Blast2GO: a comprehensive suite for functional analysis in plant genomics. *Int. J. Plant Genomics* 2008, 619832.
- de Melo, A.G., Labrie, S.J., Dumaresq, J., Roberts, R.J., Tremblay, D.M., Moineau, S., 2016. Complete genome sequence of *Brevibacterium linens* SMQ-1335. *Genome Announc.* 4, e01242-16.
- de Melo, A.G., Levesque, S., Moineau, S., 2018. Phages as friends and enemies in food processing. *Curr. Opin. Biotechnol.* 49, 185–190.
- Delcher, A.L., Bratke, K.A., Powers, E.C., Salzberg, S.L., 2007. Identifying bacterial genes and endosymbiont DNA with Glimmer. *Bioinformatics* 23, 673–679.
- Deveau, H., Labrie, S.J., Chopin, M.C., Moineau, S., 2006. Biodiversity and classification of lactococcal phages. *Appl. Environ. Microbiol.* 72, 4338–4346.
- Filée, J., Baptiste, E., Susko, E., Krisch, H.M., 2006. A selective barrier to horizontal gene transfer in the T4-type bacteriophages that has preserved a core genome with the viral replication and structural genes. *Mol. Biol. Evol.* 23, 1688–1696.
- Forquin, M.P., Duvergey, H., Proux, C., Loux, V., Mounier, J., Landaud, S., Coppée, J.Y., Gibrat, J.F., Bonnarme, P., Martin-Verstraete, I., Vallaeys, T., 2009. Identification of *Brevibacteriaceae* by multilocus sequence typing and comparative genomic hybridization analyses. *Appl. Environ. Microbiol.* 75, 6406–6409.
- Fortier, L.-C., Moineau, S., 2009. Phage production and maintenance of stocks, including expected stock lifetimes. *Methods Mol. Biol.* 501, 203–219.
- Fortier, L.C., Bransi, A., Moineau, S., 2006. Genome sequence and global gene expression of Q54, a new phage species linking the 936 and c2 phage species of *Lactococcus lactis*. *J. Bacteriol.* 188, 6101–6114.
- Fortier, L.C., Moineau, S., 2007. Morphological and genetic diversity of temperate phages in *Clostridium difficile*. *Appl. Environ. Microbiol.* 73, 7358–7366.
- Garneau, J.E., Moineau, S., 2011. Bacteriophages of lactic acid bacteria and their impact on milk fermentations. *Microb. Cell Fact.* 10, S20.
- Gasteiger, E., Gattiker, A., Hoogland, C., Ivanyi, I., Appel, R.D., Bairoch, A., 2003. ExpASY: the proteomics server for in-depth protein knowledge and analysis. *Nucleic Acids Res.* 31, 3784–3788.
- Gasteiger, E., Hoogland, C., Gattiker, A., Duvaud, S., Wilkins, M.R., Appel, R.D., Bairoch, A., 2005. Protein identification and analysis tools on the ExpASY Server. In: Walker, J.M. (Ed.), *The Proteomics Protocols Handbook*. Humana Press, Totowa, NJ, pp. 571–607.
- Gavrish, E.Y., Krauzova, V.I., Potekhina, N. V., Karasev, S.G., Plotnikova, E.G., Altyntseva, O. V., Korosteleva, L.A., Evtushenko, L.I., 2004. Three new species of *Brevibacteria*,

- Brevibacterium antiquum* sp. nov., *Brevibacterium aurantiacum* sp. nov., and *Brevibacterium permense* sp. nov. *Microbiology* 73, 176–183.
- Geagea, H., Labrie, S.J., Subirade, M., Moineau, S., 2017. The tape measure protein is involved in the heat stability of *Lactococcus lactis* phages. *Appl. Environ. Microbiol.* 84, 1–9.
- Gemayel, R., Vences, M.D., Legendre, M., Verstrepen, K.J., 2010. Variable tandem repeats accelerate evolution of coding and regulatory sequences. *Annu. Rev. Genet.* 44, 445–477.
- Guo, X., Mrázek, J., 2008. Long simple sequence repeats in host-adapted pathogens localize near genes encoding antigens, housekeeping genes, and pseudogenes. *J. Mol. Evol.* 67, 497–509.
- Guy, L., Roat Kultima, J., Andersson, S.G.E., 2010. genoPlotR: comparative gene and genome visualization in R. *Bioinformatics* 26, 2334–2335.
- Hamdi, S., Rousseau, G.M., Labrie, S.J., Tremblay, D.M., Kourda, R.S., Ben Slama, K., Moineau, S., 2017. Characterization of two polyvalent phages infecting *Enterobacteriaceae*. *Sci. Rep.* 7, 40349.
- <https://www.ncbi.nlm.nih.gov/orffinder/>, n.d. ORF Finder (Open Reading Frame Finder).
- Hyatt, D., Chen, G.-L., Locascio, P.F., Land, M.L., Larimer, F.W., Hauser, L.J., 2010. Prodigal: prokaryotic gene recognition and translation initiation site identification. *BMC Bioinformatics* 11, 119.
- Irlinger, F., Mounier, J., 2009. Microbial interactions in cheese: implications for cheese quality and safety. *Curr. Opin. Biotechnol.* 20, 142–148.
- Jacobs-Sera, D., Marinelli, L., Bowman, C., Broussard, G., Guerrero Bustamante, C., Boyle, M., Petrova, Z., Dedrick, R., Pope, W., Modlin, R., Hendrix, R.W., Hatfull, G.F., 2012. On the nature of mycobacteriophage diversity and host preference. *Virology* 434, 187–201.
- Jansen, A., Gemayel, R., Verstrepen, K.J., 2012. Unstable microsatellite repeats facilitate rapid evolution of coding and regulatory sequences. *Repetitive DNA* 7, 108–125.
- Jansena, A., Gemayela, R., Verstrepena, K.J., Jansen, A., Gemayel, R., Verstrepen, K.J., 2012. Unstable microsatellite repeats facilitate rapid evolution of coding and regulatory sequences. *Repetitive DNA* 7, 108–125.
- Jarvis, A.W., 1978. Serological studies of a host range mutant of a lactic streptococcal bacteriophage. *Appl. Environ. Microbiol.* 36, 785–789.
- Jonge, P.A. d., Meijenfeldt, F.A.B. von, Rooijen, L.E. va., Brouns, S.J.J., Dutilh, B.E., 2019. Evolution of BACON domain tandem repeats in crAssphage and novel gut bacteriophage lineages. *Viruses* 11, 1085.
- Kala, S., Cumby, N., Sadowski, P.D., Hyder, B.Z., Kanelis, V., Davidson, A.R., Maxwell, K.L., 2014. HNH proteins are a widespread component of phage DNA packaging machines. *Proc. Natl. Acad. Sci. U. S. A.* 111, 6022–6027.
- Katsura, I., Hendrix, R.W., 1984. Length determination in bacteriophage Lambda tails. *Cell* 39, 691–698.
- Klyczek, K.K., Bonilla, J.A., Jacobs-Sera, D., Adair, T.L., Afram, P., Allen, K.G., Archambault, M.L., Aziz, R.M., Bagnasco, F.G., Ball, S.L., Barrett, N.A., Benjamin, R.C., Blasi, C.J., Borst, K., Braun, M.A., Broomell, H., Brown, C.B., Brynell, Z.S., Bue, A.B., Burke, S.O., Casazza, W., Cautela, J.A., Chen, K., Chimalakonda, N.S., Chudoff, D., Connor, J.A., Cross, T.S., Curtis, K.N., Dahlke, J.A., Deaton, B.M., Degroote, S.J., Denigris, D.M., Deruff, K.C., Dolan, M., Dunbar, D., Egan, M.S., Evans, D.R., Fahnestock, A.K., Farooq, A., Finn, G., Fratus, C.R., Gaffney, B.L., Garlena, R.A., Garrigan, K.E., Gibbon, B.C., Goedde, M.A., Guerrero Bustamante, C.A., Harrison, M., Hartwell, M.C., Heckman, E.L., Huang, J., Hughes, L.E., Hyduchak, K.M., Jacob, A.E., Kaku, M., Karstens, A.W., Kenna, M.A., Khetarpal, S., King, R.A., Kobokovich, A.L.,

- Kolev, H., Konde, S.A., Kriese, E., Lamey, M.E., Lantz, C.N., Lapin, J.S., Lawson, T.O., Lee, I.Y., Lee, S.M., Lee-Soety, J.Y., Lehmann, E.M., London, S.C., Lopez, A.J., Lynch, K.C., Mageeney, C.M., Martynyuk, T., Mathew, K.J., Mavrich, T.N., McDaniel, C.M., McDonald, H., McManus, C.J., Medrano, J.E., Mele, F.E., Menninger, J.E., Miller, S.N., Minick, J.E., Nabua, C.T., Napoli, C.K., Nkangabwa, M., Oates, E.A., Ott, C.T., Pellerino, S.K., Pinamont, W.J., Pirnie, R.T., Pizzorno, M.C., Plautz, E.J., Pope, W.H., Pruett, K.M., Rickstrew, G., Rimple, P.A., Rinehart, C.A., Robinson, K.M., Rose, V.A., Russell, D.A., Schick, A.M., Schlossman, J., Schneider, V.M., Sells, C.A., Sieker, J.W., Silva, M.P., Silvi, M.M., Simon, S.E., Staples, A.K., Steed, I.L., Stowe, E.L., Stueven, N.A., Swartz, P.T., Sweet, E.A., Sweetman, A.T., Tender, C., Terry, K., Thomas, C., Thomas, D.S., Thompson, A.R., Vanderveen, L., Varma, R., Vaught, H.L., Vo, Q.D., Vonberg, Z.T., Ware, V.C., Warrad, Y.M., Wathen, K.E., Weinstein, J.L., Wyper, J.F., Yankauskas, J.R., Zhang, C., Hatfull, G.F., 2017. Tales of diversity: genomic and morphological characteristics of forty-six *Arthrobacter* phages. *PLoS One* 12, e0180517.
- Koskella, B., Meaden, S., 2013. Understanding bacteriophage specificity in natural microbial communities. *Viruses* 5, 806–823.
- Kot, W., Neve, H., Heller, K.J., Vogensen, F.K., 2014. Bacteriophages of *Leuconostoc*, *Oenococcus*, and *Weissella*. *Front. Microbiol.* 5, 186.
- Labrie, S., Vukov, N., Loessner, M.J., Moineau, S., 2004. Distribution and composition of the lysis cassette of *Lactococcus lactis* phages and functional analysis of bacteriophage ul36 holin. *FEMS Microbiol. Lett.* 233, 37-43.
- Levesque, S., de Melo, A.G., Labrie, S.J., Moineau, S., 2019. Mobilome of *Brevibacterium aurantiacum* sheds light on its genetic diversity and its adaptation to smear-ripened cheeses. *Front. Microbiol.* 10, 1270.
- Li, H., Durbin, R., 2009. Fast and accurate short read alignment with Burrows-Wheeler transform. *Bioinformatics* 25, 1754–1760.
- Li, H., Handsaker, B., Wysoker, A., Fennell, T., Ruan, J., Homer, N., Marth, G., Abecasis, G., Durbin, R., 2009. The Sequence Alignment/Map format and SAMtools. *Bioinformatics* 25, 2078–2079.
- Lowe, T.M., Eddy, S.R., 1996. TRNAscan-SE: a program for improved detection of transfer RNA genes in genomic sequence. *Nucleic Acids Res.* 25, 955–964.
- Mahony, J., Alqarni, M., Stockdale, S., Spinelli, S., Feyereisen, M., Cambillau, C., Sinderen, D. van, 2016. Functional and structural dissection of the tape measure protein of lactococcal phage TP901-1. *Sci. Rep.* 6, 36667.
- Mahony, J., Deveau, H., Mc Grath, S., Ventura, M., Canchaya, C., Moineau, S., Fitzgerald, G.F., Van Sinderen, D., 2006. Sequence and comparative genomic analysis of lactococcal bacteriophages jj50, 712 and P008: evolutionary insights into the 936 phage species. *FEMS Microbiol. Lett.* 261, 253–261.
- Mahony, J., Tremblay, D.M., Labrie, S.J., Moineau, S., van Sinderen, D., 2015. Investigating the requirement for calcium during lactococcal phage infection. *Int. J. Food Microbiol.* 201, 47–51.
- Mahony, J., van Sinderen, D., 2014. Current taxonomy of phages infecting lactic acid bacteria. *Front. Microbiol.* 5: 7.
- McDonnell, B., Mahony, J., Neve, H., Hanemaaijer, L., Noben, J.P., Kouwen, T., van Sinderen, D., 2016. Identification and analysis of a novel group of bacteriophages infecting the lactic acid bacterium *Streptococcus thermophilus*. *Appl. Environ. Microbiol.* 82, 5153–5165.
- Mercanti, D.J., Rousseau, G.M., Capra, M.L., Quiberoni, A., Tremblay, D.M., Labrie, S.J.,

- Moineau, S., 2016. Genomic diversity of phages infecting probiotic strains of *Lactobacillus paracasei*. *Appl. Environ. Microbiol.* 82, 95–105.
- Moineau, S., Lévesque, C., 2004. Control of bacteriophages in industrial fermentations. In: Kutter, E., Sulakvelidze, A. (Eds.), *Bacteriophages*. CRC Press, Boca Raton, FL, United States of America, pp. 285–296.
- Moineau, S., Pandian, S., Klaenhammer, T.R., 1994. Evolution of a lytic bacteriophage via DNA acquisition from the *Lactococcus lactis* chromosome. *Appl. Environ. Microbiol.* 60, 1832–1841.
- Motta, A.S., Brandelli, A., 2008. Properties and antimicrobial activity of the smear surface cheese coryneform bacterium *Brevibacterium linens*. *Eur. Food Res. Technol.* 227, 1299–1306.
- Mounier, J., 2015. Microbial interactions in smear-ripened cheeses. In: *Diversity, dynamics and functional role of Actinomycetes on European smear ripened cheeses*. Springer International Publishing, Cham, pp. 155–166.
- Mounier, J., Monnet, C., Vallaes, T., Arditi, R., Sarthou, A.S., Hélias, A., Irlinger, F., 2008. Microbial interactions within a cheese microbial community. *Appl. Environ. Microbiol.* 74, 172–181.
- Mrazek, J., Guo, X., Shah, A., 2007. Simple sequence repeats in prokaryotic genomes. *Proc. Natl. Acad. Sci.* 104, 8472–8477.
- Murphy, J., Bottacini, F., Mahony, J., Kelleher, P., Neve, H., Zomer, A., Nauta, A., van Sinderen, D., 2016. Comparative genomics and functional analysis of the 936 group of lactococcal Siphoviridae phages. *Sci. Rep.* 6, 21345.
- Murphy, J., Royer, B., Mahony, J., Hoyles, L., Heller, K., Neve, H., Bonestroo, M., Nauta, A., van Sinderen, D., 2013. Biodiversity of lactococcal bacteriophages isolated from 3 Gouda-type cheese-producing plants. *J. Dairy Sci.* 96, 4945–4957.
- Nurk, S., Bankevich, A., Antipov, D., Gurevich, A., Korobeynikov, A., Lapidus, A., Prjibelsky, A., Pyshkin, A., Sirotkin, A., Sirotkin, Y., Stepanauskas, R., McLean, J., Lasken, R., Clingenpeel, S.R., Woyke, T., Tesler, G., Alekseyev, M.A., Pevzner, P.A., 2013. Assembling genomes and mini-metagenomes from highly chimeric reads. In: Deng, M., Jiang, R., Sun, F., Zhang, X. (Eds.), *Research in computational molecular biology*. Springer Berlin Heidelberg, Berlin, Heidelberg, pp. 158–170.
- Onraedt, A., Soetaert, W., Vandamme, E., 2005. Industrial importance of the genus *Brevibacterium*. *Biotechnol. Lett.* 27, 527–533.
- Pham, N.-P., Layec, S., Dugat-Bony, E., Vidal, M., Irlinger, F., Monnet, C., 2017. Comparative genomic analysis of *Brevibacterium* strains: insights into key genetic determinants involved in adaptation to the cheese habitat. *BMC Genomics.* 18, 955.
- Pope, W.H., Bowman, C.A., Russell, D.A., Jacobs-Sera, D., Asai, D.J., Cresawn, S.G., Jacobs, W.R., Hendrix, R.W., Lawrence, J.G., Hatfull, G.F., 2015. Whole genome comparison of a large collection of mycobacteriophages reveals a continuum of phage genetic diversity. *eLife* 4, e06416.
- Pujato, S.A., Mercanti, D.J., Guglielmotti, D.M., Rousseau, G.M., Moineau, S., Reinheimer, J.A., Quiberoni, A. del L., 2015. Phages of dairy *Leuconostoc mesenteroides*: genomics and factors influencing their adsorption. *Int. J. Food Microbiol.* 201, 58–65.
- Rattray, F.P., Fox, P.F., 1999. Aspects of enzymology and biochemical properties of *Brevibacterium linens* relevant to cheese ripening: a review. *J. Dairy Sci.* 82, 891–909.
- Rousseau, G.M., Moineau, S., 2009. Evolution of *Lactococcus lactis* phages within a cheese factory. *Appl. Environ. Microbiol.* 75, 5336–5344.

- Sambrook, J., Russel, D.W., 2001. Molecular cloning: a laboratory manual, 3rd editio. ed. Cold Spring Harbor Laboratory Press, Cold Spring Harbor, New York.
- Sergueev, K. V., Filippov, A.A., Farlow, J., Su, W., Kvachadze, L., Balarjishvili, N., Kutateladze, M., Nikolich, M.P., 2019. Correlation of host range expansion of therapeutic bacteriophage Sb-1 with allele state at a hypervariable repeat locus. *Appl. Environ. Microbiol.* 85, e01209-19.
- Shapiro, J.W., Putonti, C., 2018. Gene co-occurrence networks reflect bacteriophage ecology and evolution. *mBio.* 9, e01870-17.
- Shine, J., Dalgarno, L., 1974. The 3'-Terminal Sequence of *Escherichia coli* 16S Ribosomal RNA: complementarity to nonsense triplets and ribosome binding sites. *Proc Natl Acad Sci U S A* 71, 1342–1346.
- Shine, J., Dalgarno, L., 1975. Determinant of cistron specificity in bacterial ribosomes. *Nature* 254, 34–38.
- Underwood, S.L., Foto, A., Ray, A.F., Nelms, A.E., Kennedy, K.L., Hartley, S.G., Ryals, L.M., Gurung, C., D'Angelo, W.A., Pope, W.H., Mavrodi, D. V., 2019. Discovery and characterization of bacteriophage LuckyBarnes. *Microbiol. Resour. Announc.* 8, e00330-19.
- Wickham, H., 2016. ggplot2, Second edi. ed, Use R! Springer International Publishing, Cham.
- Wolfe, B.E., Button, J.E., Santarelli, M., Dutton, R.J., 2014. Cheese rind communities provide tractable systems for in situ and in vitro studies of microbial diversity. *Cell* 158, 422–433.
- Zhou, K., Aertsen, A., Michiels, C.W., 2014. The role of variable DNA tandem repeats in bacterial adaptation. *FEMS Microbiol. Rev.* 38, 119–141.

Chapter 3 – Article 3

Mutations in an ATP-binding cassette transporter confer phage resistance in *Brevibacterium aurantiacum*

Alessandra G. de Melo^{1,2}, Geneviève M. Rousseau^{2,3}, Denise M. Tremblay^{2,3}, Pier-Luc Plante^{4,5}, Simon J. Labrie⁶, and Sylvain Moineau^{1,2,3*}

¹ Département de biochimie, de microbiologie et de bio-informatique, Faculté des sciences et de génie, Université Laval, Québec, QC, Canada.

² Groupe de recherche en écologie buccale, Faculté de médecine dentaire, Université Laval, Québec, QC, Canada.

³ Félix d'Hérelle Reference Center for Bacterial Viruses, Faculté de médecine dentaire, Université Laval, Québec, QC, Canada.

⁴ Centre de recherche en infectiologie de l'Université Laval, axe maladies infectieuses et immunitaires, Centre de recherche du CHU de Québec-Université Laval, Québec City, QC, Canada.

⁵ Centre de recherche en données massives, Université Laval, Québec City, Canada.

⁶ SyntBioLab, Lévis, Canada.

Résumé

Brevibacterium aurantiacum se développe à la surface de plusieurs fromages à croûte lavée, participant au développement des saveurs des fromages affinés produits dans le monde. La souche industrielle *B. aurantiacum* SMQ-1335 est utilisée pour la production de fromages, mais elle est sensible aux phages. Une façon de protéger des souches industrielles contre les attaques phagiques est de sélectionner des mutants naturels insensibles aux phages (BIMs, de l'anglais bacteriophage insensitive mutants). Ces BIMs sont sélectionnés après avoir mis en contact la souche sensible avec des phages virulents. Dans ce chapitre, nous avons cherché à comprendre comment *B. aurantiacum* peut devenir résistant au phage virulent AGM1. Pour ce faire, nous avons généré des BIM dans des milieux liquides ou solides et caractérisé 11 d'entre eux. Les analyses microbiologiques ont révélé trois phénotypes: des BIM partiellement résistants aux phages, des BIM bloquant l'adsorption des phages et des BIM entièrement résistants aux phages mais permettant l'adsorption des phages. Nous avons séquencé le génome de ces BIM et les avons comparé à celui de la souche sensible sauvage SMQ-1335. Des analyses de génomique comparative ont révélé que les trois BIM entièrement résistants aux phages et ayant un phénotype non lié à l'adsorption contenaient des mutations dans un système de transport de peptides de type ABC (de l'anglais ATP-binding cassette). Comme le phage AGM1 peut encore s'adsorber sur ces BIM, les mutations dans le transporteur ABC doivent bloquer une étape après l'adsorption virale. Nous postulons que le système de transport du peptide ABC est utilisé par le phage AGM1 pour injecter son génome dans la cellule. Étant donné que *B. aurantiacum* est récalcitrante à la transformation génétique, nous n'avons pas pu effectuer de tests de désactivation ou de complémentation dans la souche sauvage. Par conséquent, nous avons testé si l'inactivation des deux systèmes de transport par perméabilité aux oligopeptides (Opp) de *Lactococcus lactis* MG1363 conférait une résistance aux phages de lactocoques. Bien qu'il ait été possible de déléter chacun des deux systèmes Opp de *L. lactis* en utilisant la technologie CRISPR-Cas9, il n'a pas été possible de désactiver les deux dans une même souche, ce qui suggère qu'au moins un système Opp est essentiel chez *L. lactis* dans nos conditions de laboratoire. Aucune inactivation d'Opp n'a conduit à une résistance contre les phages virulents de lactocoques p2 et c2. Des expériences supplémentaires sont en cours pour caractériser les phénotypes de résistance aux phages dans les BIM de *B. aurantiacum* SMQ-1335.

Abstract

Brevibacterium aurantiacum grows on the surface of several specialty cheeses produced worldwide and participate in the development of their sought-after flavors. The industrial strain *B. aurantiacum* SMQ-1335 is used for the production of washed rind cheeses but virulent phages infecting that strain have emerged. One way to maintain the industrial use of such strains is through the selection of bacteriophage insensitive mutants (BIMs), which are naturally obtained after challenging the sensitive strain with virulent phages. This bacterial subpopulation usually contains mutations in key genes that are necessary to viral infection. Here, we aimed to understand how *B. aurantiacum* SMQ-1335 can become resistant to the virulent siphophage AGM1. We generated BIMs in either liquid or solid media and characterized 11 of them. Microbiological assays revealed three phenotypes: fully resistant adsorption-related BIMs, partially or fully resistant non-adsorption-related BIMs. We sequenced the genome of these BIMs and compared them to the one of the phage-sensitive wild-type strain SMQ-1335. Comparative genome analyses revealed that the three fully resistant non-adsorption-related BIMs contained mutations in an ATP-binding cassette (ABC) transport system, likely involved in taking up extracellular peptides. As phage AGM1 can still efficiently adsorb to these BIMs, the mutations in the ABC-transporter likely block a step following viral adsorption. We postulate that the peptide ABC transport system is used by phage AGM1 to inject its genome into the cell. As *B. aurantiacum* is recalcitrant to genetic transformation, we could not perform knockout or complementation assays in the wild-type strain. Hence, we tested if the inactivation of the two oligopeptide permeases (Opp) transport systems of *Lactococcus lactis* MG1363 would provide resistance to lactococcal siphophages. Although it was possible to knockout each of the two Opp systems of *L. lactis* using the CRISPR-Cas9 technology, it was not possible to inactivate both of them in the same strain, suggesting that at least one Opp system is essential for *L. lactis* growth under our laboratory conditions. None of the Opp inactivation led to resistance against the virulent siphophages p2 and c2. Additional experiments are underway to further characterize the phage resistance phenotypes in BIMs of *B. aurantiacum* SMQ-1335.

Abbreviations

ABC	ATP-binding cassette
Abi	Abortive infection
BIMs	Bacteriophage insensitive mutants
CFU	Colony forming units
CRISPR-Cas	Clustered regularly interspaced short palindromic repeats and CRISPR associated proteins
CRISPR-Cas9	Gene-editing tool using the nuclease Cas9
DNA	Deoxyribonucleic acid
dsDNA	Double strand DNA
LAB	Lactic acid bacteria
MOI	Multiplicity of infection
NBD	Nucleotide binding domain
OD	Optical density
Opp	Oligopeptide permease
ORF	Open reading frame
PAM	Protospacer adjacent motif
PCR	Polymerase chain reaction
PFU	Plaque forming units
PBP	Periplasmic binding protein
RM	Restriction-modification
RNA	Ribonucleic acid
rRNA	Ribosomal RNA
SBP	Substrate binding protein
TMD	Transmembrane domain
tRNA	Transfer RNA

Introduction

Brevibacterium aurantiacum is a dairy bacterium used during the ripening process of washed rind cheeses worldwide. This bacterium grows on the surface of several specialty cheeses, being an important microbial player in the color and flavor development of these sought-after cheeses (Cogan et al., 2014; Levesque et al., 2019; Pham et al., 2017). In dairy facilities, orange-pigment producing *Brevibacterium* strains are commonly identified as *B. linens* (Gavrish et al., 2004). However, recent phylogenetic studies showed that *B. aurantiacum* is prevalent in washed rind cheeses (Cogan et al., 2014; Levesque et al., 2019; Pham et al., 2017). With the recent subdivision of the *B. linens* species, industrial strains previously classified as such have been revisited (Levesque et al., 2019). This is the case of strain SMQ-1335 (de Melo et al., 2016), an industrial strain previously identified as *B. linens*, but reclassified as *B. aurantiacum* (Levesque et al., 2019; Melo et al., 2020).

Selected bacteria are used to ferment and transform milk into valuable dairy products, such as cheese and yogurt. However, the recurrent use of the same dairy strains, grown daily in large quantities in a rich substrate, put them at risk of bacteriophage (or phage) predation. While research on dairy phages focused mostly on virulent phages infecting lactic acid bacteria (LAB), other key microbial species are used during cheese production, such as ripening cultures mentioned above. The interaction of industrial strains with their viral predators in the production environment can cause technological problems during cheesemaking as it can lead to the delay in the process or inconsistencies in the final products (Garneau and Moineau, 2011).

The complex nature of the cheese rinds makes the replacement or the rotation of ripening strains rather difficult as it may alter the organoleptic attributes of the cheese and generate a product with inconsistent features, consequently affecting consumer acceptability of the cheese. Therefore, the replacement of a ripening strain is often considered as a last resort (Melo et al., 2020). However, keeping a phage-sensitive strain for cheese production puts the ripening process at risk as well as allowing persistence and buildup of viral population in the dairy facilities.

One way to protect a phage-sensitive industrial strain is through the generation of naturally resistant derivatives, called bacteriophage insensitive mutants or BIMs, which are selected after

challenging the sensitive strain with virulent phages (Deveau et al., 2008; Garneau and Moineau, 2011). A bacterial subpopulation may contain mutations in genes necessary for viral infection. Therefore, the sensitive population that comes into contact with phages will die after viral infection, but the strong selective pressure will allow to isolate a subpopulation of phage-resistant cells. Bacteria also possess several mechanisms to resist phages, such as CRISPR-Cas, restriction-modification (RM) systems, and abortive infection (Abi) to name a few (Bernheim and Sorek, 2019; Hampton et al., 2020; Labrie et al., 2010). These systems are globally widespread in bacterial strains and act to arrest phage infection after the injection of the viral genome into the cells. However, bacteria can also prevent viral infection through mutations in genes coding for phage receptors. The latter strategy is usually phage-host dependent as it involves cell components involved in other cell processes.

Here, we aimed to study how *B. aurantiacum* evolves phage resistance. Through the generation and selection of eleven BIMs with three different phenotypes, we identify mutations in several host components. A group of three BIMs presented mutations in an ATP-binding cassette (ABC) transport system, likely involved in peptide transport. The mutations in the ABC transporter led to a full resistance phenotype, although permissive to viral adsorption. These results show that these mutations provide resistance at a step after phage adsorption.

Results and Discussion

Generation of bacteriophage-insensitive mutants (BIMs)

When challenging the bacterial strain *Brevibacterium aurantiacum* SMQ-1335 with phages on a plate using a low multiplicity of infection (MOI of 0.3), numerous colonies emerged. However, several of these colonies were sensitive to viral infection. The few colonies that were phage-resistant were due to failing in phage adsorption (data not shown). In order to select mutants containing different phenotypes, we challenged *B. aurantiacum* SMQ-1335 with the virulent phage AGM1 in liquid and solid media. To generate BIMs in liquid media, an aliquot of undiluted phage lysate was combined with the overnight bacterial culture in broth and the mixture was incubated for an extended period of time (Figure 13). To obtain isolated colonies potentially resistant to the

phages, the overgrown culture was either streaked (BIM 1 and BIM 2) or diluted and plated with (BIM 3 and BIM 4) or without (BIM 5) additional phages.

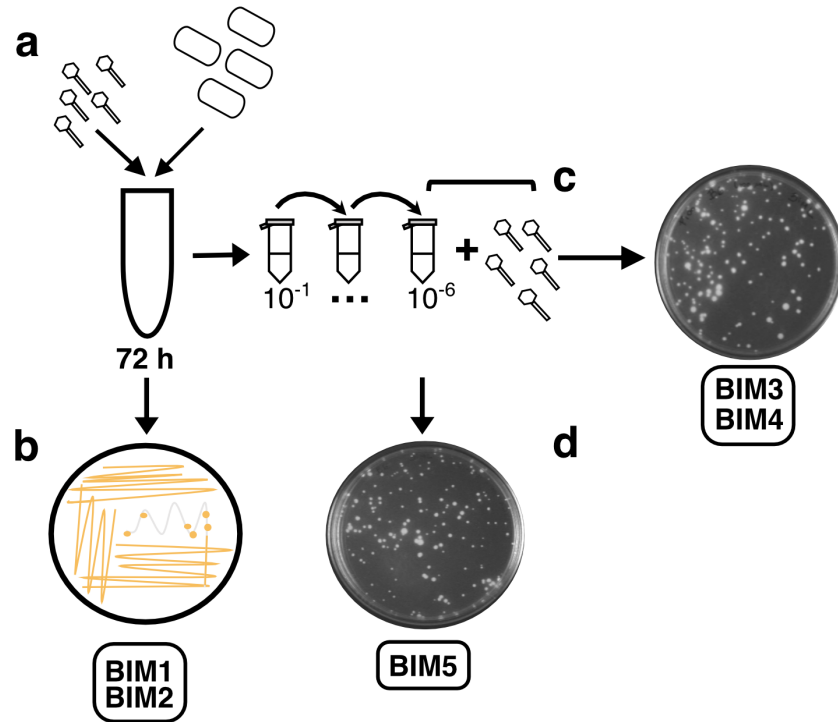


Figure 13. Schematic representation of mutants' selection from liquid media. (a) Mutants were generated by combining phages and bacteria in broth. (b) The overgrown culture was directly streaked before and after centrifugation. (c) After diluting the overgrown cells, they were directly plated with an aliquot of phage lysate or (d) without any additional phages.

We tested an alternative protocol in solid media (Figure 14), where different ratios of phages and bacteria were combined to achieve MOIs ranging from 3E-07 to 300. As expected, increasing the MOI led to a decreased in the number of surviving colonies. From this assay, we selected and purified six isolated colonies from the MOI 300 (BIM 6-8) and 30 (BIM 9-11) to be further characterized for their resistance phenotype.

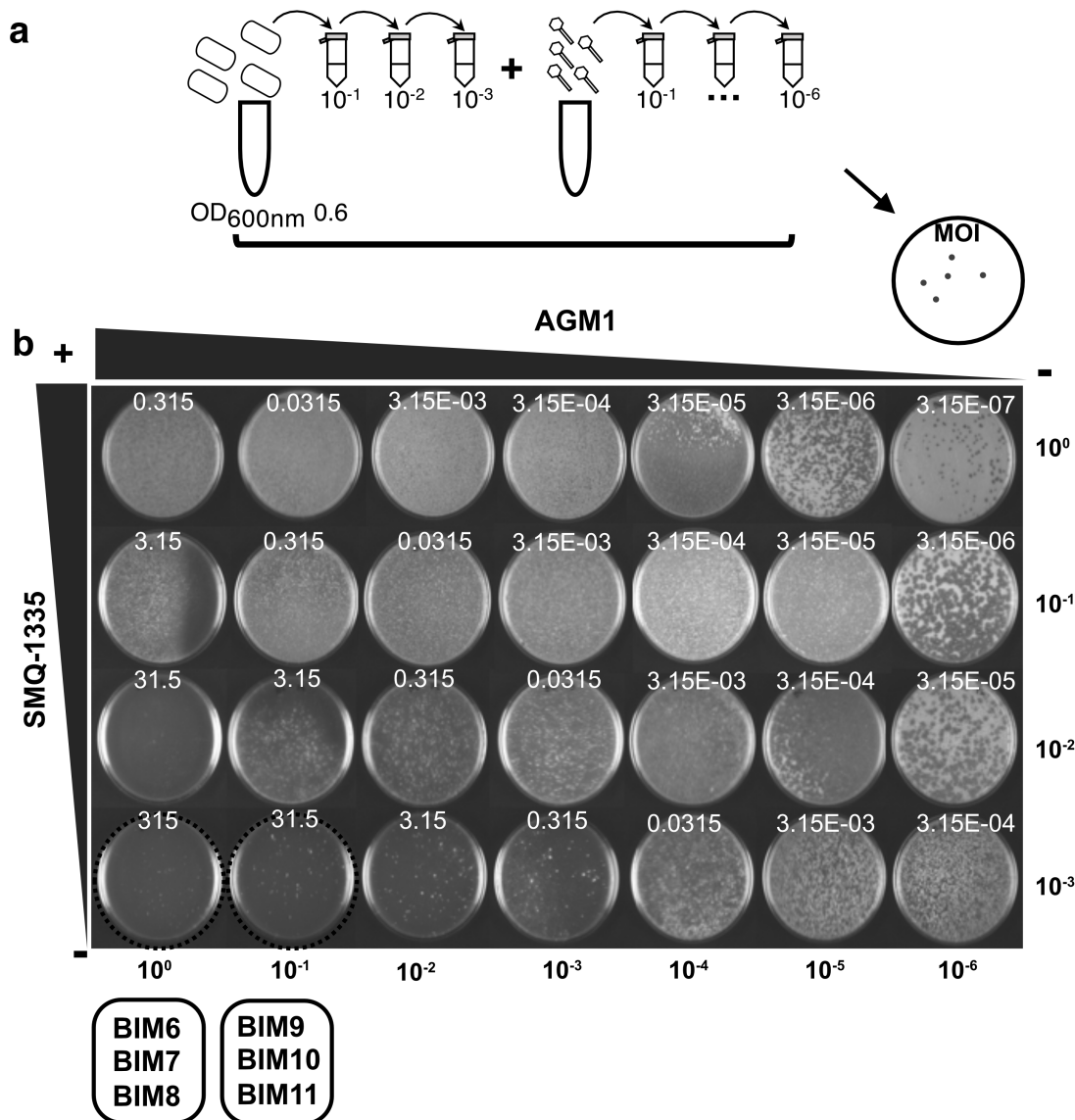


Figure 14. Schematic representation of mutants' generation and selection in solid media.

(a) Phages and bacteria were diluted and combined at several multiplicities of infection. (b) The row 10⁰ represents the BIM generation with exponentially grown undiluted bacteria (OD_{600nm} 0.6) mixed with a serially diluted phage lysate. The subsequent rows (10⁻¹ – 10⁻³) represent different dilutions of the bacteria, combined with serial dilutions of the phage lysate shown by each column (10⁰ - 10⁻⁶). Dashed circles mark the plates and conditions from which the BIMs were selected. Estimated MOIs are represented at the top of the plates.

Characterization experiments show BIMs with three different phenotypes

The eleven BIMs described in the previous sections were characterized in regard to phage adsorption and to the level of phage resistance (Figure 15). Phage AGM1 adsorbed to eight out of eleven BIMs (i.e. BIM 1, BIM 2, BIM 4 – BIM 6, BIM 9 – BIM 11). However, five of them were only partially resistant to this phage (i.e. BIM 1, BIM 5, BIM 9, BIM 10, BIM 11). The other three non-adsorption BIMs (BIM 2, BIM 4, BIM 6) and the adsorption BIMs (BIM 3, BIM 7, BIM 8) were fully resistant to the phages. Thus, BIM 2, BIM 4 and BIM 6 are fully phage resistant while still allowing phage adsorption, indicating that the resistance mechanism is blocking some step downstream adsorption. BIM 3, BIM 7 and BIM 8 are also insensitive to phage AGM1, but this virus did not adsorb to these BIMs, indicating that the resistance phenotype is likely due to mutations in receptors at the cell surface. Phage AGM1 adsorbed to the partially resistant BIM 1, BIM 5, BIM9, BIM 10 and BIM 11.

Additional phage sensitivity assays were performed using other 13 other virulent phages previously described (Melo et al., 2020). BIMs were also fully or partially resistant to these phages. We observed that when a BIM was fully resistant to phage AGM1, it was also fully resistant to the other thirteen phages tested. The same was seen for the partially resistant BIMs. However, these BIMs were slightly more sensitive to the phages AGM4, AGM9, AGM10, AGM11, AGM13, and AGM14. All these six phages have a 51-bp duplication in *orf27*, which encodes for a protein of unknown function. This duplication led to the formation of tandem repeats in these six phages (Melo et al., 2020). The genome context of the *orf27* shows this gene is located right downstream of genes belonging to the host-lysis module of these phages. Perhaps, one can speculate that the tandem repeat formed in *orf27* could potentially have an effect on the phage virulence, offering some sort of competitive advantage to these phages.

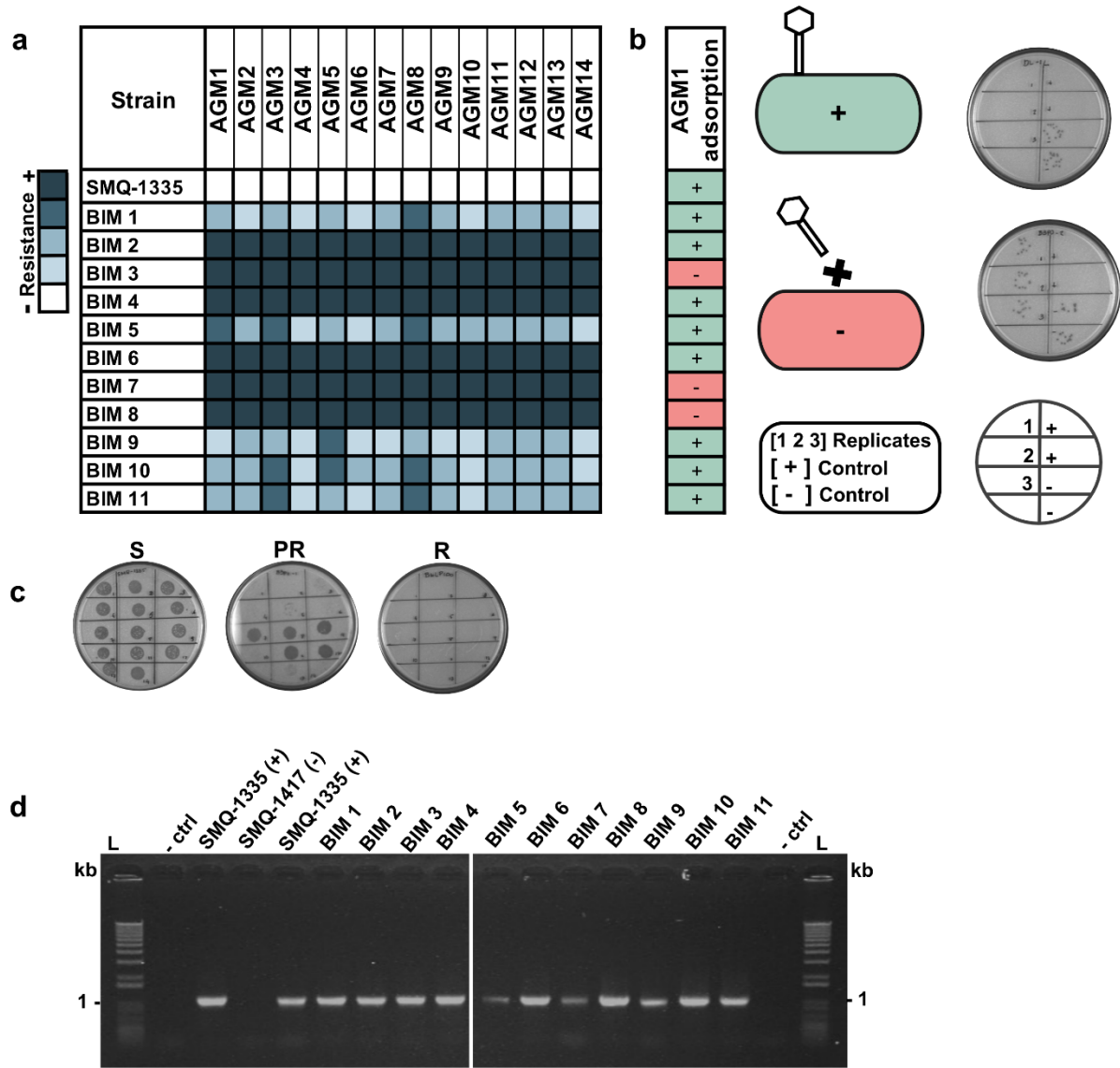


Figure 15. Characterization of phage insensitive mutants. (a) Eleven BIMs were tested for sensitivity to fourteen *B. aurantiacum* phages, with profiles ranging from fully resistant (darker blue) to partially resistant (other shades of blue) in comparison to the sensitive wild-type strain (white). (b) Phage AGM1 adsorbed (+) or not (-) to the BIMs. In the plate representation in (b), the positive control (+) is phages added to the wild-type strain and negative control (-) is phages added to media. Positive and negative controls were spotted in technical duplicates. (c) Example of sensitive (S), partially resistant (PR) and fully resistant (R) profiles are presented. (d) PCR targeting a region in SMQ-1335 genome horizontally transferred from *Micrococcus luteus* confirming that the BIMs are derivatives of SMQ-1335. L: ladder; - ctrl: negative control; (+) positive or (-) negative strains for the PCR.

BIMs are derivatives of SMQ-1335

To confirm that the BIMs were derivatives of SMQ-1335, we PCR-amplified a chromosomal region that is unique to this strain (genomic position 2,204,340 to 2,212,655 of GenBank accession number CP017150.1). We previously showed that SMQ-1335 has a genomic region of 8,316 bp acquired by horizontal gene transfer (HGT) from *Micrococcus luteus* (Levesque et al., 2019). This region encodes for a nucleotide-binding protein, a thioredoxin, a heat shock protein, transcriptional repressor HspR, a nucleotide exchange factor GrpE and molecular chaperones ClpB, DnaJ and DnaK. *B. aurantiacum* strain SMQ-1417 was used as a negative control. The targeted region was amplified for all eleven BIMs and SMQ-1335 but was negative for SMQ-1417 (Figure 15d). These results confirmed that the BIMs were indeed derivatives of SMQ-1335. Then, BIM 1 to BIM 11 were selected for genome sequencing using Illumina MiSeq and compared to the wild-type genome of SMQ-1335, which was previously sequenced using PacBio (Melo et al., 2020). The wild-type strain SMQ-1335 was also re-sequenced using Illumina MiSeq.

The new genome sequence of SMQ-1335 wild-type has divergences in comparison to the previously sequenced reference genome

Fourteen polymorphisms were found between the reference sequence and the newly sequenced genome of the wild-type strain. These differences were also found in the genome of the BIMs and can be seen in Table 3. The fact that these mutations were also found in the genome of the BIMs suggests that the laboratory stock culture used for BIM generation already contained polymorphisms. Discrepancies between data from the PacBio and Illumina have been observed previously (Labrie et al., 2015). Moreover, as they were found in both sensitive and resistant cultures, they are likely not involved in phage resistance. Therefore, they were removed from the candidate mutations that have to be present exclusively in the genome of the BIMs. These results show the importance of resequencing the genome of the wild-type strains used to generate BIMs to rule out newly acquired mutations through mutual evolution or sequencing errors. Otherwise, the search for a candidate mutation involved in phage resistance could become a much more laborious task.

Table 3. Divergences between the reference genome of SMQ-1335 (GenBank accession CP017150.1) and the new sequence from Illumina.

Genome position	Locus	Function	Mutation (nt)	Codon change	Amino acid change
2,584,293	BLSMQ_RS11950	Amino acid adenylation domain-containing protein	G > A	GAG > GAA	E > E
2,937,610	BLSMQ_RS13505	Cysteine desulfurase NifS	T > TC		Frameshift
2,937,642	BLSMQ_RS13505	Cysteine desulfurase NifS	G > GC		Frameshift
2,937,686	BLSMQ_RS13505	Cysteine desulfurase NifS	G > GC		Frameshift
2,937,798	BLSMQ_RS13505	Cysteine desulfurase NifS	T > TG		Frameshift
2,939,122	BLSMQ_RS13515	Hypothetical protein	C > CG		Frameshift
2,939,304	BLSMQ_RS13515	Hypothetical protein	AC > A		Frameshift
2,939,385	BLSMQ_RS13515	Hypothetical protein	A > AC		Frameshift
2,939,461	BLSMQ_RS13515	Hypothetical protein	G > GC		Frameshift
2,939,486	BLSMQ_RS13515	Hypothetical protein	T > TC		Frameshift
2,939,541	Intergenic		G > GC		
2,939,682	BLSMQ_RS13520	Hypothetical protein	C > CT		Frameshift
2,939,961	BLSMQ_RS13520	Hypothetical protein	G > GC		Frameshift
3,968,817	BLSMQ_RS18210	N-acetylglucosamine-6-phosphate deacetylase	T > C	GAG > GGG*	E > G

* Gene in the antiparallel strand.

Mutations in the genome of BIMs from different phenotypic groups

Only four mutations were shared among several BIMs and they are summarized in Table 4.

Table 4. Mutations shared among all BIMs.

Genome position	Locus	Function	Mutation (nt)	Codon change	Amino acid change	Shared by
569,906	Intergenic		TC > TCC			All BIMs, except BIM11
596,534	Intergenic		G > C			Partially resistant BIMs
3,539,282	BLSMQ_RS16285	Hypothetical protein	G > T	ACC > ACA*	T > T	All BIMs
3,542,973	BLSMQ_RS16305	Transcriptional regulator	CG > C		Frameshift	Partially resistant BIMs, except BIM9

* Gene in the antiparallel strand.

One silent mutation in a hypothetical protein (BLSMQ_RS16285) was shared by all the BIMs in the three observed phenotypes (Table 4), suggesting that perhaps this mutation could confer some

degree of phage resistance, but other mutations are clearly at play. Two other mutations were found in intergenic regions. The mutation at position 569,906 was found in all BIMs, except BIM 11, again alluding to a role in phage resistance but with the help of other mutations. The point mutation at position 596,534 (G to C substitution) was found only in the five BIMs (BIM 1, BIM 5, BIM 9, BIM 10, and BIM 11) with a partially phage-resistant phenotype (Table 4). This region is flanked by two *orfs* oriented in opposite directions, encoding a C4-dicarboxylate transporter DctA (BLSMQ_RS02655) and a hypothetical protein (BLSMQ_RS02660). The latter protein of unknown function is part of an operon with a histidine kinase, a response regulator, and another hypothetical protein. As we did not see a phage adsorption deficiency, this may indicate that an interference with the phage lytic cycle occurs in the steps downstream to phage adsorption. Finally, a point mutation leading to a frameshift was found in a putative transcriptional regulator (BLSMQ-16305) in ten of the eleven BIMs (Table 4).

Except for BIM 9, the ten other BIMs had unique mutations in their genomes (Table 5). The mutations that are exclusive to each BIM vary from missense, nonsense, synonymous and frameshift variations. Two groups of BIMs have mutations that generated a full viral resistance phenotype. These groups are the adsorption related BIMs, which are composed of BIM 3, BIM 7 and BIM8, or the non-adsorption-related BIMs, composed by BIM 2, BIM 4 and BIM 6.

Six set of primers (Table 8) were designed to verify the non-synonymous mutations in the genome of the fully resistant BIMs (i.e. BIM 2, BIM 3, BIM 4, BIM 6, BIM 7, and BIM 8). Each PCR amplification was performed for all eleven BIMs and the wild-type strain. The PCRs confirmed every polymorphism detected in the respective BIM, being negative for the wild-type and remaining BIMs. Of note, a seventh set of primers targeting a gene encoding for a putative integral membrane protein (BLSMQ_RS13515) was used as a control. This region diverged from the reference SMQ-1335 genome and the newly sequenced genome (Table 3). It was used to verify the sequencing results. The modifications shown in this region for the reference versus the new sequence were all confirmed by PCR for both wild-type and BIMs.

Table 5. Non-shared mutations in the genome of the BIMs.

Genome position	Locus	Function	Mutation (nt)	Codon change	Amino acid change	Mutant
961,486	BLSMQ_RS04310	ATP-dependent Clp protease proteolytic subunit	C > A	G <u>C</u> C > G <u>C</u> A	A > A	BIM3
1,104,132	BLSMQ_RS04975	DUF2520 domain-containing protein	C > T	G <u>C</u> G > G <u>T</u> G	A > V	BIM10
1,338,019	BLSMQ_RS06155	50S ribosomal protein L6	A > T	<u>A</u> AC > <u>I</u> AC	N > Y	BIM1
1,452,482	BLSMQ_RS06710	Transcriptional regulator	G > T	<u>G</u> CA > <u>I</u> CA	A > S	BIM8
1,788,753	BLSMQ_RS08270	ABC transporter substrate-binding protein	A > AC		Frameshift	BIM4
1,790,666	BLSMQ_RS08275	ABC transporter permease	T > G	T <u>A</u> I > T <u>A</u> G	Y > Stop	BIM6
1,790,812	BLSMQ_RS08275	ABC transporter permease	T > TG		Frameshift	BIM2
2,290,354	BLSMQ_RS10675	ABC transporter ATP-binding protein	G > T	A <u>C</u> C > A <u>C</u> A*	T > T	BIM6
2,333,738	BLSMQ_RS10880	Hypothetical protein	G > A	A <u>G</u> C > A <u>G</u> T*	S > S	BIM1
2,359,593	BLSMQ_RS10980	Acetyl-CoA carboxyl transferase	C > G	G <u>A</u> G > G <u>A</u> C*	E > D	BIM11
2,428,221	BLSMQ_RS11310	PhoH family protein	G > C	<u>C</u> CC > <u>C</u> GC*	P > R	BIM5
2,913,168	BLSMQ_RS13405	ABC transporter ATP-binding protein	C > A	<u>G</u> AG > <u>I</u> AG*	E > Stop	BIM4
2,936,261	BLSMQ_RS13500	tRNA 2-thiouridine(34) synthase MnmA	G > A	A <u>C</u> C > A <u>C</u> I*	T > T	BIM7
3,052,911	BLSMQ_RS13985	Hypothetical protein	G > T	G <u>T</u> G > G <u>T</u> I	V > V	BIM11
3,173,843	BLSMQ_RS14610	Type II secretion system protein	G > C	<u>G</u> GA > <u>C</u> GA	G > R	BIM6
3,486,957	BLSMQ_RS16030	Hypothetical protein	G > C	<u>C</u> CG > <u>C</u> GG*	P > R	BIM11
3,547,477	BLSMQ_RS19650	Hypothetical protein	C > A	<u>G</u> AC > <u>A</u> AC*	L > M	BIM11
3,567,410	BLSMQ_RS16410	Sodium-dependent transporter	G > A	C <u>T</u> G > C <u>T</u> A	L > L	BIM8
3,921,707	Intergenic		C > A			BIM3
4,104,277	BLSMQ_RS18790	Hypothetical protein	C > T	<u>G</u> GA > <u>A</u> GA*	G > R	BIM11

* Gene in the antiparallel strand.

Adsorption-blocking BIMs do not share exclusive mutations in similar genes or operons

We expected that BIMs belonging to the same phenotypic group would share mutations in genes or operons related to phage resistance. Surprisingly, each of the three fully resistant BIMs (BIM 3, BIM 7, BIM 8) that had a phage adsorption-blocking phenotype contained unique mutations in unrelated genes. BIM 3 has one synonymous mutation in a gene encoding an ATP-dependent protease (Clp) and a single nucleotide variation in an intergenic region upstream a diene lactone hydrolase gene. BIM 8 has one missense mutation in a transcriptional regulator gene (AraC family)

and a synonymous mutation in a gene encoding a sodium-dependent transporter. The non-synonymous mutation in BIM 8 is located at the 3' end of the transcriptional regulator gene.

BIM 7 has only one exclusive synonymous mutation in the gene coding for a tRNA 2-thiouridine (34) synthase (MnmA). Because BIM 7 only has one more mutation that could lead to phage insensitivity (as the other two were shared with partially resistant BIMs), perhaps one can assume that the synonymous mutation in the tRNA 2-thiouridine(34) synthase (MnmA) gene can confer full resistance to phage AGM1 alone or as a consequent build up from the other shared mutations. This protein catalyzes a post-transcriptional modification of the wobble position in glutamate, glutamine, and lysine tRNA molecules, which acts to stabilize the anticodon structure, improving ribosomal binding and overall efficiency of the translational process (Black and dos Santos, 2015). Consequently, the absence of the 2-thiouridine modification in tRNA has been associated to growth defects in bacteria attributed to accumulation of frame-shifting during translation (Black and dos Santos, 2015). Therefore, it is possible that the mutation in the MnmA gene has an effect not only in the protein itself, but in other cell processes associated to it. Interestingly, the genome context of the tRNA 2-thiouridine(34) synthase gene shows that this gene is located in a genomic region where several variations were found in the wild-type and BIMs in comparison to the reference genome (Table 3, BLSMQ_RS13505 to BLSMQ_RS13520), including a cysteine desulfurase NifS (BLSMQ_RS13505) that acts with MnmA in the post-translational modification of the tRNA molecules.

Growing evidence from both comparative and experimental studies suggests that synonymous mutations are not as silent as previously thought. Most often, they are either nearly neutral or deleterious and infrequently, weakly beneficial (Bailey et al., 2014). In fact, synonymous mutations may impact gene expression, mRNA stability and folding, protein folding and fitness (Bailey et al., 2014). For instance, in the Gram-negative bacteria, *Salmonella enterica*, four synonymous mutations in the rpsT gene (encoding ribosomal protein S20) reduced bacterial fitness, which was measured by the growth rate of the wild-type and mutants (Knöppel et al., 2016). Considering the possible effects of synonymous mutations in a range of genes and organisms, it is possible that the mutation in the MnmA gene of BIM 7 has an impact in phage resistance, but experimental evidence would be necessary to confirm these results. However, *B. aurantiacum* is recalcitrant to genetic transformation and as of now there is no protocol available

to transform this species, what make the test of the impact of this mutation by complementation assays, for example, currently impossible.

We also analyzed the prevalence of the tRNAs carrying the anticodons of the wild-type SMQ-1335 or the BIMs, involved in synonymous mutations (Table 6). In the specific case of BIM 7, a more frequently used codon (ACC) for the amino acid threonine was replaced for a less frequent codon (ACT), with both tRNA being present in the genome. However, when we consider the codon usage bias of only the MnmA gene, the ACC codon is used 63.3% whereas the ACT codon is not used in this gene. When we consider all the synonymous mutations found in the BIMs, we observed no specific pattern in the synonymous mutations and codon usage. In some cases, the tRNA of the mutated codon was absent in the cell, such as for tRNA-Serine (codon AGT) or tRNA-Valine (codon GTT). However, for tRNA-Lysine, for instance, a less frequent codon (AAA; 25%) was replaced by one that it is more frequently used (AAG; 75%). For the amino acid alanine, one codon in the genome was replaced by another (GCA), with more than one copy of the tRNA-Alanine. It has been suggested that synonymous mutations have an impact on the mRNA folding into its secondary and tertiary structure, which affects the rate of the mRNA degradation and the efficiency of translation (Hunt et al., 2014). Perhaps, the synonymous variation may have an effect on the mRNA secondary structure other than a direct relationship with the prevalence of the tRNA and wild-type codon usage bias.

Table 6. Codon usage for wild-type and mutated codons of BIMs synonymous mutations.

Position of synonymous mutation	tRNA	SMQ-1335 tRNAs					Codon usage	
		Total tRNA	Possible codon	Present	Absent	Repeat	Original	Replacement
961,486	tRNA-Ala	4/49	4	3	GCT	GCA	GCC (31%)	GCA (21%)
2,214,182	tRNA-Lys	2/49	2	2			AAA (25%)	AAG (75%)
2,290,354	tRNA-Thr	3/49	4	3	ACT		ACC (32%)	ACA (18%)
2,333,738	tRNA-Ser	4/49	6	4	AGT, TCT		AGC (16%)	AGT (9%)
2,936,261	tRNA-Thr	3/49	4	3			ACC (32%)	ACT (17%)
3,052,911	tRNA-Val	3/49	4	3	GTT		GTG (32%)	GTT (18%)
3,539,282	tRNA-Thr	3/49	4	3			ACC (32%)	ACA (18%)
3,567,410	tRNA-Leu	5/49	6	5	CTT		CTG (30%)	CTA (5%)

An ATP-Binding Cassette (ABC) transport system is likely involved in phage insensitivity

Among the eleven selected BIMs, three of them (i.e. BIM 2, BIM 4, BIM 6) were fully resistant to phages and it was not due to a defect in phage adsorption. Therefore, phage infection was blocked in a subsequent step of the lytic cycle. Of interest, these three BIMs have mutations in an operon coding for a putative ATP-Binding Cassette (ABC) peptide transport system (Table 5, locus BLSMQ_RS08270 and BLSMQ_RS08275). A more detailed analysis of the conserved domains is described below. Figure 16 shows a schematic representation of the genomic and functional context of this operon and the mutations found in the BIMs.

ABC transporters are a large family of bacterial proteins associated to the cell membrane. By hydrolyzing ATP as energy source, these systems import or export a wide variety of substrates, including micronutrients, sugars, amino acids and peptides, antibiotics, and antimicrobial peptides (Durmort and Brown, 2015). Import ABC transporters share a common architecture composed of a substrate-binding protein (SBP) or receptor, two transmembrane domains (TMDs, often termed permeases) and two nucleotide-binding domains (NBDs, often ATPases) (Durmort and Brown, 2015). In *B. aurantiacum* SMQ-1335, the targeted cluster is composed of four genes: one coding for a SBP, two for permeases and only one for an ATP-binding protein (Figure 16).

BIM 4 has a frameshift mutation in the gene encoding for the SBP. This mutation maintains the first 26 amino acids (out of 601) of the parental SBP sequence but generates a stop codon fifteen nucleotides after the frameshift. The SBPs are often associated with membrane protein complexes for transport or signal transduction (Berntsson et al., 2010). In Gram-positive, SBPs are anchored to the outer surface of the cell membrane through a lipid modification or covalently linked to the translocation pore (Berntsson et al., 2009; Durmort and Brown, 2015).

Both BIM 2 and BIM 6 contain mutations in the gene encoding for one of the ABC-transporter permeases (i.e. subunit B). BIM 2 has a frameshift mutation at the codon for the amino acid 75 (out of 514), thereby generating a completely different amino acid sequence after the frameshift mutation. In the BIM 6, a nonsense mutation generated in the same permease gene generated a much shorter protein with only 25 amino acids out of 514. Therefore, it is likely that both mutations inactivated this protein. Of note, the conserved domain of the wild-type permease is from the

amino acids 46 to 512. The permeases are integral membrane proteins, generally composed of 5-10 transmembrane helices, that form pores through which the substrate is transported across the cell membrane (Durmort and Brown, 2015).

BIM 2 is the only one of the fully resistant non-adsorption-related BIMs with no other unique mutation. This BIM, as the other two, shares two mutations with the other two phenotypic groups of BIMs, but the mutation in the permease gene is the only one in the genome of BIM 2 that may explain the complete phage resistance phenotype. BIM 4 has a unique nonsense mutation in a gene coding for an ATP-binding protein (BLSMQ_RS13405) of another ABC-transport operon, possibly also involved in peptide transport according to the conserved domains identified. The conserved domains of the ATP-binding protein are in the N-terminal portion of the protein (amino acid 1-327), while the nonsense mutation was found towards the C-terminal region of the protein, preserving most of the wild-type sequence (517/701 amino acids). Therefore, it is likely that this protein is still functional. BIM 6 has two other unique mutations. One is a synonymous mutation located in a gene coding for another ATP-binding protein (213/261 amino acids; BLSMQ_RS10675) of an iron transporter. The second mutation is in a gene coding for a type II secretion system protein (position 283 of 312 amino acids).

Despite BIM 4 and BIM 6 having additional mutations, the fact that all three fully resistant non-adsorption-related BIMs have mutations in a common operon strongly suggests that this ABC-transport system could be involved in phage resistance. We chose this ABC-transport operon specified in Figure 16 as the main candidate in our study of phage-host interaction. As the substrate binding protein of the ABC transporters in Gram-positive bacteria are anchored on the cell membrane (Berntsson et al., 2009), we hypothesize that the mutations in this system impede the entry of the viral genome. Therefore, after the initial contact of the viral particles with a phage receptor on the cell surface, phage AGM1 could use the peptide import ABC transporter to inject its genome into the bacterial cytoplasm. In the genome injection of the *E. coli* phage HK97, for example, after binding to the bacterial receptor LamB, the tail tape measure protein of the phage interacts with the inner membrane glucose transporter protein PtsG of the host, with the help of the periplasmic chaperone FkpA (Cumby et al., 2015).

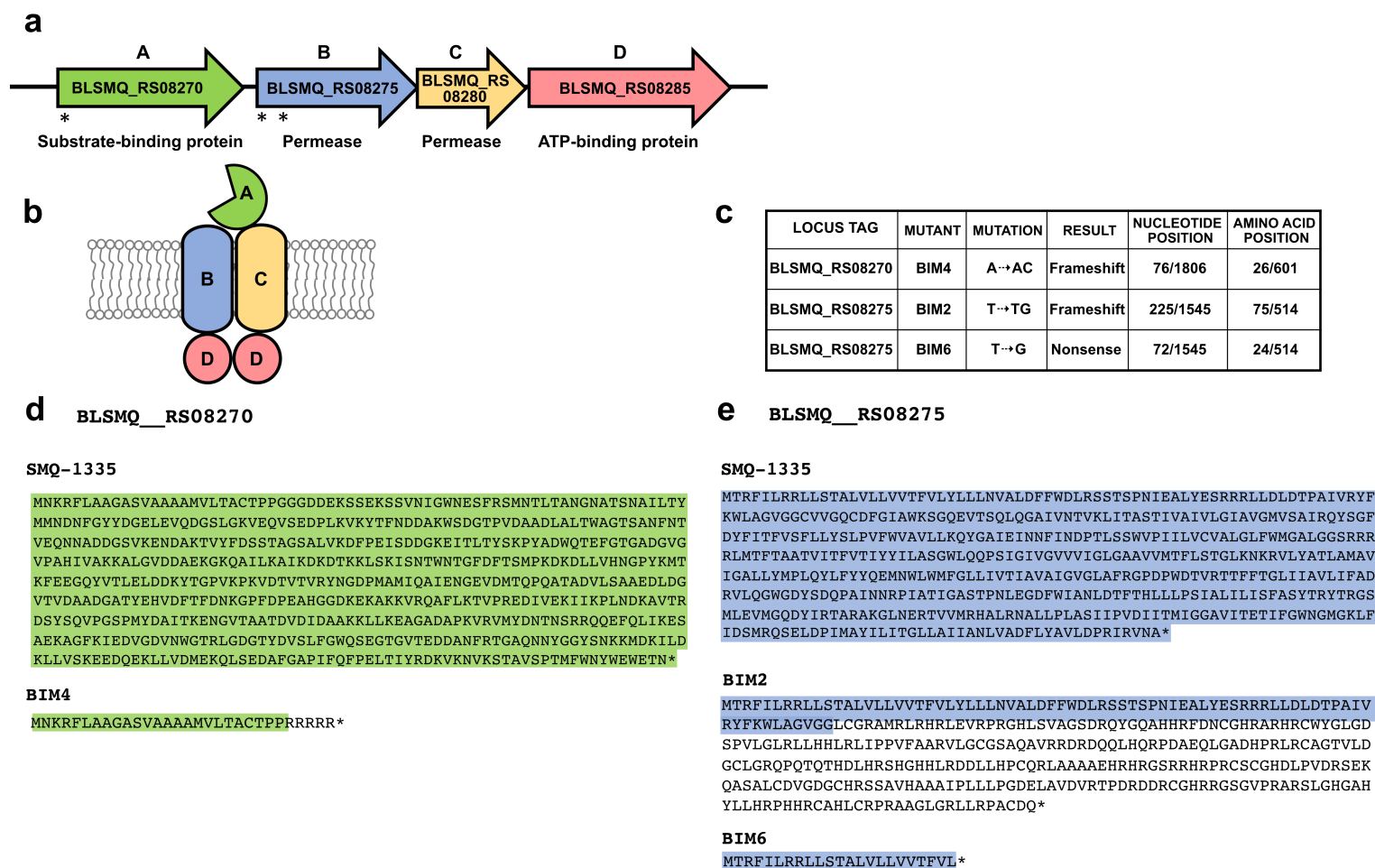


Figure 16. Schematic representation of the ABC-transport system of *B. aurantiacum* SMQ-1335 and mutations in the BIMs. (a) The ABC-transport system operon of SMQ-1335 is composed of four genes. The asterisks (*) represents the approximate location of the mutations present in the genes. The same color scheme used for the genes is also applied for the respective proteins represented in (b) and (d). (b) An example of transmembrane protein complex of ABC transport system. (c) The BIMs have mutations in the substrate-binding protein (A) or in one of the permeases (B). (d, e) Representation of the final amino acid sequences obtained when the mutations are present in the genes encoding for the substrate-binding protein (d) or in the permease I when compared to the SMQ-1335 wild-type gene.

Analysis of the ABC-transport system of *B. aurantiacum* SMQ-1335

B. aurantiacum SMQ-1335 has approximately 70 single genes or operons annotated as component of an ABC-transport systems and involved in the transport of a range of substrates, such as iron, ectoine and glycine betaine. Among these ABC transporters, six have annotations pointing to the involvement in peptide transport (data not shown). Because of the importance of peptides for growth, it is not uncommon for bacteria to have multiple peptide transport systems with overlapping functions (Wang et al., 2004). We did not find sequence homology between the mutated systems and other ABC transporters in SMQ-1335 genome. It is likely that these various systems have distinct specificities for amino acids or peptides than the one mutated in BIM 2, BIM 4 and BIM 6. The substrate specificity of ABC transporters is usually experimentally characterized using a combination of genetic and biochemical approaches. Due to the experimental limitations with *B. aurantiacum*, we first used *in silico* analysis for the presence of structural homologs, predicted transmembrane and conserved domains.

In several dairy species, such as *Lactococcus lactis* and *Streptococcus thermophilus*, the ABC transporters involved in peptide import, such as the oligopeptide permease (Opp) transport systems are composed of five subunits, which are the substrate-binding protein or receptor (OppA) that determines the specificity of the transport system, two integral membrane proteins (OppB and OppC) that form the translocation pore, and two nucleotide-binding domains (OppD and OppF) that bind and hydrolyze ATP to drive the transport process (Berntsson et al., 2009).

ABC-transport systems usually show high degree of similarity among each other. The specificity determinant of these systems is usually given by the SBP as this protein binds to the substrate and delivers to the transmembrane complex (Charbonnel et al., 2003). Previous annotations classified the mutated ABC-transporter of SMQ-1335 as an oligopeptide transport system. Although it is possible to find conserved domains for the SBP, it is often difficult to differentiate *in silico* if they are involved in oligopeptide (OppA), dipeptide (DppA) or nickel transport (NikA), due to the homology of their conserved domains. The analysis of conserved domains of SBP of SMQ-1335 showed a hit with a dipeptide-binding protein (DdpA; COG0747; amino acids 17-599), which is part of the type 2 periplasmic binding protein (PBP2) superfamily involved in the transport of nickel, dipeptides or oligopeptides (superfamily cluster accession number cl01709).

The DppA and OppA binding proteins differ not only in the length of the peptide transported, but also in the cellular processes in which they are involved. DppA binds dipeptides and is involved in peptide chemotaxis (Abouhamad et al., 1991). OppA binds to a wide range of peptides (2-35 amino acids) and plays a role in the recycling of cell wall peptides and uptake of peptides as a nutrient source (Abouhamad et al., 1991; Berntsson et al., 2009). The specificity of SBPs for peptides of a particular length is determined by salt bridges that constrain the positions of their N and C termini in the binding site (Berntsson et al., 2009). Identifying the specific substrate for an ABC transporter can be inferred by bioinformatic analysis but requires experimental support (Durmort and Brown, 2015), which is not available for the ABC transporters of *B. aurantiacum*.

The permeases components of the peptide ABC-transporters are OppB (or DppB) and OppC (or DppC). These integral membrane proteins, which contain 5 to 10 transmembrane I domains, form pores to translocate the substrate through the membrane (Durmort and Brown, 2015). The OppB/DppB-like protein (COG0601; amino acid 46-512) of SMQ-1335 has twelve TM domains, whereas the OppC/DppC-like protein (COG1173) possesses six TM domains. These two permeases have conserved regions of the inner membrane component of binding-protein-dependent transport system (BPD; pfam00528), with the most conserved region located in a cytoplasmic loop between two TM helices (amino acids 369-512 in the B subunit and 139-323 in the C subunit). They also have the TM subunit that generally bind type 2 PBPs (cd06261) or SBPs.

The cytoplasmic component of the system is the ATPase that drives the substrate translocation through the hydrolysis of ATP (Rahman et al., 2019). The nucleotide-binding domain can be formed by a single or two separated proteins (subunits D and F) (Durmort and Brown, 2015). In SMQ-1335, the mutated ABC-transporter appears to have only one ATP-binding protein. Interestingly, this protein has the approximate size of both OppD and OppF of the well-studied oligopeptide transport system of *Lactococcus lactis* MG1363. The N-terminal of the ATP-binding protein of SMQ-1335 has a non-specific hit for nickel D superfamily, whereas its C-terminal has non-specific hits for nickel E superfamily, similarly to what it is seen for MG1363 OppD and OppF, respectively. A conserved domain for an ATPase component of ABC-type glutathione transport system (GsiA; COG1123) that contains duplicated ATPase domain was identified. This result also indicates that this single protein might hold the ATPase function similar to that found in OppD and OppF in other species.

One important step in the study of phage-host interactions is to confirm the effect of any given mutation through classical gene knockout and complementation assays. However, species of the genus *Brevibacterium* has been recalcitrant to genetic transformation (Levesque, 2018). As an alternative, we used another phage-host system to evaluate if the knockout of an orthologous ABC-transporter would give resistance to phage infection. *L. lactis* MG1363 and its infecting phages were chosen as the phage-host system to test the hypothesis as they share several conserved domains in their ABC-transporter proteins.

***Lactococcus lactis* MG1363 as a model to study the role of permeases in phage resistance**

L. lactis MG1363 (Wegmann et al., 2007) and its virulent phages p2 (Higgins et al., 1988), c2 (Lubbers et al., 1995), jj50 (Mahony et al., 2006), 712 (Rincé et al., 2000) and sk1 (Chandry et al., 1997) were chosen as phage-host systems to investigate the role of the peptide ABC-transporter in phage infection. Although this phage-host system differed in many ways of *B. aurantiacum* and its phages, *L. lactis* MG1363 possesses a well-characterized oligopeptide transport system and several distinct lytic phages can infect it. Finally, an exogenous CRISPR-Cas9 genetic tool was previously designed to edit the genome of *L. lactis*.

L. lactis MG1363 has two homologous operons (Opp1 or Opp2) involved in oligopeptide transport. While Opp1 has all five complete genes (*oppABCD*), Opp2 has two genes encoding the ATP-binding proteins (i.e. *oppD2* and *oppF2*), which are classified as pseudogenes. The *oppB* genes of MG1363 have approximately 82% nucleotides identity, whereas the encoded proteins have more than 90% amino acid identity between them. A two-step strategy was designed to inactivate each *oppB* gene. Table 9 contains the primers and Table 10 the biological materials used for the genome editing experiments.

To inactivate the permease genes of the Opp systems of *L. lactis* MG1363, we used the CRISPR-Cas9 technology (Lemay et al., 2019, 2018). First, MG1363 was transformed with the plasmid pKO-B2, containing the recombination template to inactivate the *oppB2* gene. A CRISPR-Cas9 containing plasmid pL2Cas9 was designed to target the permease genes, *oppB1* or *oppB2*, which generated pL2Cas9-spB1 or pL2Cas9-spB2, respectively. MG1363::pKO-B2 was then transformed with pL2Cas9-spB2. As the Opp system is essential for growth of *L. lactis* in milk,

which is poor in amino acids (Charbonnel et al., 2003), MG1363 transformants were plated in GM17 selection plates supplemented or not with casaminoacids as the amino acids source. Colonies were screened for the presence of the deletion and also for the presence of the spacer-repeat unit in pL2Cas9-spB2. A *L. lactis* MG1363::pKO-B2::pL2Cas9-spB2 colony, containing both the target deletion and spacer-repeat unit in pL2Cas9-spB2, was then selected. *L. lactis* MG1363::pKO-B2::pL2Cas9-spB2 was grown in broth with no antibiotic pressure to lose the plasmids. Although, pL2Cas9-spB2 was readily lost after three passages, pKO-B2 was stable after 20 passages. Therefore, we use pL2Cas9-spCm targeting the chloramphenicol resistance gene of the backbone plasmid of pKO-B2 (i.e. pNZ123), which forced the loss of pKO-B2. Then, MG1363 Δ *oppB2* was tested for phage sensitivity and was found to be as phage sensitive as the wild-type strain.

As the deletion of the *oppB* genes in both operons could be necessary for phage resistance in *L. lactis*, we tried to inactivate *oppB1*. The pKO-B1 plasmid, containing the recombination template to inactivate the *oppB1* gene was transformed into MG1363 Δ *oppB2*. Then, MG1363 Δ *oppB2*::pKO-B1 was afterwards transformed with pL2Cas9-spB1, which targeted the *oppB1* gene. When compared to the controls containing empty plasmids or pL2Cas9 not targeting any site of MG1363 genome, a visible difference was found in the number of transformants. Only a few colonies were obtained with pL2Cas9 targeting *oppB1* as compared to the empty vector for which numerous colonies were obtained (data not shown). In addition, for the few colonies retrieved in these knockout experiments, we observed the deletion of the repeat-spacer unit or genome rearrangements. Taken altogether, the deletion of both *oppB* genes appears to be toxic in *L. lactis*. Therefore, one of these systems seems essential for the growth of *L. lactis* MG1363 in our experimental conditions.

Conclusion

The production of washed rind cheeses makes the rotation of ripening strains difficult. Therefore, the generation of bacteriophage insensitive mutants provides a mean to extend the use of performing bacterial strains. Here, we generated several BIMs of the ripening strain *B. aurantiacum* SMQ-1335 by challenging it with the virulent phage AGM1. By combining different strategies and phage-bacteria ratio, we selected BIMs with three phenotype groups. While two

groups did not share mutations, the three fully resistant non-adsorption-related BIMs had mutations in a common gene cluster, likely coding for a peptide import ATP-binding cassette transporter. Because these three BIMs are permissive to viral adsorption, but yet fully phage resistant, we hypothesized that this peptide ABC-transporter is used by phage AGM1 during the genome injection process. The fact that *B. aurantiacum* SMQ-1335 is currently recalcitrant to genetic transformation, we could not confirm the role of these mutations using complementation assays. Our study offers the first report on phage-host interaction in *B. aurantiacum* and perhaps also on the role of a peptide transporter in phage infection.

Materials and Methods

Bacterial growth and phage assays

B. aurantiacum cells were grown in supplemented Elliker media as previously described (Melo et al., 2020). Phage assays were also performed as reported elsewhere (Melo et al., 2020). *B. aurantiacum* strains and phages used in this study are listed in Table 7. Phage sensitive assay was performed using the lysates of fourteen phages (AGM1 to AGM14) diluted 1000-fold. Five microliters of the diluted lysates were spotted on the bacterial strains as described (Melo et al., 2020).

Generation of bacteriophage insensitive mutants (BIMs)

BIMs were isolated by challenging the wild-type sensitive host *B. aurantiacum* SMQ-1335 with phage AGM1 using different approaches. First, BIMs were generated in liquid media using an assay similar to a phage propagation, but the infected culture was incubated for a longer period of time to allow the growth of resistant derivatives. In this assay, 100 μ L of phage lysate and 100 μ L of an overnight bacterial culture were mixed in Elliker broth supplemented with 20 mM CaCl₂. The tubes were incubated for three days at 23°C while being agitated at 200 rpm until the cells started growing after the lysis of the sensitive cell population. The surviving culture was streaked on Elliker agar plates and an isolated colony was selected (BIM 1). A 1-mL aliquot of the culture was also transferred to a microtube and centrifuged at 14,243 x g for 1 min. After discarding the supernatant, part of the pellet was streaked on Elliker plates, where an isolated colony was selected and named BIM 2. Serial dilutions of the phage-challenged culture were performed up to 10⁻⁶.

Then, 100 μ L of the diluted bacteria (10^{-5} or 10^{-6}) was plated with 100 μ L of phage lysate, generating BIM 3 and BIM 4, respectively. Finally, the bacterial culture diluted to 10^{-6} was directly plated on Elliker plates to select isolated colonies, which generated BIM 5.

Table 7. List of *B. aurantiacum* strains and phages used in this study.

<i>B. aurantiacum</i> strains and phages	Characteristics	Source
Bacterial strains		
<i>B. aurantiacum</i> SMQ-1335	Host of phage AGM1 to AGM14; GenBank CP017150.1	de Melo <i>et al.</i> , 2016
BIM 1, BIM 5, BIM 9, BIM 10 and BIM11	Partially phage-insensitive mutant* derived from SMQ-1335, permissive to adsorption	This study
BIM 2, BIM 4 and BIM 6	Fully phage-insensitive mutant* derived from SMQ-1335, permissive to adsorption	This study
BIM 3, BIM 7 and BIM 8	Fully phage-insensitive mutant* derived from SMQ-1335, resistant to adsorption	This study
<i>B. aurantiacum</i> SMQ-1417	Phage resistant strain, GenBank CP02530.1	Levesque <i>et al.</i> , 2019
<i>B. aurantiacum</i> SMQ-1418	Phage resistant strain, GenBank CP02531.1	Levesque <i>et al.</i> , 2019
<i>B. aurantiacum</i> SMQ-1419	Phage resistant strain, GenBank CP02532.1	Levesque <i>et al.</i> , 2019
<i>B. aurantiacum</i> SMQ-1420	Phage resistant strain, GenBank CP02533.1	Levesque <i>et al.</i> , 2019
<i>B. aurantiacum</i> SMQ-1421	Phage resistant strain, GenBank CP02534.1	Levesque <i>et al.</i> , 2019
Phages		
AGM1	Virulent phage of <i>B. aurantiacum</i> SMQ-1335, GenBank MN023176	de Melo <i>et al.</i> , 2020
AGM2 - AGM14	Virulent phages of <i>B. aurantiacum</i> SMQ-1335, GenBank MN023177 - MN023189	de Melo <i>et al.</i> , 2020

* Phage insensitivity due to various types of mutations

BIMs were also generated using solid media. *B. aurantiacum* SMQ-1335 was grown until the optical density (OD₆₀₀) of 0.6. To achieve different multiplicity of infection (MOI), bacterial culture and phage lysate were diluted (up to 10^{-3} or 10^{-6} , respectively) and a 100 μ L aliquot of each was combined in 3 mL of Elliker soft agar supplemented with 20 mM CaCl₂ and added to a Elliker bottom layer (Melo *et al.*, 2020). Bacterial and phage dilutions were plated to determine the colony forming units (CFU) and the plaque forming units (PFU), respectively, and calculate the MOI. The plates were incubated at 23°C until the naturally resistant colonies appeared, which led to the

selection of BIM 6 to BIM 11. The selected colonies of SMQ-1335 derivatives (BIM 1 – BIM11) were streaked three times to ensure purity and stored in glycerol (15%) at -80°C.

Confirmation of BIMs as derivatives of SMQ-1335

To confirm that the BIMs were derivatives of the strain SMQ-1335, a set of primers targeting a unique genomic region of SMQ-1335 (Levesque et al., 2019) was designed and is presented in Table 8 (primer set BL_2204307-Fwd and BL_2205371-Rev). The sensitive strain, SMQ-1335, was used as a positive control for the amplification, whereas the strain *B. aurantiacum* SMQ-1417 was used as a negative control for the presence of this genomic region. This PCR was also used to assure the purity of the BIMs DNA before sequencing.

Table 8. List of primers used for *B. aurantiacum* SMQ-1335 and its derivatives.

Function	Primer	Sequence 5'→3'
Confirmation of BIMs as SMQ-1335 derivatives	BL_2204307-Fwd	CTTGCGAGCCTCTAACAAACC
	BL_2205371-Rev	GGAAGGACAGCCGTCTTTCCG
Screening for mutation in the intergenic region or non-synonymous in genes		
Intergenic region	BL_3921543-Fwd	CGCTCGTCTCTACGACTGG
	BL_3921953-Rev	CGAAGACGATCTCACCAGTCAGG
Transcriptional regulator	BLSMQ_RS06710-Fwd	GGGTTGGCTGTTGTCATTCC
	BLSMQ_RS06710-Rev	GGAATCGGCATCGTCAAGC
ABC-transporter substrate-binding protein	BLSMQ_RS08270-Fwd	CCGGTGAATTAACCTTTGAGG
	BLSMQ_RS08270-Rev	GCCATCGGACCATTGG
ABC-transporter permease	BLSMQ_RS08275-Fwd	CGGTCCGGTTCTCCTTCACC
	BLSMQ_RS08275-Rev	GCGAGAGCATTTTCGTTGTCG
ABC-transporter ATP-binding protein	BLSMQ_RS13405-Fwd	GCGACGAAGAGGTAGGACAGC
	BLSMQ_RS13405-Rev	GGCAAGATCGTCATCAATGG
Putative integral membrane protein	BLSMQ_RS13515-Fwd	CGAGAGATTGGACCAGATTTGG
	BLSMQ_RS13515-Rev	CCGTATGTGCTGATGAAGACC
Type II secretion system protein	BLSMQ_RS14610-Fwd	CGGACACATCATCAACGACTGG
	BLSMQ_RS14610-Rev	CGGTGAATCGGTTTCATCAGATGG

Adsorption assays

The sensitive strain *B. aurantiacum* SMQ-1335 or the purified BIMs were inoculated from the -80°C glycerol stocks in 10 mL Elliker broth (Melo et al., 2020) and incubated for approximately 20 h at 23°C with agitation (200 rpm). These cultures were used to perform phage adsorption assays. Phage titration was performed beforehand as previously described (Melo et al., 2020), then phage AGM1 lysate was diluted to have a solution of 1.0×10^4 PFU/mL. Subsequently, 100 µL of

the appropriate dilution was taken and added to 900 μL of Elliker broth (negative control), the sensitive strain SMQ-1335 (positive control) or the resistant derivatives in a microtube to a final titer of 1.0×10^3 PFU/mL and mixed by inversion. Phages were let to adsorb for 15 minutes at room temperature, then the tubes were centrifuged at $14,243 \times g$ for 1 min, in a microcentrifuge. Ten microliters of the supernatants were spotted on the wild-type sensitive strain SMQ-1335 to verify the positive or negative phage adsorption.

DNA isolation, genome sequencing and mutations mapping

BIMs and wild-type strain genomic DNAs were extracted as previously described (O'Sullivan and Klaenhammer, 1993) and modified elsewhere (Bissonnette et al., 2000). In addition, the incubation period was prolonged after adding lysozyme for approximately 1 hour or until cell lysis was observed. Bacterial DNA was quantified using a Quant-iT PicoGreen dsDNA Assay kit and libraries were prepared using a Nextera XT DNA Sample kit, Nextera XT Index kit, and a MiSeq Reagent kit v2, according to manufacturing instructions. Genomes were sequenced using Illumina MiSeq (Centre de recherche du CHU de Québec, Université Laval). The reads were assembled and mapped on SMQ-1335 genome (de Melo et al., 2016) as described elsewhere (Labrie et al., 2019). The average read coverages ranged from 13- to 57-fold for the BIMs and 31-fold for the wild-type strain. Results were visualized using Geneious[®] 11.1.2 (Biomatters).

Verification of mutations using PCR and Sanger sequencing

Primer sets were designed to verify that the non-synonymous mutations found in the BIMs genome sequence were absent from the wild-type strain. The primers used are listed in Table 8. PCRs for all the eleven BIMs and wild-type strain were carried out by adding G+C enhancer to the reaction to improve specificity as described elsewhere (Melo et al., 2020). PCR products were sent for Sanger sequencing (Plateforme de Séquençage et de Génotypage des Génomes du Centre Hospitalier de l'Université Laval). Sanger reads were mapped to the wild-type and BIMs genomes using Geneious[®] 11.1.2 (Biomatters) to verify the mutations.

***In silico* analysis of ABC transport system and other mutated regions in the BIMs**

BLASTp (Altschul et al., 1997) was used to verify the annotation of the wild-type proteins that were mutated in the BIMs and predict their function. The ABC transport system of BIM 2, BIM 4 and BIM 6 was analyzed according to the presence of conserved domains using the Conserved Domain Database (CDD) (Lu et al., 2020). The CDD is a database superset including NCBI curated domains and data imported from the external databases Pfam (Protein families), SMART (Simple Modular Architecture Research Tool), COG (Clusters of Orthologous Groups of proteins), PRK (Protein Klusters), and TIGRFAMs (The Institute for Genomic Research's database of protein families). A set of conserved domain models that generates overlapping annotation on the same protein sequences is considered a superfamily cluster and its accession number begins with the prefix "cl" for "cluster".

Genome editing of *L. lactis* MG1363

L. lactis MG1363 (Wegmann et al., 2007) was chosen to test the potential involvement of peptide transport systems in phage resistance. As this strain has two homologous systems in its genome, experiments were designed to inactivate sequentially the OppB1 (*llmg_0699*) and OppB2 (*llmg_2026*) genes in the two operons. Genome editing was performed using pL2Cas9 as previously described (Lemay et al., 2019). The protospacer adjacent motif (PAM) 5'-NGG-3' was searched in the *oppB1* or *oppB2* genes of *L. lactis* MG1363 using Geneious® 11.1.2 (Biomatters) to select for spacers. pL2Cas9 targeting the *oppB1* or *oppB2* genes (pL2Cas9-spB1, pL2Cas9-spB2) were construct by introducing the desired spacer sequence in pL2Cas9. The growth conditions for *L. lactis* MG1363 with or without selection markers has been described elsewhere (Lemay et al., 2019). For electroporation experiments, 300 ng of pL2Cas9 empty or pL2Cas9 targeting (pL2Cas9-spB1, pL2Cas9-spB2 and pL2Cas9-spCm) and 100 ng of pNZ123 (De Vos, 1987) and its derivatives (pKO-B1 or pKO-B2) were transformed into *L. lactis* MG1363. The list of primers is presented in Table 9 while all the bacterial strains, phages and plasmids used are listed in Table 10. These primers were used to construct pL2Cas9 with targeting spacers (pL2Cas9-spB1 or pL2Cas9-spB2) and pNZ123 with recombination templates (pKO-B1 or pKO-B2) as well as to screen for plasmids and deletions. The repair templates were designed to generate an out of frame mutation, conserving only 40 or 59 bp of the original nucleotide sequence at the 5'-end of

the 960-bp genes. The methods for plasmid construction and genome editing were described in details elsewhere (Lemay et al., 2017, 2018, 2019).

Table 9. Primers designed for the genome editing of MG1363.

Function	Primers	5'→3'	Features
Spacer cloning in pL2Cas9 targeting oppB1	SpacerB1 - Fwd SpacerB1 - Rev	<u>aaac</u> GCTAAATTGATGCCTGGTATCCTTTTTCAg <u>aaaac</u> TGAAAAAGGATCACCAGGCATCAATTTAGC	ssDNA
Repair template Insert A	oppF1 - insA - Fwd oppB1 - insA -Rev	<u>GAAAATATGCACTCGAGAAGCTTGAGCTCT</u> GCTGTTGATGGAGTAGATTTAACG <u>CCTTATTGAATCCGAATTCGTTGGTCAACC</u> GGATCATCAATAAAATACG	Overhang in pNZ123 Overhang in insert B
Repair template Insert B	oppB1 - insB - Fwd oppC1 - insB -Rev	<u>TAATTATTAGACGATTTTTATTGATGATCC</u> GGTTGACCCACGAATTCG <u>ATTACAGCTCCAGATCCAGTACTGAATTC</u> TGGTCAGCCACTCGTCTTAGT	Overhang in insert A Overhang in pNZ123
Screening for deletion of oppB1 targetting the chromosome	B1del-Fwd1 B1del-Rev1 B1del-Fwd2 B1del-Rev2	GTCATTGGGCTGCTTTGC GCACTTAGGAGTGTAGCTGC CTGGTTTCTTTAATCGAGTGAC TCACTCCTTATTGAATCCG	One of the primers bind to the chromosome and the other to the repair template
Spacer cloning in pL2Cas9 targetting oppB2	SpacerB2 - Fwd SpacerB2 - Rev	<u>aaac</u> TCTGTATGTGGCCCAATTAACCAGAGAAAg <u>aaaac</u> TTTCTCTGGTTTAATTGGCCACATACAGA	ssDNA
Repair template Insert A2	oppF2 - insA - Fwd oppB2 - insA -Rev	<u>GAAAATATGCACTCGAGAAGCTTGAGCTCT</u> GTGAGCGAAATTCCTAGTCT <u>TCCTTACTGAATCCGAATTCGAGGGTCAAC</u> CTCAGGATAAATAGTTGC	Overhang in pNZ123 Overhang in insert B
Repair template Insert B2	oppB2 - insB - Fwd oppC2 - insB -Rev	<u>ATTGATGATTCCGCAACTATTTATCCTGAG</u> GTTGACCCTCGAATTCGGATTC <u>ATTACAGCTCCAGATCCAGTACTGAATTC</u> TCTTACTGCTTGTCTTTGGTC	Overhang in insert A Overhang in pNZ123
Screening for deletion of oppB2 targetting the chromosome	B2del-Fwd1 B2del-Rev1 B2del-Fwd2 B2del-Rev2	CTGCAGTCGTTGCCAATAAAG CGTGTATTATTGATGATTCCG CCAGTTTATCATGTTTGAGTTC CAAACCGTTAAAGGAGGTG	One of the primers bind to the chromosome and the other to the repair template
Sequencing crRNA	Cas9_S.pyo_F6 crRNA_S.pyo_R	GTTCTTAGTGCATATAACAAACATAGAGAC CCAAGTAGCGAAGCGAGC	Lemay <i>et al.</i> 2018
Linearization pNZ123	pNZ_XbaI_F pNZ_XbaI_R	AGAGCTCAAGCTTCTCGAG AGAATTCAGTACTGGATCTGGAGC	Lemay <i>et al.</i> 2018
Screening inserts in pNZ123	pNZins_F pNZins_R	AATGTCACCTAACCTGCCCGG CATTGAACATGCTGAAGAGC	Lemay <i>et al.</i> 2018

Table 10. List of bacterial strains, phages and plasmids used in the genome editing of MG1363.

Bacterial strains, phages and plasmids	Characteristics	Source
Bacterial strains		
<i>E. coli</i> NEB5 α	Competent cells for cloning	NEB
<i>L. lactis</i> MG1363	Wild-type strain, GenBank NC_009004.1	Wegmann <i>et al.</i> , 2007
MG1363 Δ <i>oppB2</i>	Derivative of <i>L. lactis</i> MG1363, deletion in gene <i>limg_2026</i>	This study
Phages		
p2	Virulent phage of <i>L. lactis</i> MG1363, GenBank GQ979703	Higgins <i>et al.</i> , 1988
jj50	Lactococcal phage, GenBank NC_008371.1	Mahony <i>et al.</i> , 2006
sk1	Lactococcal phage, GenBank AF011378	Chandry <i>et al.</i> , 1997
712	Lactococcal phage, GenBank DQ227763	Rincé <i>et al.</i> , 2000
c2	Lactococcal phage, GenBank NC_001706.1	Lubbers <i>et al.</i> , 1995
Plasmids		
pNZ123	High copy number plasmid, Cm ^r , 2.5 kb	de Vos, 1987
pL2Cas9	pTRKL2::CRISPR-Cas9, Emr, 12.2 kb	Lemay <i>et al.</i> , 2018
pL2Cas9-spB1	pL2Cas9 with a spacer targeting <i>L. lactis</i> MG1363 gene <i>limg_0699</i>	This study
pL2Cas9-spB2	pL2Cas9 with a spacer targeting <i>L. lactis</i> MG1363 gene <i>limg_2026</i>	This study
pL2Cas9-spCm	pL2Cas9 with a spacer targeting Cm ^r gene of pNZ123	Unpublished
pKO-B1	pNZ123 with recombination template for Δ <i>oppB1</i> (<i>limg_0699</i>), 4.4 kb	This study
pKO-B2	pNZ123 with recombination template for Δ <i>oppB2</i> (<i>limg_2026</i>), 4.2 kb	This study

References

- Abouhamad, W.N., Manson, M., Gibson, M.M., Higgins, C.F., 1991. Peptide transport and chemotaxis in *Escherichia coli* and *Salmonella typhimurium*: characterization of the dipeptide permease (Dpp) and the dipeptide-binding protein. *Mol. Microbiol.* 5, 1035–1047.
- Altschul, S.F., Madden, T.L., Schäffer, A.A., Zhang, J., Zhang, Z., Miller, W., Lipman, D.J., 1997. Gapped BLAST and PSI-BLAST: a new generation of protein database search programs. *Nucleic Acids Res.* 25, 3389–3402.
- Bailey, S.F., Hinz, A., Kassen, R., 2014. Adaptive synonymous mutations in an experimentally evolved *Pseudomonas fluorescens* population. *Nat. Commun.* 5, 4076.
- Bernheim, A., Sorek, R., 2019. The pan-immune system of bacteria: antiviral defence as a community resource. *Nat. Rev. Microbiol.* 113–119.
- Berntsson, R.P.A., Doeven, M.K., Fusetti, F., Duurkens, R.H., Sengupta, D., Marrink, S.J., Thunnissen, A.M.W.H., Poolman, B., Slotboom, D.J., 2009. The structural basis for peptide selection by the transport receptor OppA. *EMBO J.* 28, 1332–1340.
- Berntsson, R.P.A., Smits, S.H.J., Schmitt, L., Slotboom, D.J., Poolman, B., 2010. A structural classification of substrate-binding proteins. *FEBS Lett.* 584, 2606–2617.
- Bissonnette, F., Labrie, S., Deveau, H., Lamoureux, M., Moineau, S., 2000. Characterization of mesophilic mixed starter cultures used for the manufacture of aged cheddar cheese. *J. Dairy Sci.* 83, 620–627.
- Chandry, P.S., Moore, S.C., Boyce, J.D., Davidson, B.E., Hillier, A.J., 1997. Analysis of the DNA sequence, gene expression, origin of replication and modular structure of the *Lactococcus lactis* lytic bacteriophage sk1. *Mol. Microbiol.* 26, 49–64.
- Charbonnel, P., Lamarque, M., Piard, J.C., Gilbert, C., Juillard, V., Atlan, D., 2003. Diversity of oligopeptide transport specificity in *Lactococcus lactis* species: a tool to unravel the role of OppA in uptake specificity. *J. Biol. Chem.* 278, 14832–14840.
- Cogan, T.M., Goerges, S., Gelsomino, R., Larpin, S., Hohenegger, M., Bora, N., Jamet, E., Rea, M.C., Mounier, J., Vancanneyt, M., Guéguen, M., Desmasures, N., Swings, J., Goodfellow, M., Ward, A.C., Sebastiani, H., Irlinger, F., Chamba, J.-F., Beduhn, R., Scherer, S., 2014. Biodiversity of the surface microbial consortia from Limburger, Reblochon, Livarot, Tilsit, and Gubbeen cheeses. In: *Cheese and Microbes*. American Society of Microbiology, pp. 219–250.
- Cumby, N., Reimer, K., Mengin-Lecreulx, D., Davidson, A.R., Maxwell, K.L., 2015. The phage tail tape measure protein, an inner membrane protein and a periplasmic chaperone play connected roles in the genome injection process of *E. coli* phage HK97. *Mol. Microbiol.* 96, 437–447.
- de Melo, A.G., Labrie, S.J., Dumaresq, J., Roberts, R.J., Tremblay, D.M., Moineau, S., 2016. Complete genome sequence of *Brevibacterium linens* SMQ-1335. *Genome Announc.* 4, e01242-16.
- De Vos, W.M., 1987. Gene cloning and expression in lactic streptococci. *FEMS Microbiol. Lett.* 46, 281–295.
- Durmort, C., Brown, J.S., 2015. *Streptococcus pneumoniae* lipoproteins and ABC transporters. In: *Streptococcus pneumoniae*. Elsevier, pp. 181–206.
- Garneau, J.E., Moineau, S., 2011. Bacteriophages of lactic acid bacteria and their impact on milk fermentations. *Microb. Cell Fact.* 10, S20.
- Gavrish, E.Y., Krauzova, V.I., Potekhina, N. V., Karasev, S.G., Plotnikova, E.G., Altyntseva, O.

- V., Korosteleva, L.A., Evtushenko, L.I., 2004. Three new species of *Brevibacteria*, *Brevibacterium antiquum* sp. nov., *Brevibacterium aurantiacum* sp. nov., and *Brevibacterium permense* sp. nov. *Microbiology* 73, 176–183.
- Hampton, H.G., Watson, B.N.J., Fineran, P.C., 2020. The arms race between bacteria and their phage foes. *Nature* 577, 327–336.
- Higgins, D.L., Sanozky-Dawes, R.B., Klaenhammer, T.R., 1988. Restriction and modification activities from *Streptococcus lactis* ME2 are encoded by a self-transmissible plasmid, pTN20, that forms cointegrates during mobilization of lactose-fermenting ability. *J. Bacteriol.* 170, 3435–3442.
- Hunt, R.C., Simhadri, V.L., Iandoli, M., Sauna, Z.E., Kimchi-Sarfaty, C., 2014. Exposing synonymous mutations. *Trends Genet.* 30, 308–321.
- Knöppel, A., Näsvall, J., Andersson, D.I., 2016. Compensating the fitness costs of synonymous mutations. *Mol. Biol. Evol.* 33, 1461–1477.
- Labrie, S.J., Mosterd, C., Loignon, S., Dupuis, M.-È., Desjardins, P., Rousseau, G.M., Tremblay, D.M., Romero, D.A., Horvath, P., Fremaux, C., Moineau, S., 2019. A mutation in the methionine aminopeptidase gene provides phage resistance in *Streptococcus thermophilus*. *Sci. Rep.* 9, 13816.
- Labrie, S.J., Samson, J.E., Moineau, S., 2010. Bacteriophage resistance mechanisms. *Nat. Rev. Microbiol.* 8, 317–327.
- Labrie, S.J., Tremblay, D.M., Plante, P.-L., Wasserscheid, J., Dewar, K., Corbeil, J., Moineau, S., 2015. Complete Genome Sequence of *Streptococcus thermophilus* SMQ-301, a model strain for phage-host interactions. *Genome Announc.* 3, e00480-15.
- Lemay, M.-L., Otto, A., Maaß, S., Plate, K., Becher, D., Moineau, S., 2019. Investigating *Lactococcus lactis* MG1363 response to phage p2 infection at the proteome level. *Mol. Cell. Proteomics* 18, 704–714.
- Lemay, M.-L., Renaud, A., Rousseau, G., Moineau, S., 2018. Targeted genome editing of virulent phages using CRISPR-Cas9. *Bio-Protocol* 8, e2674.
- Lemay, M.L., Tremblay, D.M., Moineau, S., 2017. Genome engineering of virulent lactococcal phages using CRISPR-Cas9. *ACS Synth. Biol.* 6, 1351-1358.
- Levesque, S., 2018. Développement d'un outil génétique pour *Brevibacterium aurantiacum* et analyse génomique comparative de souches laitières. Université Laval.
- Levesque, S., de Melo, A.G., Labrie, S.J., Moineau, S., 2019. Mobilome of *Brevibacterium aurantiacum* sheds light on its genetic diversity and its adaptation to smear-ripened cheeses. *Front. Microbiol.* 10, 1270.
- Lu, S., Wang, J., Chitsaz, F., Derbyshire, M.K., Geer, R.C., Gonzales, N.R., Gwadz, M., Hurwitz, D.I., Marchler, G.H., Song, J.S., Thanki, N., Yamashita, R.A., Yang, M., Zhang, D., Zheng, C., Lanczycki, C.J., Marchler-Bauer, A., 2020. CDD/SPARCLE: the conserved domain database in 2020. *Nucleic Acids Res.* 48, D265–D268.
- Lubbers, M.W., Waterfield, N.R., Beresford, T.P.J., Le Page, R.W.F., Jarvis, A.W., 1995. Sequencing and analysis of the prolate-headed lactococcal bacteriophage c2 genome and identification of the structural genes. *Appl. Environ. Microbiol.* 61, 4348–4356.
- Mahony, J., Deveau, H., Mc Grath, S., Ventura, M., Canchaya, C., Moineau, S., Fitzgerald, G.F., Van Sinderen, D., 2006. Sequence and comparative genomic analysis of lactococcal bacteriophages jj50, 712 and P008: evolutionary insights into the 936 phage species. *FEMS Microbiol. Lett.* 261, 253–261.

- Melo, A.G., Rousseau, G.M., Tremblay, D.M., Labrie, S.J., Moineau, S., 2020. DNA tandem repeats contribute to the genetic diversity of *Brevibacterium aurantiacum* phages. *Environ. Microbiol.* 22, 3413-3428.
- O’Sullivan, D.J., Klaenhammer, T.R., 1993. Rapid mini-prep isolation of high-quality plasmid DNA from *Lactococcus* and *Lactobacillus* spp. *Appl. Environ. Microbiol.* 59, 2730–2733.
- Pham, N.-P., Layec, S., Dugat-Bony, E., Vidal, M., Irlinger, F., Monnet, C., 2017. Comparative genomic analysis of *Brevibacterium* strains: insights into key genetic determinants involved in adaptation to the cheese habitat. *BMC Genomics.* 18, 955.
- Rahman, M.M., Machuca, M.A., Khan, M.F., Barlow, C.K., Schittenhelm, R.B., Roujeinikova, A., 2019. Molecular basis of unexpected specificity of abc transporter-associated substrate-binding protein DppA from *Helicobacter pylori*. *J. Bacteriol.* 201, e00400-19.
- Rincé, A., Tangney, M., Fitzgerald, G.F., 2000. Identification of a DNA region from lactococcal phage sk1 protecting phage 712 from the abortive infection mechanism AbiF. *FEMS Microbiol. Lett.* 182, 185–191.
- Wang, X., Kidder, J.M., Scagliotti, J.P., Klempner, M.S., Noring, R., Hu, L.T., 2004. Analysis of differences in the functional properties of the substrate binding proteins of the *Borrelia burgdorferi* oligopeptide permease (opp) operon. *J. Bacteriol.* 186, 51–60.
- Wegmann, U., O’Connell-Motherway, M., Zomer, A., Buist, G., Shearman, C., Canchaya, C., Ventura, M., Goesmann, A., Gasson, M.J., Kuipers, O.P., van Sinderen, D., Kok, J., 2007. The complete genome sequence of the lactic acid bacterium *Lactococcus lactis* subsp. *cremoris* MG1363. *J. Bacteriol.* 189, 3256-3270.

Chapter 4 – Article 4

The impact of *Brevibacterium aurantiacum* virulent phages on the production of smear surface-ripened cheeses

Alessandra G. de Melo^{1,2}, Hany Geagea^{1,2} and Sylvain Moineau^{1,2,3*}

¹ Département de biochimie, de microbiologie et de bio-informatique, Faculté des sciences et de génie, Université Laval, Québec, QC, Canada.

² Groupe de recherche en écologie buccale, Faculté de médecine dentaire, Université Laval, Québec, QC, Canada.

³ Félix d'Hérelle Reference Center for Bacterial Viruses, Faculté de médecine dentaire, Université Laval, Québec, QC, Canada.

Résumé

Les phages sont présents dans tous les écosystèmes microbiens et sont particulièrement abondants dans les environnements où les bactéries se développent rapidement, comme dans l'industrie fromagère. Malgré que l'infection des bactéries lactiques par les phages soit bien documentée, l'impact des phages sur les souches de maturation, telles que *Brevibacterium aurantiacum*, est peu connu. Dans ce chapitre, nous avons cherché à étudier l'impact de phages de *B. aurantiacum* dans la production de fromages affinés. Pour ce faire, nous avons utilisé des fromages modèles et suivi le développement de la couleur de la croûte ainsi que de sa composition microbienne de la croûte, selon que le phage AGM9 a été ajouté (groupe de traitement) ou non (témoin). Nos résultats montrent que la présence de phages virulents de *B. aurantiacum* a un impact sur le développement de la couleur orangée de la croûte des fromages modèles. Au cours des derniers jours de maturation, des phages ont également été détectés dans les caillé témoins. En analysant une région hypervariable du génome des phages de *B. aurantiacum*, nous avons détecté des phages avec des profils de répétition en tandem différents de ceux du phage AGM9, inoculés dans le groupe de traitement des fromages modèles. Par conséquent, nos résultats mettent également en évidence les risques de conserver une souche sensible aux phages dans la production de fromages affinés. Il s'agit de la première étude sur l'impact des phages de *B. aurantiacum* sur les fromages affinés.

Abstract

Phages can be found in every microbial ecosystem and are particularly abundant in environments where bacteria thrive, such as those in the cheese industry. Although it is well documented that phages infect lactic acid bacteria, their impact has been overlooked in ripening strains, such as *Brevibacterium aurantiacum*. Here, we aimed to study the impact of *B. aurantiacum* phages on the production of smear-ripened cheeses. We used model cheeses and monitored the development of the color of the cheese rind as well as of its microbial composition under untreated conditions (control group - with no added phages) and when phage AGM9 was added (treatment group). Our results show that the presence of *B. aurantiacum* phages has a negative impact on the development of the orange rind color in the model cheeses. Surprisingly in the final days of ripening, phages were also detected in the control curds. By analyzing a hypervariable region of *B. aurantiacum* phage genomes, we detected phages with tandem repeat patterns that were different from phage AGM9, which was the phage inoculated in the model cheese treatment group. Our results highlight the risks of retaining a phage-sensitive strain in smear-ripened cheese production. This paper is the first to report on the impact of *B. aurantiacum* phages in smear-ripened cheeses.

Abbreviations

CFU	Colony forming units
GMO	Genetically modified organisms
LAB	Lactic acid bacteria
NaCl	Sodium chloride
ORF	Open reading frame
PCR	Polymerase chain reaction
PDA	Potato dextrose agar
PFU	Plaque forming units
TR	Tandem repeats

Introduction

Cheeses host a dynamic ecosystem characterized by a succession of diverse microbial groups that develop during the various processes of cheesemaking, such as milk fermentation, curd maturation and storage (Irlinger and Mounier, 2009). Two different microbial communities are particularly important for the manufacturing and ripening of cheeses (Bonomo and Salzano, 2012). The first is found in the cheese core and contains primarily starter lactic acid bacteria. The second develops on the surface of the cheese, where a diverse collection of microbes composed of yeast, mold and surface bacteria make up the rind (Dutton and Wolfe, 2013). While the primary function of starter bacteria is to produce sufficient acid from the metabolism of lactose in order to reduce milk pH to the desired level (Cotter and Beresford, 2017), the secondary microbiota participate in the cheese-ripening process. This process involves microbiological and biochemical changes to the curd resulting in the flavor and texture of the particular variety of cheese (McSweeney, 2004).

The dairy industry has been selecting yeast, mold and bacteria to use as cheese surface-ripening cultures because of properties such as aroma and pigmentation (Irlinger and Mounier, 2009). In several smear-ripened cheeses, the development of the surface microflora is supported by periodically washing the cheese surface with a brine solution that contains the desired microbes in a process referred to as “smearing” (McSweeney et al., 2017). Among the carefully selected microbes, *Brevibacterium* spp. strains are widely used for the manufacturing of surface-ripened cheeses that are manufactured worldwide. The enzymatic richness of these popular strains contributes to the breakdown of lipids and proteins as well as produces volatile sulfur compounds and red-orange pigments (Pham et al., 2017). *Brevibacterium aurantiacum* is frequently isolated on the surface of a variety of surface-ripened cheeses (Bonham et al., 2017; Cogan et al., 2014). Some of these strains were previously classified as *Brevibacterium linens* but have now been reclassified as *B. aurantiacum* (Levesque et al., 2019; Pham et al., 2017).

Similar to starter cultures, *B. aurantiacum* can also be infected by bacterial viruses called bacteriophages (or phages). Phages are ubiquitous and can become pervasive if they encounter a sensitive host in cheese manufacturing plants (Garneau and Moineau, 2011). This problem becomes even more challenging if the culture is difficult to replace, such as for the industrial strain *B. aurantiacum* SMQ-1335 (Melo et al., 2020). This strain is sensitive to phages and highly

associated with the organoleptic features of surface-ripened cheeses (Melo et al., 2020). Although *B. aurantiacum* phages were very recently isolated for the first time from surface-ripened cheeses with color and flavor defects, as well as from various environmental samples collected in cheese factories (Melo et al., 2020), little is known about the effect of phages on washed rind cheeses.

Using a system that can be experimentally controlled provides a way to answer questions concerning the form, assembly, function, and evolution of microbial communities (Dutton and Wolfe, 2013). Cheese rinds have been described as being a model ecosystem to study microbial communities (Wolfe et al., 2014). Although the widespread positive and negative interactions between bacterial and fungal communities were previously described in this cheese tractable system (Wolfe et al., 2014), the effect of phages on the bacterial community of surface-ripened cheeses has been largely ignored. In this study, we aimed to shed light on the influence of phages on the *B. aurantiacum* population as well as on rind color during the cheesemaking process.

Results and Discussion

Microbiological development on the cheese rind

We prepared model curds of an orange-pigmented cheese, which were molded in small glass canning jars and covered with cheese cloth during ripening. There were enough model curds to perform both experiments in triplicate: the control experiments (no added phage) and with added *B. aurantiacum* virulent phage AGM9 in the concentration of 10^6 PFU/mL of smearing liquid. Phage titers and cheese pH were measured, and microbial counts on the rind were conducted for the control cheeses as well as for the cheeses where phages were introduced along with other microbes in the smearing liquid. These model curds proved to be systems that could be used to follow the rind microbiota, pH and color of the rind developed as expected in industrial settings.

The pH of the curd plays an essential role in the ripening process of smear-ripened cheeses as it determines the development and the succession of the microorganisms involved (Mounier et al., 2017). The pH also influences the activities of enzymes required for cheese maturation (Mounier et al., 2017). After coagulation and draining of the whey, the pH is approximately 5.0, which is not always the pH at which the growth of essential microbiota for cheese ripening occurs (Mounier et al., 2017). We monitored the pH of the model curds on Days 1, 3, 6, and 8 of the ripening process

(Figure 1). The pH on Day 1 was approximately 5.3 for both the control and phage-infected cheeses. As expected, the pH increased over time to levels higher than 6.0 in the control cheeses and reached a pH of 6.4 on Day 8. The pH in the phage-infected cheeses initially followed the same trend as the control cheeses but it subsequently dropped to 5.7 on Day 8 (Figure 17). Of note, *B. aurantiacum* usually grows at a pH that is equal to or greater than 6, but growth can also occur at a pH of 5.5, depending on NaCl concentrations (Mounier et al., 2008).

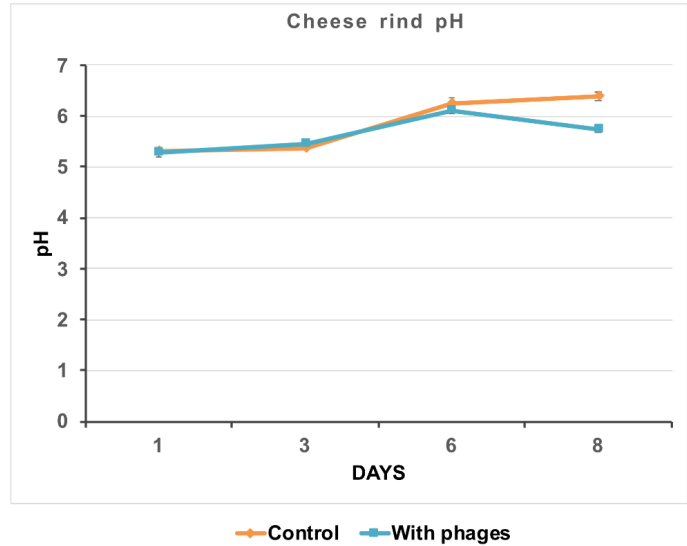


Figure 17. Deacidification of the model curd rinds during the first eight days of ripening

The increase in pH in the first few days of ripening is a result of the growth of yeasts that are inoculated on the cheese surface in the smearing liquid. The smearing liquid that was used contained the yeasts *Geotrichum candidum* and *Cryptococcus albicans* and the bacterium *B. aurantiacum*. These yeasts metabolize the lactate that is present in the curd and release growth factors (Mounier et al., 2008). They also produce alkaline metabolites, such as ammonia from deamination of amino acids, which leads to an increase in pH and enables the growth of acid-sensitive bacteria (Corsetti et al., 2001; Irlinger and Mounier, 2009; Mounier et al., 2008). Both control and phage-containing cheeses presented very similar growth of *G. candidum* and *C. albicans* (Figure 18).

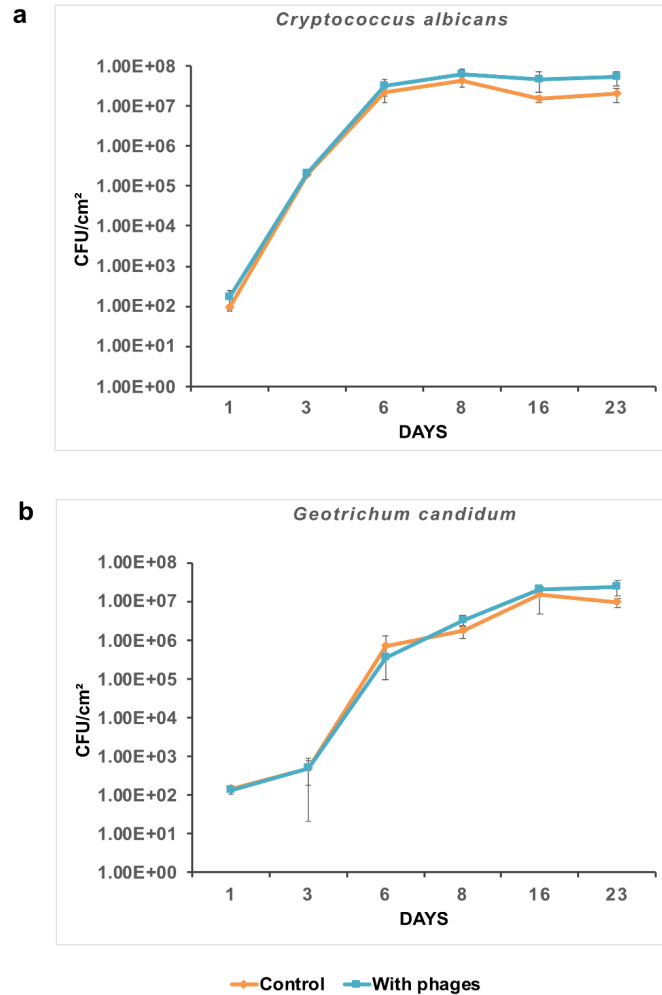


Figure 18. Growth of the yeasts (a) *Cryptococcus albicans* and (b) *Geotrichum candidum* during model cheese ripening.

G. candidum demonstrated slower population growth during the ripening process than *C. albicans*, but growth was constant and exponential (from $\sim 10^2$ to $\sim 10^7$ CFU/cm²). However, *C. albicans* grew faster in the first six days of ripening and reached a plateau in the days that followed ($\sim 10^7$ CFU/cm²). In previous studies, bacterial growth was shown to be influenced by the yeasts that were inoculated in the cheese models, with no occurrence of bacterial growth when yeasts were not inoculated (Mounier et al., 2008). Among the individual yeasts that were used (*Yarrowia lipolytica*, *Debaryomyces hansenii* and *G. candidum*) and the reactions when they were combined, the species *G. candidum* appeared to have the most positive impact on the development of *B. aurantiacum* in the cheese rind, enhancing its growth on the cheese surface (Mounier et al., 2008).

Other bacteria also grew on the surface of the cheese (Figure 19). These bacteria are present in the environments where cheese is produced and are capable of growing during the ripening process. This bacterial population was considered as a whole and it is easy to differentiate from *B. aurantiacum* based on the color of the colonies (beige, white and yellow *versus* orange colonies) (Figure 19). A two-log increase was observed in their numbers from Day 3 to Day 6 and up to 10^4 CFU/cm² in both the control and phage-inoculated cheeses (Figure 19). Interestingly, their numbers dropped to undetectable levels starting on Day 8 and remained undetectable until Day 23, the last day of sampling.

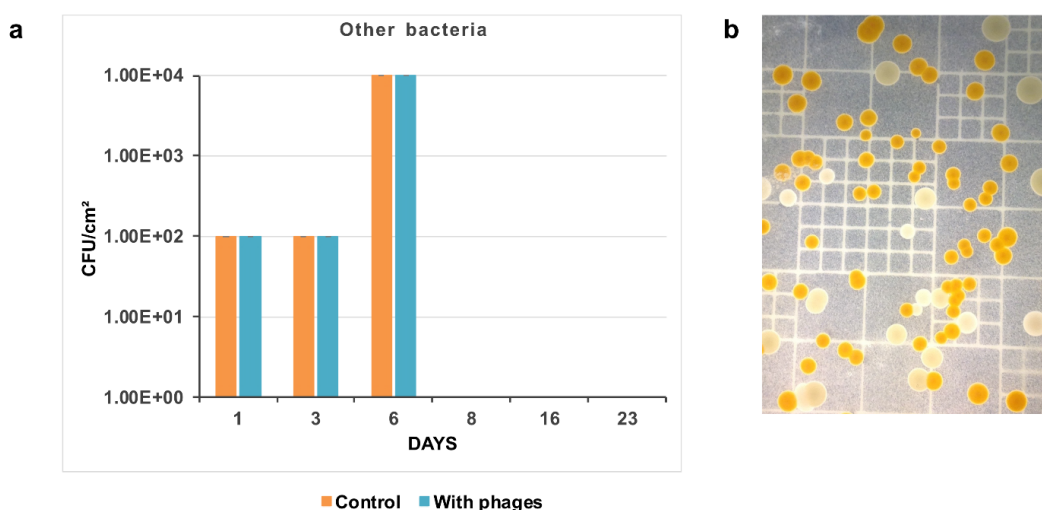


Figure 19. Development of secondary bacteria on the model cheese surface. (a) Growth of adventitious bacteria during ripening (up to Day 23). (b) Example of *B. aurantiacum* (orange colonies) growing with adventitious microbiota (white and beige colonies).

The growth of acid-sensitive bacteria, including *B. aurantiacum*, depends on the deacidification of the cheese rind. As previously mentioned, this process starts with the development of yeast on the cheese surface. *B. aurantiacum* was inoculated at specific intervals (Table 1; Day 0, 1, 3, 6, 8, 10, 13, 16, and 20) during cheese maturation and its development was monitored during ripening. As shown in Figure 20, *B. aurantiacum* counts remained nearly constant until Day 6 ($\sim 10^6$ CFU/cm²), followed by an increase in bacterial growth starting on Day 8, especially in the control curds. This observation is consistent with the deacidification of the cheese rind between Day 4 and Day 6 of the ripening process. Deacidification led to an increased rind pH of 6.0. The increased pH created the ideal conditions for the exponential growth of *B. aurantiacum* that was observed a

few days after. This growth continued until the last day of ripening (which was also the last day of the microbiological analyses). Bacterial growth increased from approximately 10^6 to 10^{10} CFU/cm². Although a difference can be observed in *B. aurantiacum* counts from Day 8 to Day 16 between the two groups of cheeses (~0.5 to 1.5 logs), the cell counts converged on Day 23, with an approximately 0.5-log difference between the control and the phage-added curds.

B. aurantiacum strains have been isolated from several types of cheese around the world (Cogan et al., 2014; Mounier et al., 2017; Pham et al., 2017). Although it has been shown that despite being massively inoculated during the ripening process of washed rind cheeses, *Brevibacterium* spp. (e.g. *Brevibacterium aurantiacum* BL2) is not always recovered in those cheeses at the end of the ripening process (Brennan et al., 2002; Mounier et al., 2006). *B. aurantiacum* SMQ-1335 is well adapted to the conditions that were present in the cheese experiment as evidenced by the cell counts ($>10^9$ CFU/cm²) on the last day of ripening, even in the presence of virulent phages.

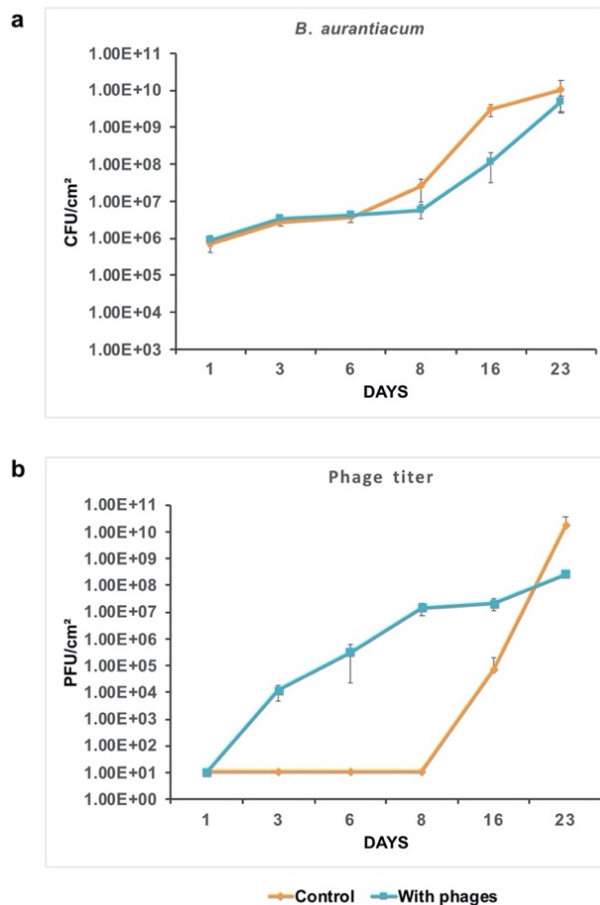


Figure 20. Development of *B. aurantiacum* (a) and phages (b) during cheese ripening.

***B. aurantiacum* phages on the cheese rind**

Although phages are well documented as being a part of the dairy ecosystem (Garneau and Moineau, 2011) and are generally reported as being a risk for starter cultures, their effect on ripening cultures is poorly documented. We recently characterized *B. aurantiacum* virulent phages that were isolated from dairy facilities (Melo et al., 2020). Limited diversity was found among the sixteen characterized phages, even though they were isolated from three different cheese factories. However, the three cheese manufacturing sites use the same *B. aurantiacum* strain, SMQ-1335, for ripening. The presence of tandem repeats (TR) in the phage genomes was the major contributor to their genetic diversity. Phage AGM9 was one of the isolated phages in these manufacturing sites and was used in this study, as it belonged to the most prevalent tandem repeat group isolated, TR5m5. One of the parameters that was evaluated in these model washed-rind cheeses was the color and how it developed on the cheese surface in the presence or absence of inoculated phages. Until the eighth day of the ripening process, both control and experimental model cheeses developed a very similar rind color (Figure 21). These first eight days of ripening also coincided the deacidification process, which promoted the growth of *B. aurantiacum*. On Day 13, the two groups of cheese could be differentiated by their rind colors. From Day 13 to Day 90, clear differences were observed between the control and the phage-containing cheeses. As *B. aurantiacum* SMQ-1335 developed on the cheese surface the phage populations also increased, which negatively affected the development of the rind color.

Surprisingly, starting on Day 16, phages were detected in all the control cheeses. The concentrations ranged from approximately 10^1 PFU/cm² to 7×10^4 PFU/cm². On Day 23, phage titers even reached a concentration of 1.7×10^{10} PFU/cm², which is higher than in the group with the phage-inoculated smear liquid (2.7×10^8 PFU/cm²). These data also indicate that phage populations can reach very high levels, even in a solid matrix. After careful examination and testing, we could not identify any source of contamination from the laboratory materials used. Thus, we hypothesized that the phages found in the control group may be different from phages added to the treatment group (AGM9) and these new phages may have come from a contamination of the ripening room. To verify this hypothesis, we used the PCR primer sets previously designed to target *B. aurantiacum* phages previously described, such as AGM9 (Melo et al., 2020).





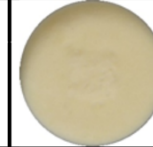
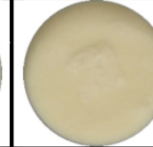





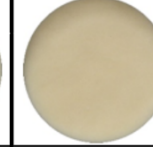



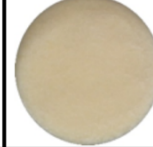






































Day	Control			With phages		
	1A	1B	1C	2A	2B	2C
3						
6						
8						
13						
16						
20						
23						
50						
90						

Figure 21. Development of the rind color of model curds. Columns represent each biological replicate in the control (1A, 1B and 1C) and in the experimental treatment with phages (2A, 2B and 2C). Rows represent the number of days of ripening (Days 3 to 23) or storage (Days 50 and 90).

Although the *B. aurantiacum* phages that infect strain SMQ-1335 are very closely related, the regions containing tandem repeats helped differentiate previous isolates. AGM9 has five TRs in its *orf50*, each one containing 198 bp. This results in a specific band pattern in the electrophoresis gel when targeted by PCR. From the 10 isolated plaques that were selected from the control curds, six yielded PCR products with bands that resemble phage AGM9, whereas four other phages (1, 8, 9, 10) yielded larger-sized PCR products, indicating that they were not phage AGM9 (Figure 22). However, only this region is not enough to differentiate the six isolates with the tandem repeat region resembling AGM9. While genome sequencing of these other phage isolates could shed light on their relationship with phage AGM9, it is clear that four isolates are different from the wild-type phage used in this study, based on their tandem repeat region. These data suggest that several *B. aurantiacum* phages are endemic in this cheese facility.

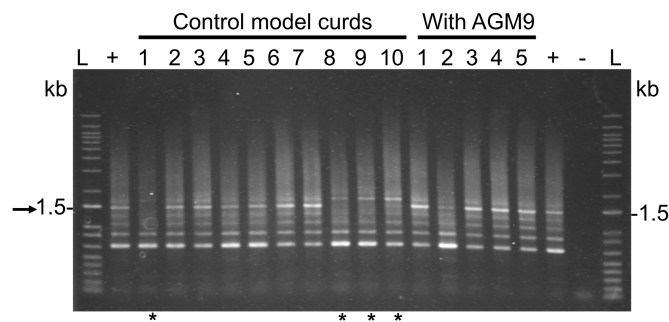


Figure 22. PCR of the tandem repeat region of isolated plaques from the model curds.

Four out of 10 plaques from the control model curds exhibited band patterns that were different from phage AGM9 (+) and are indicated by the asterisks (*). L indicates the ladder, + is the positive control or phage AGM9, and – indicates the PCR negative control. The arrow represents the expected PCR size of 1,459 bp for AGM9.

Our results also highlight the risk of using phage-sensitive strains in cheesemaking. Because these bacterial strains are already targeted by the phages found in this ecological niche, using them repeatedly could lead to an increase in this specific viral population in dairy facilities and may even favor the emergence of other phages. In addition, these data provide information about the way phage contamination affects the length of time it takes for the cheese surface to develop its color. The cheeses that were intentionally exposed to phage AGM9 developed light orange-pigments during ripening, presumably because the virulent phages killed several *B. aurantiacum* cells. The color development in these intentionally exposed cheeses was delayed compared to the

negative controls presumably due to the phages. On the other hand, the control cheeses developed typical orange-pigmented cheeses, as contamination with phages from the environment occurred later in the ripening stage.

Therefore, it seems that exposure to phages at the beginning of the cheese ripening process delays the development of color and presumably flavor in smear surface-ripened cheeses. In contrast, if exposure occurs later in the ripening process or perhaps if there is also a lower level of exposure, the development of the organoleptic features of the cheeses may be less affected, if at all. Beneficial future research could include performing these same trials with the use of bacteriophage insensitive mutants.

Phage tolerance to thermal treatments

The dairy industry employs a series of strategies to control phage contamination in its facilities. One of these control measures is the use of heat treatments to reduce the microbial load in the milk (Garneau and Moineau, 2011). The standard treatment for milk used in cheese production is pasteurization, which is usually conducted at 72°C for at least 15 seconds (Lucey, 2015). Some phages that infect lactic acid bacteria have been shown to resist heat treatment (Garneau and Moineau, 2011; Murphy et al., 2017). Although phage titers are usually low in heat-treated milk, specific viral populations can increase very rapidly if it replicates in the phage-sensitive bacterial strains used in the dairy cultures (de Melo et al., 2018; Garneau and Moineau, 2011). Testing phage tolerance to thermal treatments is part of the phage monitoring program often adopted by dairy industries to control phage contamination.

Lactococcus lactis phage P1532 has been described as a model for thermo-resistant phages. This phage showed only a 2-log reduction following heat treatment at 90°C for 15 minutes (Sadiq et al., 2019) and could still be detected after incubation at 97°C for 5 min (Atamer et al., 2009). Another phage, the lactococcal phage p2, is heat-sensitive (Geagea et al., 2017). These phages were used as controls to assess the tolerance of *B. aurantiacum* phages to heat treatments. *B. aurantiacum* phages were subjected to heat treatments with temperatures ranging from 60°C to 90°C for 5 minutes. All sixteen phage lysates tested were completely inactivated at temperatures above 65°C (Figure 23). As milk proteins have been shown to have a protective effect on phages

during heat treatments (Atamer et al., 2010; Geagea et al., 2015), we also tested the *B. aurantiacum* phages in milk. Similarly, no phage plaques were recovered after a 5-minute exposure to heat treatments of 65°C and above (data not shown). Therefore, pasteurization should sufficiently inactivate *B. aurantiacum* phages and the phage contamination observed in the control curds likely did not come from the milk used to make the cheeses, but instead originated from the environment.

≈ 10 ⁸ PFU/mL	Temperature (°C)						
	60	65	70	75	80	85	90
Phages							
P1532	Dark Teal	Dark Teal	Dark Teal	Dark Teal	Dark Teal	Dark Teal	Dark Teal
p2	Dark Teal	Dark Teal	Dark Teal	Light Teal	Light Teal	Light Teal	Light Teal
AGM1	Dark Teal	Light Teal	Light Teal	Light Teal	Light Teal	Light Teal	Light Teal
AGM2	Dark Teal	Light Teal	Light Teal	Light Teal	Light Teal	Light Teal	Light Teal
AGM3	Dark Teal	Light Teal	Light Teal	Light Teal	Light Teal	Light Teal	Light Teal
AGM4	Dark Teal	Light Teal	Light Teal	Light Teal	Light Teal	Light Teal	Light Teal
AGM5	Light Teal	Light Teal	Light Teal	Light Teal	Light Teal	Light Teal	Light Teal
AGM6	Dark Teal	Light Teal	Light Teal	Light Teal	Light Teal	Light Teal	Light Teal
AGM7	Dark Teal	Light Teal	Light Teal	Light Teal	Light Teal	Light Teal	Light Teal
AGM8	Light Teal	Light Teal	Light Teal	Light Teal	Light Teal	Light Teal	Light Teal
AGM9	Light Teal	Light Teal	Light Teal	Light Teal	Light Teal	Light Teal	Light Teal
AGM10	Dark Teal	Light Teal	Light Teal	Light Teal	Light Teal	Light Teal	Light Teal
AGM11	Light Teal	Light Teal	Light Teal	Light Teal	Light Teal	Light Teal	Light Teal
AGM12	Light Teal	Light Teal	Light Teal	Light Teal	Light Teal	Light Teal	Light Teal
AGM13	Light Teal	Light Teal	Light Teal	Light Teal	Light Teal	Light Teal	Light Teal
AGM14	Dark Teal	Light Teal	Light Teal	Light Teal	Light Teal	Light Teal	Light Teal
AGM15	Light Teal	Light Teal	Light Teal	Light Teal	Light Teal	Light Teal	Light Teal
AGM16	Dark Teal	Light Teal	Light Teal	Light Teal	Light Teal	Light Teal	Light Teal

Lysis zone at 10⁰
 Lysis plaque at 10⁰
 Phage inactivation

Figure 23. Stability of *B. aurantiacum* phages (AGM1 – AGM16) after heat treatment at 60°C to 90°C for 5 min in Elliker medium.

Conclusion

In this study, we demonstrate the impact of *B. aurantiacum* phages on the ripening process of washed-rind cheeses. Because the industrial strain *B. aurantiacum* SMQ-1335 is sensitive to phages, we could monitor the viral impact using bacterial counts, phage titer and the color development of the cheese rinds of model curds. Viral contamination at the beginning of the cheese ripening period prevents or delays color development of the surface of these cheeses. On the other hand, if phage contamination occurs later in the ripening process, it appears to have limited effect

on color development. As SMQ-1335 and other ripening strains are particularly linked to the organoleptic features of certain varieties of cheeses, the introduction of bacteriophage insensitive mutants derived from industrial strains into the cheese ripening process could be a way to protect these ripening strains from phages, while retaining the metabolic qualities that lead to their choice as ripening strains.

Materials and Methods

Culture methods and phage assays

The presence of the yeasts *Geotrichum candidum* and *Cryptococcus albicans* were detected using modified Potato Dextrose Agar (PDA)-milk plates with the following composition: potato starch, 4 g/L; dextrose, 20 g/L; agar, 15 g/L; with the addition of 1% (v/w) sterile milk and 2% (w/w) tartaric acid after sterilization. The counts of the bacterial secondary flora were determined on LGCS agar plates containing meat extract, 3 g/L; peptone, 5 g/L; casitone, 5 g/L; glucose, 5 g/L; NaCl, 55 g/L; and agar, 15 g/L; with 0.5% CaCO₃ and 10 µg/mL of pimarinic added after sterilization (Toolens and Koning-Theune, 1970). Phages and *B. aurantiacum* cells were enumerated in modified Elliker media as previously described (Melo et al., 2020).

Model curd preparation

Figure 24 presents the general steps for the preparation of the model curds. The curds were prepared using pasteurized milk and mesophilic starter cultures and before being pressed and molded. Then, unmolded non-brined curds were shredded and kept at -20°C until the day of the experiments. The shredded cheeses were subsequently thawed overnight at 4°C and weighed aseptically. Of the total ingredients added in an industrial blender, 93% (w/w) consisted of shredded cheese which was homogenized for a few minutes. Afterwards, 2% (w/w) of sterile and dry sodium chloride was added and mixed, followed by sterile water to make up the final 5% (v/w). Then, 100 g of the prepared curd was weighed in small glass canning jars with two-component metal lids, being careful to avoid bubbles between the layers. Using sterile gloves under the microbiological hood, cheeses were pressed in order to shape and remove any remaining bubbles. With the aid of a sterile spatula, the surface of the model curd was evenly distributed, and the holes

and deformities were filled to avoid imperfections. Each model curd was then covered with a cheese cloth that was secured using the metal ring of the canning jar lid. The model curds were then transferred into a commercial ripening room and stored at 13°C and 96% humidity.

Rind care

The smear liquid was prepared by adding *Brevibacterium aurantiacum* SMQ-1335 ($\sim 2.9 \times 10^4$ CFU/mL), *Geotrichum candidum* ($\sim 1.7 \times 10^4$ CFU/mL), and *Cryptococcus albicans* ($\sim 7.2 \times 10^3$ CFU/mL) in 1 liter of sterile distilled water for the control experiment. To evaluate the impact of *B. aurantiacum* phages on the cheese rind, an aliquot of smear liquid was also inoculated with phage AGM9 at 10^6 PFU/mL. Using small sterile sponges, the smear liquid was carefully spread on the surface of the model cheeses to inoculate them with the microorganisms of interest. Rind care was performed on Day 0 (i.e. when the curd was prepared), in addition to days 1, 3, 6, 8, and 10. For days 13, 16, and 20, the care solution was replaced by a 2% (w/v) saline solution that contained either *B. aurantiacum* SMQ-1335 alone or both *B. aurantiacum* SMQ-1335 and phage AGM9. For each day of the rind wash, the order of treatment was alternated, so the model cheese that was washed first on one day was washed last the following day of smearing. The analyses of the model curds were performed according to Table 1.

pH measurements of the model curds

The pH of each model curd was measured using a surface electrode on three different areas of the curd surface. The tip of an electrode was inserted into the cheese to evaluate differences in acidity on the surface and interior of the cheese.

Microbial composition of the rind

The microbial composition of the model cheese rinds was evaluated on days 1, 3, 6, 8, 16 and 23 (Table 1). Sampling was performed using a 4 cm² (2 x 2 cm) template by scratching the cheese surface with a sterile scalpel. The samples were added to 9 mL of 2% (w/v) citrate solution and mixed for a few seconds using a rotor-stator homogenizer containing a sterile probe, which was changed between samples. This suspension was used to evaluate the yeast and bacterial counts and subsequently filtered to titer phages. To evaluate the presence of the yeasts *Geotrichum candidum*

and *Cryptococcus albicans*, serial dilutions of the samples were performed and 100 μ L of the proper dilutions were plated on PDA plates. Bacterial counts were evaluated by plating 100 μ L of the serial dilutions on agar plates of the selective medium LGCS (Toolens and Koning-Theune, 1970). Phage plaque assays and propagation were performed as previously described (Melo et al., 2020).

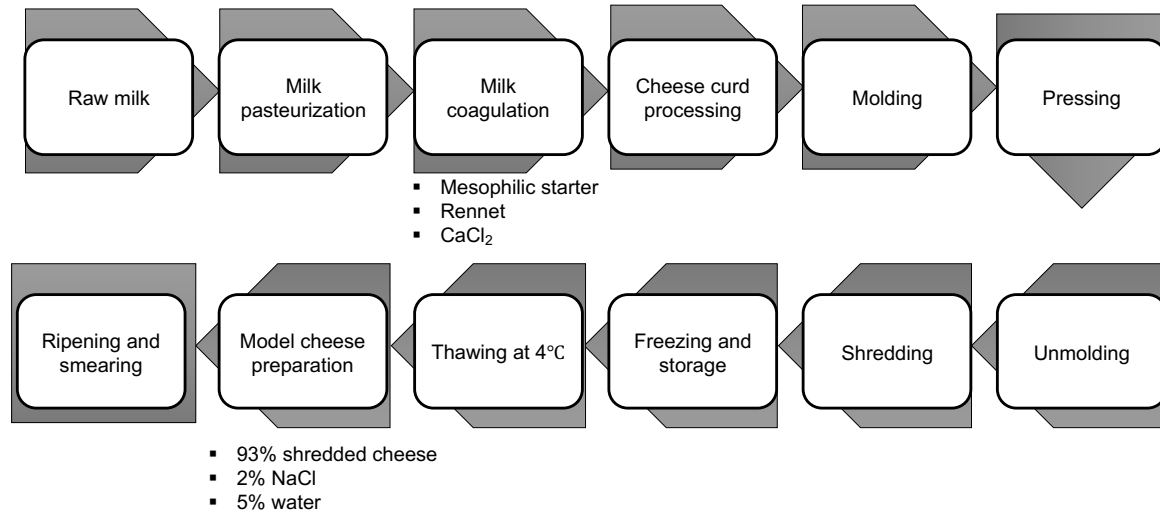


Figure 24. Basic steps for the preparation of model cheeses.

Table 1. Analysis of the model cheeses during ripening.

Day	Smearing	Microbiology of the rind	Microbiology of the smearing liquid	Photo	Rind pH
0					
1					
3					
6					
8					
10					
13	*				
16	*				
20	*				
23					
50					
90					

*2% saline solution containing only *B. aurantiacum* as the ripening culture. Grey shading represents when the analyses were performed.

Development of the rind color

The development of the color of the rind was monitored using a Sony Cyber Shot digital camera attached to a support and maintained at a consistent distance from the model curds. The pictures were taken without the use of a flash, at a 2.4x zoom and in the 4:3 20M format. The pictures were cropped using ImageJ software.

Thermal stability of *Brevibacterium aurantiacum* phages

The thermal resistance of *Brevibacterium* phages AGM1 to AGM16 was tested using Elliker broth (Melo et al., 2020) with a temperature gradient ranging from 60°C to 90°C for 5 minutes as described elsewhere (Geagea et al., 2017). The test was also repeated in 2% skim milk with temperatures ranging from 60°C to 70°C for 5 minutes. Phage titrations (Melo et al., 2020) were performed before and after the heat treatment as previously described (Melo et al., 2020). Approximately 10^8 PFU/mL of phages were added in Elliker or milk.

Acknowledgements

We are grateful to our industry partner for providing access to their ripening room. AGM earned a scholarship from the National Council for Scientific and Technological Development (CNPq-Brazil) in partnership with CALDO (Canada). This work was funded by Natural Sciences and Engineering Research Council of Canada. SM holds the Tier 1 Canada Research Chair in Bacteriophages.

References

- Atamer, Z., Dietrich, J., Müller-Merbach, M., Neve, H., Heller, K.J., Hinrichs, J., 2009. Screening for and characterization of *Lactococcus lactis* bacteriophages with high thermal resistance. *Int. Dairy J.* 19, 228-235.
- Atamer, Z., Dietrich, J., Neve, H., Heller, K.J., Hinrichs, J., 2010. Influence of the suspension media on the thermal treatment of mesophilic lactococcal bacteriophages. *Int. Dairy J.* 20, 408-414.
- Bonham, K.S., Wolfe, B.E., Dutton, R.J., 2017. Extensive horizontal gene transfer in cheese-associated bacteria. *eLife* 6, 1–23.
- Bonomo, M.G., Salzano, G., 2012. Microbial diversity and dynamics of Pecorino di Filiano PDO, a traditional cheese of Basilicata region (Southern Italy). *Int. J. Dairy Technol.* 65, 531–541.
- Brennan, N.M., Ward, A.C., Beresford, T.P., Fox, P.F., Goodfellow, M., Cogan, T.M., 2002. Biodiversity of the bacterial flora on the surface of a smear cheese. *Appl. Environ. Microbiol.* 68, 820–830.
- Cogan, T.M., Goerges, S., Gelsomino, R., Larpin, S., Hohenegger, M., Bora, N., Jamet, E., Rea, M.C., Mounier, J., Vancanneyt, M., Guéguen, M., Desmasure, N., Swings, J., Goodfellow, M., Ward, A.C., Sebastiani, H., Irlinger, F., Chamba, J.-F., Beduhn, R., Scherer, S., 2014. Biodiversity of the surface microbial consortia from Limburger, Reblochon, Livarot, Tilsit, and Gubbeen cheeses. In: *Cheese and Microbes*. American Society of Microbiology, pp. 219–250.
- Corsetti, A., Rossi, J., Gobbetti, M., 2001. Interactions between yeasts and bacteria in the smear surface-ripened cheeses. *Int. J. Food Microbiol.* 69, 1–10.
- Cotter, P.D. and Beresford, T.P. (2017) Microbiome changes during ripening. In: *Cheese*. Elsevier, pp. 389–409.
- de Melo, A.G., Levesque, S., Moineau, S., 2018. Phages as friends and enemies in food processing. *Curr. Opin. Biotechnol.* 49, 185–190.
- Dutton, R.J., Wolfe, B.E., 2013. Towards an ecosystem approach to cheese microbiology. *Microbiol. Spectr.* 1, 10.1128/microbiolspec.CM-0012-12.
- Garneau, J.E., Moineau, S., 2011. Bacteriophages of lactic acid bacteria and their impact on milk fermentations. *Microb. Cell Fact.* 10, S20.
- Geagea, H., Gomaa, A.I., Remondetto, G., Moineau, S., Subirade, M., 2015. Investigation of the protective effect of whey proteins on lactococcal phages during heat treatment at various pH. *Int. J. Food Microbiol.* 210, 33–41.
- Geagea, H., Labrie, S.J., Subirade, M., Moineau, S., 2017. The tape measure protein is involved in the heat stability of *Lactococcus lactis* phages. *Appl. Environ. Microbiol.* 84, e02082-17.
- Irlinger, F., Mounier, J., 2009. Microbial interactions in cheese: implications for cheese quality and safety. *Curr. Opin. Biotechnol.* 20, 142–148.
- Levesque, S., de Melo, A.G., Labrie, S.J., Moineau, S., 2019. Mobilome of *Brevibacterium aurantiacum* sheds light on its genetic diversity and its adaptation to smear-ripened cheeses. *Front. Microbiol.* 10, 1270.
- Lucey, J.A., 2015. Raw milk consumption: risks and benefits. *Nutr. Today* 50, 189–193.
- McSweeney, P.L.H., 2004. Biochemistry of cheese ripening. *Int. J. Dairy Technol.* 57, 127–144.
- McSweeney, P.L.H., Ottogalli, G., Fox, P.F., 2017. Diversity and classification of cheese varieties: an overview. In: *Cheese*. Elsevier, pp. 781–808.

- Melo, A.G., Rousseau, G.M., Tremblay, D.M., Labrie, S.J., Moineau, S., 2020. DNA tandem repeats contribute to the genetic diversity of *Brevibacterium aurantiacum* phages. *Environ. Microbiol.* 22, 3413-3428.
- Mounier, J., Coton, M., Irlinger, F., Landaud, S., and Bonnarme, P. (2017) Smear-ripened cheeses. In: *Cheese*. Elsevier, pp. 955–996.
- Mounier, J., Goerges, S., Gelsomino, R., Vancanneyt, M., Vandemeulebroecke, K., Hoste, B., Brennan, N.M., Scherer, S., Swings, J., Fitzgerald, G.F., Cogan, T.M., 2006. Sources of the adventitious microflora of a smear-ripened cheese. *J. Appl. Microbiol.* 101, 668–681.
- Mounier, J., Monnet, C., Vallaey, T., Arditi, R., Sarthou, A.S., Hélias, A., Irlinger, F., 2008. Microbial interactions within a cheese microbial community. *Appl. Environ. Microbiol.* 74, 172–181.
- Murphy, J., Mahony, J., Fitzgerald, G.F., van Sinderen, D., 2017. Bacteriophages infecting lactic acid bacteria. *Cheese Chem. Phys. Microbiol.* Fourth Ed. 1, 249–272.
- Pham, N.-P., Layec, S., Dugat-Bony, E., Vidal, M., Irlinger, F., Monnet, C., 2017. Comparative genomic analysis of *Brevibacterium* strains: insights into key genetic determinants involved in adaptation to the cheese habitat. *BMC Genomics.* 18, 955.
- Sadiq, F.A., He, G.Q., Sakandar, H.A., Li, Y.J., Ou, K., 2019. *Lactococcus lactis* phages from the perspective of their diversity, thermal and biocidal resistance. *Int. Dairy J.* 90, 28–38.
- Toolens, H.P., Koning-Theune, W., 1970. A selective medium for the detection of *Brevibacterium linens* in cheese. *Milchwissenschaft* 25, 79–83.
- Wolfe, B.E., Button, J.E., Santarelli, M., Dutton, R.J., 2014. Cheese rind communities provide tractable systems for *in situ* and *in vitro* studies of microbial diversity. *Cell* 158, 422–433.

Conclusion and perspectives

Cheese rind was recently shown as a tractable system to study microbial community formation and succession (Wolfe et al., 2014). We have seen as part of our studies that phages infecting *Brevibacterium aurantiacum* have an impact on the stability of the washed rind cheese community. The microbiome of the cheese rind is subject to extensive horizontal gene transfer (Bonham et al., 2017) and it is likely that phages represent an evolutionary pressure on the cheese-associated bacterial community.

In our study, the industrial strain used for the production of washed rind cheeses, *Brevibacterium aurantiacum* SMQ-1335, was permissive to infection by several, albeit related, virulent phages. As a means of phage control, the cheese industry employs a rotation of starter strains to avoid the build-up of a specific phage population due to the repetitive phage infection of the same strain, and to minimize the impact of phages on milk fermentation (Garneau and Moineau, 2011). However, the complex nature of cheese rinds makes the replacement or rotation of ripening strains, such as *B. aurantiacum*, nearly impossible. The establishment of these species on the surface of cheese depends on their metabolism and their ability to interact with other members of the complex cheese microbial community (Mounier et al., 2008; Pham et al., 2017). Once a ripening strain has been established in the manufacturing process of award-winning fine cheeses, changing the strain is considered a last resort, as it can alter the premium organoleptic attributes of the washed rind cheese, and consequently, the consumer acceptability of the final product.

Comparative genome analyses of *B. aurantiacum* phages indicate a high relatedness among these phages, with most of the diversity attributed to the presence of DNA tandem repeats in an intragenic genomic region. In terms of phage biology, phage AGM1 has a long latency period and releases a small number of virions per infected cell. As the cheese ripening takes place in conditions that might slow down the metabolism of the host, the latency period might be even longer in manufacturing settings. Considering the long ripening period for washed-rind cheeses, phages with short lytic cycles and large burst sizes could, in theory, nearly deplete the hosts and consequently, stop its own propagation leading to its extinction overtime. If long lytic cycles and small burst sizes are common for other *B. aurantiacum* phages infecting industrial strains, this

could be a reason as to why these phages have not often been reported. Overall, comparative genome analyses indicate that *B. aurantiacum* phages analyzed here evolved from the same ancestor, despite being isolated from three different cheese manufacturing sites. Furthermore, the isolation of new phages from other washed rind cheeses around the globe would certainly broaden our knowledge on the diversity of *B. aurantiacum* phages.

When a sensitive host is present during cheese manufacturing, phage propagation is controlled mostly by the environment, growth of the host and by the phage itself. However, considering that genomic variations are created by a combination of mutations induced by replication errors, recombination, and mutagens (Koonin and Wolf, 2012), one can speculate that over time, with the persistence of phages in the manufacturing facilities, mutations are inevitable. These mutations may perhaps increase phage fitness or give them the ability to infect other strains, leading to the rise of new phages with more diverse genetic structures. For example, here we have observed that tandem repeats acted as promoters of diversity among *B. aurantiacum* phages. The presence of these repeats is itself one of the drivers of genomic plasticity (Zhou et al., 2014), with mutations in the repeats region introduced during various cellular processes affecting the DNA, including replication, recombination and repair mechanisms (Mrázek et al., 2007). The frequency of repeat mutations has been shown to depend on a mutational bias that promotes their expansion or contraction, such as their identity and composition, and a lack of strong negative selection against them (Gemayel et al., 2012; Mrázek et al., 2007). Thus, the longer and identical the repeats are, the higher is the mutation frequency, whereas the shorter and less identical, the lower the mutation frequency (Gemayel et al., 2012). Although we could not attribute a function and/or determine whether or not these structures give a competitive advantage to phages, it is possible that coding macrosatellites have an impact on protein structure and/or folding of ORF50.

Considering the ubiquity of phages in manufacturing environments, the isolation of natural phage-resistant bacteria is one alternative to control phage outbreaks in these facilities (Deveau et al., 2010; Marcó et al., 2012). While these emerging cells are resistant to virulent phages, they also often retain technologically important attributes from the wild-type culture (Mahony et al., 2012). We generated and characterized bacteriophage insensitive mutants derived from *B. aurantiacum* SMQ-1335 and their genome analysis suggested that an ABC-transporter may be involved in phage resistance, perhaps blocking DNA entry. While their receptors are still elusive, these phages

appear to be strain specific as they did not infect other strains than their host. This was not entirely surprising as viral specialists are almost always observed in the dairy environs. One of the biggest challenges in studying the interaction between *B. aurantiacum* and its phages is the fact that this species is recalcitrant to genetic transformation. As extensive horizontal gene transfer has been proposed for cheese-associated strains of *B. aurantiacum* (Bonham et al., 2017; Levesque et al., 2019), it is tempting to speculate that DNA uptake is taking place in the cheese ecosystem. Perhaps this species has a community requirement to uptake DNA, needs specific abiotic conditions not identified yet or even possesses mechanisms constraining DNA transformation in laboratory conditions. DNA transformation protocol could possibly include a community approach instead of a single and pure culture. Conjugation could also be investigated as an alternative DNA transfer method as it has been successful for in other microbes proven hard to be transformed, such as Bifidobacterial (Dominguez and O’Sullivan, 2013). During conjugation the DNA is transferred as single strand DNA and methylated when the second strand is synthesized, therefore not subject of restriction-modification systems. Additionally, there is no constraints regarding plasmid size (Dominguez and O’Sullivan, 2013).

Regardless of genetic transformation difficulties, other experiments could be used to further characterize *B. aurantiacum* BIMs. One of these alternatives is the use of fluorescence microscopy. As the three BIMs with mutations in the ABC system are permissive to viral adsorption, yet fully resistant to phages, the resistance must happen at some step following adsorption. Phage DNA accumulation or injection blocking could be verified under fluorescence microscopy after viral adsorption. For example, the phage genome and the bacterial cytoplasmic membrane could be differentially stained and followed under a fluorescence microscope as done previously with *Campylobacter jejuni* and its phage F341 (Baldvinsson et al., 2014). Another alternative assay could be to perform a time course infection and determined if the phage DNA replicate inside the BIMs as described for lactococcal strains and their phages (Boucher et al., 2000; Hill et al., 1991). In the event of phage DNA replication, one would conclude that the interference does not occur at the DNA injection level, but at another step of the phage lytic cycle.

In our study, we also evaluated the impact of virulent *B. aurantiacum* phages during the production of washed rind cheeses. As a result, phages affected the color development of the cheeses in which they were added, indicating that *B. aurantiacum* phage contamination can negatively impact the

production of washed rind cheeses and lead to a longer ripening time. Surprisingly, *B. aurantiacum* phages were also found in the control cheeses where they were not added, substantiating the risk of keeping a phage-sensitive strain in cheese production. A PCR characterization showed that at least four out of ten phage isolates found in the control cheeses have a different repeat array than the phage AGM9 added in the treatment group. Further PCR characterization or whole genome sequencing would be necessary to verify if the other six isolates sharing the same type of repeat array as AGM9 are different isolates or if it is phage AGM9 that contaminated our controls. It would also be interesting to perform similar cheese experiment with the various BIMs developed in the Chapter 3. Finally, while they seem to be a minor and temporary component of the microbial community in washed rind cheeses, it may be of interest to further characterize the secondary bacteria that were detected in the early days of the ripening period in the model curds.

Increased knowledge about phage-host interactions in *B. aurantiacum*, the biology of these phages as well as the selection of phage-resistant strains could enable the industry to improve strategies to control phage proliferation in cheese ripening processes. Hopefully, the knowledge acquired in this thesis will also contribute to increase the general interest in *B. aurantiacum* phages as well as to perhaps isolate and characterize additional phages from diverse cheeses produced worldwide.

References

- Adriaenssens, E.M., Sullivan, M.B., Knezevic, P., van Zyl, L.J., Sarkar, B.L., Dutilh, B.E., Alfenas-Zerbini, P., Łobocka, M., Tong, Y., Brister, J.R., Moreno Switt, A.I., Klumpp, J., Aziz, R.K., Barylski, J., Uchiyama, J., Edwards, R.A., Kropinski, A.M., Petty, N.K., Clokie, M.R.J., Kushkina, A.I., Morozova, V. V., Duffy, S., Gillis, A., Rumnieks, J., Kurtböke, I., Chanishvili, N., Goodridge, L., Wittmann, J., Lavigne, R., Jang, H. Bin, Prangishvili, D., Enault, F., Turner, D., Poranen, M.M., Oksanen, H.M., Krupovic, M., 2020. Taxonomy of prokaryotic viruses: 2018-2019 update from the ICTV bacterial and archaeal viruses subcommittee. *Arch. Virol.* 165, 1253-1260.
- Adriaenssens, E.M., Wittmann, J., Kuhn, J.H., Turner, D., Sullivan, M.B., Dutilh, B.E., Jang, H. Bin, van Zyl, L.J., Klumpp, J., Łobocka, M., Moreno Switt, A.I., Rumnieks, J., Edwards, R.A., Uchiyama, J., Alfenas-Zerbini, P., Petty, N.K., Kropinski, A.M., Barylski, J., Gillis, A., Clokie, M.R.C., Prangishvili, D., Lavigne, R., Aziz, R.K., Duffy, S., Krupovic, M., Poranen, M.M., Knezevic, P., Enault, F., Tong, Y., Oksanen, H.M., Rodney Brister, J., 2018. Taxonomy of prokaryotic viruses: 2017 update from the ICTV bacterial and archaeal viruses subcommittee. *Arch. Virol.* 163, 1125–1129.
- Almena-Aliste, M., Mietton, B., 2014. Cheese classification, characterization, and categorization: a global perspective. *Microbiol. Spectr.* 2, CM-0003-2012.
- Anast, J.M., Dzieciol, M., Schultz, D.L., Wagner, M., Mann, E., Schmitz-Esser, S., 2019. *Brevibacterium* from Austrian hard cheese harbor a putative histamine catabolism pathway and a plasmid for adaptation to the cheese environment. *Sci. Rep.* 9, 6164.
- Ardö, Y., McSweeney, P.L.H., Magboul, A.A.A., Upadhyay, V.K., Fox, P.F., 2017. Biochemistry of cheese ripening: proteolysis. In: *Cheese: Chemistry, Physics and Microbiology: Fourth Edition*.
- Arfi, K., Landaud, S., Bonnarme, P., 2006. Evidence for distinct L-methionine catabolic pathways in the yeast *Geotrichum candidum* and the bacterium *Brevibacterium linens*. *Appl. Environ. Microbiol.* 72, 2155–2162.
- Baldvinsson, S.B., Holst Sørensen, M.C., Vegge, C.S., Clokie, M.R.J., Brøndsted, L., 2014. *Campylobacter jejuni* motility is required for infection of the flagellotropic bacteriophage F341. *Appl. Environ. Microbiol.* 80, 7096–7106.
- Bertozi Silva, J., Storms, Z., Sauvageau, D., 2016. Host receptors for bacteriophage adsorption. *FEMS Microbiol. Lett.* 363, fnw002.
- Bondy-Denomy, J., Davidson, A.R., 2014. When a virus is not a parasite: the beneficial effects of prophages on bacterial fitness. *J. Microbiol.* 52, 235–242.
- Bonham, K.S., Wolfe, B.E., Dutton, R.J., 2017. Extensive horizontal gene transfer in cheese-associated bacteria. *eLife* 6, e22144.
- Bonnarme, P., Psoni, L., Spinnler, H.E., 2000. Diversity of L-methionine catabolism pathways in cheese-ripening bacteria. *Appl. Environ. Microbiol.* 66, 5514–5517.
- Bonomo, M.G., Salzano, G., 2012. Microbial diversity and dynamics of Pecorino di Filiano PDO, a traditional cheese of Basilicata region (Southern Italy). *Int. J. Dairy Technol.* 65, 531–541.
- Boucher, I., Émond, E., Dion, E., Montpetit, D., Moineau, S., 2000. Microbiological and molecular impacts of AkiK on the lytic cycle of *Lactococcus lactis* phages of the 936 and P335 species. *Microbiology* 146, 445–453.
- Breed, R.S., Murray, E.G.D., Smith, N.R., 1957. *Bergey's manual of systematic bacteriology*,

- Igarss 2014.
- Brüssow, H., Hendrix, R.W., 2002. Phage Genomics: Small is beautiful. *Cell* 108, 13–16.
- Campbell, A., 2003. The future of bacteriophage biology. *Nat. Rev. Genet.* 4, 471–477.
- Caridi, A., Micari, P., Caparra, P., Cufari, A., Sarullo, V., 2003. Ripening and seasonal changes in microbial groups and in physico-chemical properties of the ewes' cheese Pecorino del Poro. *Int. Dairy J.* 13, 191–200.
- Chapot-Chartier, M.P., 2014. Interactions of the cell-wall glycopolymers of lactic acid bacteria with their bacteriophages. *Front. Microbiol.* 5, 236.
- Chibani-chennoufi, S., Bruttin, A., Brüssow, H., Dillmann, M., Bru, H., 2004. Phage-host interaction : an ecological perspective. *J. Bacteriol.* 186, 3677–3686.
- Cogan, T.M., Goerges, S., Gelsomino, R., Larpin, S., Hohenegger, M., Bora, N., Jamet, E., Rea, M.C., Mounier, J., Vancanneyt, M., Guéguen, M., Desmasures, N., Swings, J., Goodfellow, M., Ward, A.C., Sebastiani, H., Irlinger, F., Chamba, J.-F., Beduhn, R., Scherer, S., 2014. Biodiversity of the surface microbial consortia from Limburger, Reblochon, Livarot, Tilsit, and Gubbeen cheeses. In: *Cheese and Microbes*. American Society of Microbiology, pp. 219–250.
- Corsetti, A., Rossi, J., Gobbetti, M., 2001. Interactions between yeasts and bacteria in the smear surface-ripened cheeses. *Int. J. Food Microbiol.* 69, 1–10.
- Cotter, P.D. and Beresford, T.P. (2017) Microbiome Changes During Ripening. In: *Cheese*. Elsevier, pp. 389–409.
- de Melo, A.G., Labrie, S.J., Dumaresq, J., Roberts, R.J., Tremblay, D.M., Moineau, S., 2016. Complete genome sequence of *Brevibacterium linens* SMQ-1335. *Genome Announc.* 4, e01242-16.
- Deveau, H., Garneau, J.E., Moineau, S., 2010. CRISPR/Cas system and its role in phage-bacteria interactions. *Annu. Rev. Microbiol.* 64, 475–493.
- Dion, M.B., Oechslin, F., Moineau, S., 2020. Phage diversity, genomics and phylogeny. *Nat. Rev. Microbiol.* 18, 125–138.
- Dominguez, W., O'Sullivan, D.J., 2013. Developing an efficient and reproducible conjugation-based gene transfer system for *Bifidobacteria*. *Microbiol.* 159, 328–338.
- Doron, S., Melamed, S., Ofir, G., Leavitt, A., Lopatina, A., Keren, M., Amitai, G., Sorek, R., 2018. Systematic discovery of antiphage defense systems in the microbial pangenome. *Science* 359, eaar4120.
- Duplessis, M., Lévesque, C.M., Moineau, S., 2006. Characterization of *Streptococcus thermophilus* host range phage mutants. *Appl. Environ. Microbiol.* 72, 3036–3041.
- Duplessis, M., Moineau, S., 2001. Identification of a genetic determinant responsible for host specificity in *Streptococcus thermophilus* bacteriophages. *Mol. Microbiol.* 41, 325–336.
- Dutton, R.J., Wolfe, B.E., 2013. Towards an ecosystem approach to cheese microbiology. *Microbiol. Spectr.* 1, 10.1128/microbiolspec.CM-0012-12.
- Feiner, R., Argov, T., Rabinovich, L., Sigal, N., Borovok, I., Herskovits, A.A., 2015. A new perspective on lysogeny: prophages as active regulatory switches of bacteria. *Nat. Rev. Microbiol.* 13, 641–650.
- Forquin, M.P., Duvergey, H., Proux, C., Loux, V., Mounier, J., Landaud, S., Coppée, J.Y., Gibrat, J.F., Bonnarme, P., Martin-Verstraete, I., Vallaeys, T., 2009. Identification of *Brevibacteriaceae* by multilocus sequence typing and comparative genomic hybridization analyses. *Appl. Environ. Microbiol.* 75, 6406–6409.
- Fox, P.F., McSweeney, P.L.H., 2017. Cheese: an overview. In: *Cheese*. Elsevier, pp. 5–21.

- Garneau, J.E., Moineau, S., 2011. Bacteriophages of lactic acid bacteria and their impact on milk fermentations. *Microb. Cell Fact.* 10, S20.
- Gavrish, E.Y., Krauzova, V.I., Potekhina, N. V, Karasev, S.G., Plotnikova, E.G., Altyntseva, O. V., Korosteleva, L.A., Evtushenko, L.I., 2004. Three new species of *Brevibacteria*, *Brevibacterium antiquum* sp. nov., *Brevibacterium aurantiacum* sp. nov., and *Brevibacterium permense* sp. nov. *Microbiology* 73, 176–183.
- Gemayel, R., Cho, J., Boeynaems, S., Verstrepen, K.J., 2012. Beyond junk-variable tandem repeats as facilitators of rapid evolution of regulatory and coding sequences. *Genes* 3, 461–480.
- Goldfarb, T., Sberro, H., Weinstock, E., Cohen, O., Doron, S., Charpak-Amikam, Y., Afik, S., Ofir, G., Sorek, R., 2015. BREX is a novel phage resistance system widespread in microbial genomes. *EMBO J.* 34, 169–83.
- Hampton, H.G., Watson, B.N.J., Fineran, P.C., 2020. The arms race between bacteria and their phage foes. *Nature* 577, 327–336.
- Hatfull, G.F., 2008. Bacteriophage genomics. *Curr. Opin. Microbiol.* 11, 447–453.
- Hill, C., Massey, I.J., Klaenhammer, T.R., 1991. Rapid method to characterize lactococcal bacteriophage genomes. *Appl. Environ. Microbiol.* 57, 283–288.
- Irlinger, F., Layec, S., Hélinck, S., Dugat-Bony, E., 2015. Cheese rind microbial communities: Diversity, composition and origin. *FEMS Microbiol. Lett.* 362, 1–11.
- Irlinger, F., Mounier, J., 2009. Microbial interactions in cheese: implications for cheese quality and safety. *Curr. Opin. Biotechnol.* 20, 142–148.
- Kenny, J.G., McGrath, S., Fitzgerald, G.F., Van Sinderen, D., 2004. Bacteriophage Tuc2009 encodes a tail-associated cell wall-degrading activity. *J. Bacteriol.* 186, 3480–3491.
- Koonin, E. V., Wolf, Y.I., 2012. Evolution of microbes and viruses: a paradigm shift in evolutionary biology? *Front. Cell. Infect. Microbiol.* 2, 119.
- Koskella, B., Brockhurst, M.A., 2014. Bacteria-phage coevolution as a driver of ecological and evolutionary processes in microbial communities. *FEMS Microbiol. Rev.* 38, 916–931.
- Labrie, S.J., Samson, J.E., Moineau, S., 2010. Bacteriophage resistance mechanisms. *Nat. Rev. Microbiol.* 8, 317–327.
- Letarov, A. V., Kulikov, E.E., 2017. Adsorption of bacteriophages on bacterial cells. *Biochem.* 82, 1632–1658.
- Levesque, S., de Melo, A.G., Labrie, S.J., Moineau, S., 2019. Mobilome of *Brevibacterium aurantiacum* sheds light on its genetic diversity and its adaptation to smear-ripened cheeses. *Front. Microbiol.* 10, 1270.
- Mahony, J., Ainsworth, S., Stockdale, S., van Sinderen, D., 2012. Phages of lactic acid bacteria: the role of genetics in understanding phage-host interactions and their co-evolutionary processes. *Virology* 434, 143–150.
- Mahony, J., van Sinderen, D., 2012. Structural aspects of the interaction of dairy phages with their host bacteria. *Viruses* 4, 1410–1424.
- Makarova, K.S., Wolf, Y.I., Snir, S., Koonin, E. V., 2011. Defense islands in bacterial and archaeal genomes and prediction of novel defense systems. *J. Bacteriol.* 193, 6039–6056.
- Malone, L.M., Warring, S.L., Jackson, S.A., Warnecke, C., Gardner, P.P., Gumy, L.F., Fineran, P.C., 2019. A jumbo phage that forms a nucleus-like structure evades CRISPR – Cas DNA targeting but is vulnerable to type III RNA-based immunity. *Nat. Microbiol.* 5, 48–55.
- Marcó, M.B., Moineau, S., Quiberoni, A., 2012. Bacteriophages and dairy fermentations. *Bacteriophage* 2, 149–158.

- Mc Grath, S., Fitzgerald, G.F., van Sinderen, D., 2007. Bacteriophages in dairy products: pros and cons. *Biotechnol. J.* 2, 450–455.
- McSweeney, P.L.H., 2004. Biochemistry of cheese ripening. *Int. J. Dairy Technol.* 57, 127–144.
- McSweeney, P.L.H., 2017. Biochemistry of cheese ripening: introduction and overview. *Cheese Chem. Phys. Microbiol. Fourth Ed.* 1, 379–387.
- McSweeney, P.L.H., Fox, P.F., Ciocia, F., 2017a. Metabolism of residual lactose and of lactate and citrate. *Cheese Chem. Phys. Microbiol. Fourth Ed.* 1, 411–421.
- McSweeney, P.L.H., Ottogalli, G., Fox, P.F., 2017b. Diversity and classification of cheese varieties: an overview. In: *Cheese*. Elsevier, pp. 781–808.
- Melo, A.G., Rousseau, G.M., Tremblay, D.M., Labrie, S.J., Moineau, S., 2020. DNA tandem repeats contribute to the genetic diversity of *Brevibacterium aurantiacum* phages. *Environ. Microbiol.* 22, 3413–3428.
- Mendoza, S.D., Nieweglowska, E.S., Govindarajan, S., Leon, L.M., Berry, J.D., Tiwari, A., Chaikeeratisak, V., Pogliano, J., Agard, D.A., Bondy-Denomy, J., 2019. A bacteriophage nucleus-like compartment shields DNA from CRISPR nucleases. *Nature* 577, 244–248.
- Monnet, C., Back, A., Irlinger, F., 2012. Growth of aerobic ripening bacteria at the cheese surface is limited by the availability of iron. *Appl. Environ. Microbiol.* 78, 3185–3192.
- Motta, A.S., Brandelli, A., 2008. Properties and antimicrobial activity of the smear surface cheese coryneform bacterium *Brevibacterium linens*. *Eur. Food Res. Technol.* 227, 1299–1306.
- Mounier, J., Coton, M., Irlinger, F., Landaud, S., Bonnarme, P., 2017. Smear-ripened cheeses. In: *Cheese*. Elsevier, pp. 955–996.
- Mounier, J., Monnet, C., Vallaey, T., Arditi, R., Sarthou, A.S., Hélias, A., Irlinger, F., 2008. Microbial interactions within a cheese microbial community. *Appl. Environ. Microbiol.* 74, 172–181.
- Mrázek, J., Guo, X., Shah, A., 2007. Simple sequence repeats in prokaryotic genomes. *Proc. Natl. Acad. Sci. U. S. A.* 104, 8472–8477.
- Ofir, G., Melamed, S., Sberro, H., Mukamel, Z., Silverman, S., Yaakov, G., Doron, S., Sorek, R., 2018. DISARM is a widespread bacterial defence system with broad anti-phage activities. *Nat. Microbiol.* 3, 90–98.
- Oliveira, H., Melo, L.D.R., Santos, S.B., Nobrega, F.L., Ferreira, E.C., Cerca, N., Azeredo, J., Kluskens, L.D., 2013. Molecular aspects and comparative genomics of bacteriophage endolysins. *J. Virol.* 87, 4558–4570.
- Onraedt, A., Soetaert, W., Vandamme, E., 2005. Industrial importance of the genus *Brevibacterium*. *Biotechnol. Lett.* 27, 527–533.
- Pham, N.-P., Layec, S., Dugat-Bony, E., Vidal, M., Irlinger, F., Monnet, C., 2017. Comparative genomic analysis of *Brevibacterium* strains: insights into key genetic determinants involved in adaptation to the cheese habitat. *BMC Genomics* 18, 955.
- Rattray, F.P., Fox, P.F., 1999. Aspects of enzymology and biochemical properties of *Brevibacterium linens* relevant to cheese ripening: a review. *J. Dairy Sci.* 82, 891–909.
- Roux, S., Krupovic, M., Daly, R.A., Borges, A.L., Nayfach, S., Schulz, F., Sharrar, A., Matheus Carnevali, P.B., Cheng, J.F., Ivanova, N.N., Bondy-Denomy, J., Wrighton, K.C., Woyke, T., Visel, A., Kyrpides, N.C., Eloe-Fadrosh, E.A., 2019. Cryptic inoviruses revealed as pervasive in bacteria and archaea across Earth's biomes. *Nat. Microbiol.* 4, 1895–1906.
- Samson, J.E., Magadán, A.H., Sabri, M., Moineau, S., 2013. Revenge of the phages: Defeating bacterial defences. *Nat. Rev. Microbiol.* 11, 675–687.
- Thierry, A., Collins, Y.F., Abeijón Mukdsi, M.C., McSweeney, P.L.H., Wilkinson, M.G.,

- Spinner, H.E., 2017. Lipolysis and metabolism of fatty acids in cheese. *Cheese Chem. Phys. Microbiol.* Fourth Ed. 1, 423–444.
- Underwood, S.L., Foto, A., Ray, A.F., Nelms, A.E., Kennedy, K.L., Hartley, S.G., Ryals, L.M., Gurung, C., D'Angelo, W.A., Pope, W.H., Mavrodi, D. V., 2019. Discovery and characterization of bacteriophage LuckyBarnes. *Microbiol. Resour. Announc.* 8, e00330-19.
- Wolfe, B.E., Button, J.E., Santarelli, M., Dutton, R.J., 2014. Cheese rind communities provide tractable systems for in situ and in vitro studies of microbial diversity. *Cell* 158, 422–433.
- Zhou, K., Aertsen, A., Michiels, C.W., 2014. The role of variable DNA tandem repeats in bacterial adaptation. *FEMS Microbiol. Rev.* 38, 119–141.

Annex A: Mobilome of *Brevibacterium aurantiacum* sheds light on its genetic diversity and its adaptation to smear-ripened cheeses

Sébastien Levesque¹, Alessandra Gonçalves de Melo¹, Simon J. Labrie², and Sylvain Moineau^{1,3*}

¹ Département de biochimie, de microbiologie, et de bio-informatique, Faculté des sciences et de génie, Groupe de recherche en écologie buccale, Faculté de médecine dentaire, Université Laval, Québec City, QC, Canada

² Syntbiolab, Lévis, QC, Canada

³ Félix d'Hérelle Reference Center for Bacterial Viruses, Faculté de médecine dentaire, Université Laval, Québec City, QC, Canada

Abstract

Brevibacterium aurantiacum is an actinobacterium that confers key organoleptic properties to washed-rind cheeses during the ripening process. Although this industrially relevant species has been gaining an increasing attention in the past years, its genome plasticity is still understudied due to the unavailability of complete genomic sequences. To add insights on the mobilome of this group, we sequenced the complete genomes of five dairy *Brevibacterium* strains and one non-dairy strain using PacBio RSII. We performed phylogenetic and pan-genome analyses, including comparisons with other publicly available *Brevibacterium* genomic sequences. Our phylogenetic analysis revealed that these five dairy strains, previously identified as *B. linens*, belong instead to the *B. aurantiacum* species. A high number of transposases and integrases were observed in the *Brevibacterium* spp. strains. In addition, we identified 14 and 12 new insertion sequences in *B. aurantiacum* and *B. linens* genomes, respectively. Several stretches of homologous DNA sequences were also found between *B. aurantiacum* and other cheese rind actinobacteria, suggesting horizontal gene transfer (HGT). A HGT region from an iRon Uptake/Siderophore Transport Island (RUSTI) and an iron uptake composite transposon were found in five *B. aurantiacum* genomes. These findings suggest that low iron availability in milk is a driving force in the adaptation of this bacterial species to this niche. Moreover, the exchange of iron uptake systems suggests cooperative evolution between cheese rind actinobacteria. We also demonstrated that the integrative and conjugative element BreLI (*Brevibacterium* Lanthipeptide Island) can excise from *B. aurantiacum* SMQ-1417 chromosome. Our comparative genomic analysis suggests that mobile genetic elements played an important role into the adaptation of *B. aurantiacum* to cheese ecosystems.

Introduction

The coexistence and succession of diverse microorganisms over time lead to the development of distinct organoleptic properties in a wide variety of aged cheeses (Irlinger and Mounier, 2009). During the ripening period, the surface of smear-ripened cheeses is regularly washed with a microbial-rich brine, which allows the colonization of an orange microbial mat composed of various species of yeasts and bacteria (Brennan et al., 2002). The early surface microbiota of washed-rind cheeses is primarily composed of yeasts that release growth factors and alkalize the cheese surface by metabolizing the lactate produced by lactic acid bacteria added as starter cultures (Alper et al., 2013). These processes promote the growth of acid-sensitive, salt-tolerant bacterial strains primarily composed of coryneform actinobacteria from the *Micrococcaeae*, *Corynebacteriaceae* and *Brevibacteriaceae* families (Brennan et al., 2002). The combined metabolic activities of this complex microbiota are responsible for the typical texture, color, and aroma of this type of cheeses (Schröder et al., 2011).

Strains of *Brevibacterium linens* have been acknowledged as widely used for washed rind cheese ripening as they produce volatile sulfur compounds (VSCs) (Amarita et al., 2004; Hanniffy et al., 2009), carotenoids (Krubasik and Sandmann, 2000; Leclercq-Perlat et al., 2004), lipolytic and proteolytic enzymes (Leclercq-Perlat et al., 2000; Rattray and Fox, 1999), which drive the development of the organoleptic features of smear-ripened cheeses. The dairy strains previously identified as *B. linens* ATCC 9175 and *B. linens* BL2 were reported to produce VSCs and carotenoids (Amarita et al., 2004; Dufossé and De Echanove, 2005; Hanniffy et al., 2009) but they were separated from the type strain *B. linens* ATCC 9172 and reclassified as *B. aurantiacum* according to their genetic, physiological, and biochemical characteristics (Forquin et al., 2009; Gavrish et al., 2004). A recent study also identified *B. aurantiacum* as the dominant bacterial species in five different smear-ripened cheeses (Cogan et al., 2014), suggesting that the taxonomic position of industrial *Brevibacterium* cheese isolates may need to be revisited.

Traditionally, the cheese ripening process involved the transfer of an undefined microbiota from mature to fresh unripened cheeses, thereby selecting for microorganisms well adapted to this ecosystem (Monnet et al., 2010). Hence, smear-ripened cheese is an interesting model to study the adaptation of microorganisms to a new habitat. The prevalence of horizontal gene transfer (HGT)

in cheese rind microbiomes has recently been described, with genes involved in iron siderophore acquisition shown to be widespread in the rind microbiomes of cheeses from Europe and the USA (Bonham et al., 2017). Interestingly, the low iron concentration found in cheese rinds appears to be one of the major metabolic determinants for the growth of ripening bacteria (Monnet et al., 2012; Noordman et al., 2006). In addition, a recent study performing the comparative analysis of 23 *Brevibacterium* spp. genomes, including 12 isolates from cheeses, identified genetic determinants involved in adaptation to the cheese habitat (Pham et al., 2017). Their gene repertoire involved in iron acquisition, osmotic tolerance, and bacteriocin production has been described as well as the ability of this microbial group to use the energy compounds present in cheeses, such as carbohydrates, amino acids, proteins, and lipids (Pham et al., 2017).

While our knowledge on the factors involved on *Brevibacterium* spp. niche adaptation has broaden, we still have a limited comprehension of the mobilome of these species. In fact, most *Brevibacterium* spp. isolated from cheeses previously studied were sequenced using short-read sequencing and their genome sequences remained at the draft level. As such, an in-depth investigation of the mobile genetic elements could not be performed as the analysis of transposon-rich genomes, for example, critically depend on long read sequencing technology (Koren et al., 2013; Pfeiffer et al., 2018).

Here, we report the complete genome sequences of five industrial dairy strains of *B. aurantiacum* and one strain of *B. linens* using the PacBio RSII platform. We performed 16S rRNA and core-genome phylogenetic analyses, which led to the reclassification of dairy strains into the *B. aurantiacum* species. Additionally, we carried out comparative analysis to describe the mobilome of *B. aurantiacum* involved in genome plasticity and adaptation of this species to smear-ripened cheeses.

Materials and Methods

Bacterial strains and DNA sequencing

Brevibacterium strains used in this study are listed in Table 1. They were routinely cultivated in Luria Bertani (LB) or Brain Heart Infusion (BHI) medium at 30°C with agitation (200 rpm). Pulsed-Field Gel Electrophoresis (PFGE) was performed as described previously (Le Bourgeois

et al., 1989; Simpson et al., 2003), using the restriction enzymes AseI and PstI. Genomic DNA was purified using a QIAGEN Genomic tip 20/G kit, according to manufacturer instructions. Single Molecule Real-Time (SMRT) sequencing was performed on a PacBio RSII sequencer (G enome Qu ebec Innovation Centre). Basic Local Alignment with Successive Refinement (BLASR) (Chaisson and Tesler, 2012) was used to align and preassemble the sequences using the longest reads as seeds to which the other subreads were recruited and mapped to correct random errors. Celera assembler (Myers et al., 2000) was used to assemble long and corrected reads into contigs. The sequences were refined using Quiver and genomes were then assembled into one contig using the Hierarchical Genome Assembly Process (HGAP) (Chin et al., 2013). The native plasmid pBLA8 from *B. linens* ATCC 19391 was purified using a QIAGEN Plasmid Maxi kit according to the manufacturer's instructions. Genome libraries were also made using the Nextera XT DNA library preparation kit (Illumina) and sequenced using a MiSeq reagent kit v2 (Illumina, 500 cycles) on a MiSeq system. De novo assembly was performed with Ray assembler version 2.2.0 (Boisvert et al., 2010). Nucleotide coverage, ranging from 3,700x to more than 20,000x for each nucleotide, was calculated with SAMtools (Li et al., 2009).

General genome features prediction

The *Ori* regions were set upstream of the gene coding for the chromosomal replication initiator protein DnaA, as described (de Melo et al., 2016). Gene prediction and annotation were performed with the NCBI prokaryotic genome annotation pipeline (Haft et al., 2018; Tatusova et al., 2016). Gene annotation was also performed separately with the RAST server (Overbeek et al., 2014) and BLASTp (Altschul et al., 1997). Table 2 presents the general genome features of *Brevibacterium* strains. For pBLA8, open reading frames (ORF) were identified with GeneMark.hmm (Besemer et al., 2001) while BLASTp (Altschul et al., 1997) was used to predict ORF function. The presence of CRISPR (Clustered Regularly Interspaced Short Palindromic Repeats) arrays and their associated (*cas*) genes was assessed using CRISPRCasFinder (Couvin et al., 2018). Additionally, genes related to the production of bacteriocins or antimicrobial posttranslational modified peptides were predicted using Bagel4 (Van Heel et al., 2018). Prophages prediction was performed using PHASTER (Arndt et al., 2016) coupled with manual inspection of the regions flanking putative prophages, especially when no genes encoding structural proteins were identified.

Table 1. *Brevibacterium* spp. strains used in this study.

Strain	GenBank numbers	Source	Sequencing technology	Year	Genome status	References
<i>B. aurantiacum</i>						
SMQ-1417	CP025330	Dairy strain	PacBio SMRT	2017	Complete	This study
SMQ-1418	CP025331	Dairy strain	PacBio SMRT	2017	Complete	This study
SMQ-1419	CP025333	Dairy strain	PacBio SMRT	2017	Complete	This study
SMQ-1420	CP025334	Dairy strain	PacBio SMRT	2017	Complete	This study
SMQ-1421	CP025332	Dairy strain	PacBio SMRT	2017	Complete	This study
JB5	NZ_NRGX01000001.1	Dairy isolate	PacBio SMRT	2017	Complete	(Bonham et al., 2017)
SMQ-1335	NZ_CP017150.1	Dairy strain	PacBio SMRT	2016	Complete	(de Melo et al., 2016)
<i>B. linens</i>						
ATCC 19391	CP026734	Unknown	PacBio SMRT	2017	Complete	(Leret et al., 1998)
BS258	NZ_CP014869.1	Marine sediment	PacBio SMRT	2016	Complete	(Zhu et al., 2016)
Additional <i>B. aurantiacum</i> draft genomes used for the pan-genome analysis						
Strain	WGS accession numbers	Source	Sequencing technology	Year	Genome status	References
ATCC 9175	<u>FXZB01000001</u> : <u>FXZB01000070</u>	Camembert cheese	Illumina MiSeq	2017	Permanent draft (70 contigs)	(Pham et al., 2017)
CNRZ 920	<u>FXZG01000001</u> : <u>FXZG01000073</u>	Beaufort cheese	Illumina MiSeq	2017	Permanent draft (73 contigs)	(Pham et al., 2017)
6(3)	<u>FXZI01000001</u> : <u>FXZI01000097</u>	Langres cheese	Illumina MiSeq	2017	Permanent draft (97 contigs)	(Pham et al., 2017)
8(6)	<u>FXYZ01000001</u> : <u>FXYZ01000091</u>	Reblochon cheese	Illumina MiSeq	2017	Permanent draft (91 contigs)	(Pham et al., 2017)

Table 2. General genome features of *B. aurantiacum*, *B. linens* and *B. epidermidis*.

Strain	Genome length (Mb)	G+C content (%)	Predicted CDS	Hypothetical protein (%)	Assigned function (%)	rRNA	tRNA
<i>B. aurantiacum</i>							
SMQ-1335	4.210	62.63	3 807	21.4	78.6	12	49
SMQ-1417	4.424	62.76	3 990	21.2	78.8	12	49
SMQ-1418	4.193	62.77	3 751	19.7	80.3	12	50
SMQ-1419	4.039	62.71	3 668	21.2	78.8	12	49
SMQ-1420	4.329	62.73	3 874	21.1	78.9	12	49
SMQ-1421	4.085	62.76	3 687	20.1	79.9	12	49
JB5	4.311	62.79	3 859	20.1	79.9	12	49
<i>B. linens</i>							
ATCC19391	3.807	64.79	3 377	23.7	76.3	12	48
BS258	3.862	64.16	3 364	19.1	80.9	12	47

Phylogenetic analysis of *B. linens* and *B. aurantiacum*

We used a broad phylogenetic distribution of 82 *Brevibacterium* spp. 16S rRNA gene sequences from the NCBI database, including the strains described in this study, to perform a phylogenetic analysis using MEGA 7.0.26 software (Kumar et al., 2016). *Glutamicibacter arilaitensis* RE117 and *Corynebacterium casei* LMG S-19264 were used as out-groups. We trimmed the sequences to start and finish in the same conserved regions using Geneious® 11.1.2 (Biomatters, New Zealand). We then aligned the sequences with Multiple Sequence Comparison by Log-Expectation (MUSCLE) (Edgar, 2004). The phylogenetic tree (Figure 1) was constructed using the neighbor-joining method (Saitou and Nei, 1987; Tamura et al., 2004). We performed the analysis with 1,000 bootstraps and the percentage of trees in which the associated taxa clustered together is shown next to the branches (Felsenstein, 1985). The tree is drawn to scale with branch lengths measured in the number of substitutions per site. All positions containing gaps and missing data were eliminated and there were a total of 1,165 positions in the final dataset.

Core and pan-genome analyses

The protein sequences of seven complete and four draft genomes of *B. aurantiacum* were extracted from GenBank and added to the pan-genome analyses. All genomes used in our analyses were annotated with the NCBI pipeline. The clustering of the protein sequences in orthologous groups was conducted with USEARCH (Edgar, 2010), requiring greater than 60% identity with alignment over more than 75% of the protein sequence. In-house Python scripts were used to extract the pan- and the core-genome of the *B. aurantiacum* strains. Figure 2 illustrates the core- and pan-genome generated with in-house R scripts using ggPlot2 (Ito and Murphy, 2013). Genes present in only one genome (ORFans) were classified into Rapid Annotation using Subsystem Technology (RAST) subsystem categories (Overbeek et al., 2014) (Figure 2C). A total of 279 genes were classified into subsystem categories using the RAST server and the remaining 393 ORFans were classified manually. The genomic position of the ORFans from complete genomes were extracted and used to generate Supplementary Figure S1. The concatenated protein sequences of the core-genomes of *B. aurantiacum* and *B. linens* complete genomes were used to generate the phylogenetic tree seen in Figure 5. The concatenated sequences of core proteins were aligned using MAFFT (with the flag-auto for the best alignment) (Katoh and Standley, 2013) and the alignment

was divided into partitions using the Alignment Manipulation and Summary (AMAS) tool (Borowiec, 2016). Additionally, the best amino-acid substitution model and tree were determined for each partition using IQ-Tree software (Nguyen et al., 2015).

Insertion sequence and HGT identification

ISFinder database was used to identify ISBli1-ISBli5 in the genomes while ISBli6-ISBli35 were identified manually, as follow. We searched for transposase and mobile element annotations with identical lengths, and the corresponding CDS were extracted with 1000 bp upstream and downstream, as previously described (Monnet et al., 2010; Siguier et al., 2009). These sequences were aligned to *Brevibacterium* spp. genomes using BLASTn to confirm the presence of multiple IS copies. When multiple IS copies were identified, inverted repeats were manually annotated. ISs identified manually were submitted to the ISFinder database under the accession name ISBli6 to ISBli35. Four ISs (ISBli18, ISBli20, ISBli22, and ISBli27) were not validated and removed from the dataset. The other IS elements were validated by the ISFinder database. Complete ISs, transposases, and repeat sequences are available in the ISFinder database. To identify putative HGT regions, whole *Brevibacterium* spp. genomes were aligned against the NCBI database using BLASTn. Alignment hits were considered as probable HGT regions when nucleotide sequences larger than 2,000 bp shared more than 90% identity with other bacterial species.

Prophage induction experiments

Prophage induction assays with mitomycin C was performed with six *B. aurantiacum* strains as described elsewhere (Capra et al., 2010; Moineau et al., 1994). *B. aurantiacum* SMQ-1335 and other five *B. aurantiacum* strains (SMQ-1417 – SMQ-1421) were grown in Elliker media with different concentrations of mitomycin C (0.5, 1.0, 2.0, 5.0, and 10 µg/ml) and incubated at 20°C with 200 rpm agitation. The lysogenic strain *Lactobacillus paracasei* A was used as a positive control, while each culture without mitomycin C was used as negative controls.

Growth curve with limited iron availability

B. linens ATCC 19391 and *B. aurantiacum* strains (SMQ-1335, JB5, SMQ-1417 – SMQ-1421) were grown in mineral salts media (MSM) supplemented with trace elements solution (0.53 g/l

CaCl₂, 0.2 g/l FeSO₄.7H₂O, 0.01 g/l ZnSO₄.7H₂O, 0.01 g/l H₃BO₃, 0.01 g/l CoCl₂.6H₂O, 0.004 g/l MnSO₄.5H₂O, 0.003 g/l Na₂MoO₄.2H₂O, 0.002 g/l NiCl₂.6H₂O) (Janssen et al., 1984; Noordman et al., 2006) for 24 h at 30°C, 200 rpm. The cultures were then transferred to fresh MSM in the presence of different concentrations (10, 50 and 100 µM) of the chelating agent ethylenediamine-di-o-hydroxyphenylacetic acid (EDDHA). EDDHA stocks solution (1 mM) was prepared in water (pH 7,0) and filter sterilized. A culture without EDDHA was added as a control to the experiments. Bacterial growth was followed through optical density (OD_{600nm}) for 21 h.

PCR testing of BreLI chromosome excision

To verify the excision of iRon Uptake/Siderophore Transport Island (RUSTI) (Bonham et al., 2017), we designed an approach targeting the BreLI genomic region based on the strategy described elsewhere (Figure 8). *B. aurantiacum* was cultivated in BHI containing 1% (w/v) agar for 48 hours at 30°C and one colony was used for each PCR reaction. PCR was performed using Taq polymerase Mastermix (Feldan) according to the manufacturer's instructions. All primers used are listed in Table 3. PCR reactions were optimized by adding 10% (v/v) DMSO to the PCR reaction mix. An annealing temperature of 56°C was used to obtain PCR products with a minimum of non-specific bands. Primers 2 and 5 should only form a PCR product if BreLI is excised from the chromosome and is present in a circular form. Sanger sequencing (Plateforme de séquençage et de génotypage des génomes, Québec, QC, Canada) was performed to confirm BreLI excision.

Table 3. List of primers used for the amplification of BreLI.

Primer name	Sequence (5' → 3')
1. BreLi1 Fwd	AGTCAGTTGAGATGAGCAGCTG
2. BreLi1 Rev	CTCGATTCTGGTGTTCATGG
3. BreLi2 Fwd	GAACGACCCGATCAACCTGTTC
4. BreLi2 Rev	CTTCTTCAGACTCGGGAATCAG
5. BreLi3 Fwd	CATCGACCGGATGGGAGCTT
6. BreLi3 Rev	ACGTACCTGCAACTTGGAAG

Production and activity of antimicrobial peptides

In vitro production and activity of antimicrobial peptides was tested for actinobacteria and lactic acid bacteria. *B. linens* ATCC 19391, *Corynebacterium glutamicum* ATCC 21086, *B. aurantiacum* SMQ-1417 to SMQ-1421, SMQ-1335, and JB5 were cultivated in Elliker broth at 30°C, 200 rpm.

The antimicrobial activity of the filtered supernatants of these strains was tested by spotting 5 μ l on a lawn of each of the strains. Additionally, activity was tested against *Micrococcus luteus* HER1157, *Corynebacterium glutamicum* HER1229, *Arthrobacter arilaitensis* LMA-1184, *Lactococcus lactis* MG1363 and SMQ-1200, *Streptococcus thermophilus* HER1458 and HER1368. The nisin-producing strain *Lactococcus lactis* SMQ-1200 was grown in Elliker and incubated overnight at 30°C. This strain was used as a positive control for the experiments against all the bacteria mentioned above.

Availability of data and materials

B. aurantiacum strains with a SMQ number are available upon request. All IS elements were validated by the ISFinder database under the name ISBli6-ISBli35. Genomes have been deposited in the NCBI genome database (See Table 1 for accession numbers). The complete sequence of pBLA8 was deposited under GenBank accession number CP026735. A list of locus tag identifiers and predicted functions for *B. aurantiacum* ORFans are provided in Supplementary Table S1 (A-C). A list of genes in the HGT regions described in this study is provided with their genomic positions and predicted functions in in Supplementary Tables S2 and S3. All in-house Python and R scripts used in this study are available upon request to the corresponding author.

Results

Taxonomic classification of *B. linens* and *B. aurantiacum*

Our laboratory has access to seven *Brevibacterium* spp. strains, including the dairy strain SMQ-1335 for which its genome was previously sequenced (de Melo et al., 2016), five additional dairy strains (SMQ-1417 to SMQ-1421) used in Canada and a strain from the American Type Culture Collection (ATCC 19391) (Table 1). First, we performed their 16S rRNA gene phylogenetic analysis by comparing them with 75 other *Brevibacterium* sequences from GenBank database (NCBI), including type strains for the different species of *Brevibacterium* (Figure 1). With approximately 97% identity, we observed a significant separation between the type strain *B. linens* ATCC 9172 and the six dairy strains from our collection, which were previously believed to belong to the *B. linens* species. Indeed, strain SMQ-1335 as well as the five strains SMQ-1417 to SMQ-1421 grouped with the type strain of *B. aurantiacum* ATCC 9175. Although several other characterized strains (AE038-8, BS258, VKM Ac-2119) have been previously classified as *B. linens*, their 16S rRNA phylogenetic analysis grouped them with the type strain *Brevibacterium epidermidis* (P159), suggesting that these strains should have their taxonomic classification reassessed. Surprisingly, only three strains grouped with *B. linens* type strain ATCC 9172, which are *B. linens* ATCC 19391, VCM10, and Mu101. Only *B. linens* Mu101 and ATCC 9172 were isolated from cheeses. These results suggest that most of the strains used for commercial cheese ripening belong to the *B. aurantiacum* species. For years, *B. linens* has been recognized as a key player on the production of orange-pigmented washed-rind cheeses (Pham et al., 2017; Rattray and Fox, 1999). Whether *B. linens* and *B. aurantiacum* have equal or distinct roles in cheese ripening, remains to be investigated. However, the subdivisions of the *Brevibacterium* species (Gavrish et al., 2004) and new studies involving this group (Cogan et al., 2014; Pham et al., 2017)

have highlighted the importance of *B. aurantiacum* in aged cheese production.

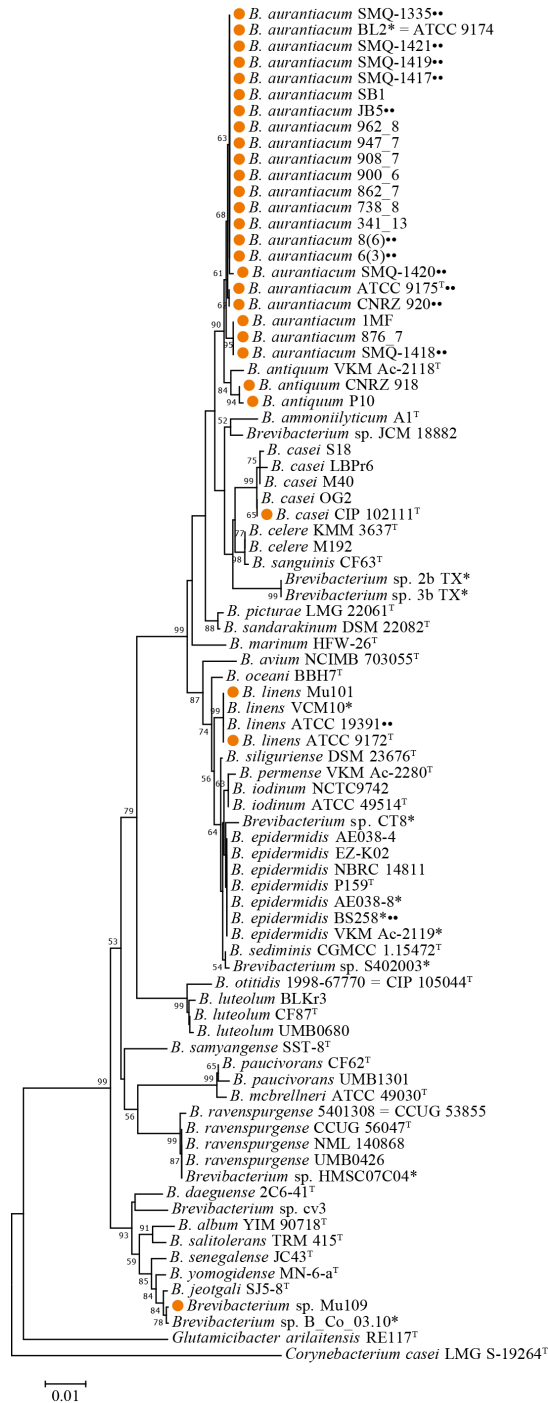


Figure 1. Phylogenetic tree of 82 *Brevibacterium* spp. 16S rRNA nucleotide sequences. The phylogenetic tree was constructed with MEGA 7.0.26 using the neighbor joining method with 1,000 bootstraps (only bootstrap values >50 are shown next to the nodes). *Brevibacterium* dairy strains have their names preceded by orange circles. Strains used in this study are marked with two black circles. Type strains are identified with T superscript. Strains marked with an asterisk should

have the taxonomic classification revisited on GenBank. *C. casei* LMG S-19264 and *G. arilaitensis* RE117 were used as out-groups

General genome features and plasmid content

To confirm that our seven *Brevibacterium* strains (SMQ-1335, SMQ-1417 to SMQ-1421, ATCC 19391) were genetically distinct, we first performed Pulsed-Field Gel Electrophoresis (PFGE). The seven strains presented a unique PFGE profile using restriction enzymes AseI and PsiI (data not shown). Then to shed light on their genomic diversity, we sequenced the genomes of six strains (*B. aurantiacum* SMQ-1417 to SMQ-1421, *B. linens* ATCC 19391) using PacBio RSII. Before performing bioinformatic analyses on these six complete genomes, we added to our analyses three other complete genomes (*B. aurantiacum* SMQ-1335 and JB5 as well as *B. epidermidis* BS258), previously sequenced with the same technology (Table 1). The genome length of *B. aurantiacum* strains ranged from 4.035 to 4.424 Mbp with a high G+C content of 62.63% to 62.79% (Table 2). *B. linens* ATCC 19391 and *B. epidermidis* BS258 had smaller genomes (3.862 and 3.807 Mbp) and higher G+C contents (64.16% and 64.79%). The number of predicted coding sequences (CDS) in these two genomes was also lower than in *B. aurantiacum*, correlating with the smaller genome sizes. Four rRNA operons were observed in all *Brevibacterium* strains analyzed. The average number of CDS per *B. aurantiacum* genome was 3,805, of which 79.3% could be assigned a predicted function. We also investigated the presence of CRISPR-Cas system in *B. aurantiacum* or *B. linens* ATCC 19391, but no CRISPR array with the associated Cas genes was predicted in any of the genomes.

The presence of plasmids in *Brevibacterium* is rare with only a few described in the literature (Anast et al., 2019; Ankri et al., 1996; Kato et al., 1989; Moore et al., 2003; Nardi et al., 2005; Sandoval et al., 1985). We searched for the presence of plasmids and only one strain, *B. linens* ATCC 19391, harbored one. The 7,590 bp plasmid named pBLA8 has been described previously and partially sequenced (Leret et al., 1998). We completed pBLA8 sequence (GenBank CP026735) using Illumina MiSeq and identified 16 Open Reading Frames (ORFs). One protein involved in plasmid partitioning and two replication proteins were identified in the theta-replicating plasmid, while the other 13 ORFs have unknown function. We performed a pairwise alignment of pBLA8 with pLIM (7,610 bp), the only other fully sequenced *B. linens* plasmid available (Moore et al., 2003). The alignment revealed that both plasmids are significantly

different since the alignment covers only 60% of the longest sequence (88% identity). Interestingly, different regions from pBLA8 were found in five *B. aurantiacum* genomes ($\geq 99\%$ identity), suggesting genetic exchange between these two closely related species (Supplementary Figure S2). These genomic regions could also correspond to an ancestral version of pBLA8 present in a common *Brevibacterium* ancestor that became unable to replicate autonomously. Up to 80% of the plasmid was found into different regions of the genomes of *B. aurantiacum* SMQ-1417 and SMQ-1335, including regions coding for RepA and RepB. The only plasmid regions absent in these two bacterial genomes were the origin of replication (*ori*) and genes encoding an additional non-essential replication protein and a hypothetical protein (ORF16). Of note, we found orthologs of JetA, JetB, JetC, and JetD of the recently described anti-plasmid system Wadjet (Doron et al., 2018) in the genome of *B. linens* ATCC 19391 and *B. epidermidis* BS258 as well as in all seven *B. aurantiacum* strains studied here. Although other unknown systems could be involved, this anti-plasmid system could be partly responsible for the absence of plasmids in *B. aurantiacum* strains analyzed here.

Core-genome and pan-genome

To determine the genetic diversity of *B. aurantiacum*, we performed a pan-genome analysis. In addition to the seven *B. aurantiacum* complete genomes now available, we added four *B. aurantiacum* draft genomes recently sequenced with a different technology (Pham et al., 2017). Our analysis revealed that the open pan-genome for 11 *B. aurantiacum* strains reaches 6,259 genes (Figure 2A). We also analyzed the number of genes present in different number of k genomes. The two major groups composed the core genome (k = 11 genomes) and the orphan genes (k = 1 genome), with 2,612 and 1,790 genes, respectively (Figure 2B). Hence, most of *B. aurantiacum* genes are either conserved in all genomes or specific to one strain (Figure 2B). The orphan genes/proteins, also called ORFans, increase the size of *B. aurantiacum* pan-genome. To explore the functions of these orphan genes, we annotated and classified them into categories using RAST. Manual curation was also performed for proteins that were not classified by RAST (Supplementary Table S1 A-C). Of 1,790 ORFans, 886 (49.5%) were hypothetical proteins. From the remaining, 125 (7.0%) had putative functions, 100 (5.6%) were considered miscellaneous, and 679 proteins (37.9%) were classified into RAST subsystem categories (Figure 2C). In RAST, phage and mobile element proteins had 112 representatives, which represented the main functional categories of

ORFans, suggesting that *B. aurantiacum* contains a diverse array of mobile genetic elements. Proteins involved in membrane transport (104 genes), DNA and RNA metabolism (99 genes) and transcriptional regulators (83 genes) also accounted for several ORFans. A total of 20 Type I restriction-modification (R-M) systems and 6 Type III R-M methylation subunits were identified in the DNA and RNA metabolism category, perhaps offering broad protection against phage infection. Another intriguing category among *B. aurantiacum* ORFans was ATP-Binding Cassette (ABC) transporter proteins, such as components of iron siderophore transport system. In the cheese environment where iron is poorly available, these genes could improve growth on cheese rinds. Furthermore, we analyzed the genomic context of the ORFans and found that these genes were dispersed into *B. aurantiacum* genomes (Supplementary Figure S1). A slightly higher concentration of ORFans was observed 2.5 Mbp downstream of the *ori* region (upstream *dnaA*) in all eleven *B. aurantiacum* genomes suggesting that this chromosomal region is less conserved in this species.

Transposable elements

After observing parts of pBLA8 and several mobile elements in the *B. aurantiacum* pan-genome, we analyzed the *B. aurantiacum* mobilome. In the largest *B. aurantiacum* genome (strain SMQ-1417), we identified 116 transposases and 68 integrases indicating that this species contains several mobile genetic elements, such as prophages and insertion sequences. A putative prophage was previously identified in the genome of SMQ-1335 (de Melo et al., 2016). Although the presence of several transposases in this putative prophage suggested that it was not functional, we tested SMQ-1335 and the other *B. aurantiacum* strains from our collection for the presence of inducible prophages. Even though the cultures with mitomycin C grew slower than the control without the chemical, no significant drop on bacterial optical density was observed for *B. aurantiacum* cultures. These results suggested that these strains did not carry functional prophages in their genome or that they could not be induced in the conditions tested.

Once the genome was annotated, we observed genes encoding putative phage proteins (e.g. holin, portal, major capsid protein, tail tape measure protein) spread in the genomes of all six *Brevibacterium* strains recently sequenced, suggesting the presence of prophage remnants. We then used *in silico* analyses to detect putative prophages throughout the genomes of *B. linens*

ATCC 19391 and *B. aurantiacum* SMQ-1417 – SMQ-1421. Similar to SMQ-1335, several integrases, transposases and other mobile elements were inserted within prophage-like regions,

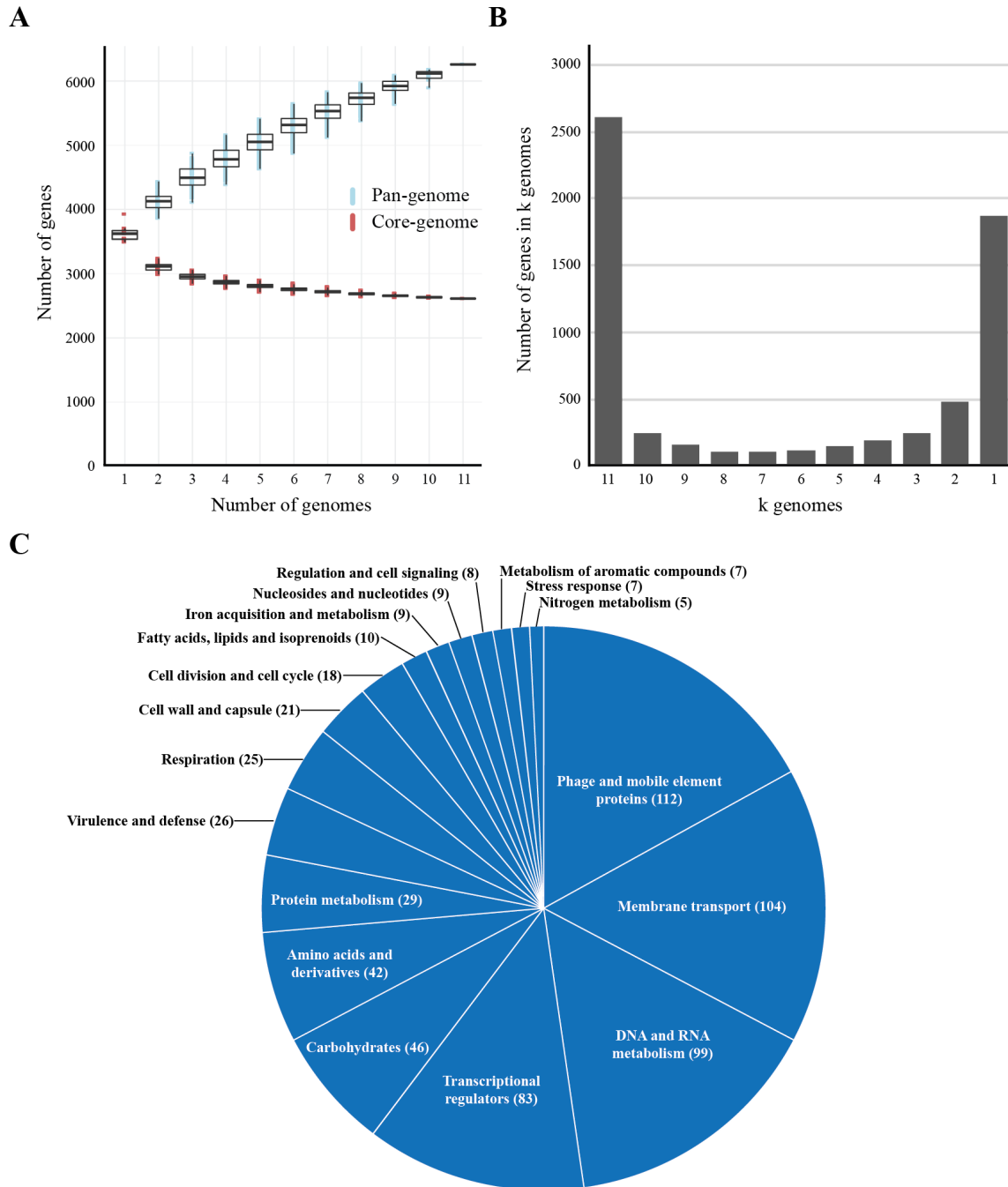


Figure 2. Pan-genome analysis of *B. aurantiacum*. (A) Accumulated number of new genes in the pan-genome and genes attributed to the core-genome are plotted against the number of added genomes. (B) Accumulated number of genes in k genomes are plotted against the number of k genomes. The number of core genes present in all 11 *B. aurantiacum* genomes can be observed

with $k = 11$ genomes. (C) Functional classification of *B. aurantiacum* orphan genes in RAST subsystem categories. Similar metabolic subsystem categories are fused together and only categories with >5 gene counts are shown. Proteins with hypothetical and putative function are not shown.

suggesting that they were likely inactivated overtime. Of note, a seemingly incomplete prophage (27.3 kbp) was detected in the genome of *B. aurantiacum* SMQ-1419. Although no structural gene was predicted, we performed a manual inspection of the regions flanking the putative prophage and found a gene encoding a putative tail tape measure protein (TMP) located a few ORFs upstream of PHASTER predicted attachment site *attL*. The BLASTp analysis of other ORFs surrounding the TMP also showed the presence of other genes involved in phage morphogenesis, such as putative genes coding for minor tail proteins, tail assembly chaperone and major capsid protein. We also identified genes involved in phage DNA packaging (e.g. portal and terminase). This extended 45-kbp putative prophage in SMQ-1419 was not found in other *B. aurantiacum* strains.

As part of *B. aurantiacum* mobilome, insertion sequences (IS) also play an important role in bacterial evolution by spreading into a genome and creating genetic variations (Wright et al., 2016). They can inactivate genes when integrated into a coding region or a promoter region as well as activate gene expression by providing an alternative promoter (Vandecraen et al., 2017). Moreover, neighbouring genes can be translocated by two flanking IS in a so-called composite transposon (Vandecraen et al., 2017; Varani et al., 2015). Using the ISFinder database, we detected five ISs (ISBli1-ISBli5) in *B. aurantiacum* genomes, often in several copies. Manually curating the annotated genomes led to the identification of 14 additional types of ISs in *B. aurantiacum* and 12 distinct in *B. linens* (ISBli6-ISBli35). A total of 26 ISs were validated by the ISFinder database, whereas four (ISBli18, ISBli20, ISBli22, and ISBli27) were not validated for not being discriminating enough to the others and were then removed from our analysis. We observed a dichotomy in the abundance and the type of ISs detected in *B. aurantiacum* and *B. linens* genomes (Figure 3A), suggesting a role in the diversification of these two closely related species. While a total of 56 copies of ISBli2 were identified in all seven *B. aurantiacum* genomes (5 to 13 copies/genome), only one copy was identified in *B. linens* ATCC 19391.

Interestingly, we found ISBli2 integrated into a gene coding for a putative abortive phage resistance protein in the genomes of *B. aurantiacum* SMQ-1417, SMQ-1419, SMQ-1421, and SMQ-1335 (Figure 3B). In SMQ-1335, the same gene was also disrupted by ISBli4. This putative anti-phage gene was identified in all *B. aurantiacum* genomes but was intact in *B. aurantiacum* SMQ-1418, SMQ-1420, and JB5. Therefore, we hypothesize that ISBli2 and ISBli4 may have inactivated this phage resistance protein in four out of seven *B. aurantiacum* genomes. Bacteriophages (or simply phages) infecting dairy cultures are well documented (de Melo et al., 2018; Marcó et al., 2012) and the presence of an intact abortive phage infection protein could provide protection against *Brevibacterium* phages during cheese ripening.

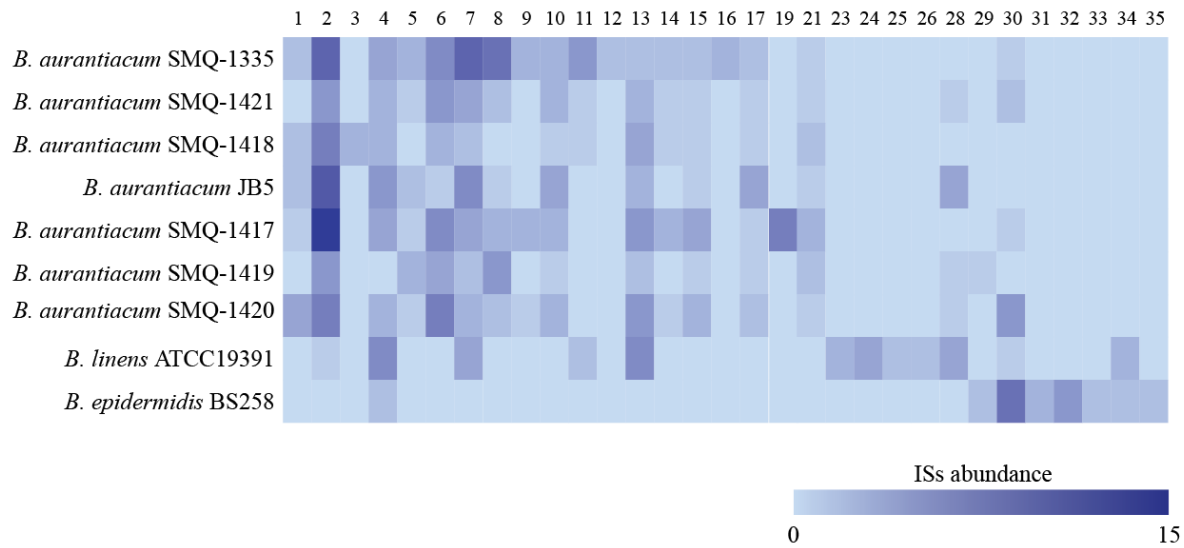
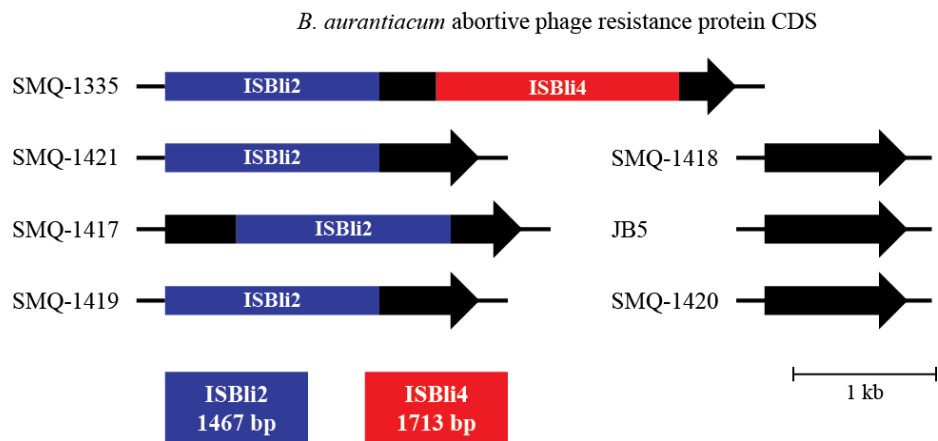
A*Brevibacterium* Insertion Sequences (ISBli1-ISBli35)**B**

Figure 3. *Brevibacterium* Insertion Sequences (ISBli1-ISBli35). (A) Abundance of ISs in *B. aurantiacum* and *B. linens* genomes. ISBli1-ISBli5 were identified with the ISFinder database and ISBli6-ISBli35 were identified manually. (B) Schematic representation of the integration of ISBli2 and ISBli4 in the coding region of an abortive phage resistance protein CDS in *B. aurantiacum* genomes. Coding sequences correspond to locus tags BLSMQ_RS02885 - BLSMQ_RS02895 of *B. aurantiacum* SMQ-1335 (GenBank: NZ_CP017150.1).

We found ISs from two other actinobacteria species used for cheese production in *B. aurantiacum* genomes. We identified ISPfr2, from *Propionibacterium freudenreichii*, in all *B. aurantiacum* strains. ISAar24, ISAar39, and ISAar42 from *Glutamicibacter arilaitensis* were also identified, but only in *B. aurantiacum* SMQ-1335 and SMQ-1420. The presence of these IS elements strongly suggests genetic exchange between cheese rind actinobacteria (Bonham et al., 2017). In-depth analysis of the 11,797 bp region containing homologues of the *G. arilaitensis* ISs also revealed an

iron uptake gene cluster between ISAar24 and ISAar39 (Figure 4) in both *B. aurantiacum* strains. *B. aurantiacum* iron uptake gene cluster shares 99% nucleotide identity with the one found in the strain *G. arilaitensis* RE117. ISAar39 and ISAar42 flanks the 11,797 bp genomic region and contain ISL3 family transposases sharing 65% amino acid sequence identity. The right inverted repeats of these two IS share 73.2% nucleotide sequence identity. Therefore, this region could be a composite transposon. Of note, the three integrase genes between ISAar24 and ISAar42 in *B. aurantiacum* SMQ-1335 and SMQ-1420 are absent in *G. arilaitensis* RE117, suggesting that their presence in *B. aurantiacum* occurred after the integration of the composite transposon (Figure 4). Interestingly, the iron uptake/siderophore operon was also identified in *Corynebacterium variabile* DSM 44702 (99% identity), but without the IS (Figure 4). We hypothesize that this operon originated from this species before being mobilized between other cheese rind actinobacteria.

Horizontal gene transfer regions

While performing BLAST analysis, we noticed that all *B. aurantiacum* genomes contained homologous nucleotide sequences (92-99% identity) with other species of cheese rind actinobacteria (Figure 5). Genomic positions, description, and gene annotations of these putative HGT regions are provided in Supplementary Tables S2 and S3. An HGT region (12,314 bp) from the previously described iRon Uptake/Siderophore Transport Island (Bonham et al., 2017) was identified in four *B. aurantiacum* genomes (Figure 5). The largest HGT region (99,628 bp) was observed in SMQ-1417 and shared 99% identity over 96% of its length with *Corynebacterium casei* LMG S-19264. This region has been previously described as the *Brevibacterium* Lanthipeptide Island (BreLI) (Pham et al., 2017; Walter et al., 2014). It is noteworthy that only two genes related to lanthipeptides synthesis has been assigned a function in the HGT region found in the strains from our collection.

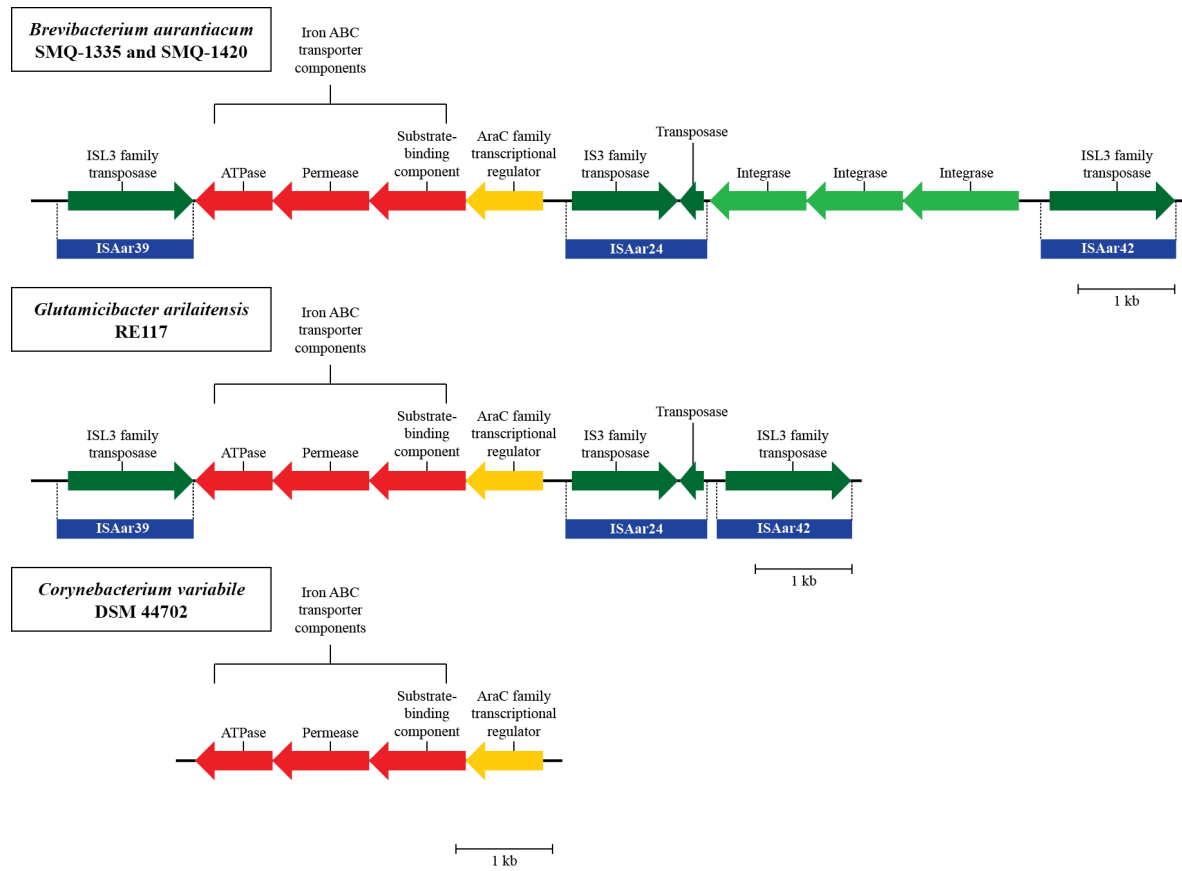


Figure 4. Schematic representation of the iron uptake composite transposon identified in *B. aurantiacum* SMQ-1335 and SMQ-1420. The homologous iron uptake gene clusters found in *Glutamicibacter arilaitensis* RE117 and *Corynebacterium variabile* DSM 44702 are also illustrated. Genes involved in iron transport are shown in red and the AraC family transcriptional regulator is shown in yellow. Mobile element proteins are shown in green and the ISs from *G. arilaitensis* are shown in blue. Coding sequences correspond to locus tags BLSMQ_RS13730 - BLSMQ_RS13785 of *B. aurantiacum* SMQ-1335 (GenBank: NZ_CP017150.1).

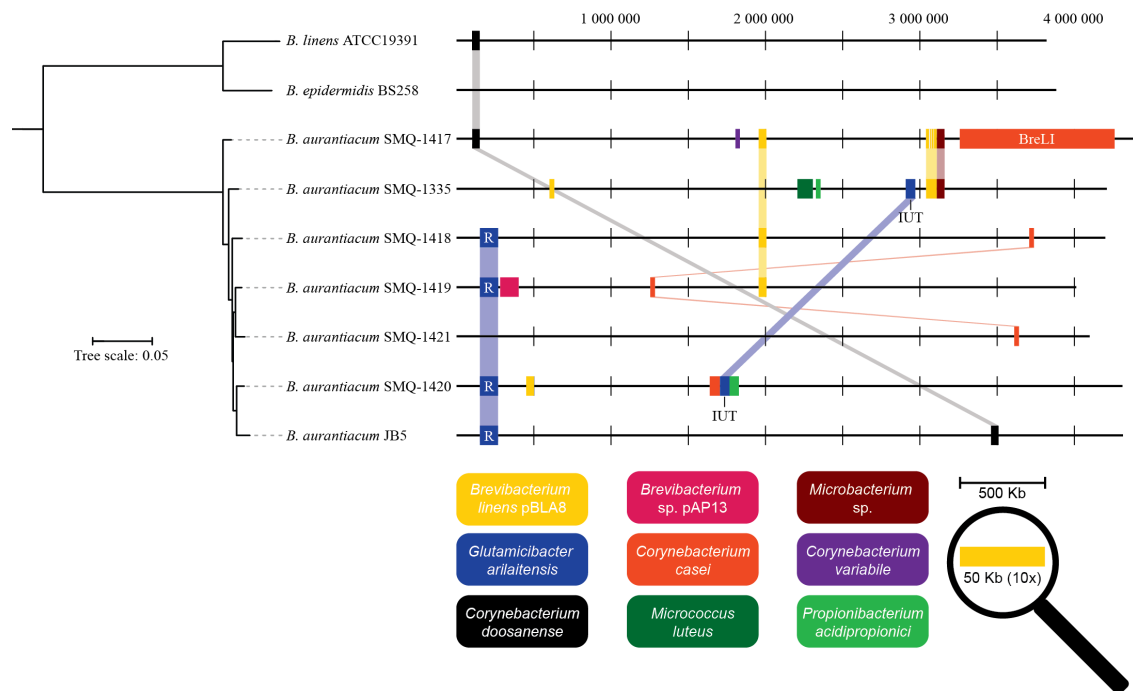


FIGURE 5 Schematic representation of HGT regions identified in *Brevibacterium* genomes. Homologous DNA sequences present in different species were identified with BLAST alignments. Identical HGT regions present in different genomes are linked together. HGT region sizes are increased 10x for presentation purposes and only regions with >90% identity are shown. The phylogenetic tree was generated with the concatenated protein sequences of the core-genomes of *B. aurantiacum*, *B. linens* and *B. epidermidis*. R; iRon Uptake Siderophore/Transport Island (RUSTI). IUT; Iron Uptake Transposon. BreLI; *Brevibacterium* Lanthipeptide Island.

We extracted annotations from all HGT regions identified in *B. aurantiacum* genomes and clustered them into functional groups based on the RAST subsystem categories (Figure 6). For representation purposes, we combined similar metabolic subsystem categories. The hypothetical proteins category contains the highest number of genes (89). The mobile elements (transposases, integrases, etc) and plasmid protein category contains 22 genes. We also identified a total of 34 genes involved in membrane transport and 24 genes involved in iron acquisition and metabolism. Moreover, 7 of the 20 transcriptional regulators observed in the HGT regions correspond to the AraC family. This family of transcriptional regulators is often found in the iron uptake gene clusters (Bonham et al., 2017). This observation suggests that efficient transport systems could confer a selective growth advantage to *B. aurantiacum* strains by helping them to efficiently acquire nutrients and minerals from the cheese environment. Of note, genes involved in DNA mobilization, membrane transport and iron acquisition were also the most prevalent horizontally transferred genes previously observed in 165 cheese rind bacteria (Bonham et al., 2017). Taken

altogether, these observations suggest high rates of HGT between cheese rind actinobacteria and cooperative adaptation to the cheese surface.

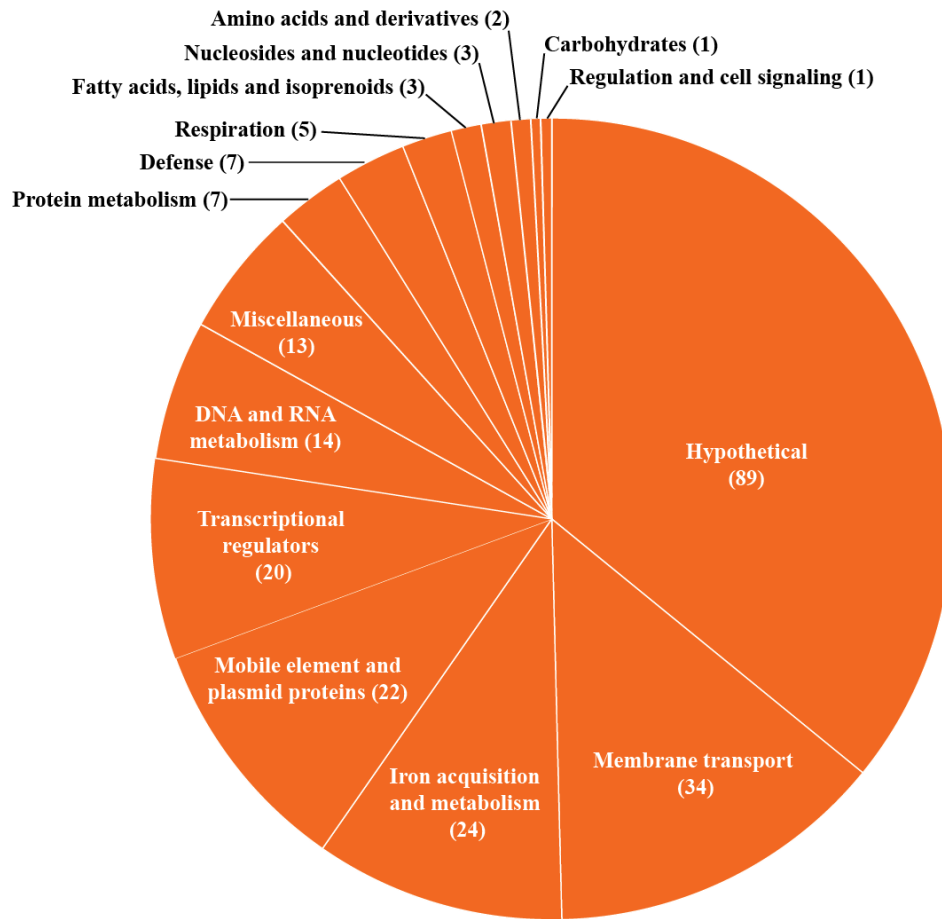


Figure 6. Functional classification of *B. aurantiacum* horizontally transferred genes. Similar metabolic subsystem categories are fused together and the percentage of HGT genes in each RAST subsystem category is shown.

Iron uptake and siderophore synthesis

Efficient iron acquisition systems are a driving force in adaptation to the iron-depleted cheese surface (Bonham et al., 2017; Monnet et al., 2012). Iron acquisition is mediated by siderophores, which are secreted by bacteria in response to iron depletion and act as chelating agents to scavenge iron (Andrews et al., 2003). In Gram-positive bacteria, iron uptake is mediated by three components: a membrane-anchored binding protein, permease, and ATP-binding protein cassette (Andrews et al., 2003). Different patterns of siderophore production and utilization in *Brevibacterium* spp. were previously described and some strains were shown to be auxotrophic for

iron siderophores (Noordman et al., 2006). Hence, the addition of siderophores or co-cultivation of siderophore-producing strains with auxotrophic strains can stimulate the growth of the latter (Noordman et al., 2006). To study the influence of the iron metabolism on *B. aurantiacum*, we analyzed the predicted genes involved in iron siderophores synthesis and acquisition. Iron ABC transporter components were more abundant in *B. aurantiacum* SMQ-1418, SMQ-1419, SMQ-1420, and JB5 than in the other strains (Supplementary Table S4). The genome of *B. aurantiacum* JB5 harbors 26 genes linked to iron uptake, the highest number in the set of genomes analyzed in this study.

Three iron ABC transporter components are clustered together in *B. aurantiacum*, *B. linens* and *B. epidermidis* genomes. In addition to the two clusters originating from the RUSTI region and the iron uptake transposon, three different iron uptake gene clusters were identified in the genome of all seven *B. aurantiacum* strains from our collection. A putative hydroxamate-type siderophore biosynthesis cluster encoding a siderophore synthetase, a lysine N6-hydroxylase, and a L-2,4-diaminobutyrate decarboxylase was recently described (Pham et al., 2017). Excluding *B. linens* ATCC 19391, this siderophore gene cluster was identified in *B. epidermidis* BS258 and all seven *B. aurantiacum* genomes. The additional putative catecholate siderophore gene cluster (Pham et al., 2017) was also observed in *B. aurantiacum* SMQ-1420 and JB5. Thus, all dairy strains from our dataset seem to be able to produce iron siderophore.

Considering the diverse amount of iron uptake gene clusters observed in *B. linens* ATCC 19391 and *B. aurantiacum* strains (SMQ-1335, JB5, SMQ-1417 to SMQ-1421), we performed growth curves in a mineral salts media (MSM) with limited iron availability and the presence of increasing concentrations of EDDHA as a chelating agent (Figure 7). We hypothesized that the acquisition of horizontally transferred iron uptake genes would confer growth fitness in an iron-limited media. SMQ-1419 did not grow well in MSM under the conditions tested, which can be either related to iron availability or another growth requirement missing in the media for this strain. In general, bacterial growth was inversely proportional to the concentration of EDDHA in the media, but the strains grew in presence or absence of chelator. In comparison with the *B. aurantiacum* strains, our experiments showed that *B. linens* ATCC 19391 is better adapted to iron-limited conditions, growing well in all concentrations of chelating agent tested. It has been previously shown (Noordman et al., 2006) that 100 μ M EDDHA is a stringent condition for the growth of

siderophore-auxotrophic strains, however it is likely less strict than in the cheese habitat. In stringent condition, SMQ-1417 grew better among *B. aurantiacum* strains, reaching approximately OD_{600nm} 0.7 after 21 h in the conditions tested. On the other hand, SMQ-1421 grew the least and also presented a larger growth difference between the control (without EDDHA) and cultures with the addition of chelating agent. Since SMQ-1421 is the strain with the lower number of iron-uptake components, this result supports the premise that the presence of genes/proteins cluster involved in iron acquisition is likely to confer adaptive growth on the cheese surface. However, they are not directly proportional as can be seen with JB5, which is the strain with more iron acquisition components. JB5 presented a similar growth in all three EDDHA concentrations, but the control culture that grew faster and reached a higher optical density. These results suggest that most of *Brevibacterium* strains tested are adapted to the growth in iron-limited medium.

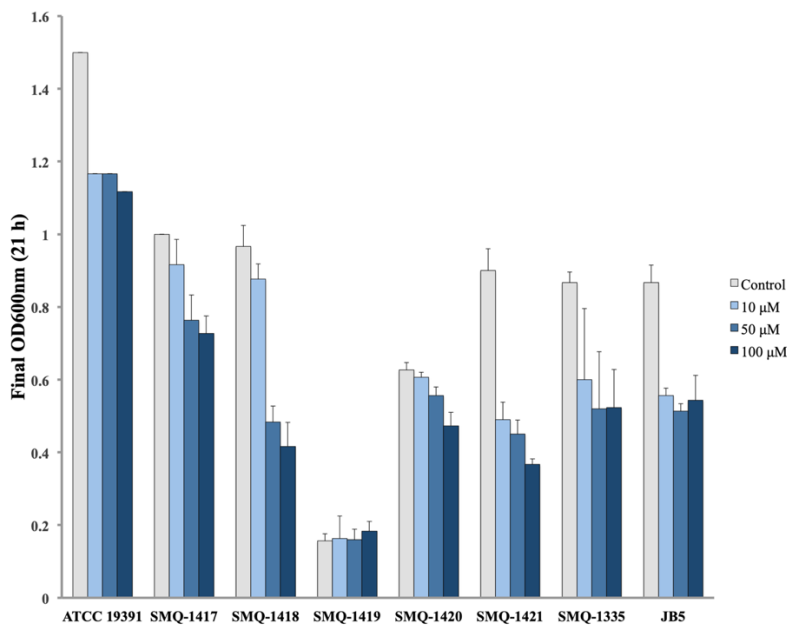


Figure 7. Growth of *Brevibacterium* spp. in iron-limited conditions. The final optical density after 21 hours growing in the presence or absence of EDDHA (0, 10, 50 or 100 μM) is shown in the graph for *B. linens* ATCC 19391 and *B. aurantiacum* strains.

***Brevibacterium* Lanthipeptide Island (BreLI)**

Another factor that can influence the microbial community on cheese surface is the production of antimicrobials, such as bacteriocins. For example, lanthionine-containing peptides (lanthipeptides) can inhibit the growth of undesirable microorganisms (Gomes et al., 2017) and confer a selective

advantage to the producing cultures. These antimicrobials are usually synthesized as inactive precursor peptides that undergo post-translational modifications to generate active molecules (Gomes et al., 2017). A probable Integrative Conjugative Element (ICE) coding for a lanthipeptide synthesis gene cluster has been previously identified in six cheese-associated *Brevibacterium* strains (*B. antiquum* CNRZ 918 and P10, *B. aurantiacum* ATCC 9174 and CNRZ 920, *B. linens* ATCC 9172 and Mu101) (Pham et al., 2017). This 96-100 kbp genomic island, called *Brevibacterium* Lanthipeptide Island (BreLI), was also observed in *C. casei* LMG S-19264 (Walter et al., 2014). This ICE integrated at the 3' end of a gene encoding a class Ib ribonucleotide reductase beta subunit, which resulted in 12 bp repeat sequence (5'-AGAAGTCCCAGT-3') flanking each side of BreLI (Pham et al., 2017). We identified this genomic island in the genome of *B. aurantiacum* SMQ-1417. ICE elements can be identified by the presence of signature genes/proteins associated with the core conjugation functions of (i) integration and excision from the host genome, (ii) replication as an extrachromosomal element, and (iii) conjugation between host and recipient cells (Ghinet et al., 2011). Genes involved in all three core functions were identified in *B. aurantiacum* SMQ-1417 BreLI region. An integrase (CXR23_14705) and a site-specific integrase (CXR23_15110) were observed at the two borders of BreLI, directly beside the repeats. Two other integrases (CXR23_14820, CXR23_14825), and one excisionase (CXR23_14930) were also identified and these five genes are likely involved in the integration and excision of BreLI.

To our knowledge, no experiment had been previously performed to determine whether this ICE element is active. To confirm excision from the genome, we designed PCR primers to amplify different regions of the *B. aurantiacum* SMQ-1417 ICE element (Figure 8). When combined, primers 2 and 5 were expected to generate a PCR product only if BreLI was excised from the chromosome. The detection and sequence of the PCR products confirmed the excision of BreLI and its presence in a circular form (Figure 8). Thus, this ICE element could still excise from the *B. aurantiacum* SMQ-1417 chromosome and potentially perform conjugation.

In terms of DNA replication, *B. aurantiacum* SMQ-1417 BreLI contains two helicases (CXR23_14715, CXR23_15070), a DNA polymerase III subunit alpha (CXR23_14790) and a DNA primase (CXR23_14925). The majority of actinobacterial ICEs utilizes a FtsK homolog-based conjugative DNA-translocation system to exchange double-stranded DNA (Bordeleau et al.,

2012). A conjugal transfer protein (CXR23_14800), a chromosome partitioning protein ParB (CXR23_14945), a conjugal transfer protein TrbL (CXR23_14995), a type VI secretion protein (CXR23_15060), and a single-stranded DNA-binding protein (CXR23_15075) are also present in BreLI. These results suggest that BreLI uses a single-stranded DNA (ssDNA) transfer system. Interestingly, the *G. arilaitensis* JB182 RUSTI, observed in four *B. aurantiacum*, is also believed to use a ssDNA transfer mechanism (Bonham et al., 2017).

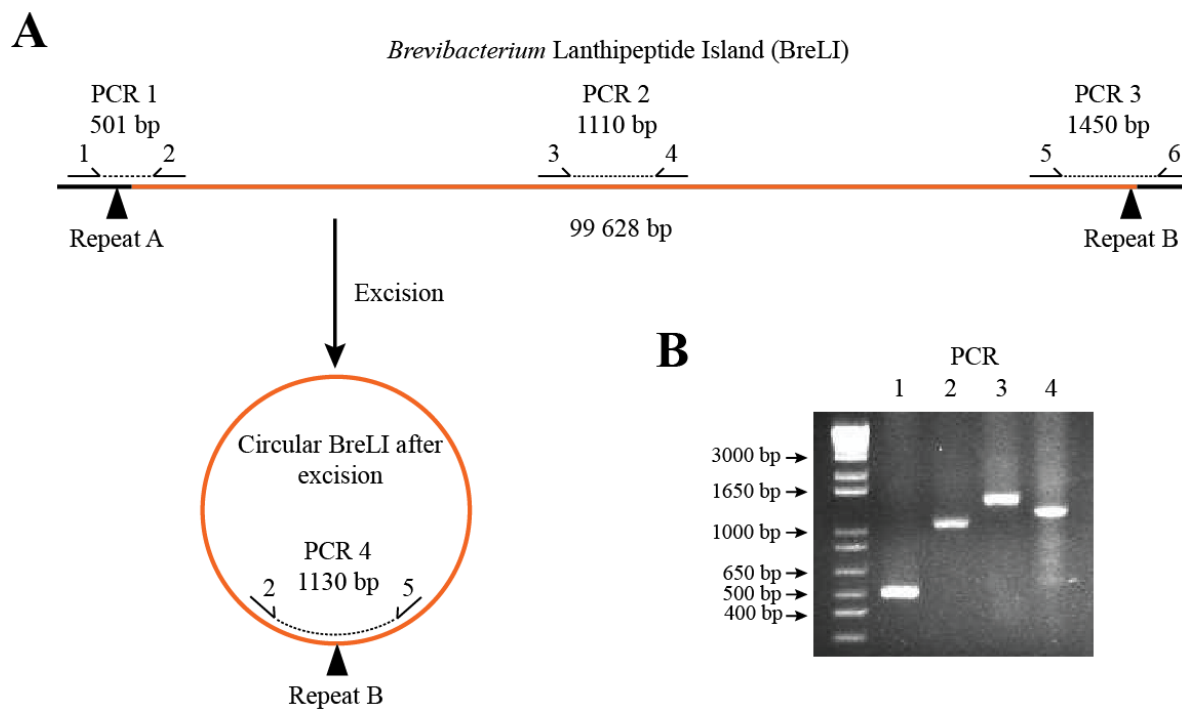


Figure 8. PCR amplification of *B. aurantiacum* SMQ-1417 BreLI. (A) Schematic for PCR primer design. (B) PCR testing for the presence of BreLI and for the excision of the ICE from the chromosome of *B. aurantiacum* SMQ-1417. PCR products were migrated on a 2% agarose gel for 35 min at 110 V and the gel was stained with ethidium bromide before UV observation.

We used Bagel4 to find genes involved in the biosynthesis of bacteriocins or bactericidal posttranslational modified peptides in the genome of *B. aurantiacum* strains and *B. linens* ATCC 19391. *B. linens* ATCC 19391 and all five *B. aurantiacum* strains sequenced here as well as SMQ-1335 contain a gene encoding a homolog of linocin. SMQ-1417 and ATCC 19391 possess a gene cluster involved in the synthesis of the lanthipeptide NAI-112, including a homolog for the core peptide. SMQ-1417, SMQ-1418 and SMQ-1419 have also genes involved in corynazolicin

synthesis (e.g. core peptide) and linaridin modification and transport, whereas SMQ-1420 and SMQ-1421 only have the genes involved in biosynthesis. SMQ-1335, SMQ-1418 and SMQ-1419 contain a putative gene cluster involved in sactipeptide production, although they do not encode putative antimicrobial peptide precursors.

We tested the *in vitro* antimicrobial activity of *Brevibacterium* spp. filtered supernatant against different bacterial species. We used the class I lantibiotic nisin-producing strain *L. lactis* SMQ-1220 as a positive control in our experiments. Although nisin-containing supernatants of SMQ-1220 were active against the bacterial strains tested (see materials and methods for the list), we did not observe antimicrobial activity for the filtered supernatants of *Brevibacterium* strains in the conditions tested. Perhaps, the lack of activity is related to experimental parameters, but it can also be due to genetic features of the host cells that prevent the expression of the laterally shared genes, such as promoter incompatibilities (Ochman et al., 2000) or absence of some components that act in the post-translational modification of the peptide (Gomes et al., 2017).

Discussion and conclusion

Comparative genomic studies have led to a better understanding of the genetic adaptation of dairy bacteria, such as *Streptococcus thermophilus* (Goh et al., 2011), *Lactococcus lactis* (Kelleher et al., 2017), *C. variable* (Schröder et al., 2011), *G. arilaitensis* (Monnet et al., 2010) and *P. freudenreichii* (Falentin et al., 2010) to cheese. A recent comparative analysis of mostly draft genomes of 23 *Brevibacterium* strains also provided insights into their adaptation to the cheese habitat (Pham et al., 2017). Overall, these studies shed light on the evolution and role of each bacterium in the development of cheese aromas and flavors.

Given the prevalence of mobile genetic elements in *Brevibacterium* spp. and other cheese actinobacteria (Bonham et al., 2017; Pham et al., 2017), we used PacBio long read sequencing technology to obtain six new complete *Brevibacterium* genome sequences and added information on the mobilome of these bacteria. Our phylogenetic analysis support previous findings (Cogan et al., 2014; Pham et al., 2017) and shows that most *Brevibacterium* strains used for cheese production belong to the *B. aurantiacum* species, making this species a key player in the dairy

industry. Therefore, the taxonomic position of commercial *Brevibacterium* strains should be revisited.

We used environmental strains of *B. linens* and *B. epidermidis* to compare with *B. aurantiacum* dairy strains and understand the cheese domestication of *B. aurantiacum*. Despite being the most prevalent (Cogan et al., 2014; Dugat-Bony et al., 2016), *B. aurantiacum* is not the only *Brevibacterium* species able to grow on cheese. For example, *B. antiquum*, *B. casei*, and *B. linens* have been isolated from cheeses (Monnet et al., 2015; Pham et al., 2017). However, certain genetic traits may explain the prevalence of *B. aurantiacum* in the dairy ecosystem. Multiple horizontal gene transfers have been documented between cheese rind bacteria (Bonham et al., 2017) and between cheesemaking fungi (Cheeseman et al., 2014), suggesting a complex network of gene exchanges that are shaping the evolution and adaptation of cheese-associated microorganisms. Our comparative analyses found significant differences between the mobilome of *B. aurantiacum* dairy strains and environmental strains of *B. linens* and *B. epidermidis*. *B. aurantiacum* strains seem to have acquired heterologous genes from other dairy actinobacteria, such as *G. arilaitensis*, *C. variabile*, and *C. casei*. The high percentage of identity between these DNA segments suggests that these genes were recently transferred. Moreover, mobile genetic elements are expanding *B. aurantiacum* pan-genome and they contribute to its genetic diversity. It is noteworthy that *B. aurantiacum* pan-genome is still open and more genomes should be analyzed to appreciate the diversity of its gene repertoire.

The use of commercial ripening cultures with active mobile genetic elements could explain the prevalence of nearly identical DNA sequences between cheese rind actinobacteria (Bonham et al., 2017), such as the lanthipeptide genomic island present in *Brevibacterium* spp. genomes. PCR amplifications of BreLI confirmed that this ICE was still active in *B. aurantiacum* SMQ-1417. Although *in vitro* tests did not confirm antimicrobial activity, it is still likely that an efficient production of active lanthipeptides could confer a selective advantage for the producing strain. Also observed in *C. casei* LMG S-19264, BreLI is likely to have been mobilized from a *Brevibacterium* spp., perhaps during cheese ripening (Walter et al., 2014). With these observations, one can speculate that as a species commonly used in commercial ripening cultures, *B. aurantiacum* is likely a player in the widespread distribution of mobile genetic elements.

Here we found horizontally transferred regions involved in iron uptake in five out of seven *B. aurantiacum* genomes. As previously showed (Bonham et al., 2017), genes associated with iron uptake were the most common genes exchanged between cheese actinobacteria. To assess if strains with efficient iron uptake systems are likely more adapted to the iron-depleted cheese surface, we performed growth curves of *Brevibacterium* strains in media with limited iron availability. Except with SMQ-1419, that was not able to grow in the media, all the other strains grew in increasing amount of iron chelating agent, with variability in the growth pattern. The strain SMQ-1421 was the less fit in iron-limited media, which corroborates with the lower abundance of iron acquisition and siderophore biosynthesis genes. On the other hand, the environmental strain *B. linens* ATCC 19391 was the better adapted when growing in the presence or absence of chelating agent.

Growth on the surface of smear-ripened cheeses is dependent of the capability to use substrates available in the cheese habitat. Additionally, it depends on its interactions with members of the microbial community present during ripening. Further studies could be done to explore the capacity of different *Brevibacterium* strains to grow, alone or in combination, in iron-depleted environments. Some *B. aurantiacum* strains with high aromatic potential could be auxotrophic for iron siderophores and dependent on other strains or species to grow well on cheese. Cheesemakers are sometimes faced with unstable ripening activity or the growth of undesirable microorganisms (Monnet et al., 2016). The optimization of ripening cultures while addressing these issues may improve the production of high-quality smear-ripened cheeses.

In conclusion, the addition of six complete genomic sequences of *Brevibacterium* spp. allowed an in-depth analysis of the mobilome of commercial *B. aurantiacum* strains and complement previous comparative analysis targeting cheese-related actinobacteria. Our phylogenetic analysis demonstrated that the industrial strains used for cheese production belong to the *B. aurantiacum* species. Our study also revealed that mobile genetic elements are widespread among the strains analyzed here and contribute to *B. aurantiacum* genetic diversity. Moreover, iron uptake HGT demonstrate the cooperative evolution of cheese actinobacteria, allowing their niche adaptation to the iron-depleted cheese surface. Regardless of the strong selective pressure exerted on the surface of smear-ripened cheeses, *B. aurantiacum* strains seem to be well adapted to thrive in this ecological niche. This comprehensive genomic information will serve as a tool to continue

improving our understanding of the complex interactions taking place in smear-ripened cheese microbial communities.

Conflict of interest

The authors declare they have no conflict of interest.

Author contributions

SL and SM designed the research protocol. SL, AGM, and SJL performed the research. SJL wrote the in-house python and R scripts and performed the pan/core-genome analysis. SL and AGM analyzed the data. SL, AGM, and SM wrote the paper.

Contribution to the field

Only two complete *B. aurantiacum* genomes were available in public databases prior to this study. *B. aurantiacum* genomes contain a high number of transposable elements and their genome sequences remain at the draft level when sequenced with short-read sequencing technologies, which precludes in-depth analysis of mobile genetic elements and genome plasticity. Here, we used long-read sequencing technology to provide six new complete *Brevibacterium* genomes. We identified a high number of mobile genetic elements that could be involved in the growth fitness of *B. aurantiacum* on the surface of smear-ripened cheeses. These genetic traits are shared between cheese rind actinobacteria and they seem involved in iron acquisition. Our study shows that mobile genetic elements are widespread in *B. aurantiacum* and contribute to its genomic diversity.

Funding

This work was supported by Agropur and the Natural Sciences and Engineering Research Council of Canada (CRD Program). SL is a recipient of scholarships from Op+Lait and PROTEO. AGM has a scholarship from the National Council for Scientific and Technological Development (CNPq-Brazil) in partnership with CALDO (Canada). SM holds a Tier 1 Canada Research Chair in Bacteriophages.

Acknowledgments

We thank Barb Conway for editorial assistance.

Supplementary materials

The supplementary material for this article can be found at: [10.3389/fmicb.2019.01270](https://doi.org/10.3389/fmicb.2019.01270).

Supplementary Figure S1 ORFans distribution in *B. aurantiacum* genomes. ORFans genomic positions and abundance are presented. Diamond colors correspond to RAST subsystem categories.

Supplementary Figure S2 Distribution of pBLA8 fragments in the genomes of *B. aurantiacum* strains. pBLA8 CDS genomic positions and predicted functions are available in Suppl. Table S3.

Supplementary Table S1 Functional classification of *B. aurantiacum* orphan genes. List of all orphan genes with genomes, locus tag identifiers, genomic positions, predicted function, and subsystem category assigned by RAST. Table S1 (A) – ORFans – RAST classification. Table S1 (B) – ORFans analysis. Table S1 (C) – ORFans – Manual classification.

Supplementary Table S2 HGT regions identified in *B. aurantiacum* and *B. linens* genomes.

Supplementary Table S3 CDS present in HGT regions described in this study. List of CDS genomic positions and predicted functions.

Supplementary Table S4 Iron acquisition and siderophore biosynthesis gene annotations and genome position.

References

- Alper, I., Frenette, M., Labrie, S., 2013. Genetic diversity of dairy *Geotrichum candidum* strains revealed by multilocus sequence typing. *Appl. Microbiol. Biotechnol.* 97, 5907–5920.
- Altschul, S.F., Madden, T.L., Schäffer, A.A., Zhang, J., Zhang, Z., Miller, W., Lipman, D.J., 1997. Gapped BLAST and PSI-BLAST: a new generation of protein database search programs. *Nucleic Acids Res.* 25, 3389–3402.
- Amarita, F., Yvon, M., Nardi, M., Chambellon, E., Delettre, J., Bonnarme, P., 2004. Identification and functional analysis of the gene encoding methionine-gamma-lyase in *Brevibacterium linens*. *Appl. Environ. Microbiol.* 70, 7348–7354.
- Anast, J.M., Dzieciol, M., Schultz, D.L., Wagner, M., Mann, E., Schmitz-Esser, S., 2019. *Brevibacterium* from Austrian hard cheese harbor a putative histamine catabolism pathway and a plasmid for adaptation to the cheese environment. *Sci. Rep.* 9, 6164.
- Andrews, S.C., Robinson, A.K., Rodríguez-Quiñones, F., 2003. Bacterial iron homeostasis. *FEMS Microbiol. Rev.* 27, 215–237.
- Ankri, S., Bouvier, I., Reyes, O., Predali, F., Leblon, G., 1996. A *Brevibacterium linens* pRBL1 replicon functional in *Corynebacterium glutamicum*. *Plasmid* 36, 36–41.
- Arndt, D., Grant, J.R., Marcu, A., Sajed, T., Pon, A., Liang, Y., Wishart, D.S., 2016. PHASTER: a better, faster version of the PHAST phage search tool. *Nucleic Acids Res.* 44, W16–W21.
- Besemer, J., Lomsadze, A., Borodovsky, M., 2001. GeneMarkS: a self-training method for prediction of gene starts in microbial genomes. Implications for finding sequence motifs in regulatory regions. *Nucleic Acids Res.* 29, 2607–2618.
- Boisvert, S., Laviolette, F., Corbeil, J., 2010. Ray: simultaneous assembly of reads from a mix of high-throughput sequencing technologies. *J. Comput. Biol.* 17, 1519–1533.
- Bonham, K.S., Wolfe, B.E., Dutton, R.J., 2017. Extensive horizontal gene transfer in cheese-associated bacteria. *eLife* 6, 1–23.
- Bordeleau, E., Ghinet, M.G., Burrus, V., 2012. Diversity of integrating conjugative elements in actinobacteria. *Mob. Genet. Elements* 2, 119–124.
- Borowiec, M.L., 2016. AMAS: a fast tool for alignment manipulation and computing of summary statistics. *PeerJ* 4, e1660.
- Brennan, N.M., Ward, A.C., Beresford, T.P., Fox, P.F., Goodfellow, M., Cogan, T.M., 2002. Biodiversity of the bacterial flora on the surface of a smear cheese. *Appl. Environ. Microbiol.* 68, 820–830.
- Capra, M.L., Mercanti, D.J., Reinheimer, J.A., Quiberoni, A.L., 2010. Characterisation of three temperate phages released from the same *Lactobacillus paracasei* commercial strain. *Int. J. Dairy Technol.* 63, 396–405.
- Chaisson, M.J., Tesler, G., 2012. Mapping single molecule sequencing reads using basic local alignment with successive refinement (BLASR): application and theory. *BMC Bioinformatics* 13, 238.
- Cheeseman, K., Ropars, J., Renault, P., Dupont, J., Gouzy, J., Branca, A., Abraham, A.L., Ceppi, M., Conseiller, E., Debuchy, R., Malagnac, F., Goarin, A., Silar, P., Lacoste, S., Sallet, E., Bensimon, A., Giraud, T., Brygoo, Y., 2014. Multiple recent horizontal transfers of a large genomic region in cheese making fungi. *Nat. Commun.* 5, 2876.
- Chin, C.-S., Alexander, D.H., Marks, P., Klammer, A.A., Drake, J., Heiner, C., Clum, A., Copeland, A., Huddleston, J., Eichler, E.E., Turner, S.W., Korlach, J., 2013. Nonhybrid, finished microbial genome assemblies from long-read SMRT sequencing data. *Nat. Methods*

10, 563–569.

- Cogan, T.M., Goerges, S., Gelsomino, R., Larpin, S., Hohenegger, M., Bora, N., Jamet, E., Rea, M.C., Mounier, J., Vancanneyt, M., Guéguen, M., Desmasures, N., Swings, J., Goodfellow, M., Ward, A.C., Sebastiani, H., Irlinger, F., Chamba, J.-F., Beduhn, R., Scherer, S., 2014. Biodiversity of the surface microbial consortia from Limburger, Reblochon, Livarot, Tilsit, and Gubbeen cheeses. In: Cheese and Microbes. American Society of Microbiology, pp. 219–250.
- Couvin, D., Bernheim, A., Toffano-Nioche, C., Touchon, M., Michalik, J., Néron, B., Rocha, E.P.C., Vergnaud, G., Gautheret, D., Pourcel, C., 2018. CRISPRCasFinder, an update of CRISRFinder, includes a portable version, enhanced performance and integrates search for Cas proteins. *Nucleic Acids Res.* 46, W246–W251.
- de Melo, A.G., Labrie, S.J., Dumaresq, J., Roberts, R.J., Tremblay, D.M., Moineau, S., 2016. Complete genome sequence of *Brevibacterium linens* SMQ-1335. *Genome Announc.* 4, e01242-16.
- de Melo, A.G., Levesque, S., Moineau, S., 2018. Phages as friends and enemies in food processing. *Curr. Opin. Biotechnol.* 49, 185–190.
- Doron, S., Melamed, S., Ofir, G., Leavitt, A., Lopatina, A., Keren, M., Amitai, G., Sorek, R., 2018. Systematic discovery of antiphage defense systems in the microbial pangenome. *Science* 359, eaar4120.
- Dufossé, L., De Echanove, M.C., 2005. The last step in the biosynthesis of aryl carotenoids in the cheese ripening bacteria *Brevibacterium linens* ATCC 9175 (*Brevibacterium aurantiacum* sp. nov.) involves a cytochrome P450-dependent monooxygenase. *Food Res. Int.* 38, 967–973.
- Dugat-Bony, E., Garnier, L., Denonfoux, J., Ferreira, S., Sarthou, A.S., Bonnarme, P., Irlinger, F., 2016. Highlighting the microbial diversity of 12 French cheese varieties. *Int. J. Food Microbiol.* 238, 265–273.
- Edgar, R.C., 2004. MUSCLE: multiple sequence alignment with high accuracy and high throughput. *Nucleic Acids Res.* 32, 1792–1797.
- Edgar, R.C., 2010. Search and clustering orders of magnitude faster than BLAST. *Bioinformatics* 26, 2460–2461.
- Falentin, H., Deutsch, S.M., Jan, G., Loux, V., Thierry, A., Parayre, S., Maillard, M.B., Dherbécourt, J., Cousin, F.J., Jardin, J., Siguier, P., Couloux, A., Barbe, V., Vacherie, B., Wincker, P., Gibrat, J.F., Gaillardin, C., Lortal, S., 2010. The complete genome of *Propionibacterium freudenreichii* CIRM-BIA1T, a hardy actinobacterium with food and probiotic applications. *PLoS One* 5, e11748.
- Felsenstein, J., 1985. Confidence limits on phylogenies: an approach using the bootstrap. *Evolution* 39, 783–791.
- Forquin, M.P., Duvergey, H., Proux, C., Loux, V., Mounier, J., Landaud, S., Coppée, J.Y., Gibrat, J.F., Bonnarme, P., Martin-Verstraete, I., Vallaeys, T., 2009. Identification of *Brevibacteriaceae* by multilocus sequence typing and comparative genomic hybridization analyses. *Appl. Environ. Microbiol.* 75, 6406–6409.
- Gavrish, E.Y., Krauzova, V.I., Potekhina, N. V., Karasev, S.G., Plotnikova, E.G., Altyntseva, O. V., Korosteleva, L.A., Evtushenko, L.I., 2004. Three new species of *Brevibacterium*, *Brevibacterium antiquum* sp. nov., *Brevibacterium aurantiacum* sp. nov., and *Brevibacterium permense* sp. nov. *Microbiology* 73, 176–183.
- Ghinet, M.G., Bordeleau, E., Beaudin, J., Brzezinski, R., Roy, S., Burrus, V., 2011. Uncovering the prevalence and diversity of integrating conjugative elements in actinobacteria. *PLoS One*

6, e27846.

- Goh, Y.J., Goin, C., O’Flaherty, S., Altermann, E., Hutkins, R., 2011. Specialized adaptation of a lactic acid bacterium to the milk environment: the comparative genomics of *Streptococcus thermophilus* LMD-9. *Microb. Cell Fact.* 10, S22.
- Gomes, K.M., Duarte, R.S., Bastos, M. do C. de F., 2017. Lantibiotics produced by *Actinobacteria* and their potential applications (A review). *Microbiol. (United Kingdom)* 163, 109–121.
- Haft, D.H., DiCuccio, M., Badretdin, A., Brover, V., Chetvernin, V., O’Neill, K., Li, W., Chitsaz, F., Derbyshire, M.K., Gonzales, N.R., Gwadz, M., Lu, F., Marchler, G.H., Song, J.S., Thanki, N., Yamashita, R.A., Zheng, C., Thibaud-Nissen, F., Geer, L.Y., Marchler-Bauer, A., Pruitt, K.D., 2018. RefSeq: An update on prokaryotic genome annotation and curation. *Nucleic Acids Res.* 46, D851–D860.
- Hanniffy, S.B., Philo, M., Peláez, C., Gasson, M.J., Requena, T., Martínez-Cuesta, M.C., 2009. Heterologous production of methionine- γ -lyase from *Brevibacterium linens* in *Lactococcus lactis* and formation of volatile sulfur compounds. *Appl. Environ. Microbiol.* 75, 2326–2332.
- Irlinger, F., Mounier, J., 2009. Microbial interactions in cheese: implications for cheese quality and safety. *Curr. Opin. Biotechnol.* 20, 142–148.
- Ito, K., Murphy, D., 2013. Tutorial: Application of ggplot2 to pharmacometric graphics. *CPT Pharmacometrics Syst. Pharmacol.* 2, 1–16.
- Janssen, D., Scheper, A., Withold, B., 1984. Biodegradation of 2-chloroethanol and 1,2-dichloroethane by pure bacterial cultures. *Prog. Ind. Microbiol.* 20, 169–178.
- Kato, F., Hara, N., Matsuyama, K., Hattori, K., Ishii, M., Murata, A., 1989. Isolation of plasmids from *Brevibacterium*. *Agric. Biol. Chem.* 53, 879–881.
- Katoh, K., Standley, D.M., 2013. MAFFT multiple sequence alignment software version 7: improvements in performance and usability. *Mol. Biol. Evol.* 30, 772–780.
- Kelleher, P., Bottacini, F., Mahony, J., Kilcawley, K.N., van Sinderen, D., 2017. Comparative and functional genomics of the *Lactococcus lactis* taxon; insights into evolution and niche adaptation. *BMC Genomics* 18, 267.
- Koren, S., Harhay, G.P., Smith, T.P., Bono, J.L., Harhay, D.M., Mcvey, S.D., Radune, D., Bergman, N.H., Phillippy, A.M., 2013. Reducing assembly complexity of microbial genomes with single-molecule sequencing. *Genome Biol.* 14, R101.
- Krubasik, P., Sandmann, G., 2000. A carotenogenic gene cluster from *Brevibacterium linens* with novel lycopene cyclase genes involved in the synthesis of aromatic carotenoids. *Mol. Gen. Genet.* 263, 423–432.
- Kumar, S., Stecher, G., Tamura, K., 2016. MEGA7: molecular evolutionary genetics analysis Version 7.0 for Bigger Datasets. *Mol. Biol. Evol.* 33, 1870–1874.
- Le Bourgeois, P., Mata, M., Ritzenthaler, P., 1989. Genome comparison of *Lactococcus* strains by pulsed-field gel electrophoresis. *FEMS Microbiol. Lett.* 50, 65–69.
- Leclercq-Perlat, M.-N., Corrieu, G., Spinnler, H.-E., 2004. The color of *Brevibacterium linens* depends on the yeast used for cheese deacidification. *J. Dairy Sci.* 87, 1536–1544.
- Leclercq-Perlat, M.-N., Oumer, A., Buono, F., Bergere, J.-L., Spinnler, H.-E., Corrieu, G., 2000. Behavior of *Brevibacterium linens* and *Debaryomyces hansenii* as ripening flora in controlled production of soft smear cheese from reconstituted milk: protein degradation. *J. Dairy Sci.* 83, 1674–1683.
- Leret, V., Trautwetter, A., Rincé, A., Blanco, C., 1998. pBLA8, from *Brevibacterium linens*, belongs to a Gram-positive subfamily of ColE2-related plasmids. *Microbiology* 144, 2827–2836.

- Li, H., Handsaker, B., Wysoker, A., Fennell, T., Ruan, J., Homer, N., Marth, G., Abecasis, G., Durbin, R., 2009. The sequence alignment/map format and SAMtools. *Bioinformatics* 25, 2078–2079.
- Marcó, M.B., Moineau, S., Quiberoni, A., 2012. Bacteriophages and dairy fermentations. *Bacteriophage* 2, 149–158.
- Moineau, S., Pandian, S., Klaenhammer, T.R., 1994. Evolution of a lytic bacteriophage via DNA acquisition from the *Lactococcus lactis* chromosome. *Appl. Environ. Microbiol.* 60, 1832–1841.
- Monnet, C., Back, A., Irlinger, F., 2012. Growth of aerobic ripening bacteria at the cheese surface is limited by the availability of iron. *Appl. Environ. Microbiol.* 78, 3185–3192.
- Monnet, C., Dugat-Bony, E., Swennen, D., Beckerich, J.-M., Irlinger, F., Fraud, S., Bonnarme, P., 2016. Investigation of the activity of the microorganisms in a Reblochon-style cheese by metatranscriptomic analysis. *Front. Microbiol.* 7, 536.
- Monnet, C., Landaud, S., Bonnarme, P., Swennen, D., 2015. Growth and adaptation of microorganisms on the cheese surface. *FEMS Microbiol. Lett.* 362, 1–9.
- Monnet, C., Loux, V., Gibrat, J.F., Spinnler, E., Barbe, V., Vacherie, B., Gavory, F., Gourbeyre, E., Siguier, P., Chandler, M., Elleuch, R., Irlinger, F., Vallaeys, T., 2010. The *Arthrobacter arilaitensis* Rel17 genome sequence reveals its genetic adaptation to the surface of cheese. *PLoS One* 5, e15489.
- Moore, M., Svenson, C., Bowling, D., Glenn, D., 2003. Complete nucleotide sequence of a native plasmid from *Brevibacterium linens*. *Plasmid* 49, 160–168.
- Myers, E., Sutton, G., Delcher, A., IM, D., DP, F., MJ, F., SA, K., CM, M., KHJ, R., KA, R., EL, A., RA, B., HH, C., CM, J., AL, H., S, L., EM, B., RC, B., L, C., PJ, D., Z, L., Y, L., DR, N., M, Z., Q, Z., X, Z., GM, R., MD, A., JC, V., 2000. A Whole-Genome Assembly of *Drosophila*. *Science* 287, 2196–2204.
- Nardi, M., Sextius, P., Bonnarme, P., Spinnler, H.E., Monnet, V., Irlinger, F., 2005. Genetic transformation of *Brevibacterium linens* strains producing high amounts of diverse sulphur compounds. *J. Dairy Res.* 72, 179–187.
- Nguyen, L.T., Schmidt, H.A., Von Haeseler, A., Minh, B.Q., 2015. IQ-TREE: A fast and effective stochastic algorithm for estimating maximum-likelihood phylogenies. *Mol. Biol. Evol.* 32, 268–274.
- Noordman, W.H., Reissbrodt, R., Bongers, R.S., Rademaker, J.L.W., Bockelmann, W., Smit, G., 2006. Growth stimulation of *Brevibacterium* sp. by siderophores. *J. Appl. Microbiol.* 101, 637–646.
- Ochman, H., Lawrence, J.G., Groisman, E.A., 2000. Lateral gene transfer and the nature of bacterial innovation. *Nature* 405, 299–304.
- Overbeek, R., Olson, R., Pusch, G.D., Olsen, G.J., Davis, J.J., Disz, T., Edwards, R.A., Gerdes, S., Parrello, B., Shukla, M., Vonstein, V., Wattam, A.R., Xia, F., Stevens, R., 2014. The SEED and the Rapid annotation of microbial genomes using subsystems technology (RAST). *Nucleic Acids Res.* 42, 206–214.
- Pfeiffer, F., Zamora-Lagos, M.A., Blettinger, M., Yeroslaviz, A., Dahl, A., Gruber, S., Habermann, B.H., 2018. The complete and fully assembled genome sequence of *Aeromonas salmonicida* subsp. *pectinolytica* and its comparative analysis with other *Aeromonas* species: investigation of the mobilome in environmental and pathogenic strains. *BMC Genomics* 19, 20.
- Pham, N.-P., Layec, S., Dugat-Bony, E., Vidal, M., Irlinger, F., Monnet, C., 2017. Comparative

- genomic analysis of *Brevibacterium* strains: insights into key genetic determinants involved in adaptation to the cheese habitat. *BMC Genomics*. 18, 955.
- Rattray, F.P., Fox, P.F., 1999. Aspects of enzymology and biochemical properties of *Brevibacterium linens* relevant to cheese ripening: a review. *J. Dairy Sci.* 82, 891–909.
- Saitou, N., Nei, M., 1987. The neighbor-joining method: a new method for reconstructing phylogenetic trees. *Mol. Biol. Evol.* 4, 406–425.
- Sandoval, H., del Real, G., Mateos, L.M., Aguilar, A., Martín, J.F., 1985. Screening of plasmids in non-pathogenic corynebacteria. *FEMS Microbiol. Lett.* 27, 93–98.
- Schröder, J., Maus, I., Trost, E., Tauch, A., 2011. Complete genome sequence of *Corynebacterium variabile* DSM 44702 isolated from the surface of smear-ripened cheeses and insights into cheese ripening and flavor generation. *BMC Genomics* 12, 545.
- Siguier, P., Gagnevin, L., Chandler, M., 2009. The new IS1595 family, its relation to IS1 and the frontier between insertion sequences and transposons. *Res. Microbiol.* 160, 232–241.
- Simpson, P.J., Stanton, C., Fitzgerald, G.F., Ross, R.P., 2003. Genomic diversity and relatedness of bifidobacteria isolated from a porcine cecum. *J. Bacteriol.* 185, 2571–2581.
- Tamura, K., Nei, M., Kumar, S., 2004. Prospects for inferring very large phylogenies by using the neighbor-joining method. *Proc. Natl. Acad. Sci.* 101, 11030–11035.
- Tatusova, T., Dicuccio, M., Badretdin, A., Chetvernin, V., Nawrocki, E.P., Zaslavsky, L., Lomsadze, A., Pruitt, K.D., Borodovsky, M., Ostell, J., 2016. NCBI prokaryotic genome annotation pipeline. *Nucleic Acids Res.* 44, 6614–6624.
- Van Heel, A.J., De Jong, A., Song, C., Viel, J.H., Kok, J., Kuipers, O.P., 2018. BAGEL4: A user-friendly web server to thoroughly mine RiPPs and bacteriocins. *Nucleic Acids Res.* 46, W278–W281.
- Vandecraen, J., Chandler, M., Aertsen, A., Van Houdt, R., 2017. The impact of insertion sequences on bacterial genome plasticity and adaptability. *Crit. Rev. Microbiol.* 43, 709–730.
- Varani, A., Chandler, M., Gourbeyre, E., Ton-Hoang, B., Siguier, P., 2015. Everyman’s guide to bacterial insertion sequences. *Microbiol. Spectr.* 3, MDNA3-0030-2014.
- Walter, F., Albersmeier, A., Kalinowski, J., Rückert, C., 2014. Complete genome sequence of *Corynebacterium casei* LMG S-19264 T (=DSM 44701 T), isolated from a smear-ripened cheese. *J. Biotechnol.* 189, 76–77.
- Wright, M.S., Bishop, B., Adams, M.D., 2016. Quantitative assessment of insertion sequence impact on bacterial genome architecture. *Microb. Genomics* 2, e000062.